Anions in Supramolecular Chemistry:

Binding, Sensing and Assembly

By

Salvatore Camiolo

A thesis submitted for the degree of

DOCTOR OF PHILOSOPHY

at the

Department of Chemistry

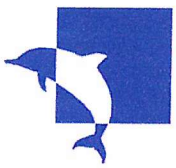

University of Southampton

2002

UNIVERSITY OF SOUTHAMPTON

ABSTRACT

FACULTY OF SCIENCE
CHEMISTRY

Doctor of Philosophy

ANIONS IN SUPRAMOLECULAR CHEMISTRY: BINDING, SENSING AND ASSEMBLY

by Salvatore Camiolo

This thesis deals with the synthesis and study of the anion complexation properties of new organic anion receptors. Firstly a series of pyrrole amide cleft receptors has been produced in order to investigate whether such simple molecules may behave as efficient anion coordinating agents. Indeed, high selectivity for oxoanions such as benzoate and dihydrogenphosphate has been observed with these receptors. The synthesis of new pyrrole amide clefts combining electron withdrawing groups at the 3- and 4- position of the pyrrole or directly appended at the amide positions has also been achieved. The aim of this project was to discover whether enhancing the acidity of the pyrrole NH or the amide NH groups via the introduction of chloro- or nitro- groups in the receptor skeleton could result in an enhanced interaction strength of the resulting receptor/anion complex. Not only was this target achieved, additionally the new electron withdrawing functionalized pyrroles clefts revealed unexpected properties such as the ability to form novel anionic dimers in the solid state and to selectively sense fluoride anions via a colorimetric response.

New 'super-extended' cavity calix[4]pyrroles have also been synthesised and the anion coordination properties of these receptors studied. These new compounds were found to bind fluoride anions exclusively in DMSO solution. The preference for fluoride was found to be so evident that these receptors were able to detect half of one equivalent of fluoride anions even in the presence of 100 equivalents of other undetected anions such as chloride, bromide, iodide, hydrogensulfate and hydrogenphosphate. The high selectivity for fluoride has been rationalized by molecular modelling studies carried out in collaboration with Dr. J.W. Essex at the University of Southampton.

Finally the carboxylate and dicarboxylate complexation properties of two amidinium derivatized calix[4]arenes previously reported in literature have been studied. The presence of two amidinium groups appended to the calix[4]arene scaffold results in quite complex binding processes that involve different binding modes between the amidinium moiety and the carboxylate anions, and the possibility of multiple equilibria in solution.

Contents

Acknowledgments

I would like to thank Dr. P.A. Gale for allowing me to work in his research group – that consisted of one member when I started (me!). I would like to thank him for his supervision and his help over the last three years as well as for his friendship. Statements such as "come on Salvo it's just a matter of doing other ten NMR titrations..." will probably survive in my memory forever.

I would like to thank the EPSRC Crystallographic Center that has solved the majority of the structures reported in this thesis. Especially my thanks go to Dr. Simon Coles and Dr. Mark Light who supported me over the last years and Prof. Mike Hursthouse. Thanks also to Prof. A.H. White and Dr. B. Skelton at UWA and Dr M.I. Ogden at Curtin who helped me in the investigation of the solid state properties of the compounds reported in chapter 4.

Many thanks to Mr. Chris Woods and Dr. J.W. Essex for the molecular modelling studies reported in chapter 3.

My thanks also go to the members of the Gale group. Among them I would like to thank Colin Warriner, for his advice in the lab as well as for teaching me the difference between a lager and a bitter and how to roll tobacco (target not yet achieved). I would like to thank him also for his company during the 233342 cigarettes smoked together (this number is not reliable since it is calculated at the moment of the submission of the thesis, and therefore will need to be updated). Korakot Navakhun, for his huge smile always present all over his face, that is able to change a black day in a..... grey day. Thanks also to all the project students who worked in the lab with me for their help and friendship (among all, G. Tizzard, A. Shi and C. Chapman).

Glossary

Anal.	Analysis
Arom.	Aromatic proton
Bu	Butyl
b s	Broad singlet (NMR)
Calcd.	Calculated
d	Doublet (NMR)
Δ	Standard Error on HRMS analysis
Decom.	Decomposition
DMAP	4,4'-Dimethylaminopyridine
DMF	Dimethyl Formamide
DMSO	Dimethyl Sulfoxide
Equiv.	Equivalent
ES^+/ES^-	Positive/negative electrospray
Et	Ethyl
HRMS	High resolution mass spectrometry
Hz	Hertz
i.e.	*id est* (Latin: that is)
m	Multiplet (NMR)
M	Molecular ion
Mp	Melting point
Me	Methyl
MS	Mass spectrometry
NMR	Nuclear Magnetic Resonance
PBP	Phosphate binding proteins
Ph	Phenyl
ppm	Part per million
Pyrr.	Pyrrolic proton
q	Quartet (NMR)
s	Singlet (NMR)

SBP	Sulphate binding protein
t	Triplet (NMR)
TBA	Tetrabutylammonium
TFA	Trifluoroacetic acid
THF	Tetrahydrofuran
Ts	*p*-Toluensulfonyl
UV/Vis	Ultraviolet/Visible

1. Introduction

1.1 Anion coordination

The exploration of the coordination chemistry of metal cations has been the *raison d'etre* of many research groups around the world from the pioneering work of Werner[1] to the birth of supramolecular chemistry with the cation receptors from the laboratories of Lehn,[2] Pederson[3,4] and Cram[5] and onwards to the production of transition metal assembled structures from capsules[6] to racks,[7] helicates[8] and grids.[9]

More recently, coordination chemistry has expanded and now interest and research effort are being directed not only at binding metals but also at the coordination of anionic and neutral species thus forming the molecular recognition component of modern supramolecular chemistry. It was only in the last quarter of the twentieth century that real effort began to be devoted to binding anions (after the first report of a synthetic anion receptor in 1968 by Park and Simmons[10]). The coordination of anionic species presents a number of challenges. Anions are generally large species (certainly larger than isoelectronic cations) and hence have a lower charge to radius ratios decreasing the effectiveness of electrostatic interactions in binding. Additionally, the variety of geometries (e.g., tetrahedral for phosphate and sulfate, trigonal for nitrate etc.) makes the coordination of anionic species a more challenging task in that receptors must be designed to be complementary to the anionic guest.

One may wonder why the coordination of anionic species is important enough to employ such effort in synthesising new receptors? Agricultural land is often fertilized to increase the concentration of phosphates and nitrates; the subsequent leaking of these substances into lakes and rivers leads to serious pollution problems. Furthermore

phosphate based domestic detergents contribute to the alteration of the natural concentration of phosphorus in these environments. These phenomena lead to the formation of blue-green algal blooms that can end up covering large areas of lakes and rivers, preventing oxygenation of the water (eutrophication[11]) with consequent problems for aquatic life (Figure 1.1). One goal in the anion recognition arena is to produce sensors for phosphate and nitrate that might give early warning of the run-off of fertilizer into waterways.

Figure 1.1: Aerial view of two experimental lakes. The bright green colour is caused by algae formed because of the alteration of phosphate concentration due to fertilization.The lake in background is unfertilised.

Anions play an important role in several aspect of biology. In fact the exchange, the concentration modulation, and the elimination of anions are essential processes for every biological system, including humans. For example cystic fibrosis is caused by the mis-regulation of chloride anion channels in cell walls.[12]

Probably the most important anionic species within the human cell is the DNA double helix (Figure 1.2). It is made up of deoxyribonucleotides, each constituted from a base, sugar and phosphate group. It carries genetic code information and therefore an alteration of its structure can be the main cause of many diseases including cancer. The effect of a variety of drugs is attributed to a direct interaction with the DNA double helix[13], and its analogue RNA.[14]

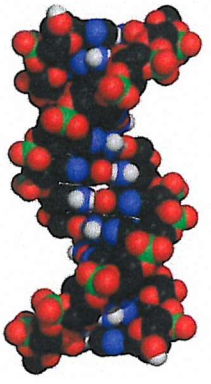

Figure 1.2: The DNA double helix.

Other examples of anion recognition in biological systems occur in proteins and enzymes. Enzymes, for example, catalyse reactions and are characterised by a high selectivity toward the substrates that they bind. For example, in carboxypeptidase-A the C-terminus of polypeptide chains is bound *via* a salt-bridge interaction to an arginine group containing a guanidinium moiety.[15] Good examples of highly selective anion recognition in biological system are shown by the phosphate binding proteins (PBP) and sulfate binding proteins (SBP) which bind and transport these anions in bacteria (Figure 1.3).[16]

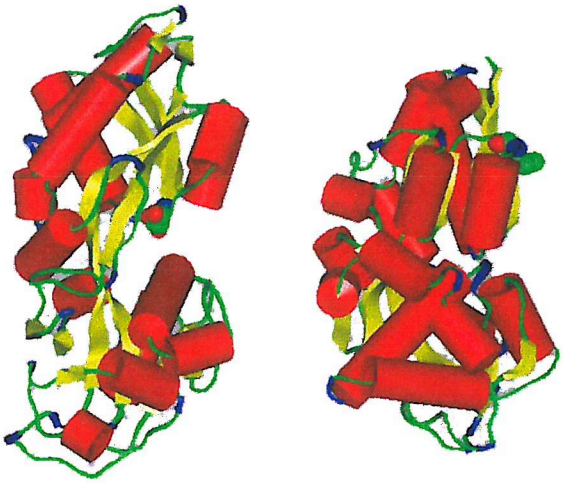

Figure 1.3: Crystal structures of the PBP (left) and SBP (right).

Complexation of the anionic substrate is a consequence of a highly specific interaction through the formation of multiple hydrogen bonds (in the case of the SBP) and electrostatic interactions (the PBP uses both hydrogen bonds and electrostatic interactions to form the complex). The ability of SBP and PBP to discriminate between sulfate and hydrogenphosphate ions is believed to be due to the fact that at physiological pH phosphate is mono-protonated whereas sulfate is not (Figure 1.4). The PBP contains a hydrogen bond acceptor residue in its binding site (Asp – marked in blue in Figure 1.4a) that can further stabilise the complex.[17]

Anions also play an important role in industry. As an example, $^{99}TcO_4^-$ is a radioactive product of nuclear fuel reprocessing, and therefore coordination and elimination of this anionic species represents a relevant achievement. Fluoride is found as an impurity in the wine production process. Again removal of this anion represents an important target to increase the quality of this beverage.

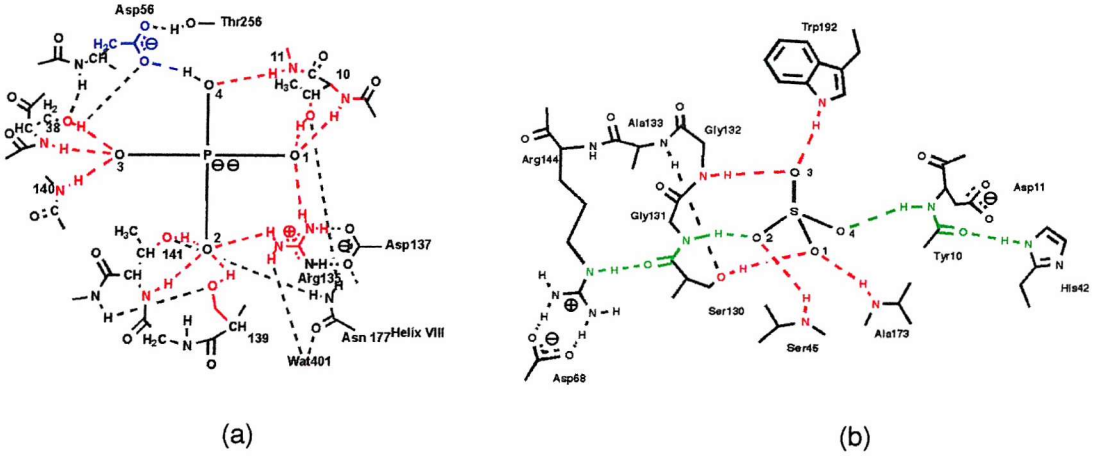

(a) (b)

Figure 1.4: The binding motif of the complex PBP/hydrogenphosphate (a) and SBP/sulfate (b).

Synthetic anion receptors therefore have a number of potential uses in binding and sensing anions in a variety of medical, environmental and industrial applications.

1.2 Synthetic anion receptors

Coordination of anionic species can be achieved by synthesising receptors containing groups that can interact with the anion through hydrogen bonding and/or electrostatic interactions. Other groups have employed Lewis acid metal centres in receptors for anionic species but these systems will not be discussed here.[18] The amide group for example can be used as a hydrogen bond donor due to the polarization of the NH bond. The presence of several amide groups can enhance the stability of the host/guest complex and the correct orientation of these groups can influence the host selectivity.

In 1997 Crabtree and co-workers reported the synthesis of two simple amide based anion receptors.[19] Binding studies, carried out in dichloromethane solution, revealed that isophthalamide derivatives **1** and **2** form anion complexes with exclusively 1:1 host:anion stoichiometry. Compound **2** was found to bind selectively spherical anions such as chloride and bromide over other putative anions ($K_{1\text{-Chloride}}$= $6.1\text{x}10^4$ M^{-1}, $K_{1\text{-Bromide}}$= $7.1\text{x}10^3$ M^{-1}) in dichloromethane solution. Crystallographic analysis revealed that receptor **1** adopts an unfavourable conformation in the host/bromide complex, with the two amide bonds twisted significantly out of the central ring plane (Figure 1.5)

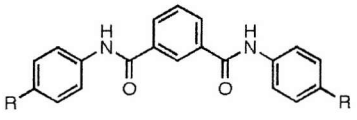

1 R = H
2 R = n-Bu

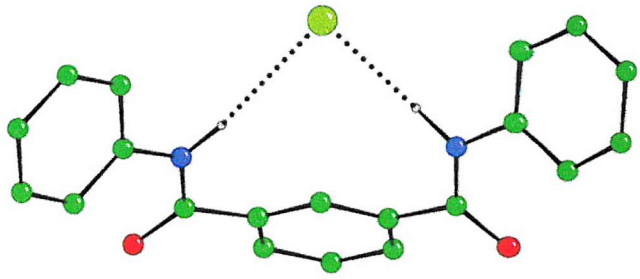

Figure 1.5: Crystal structure of the complex **1**/Bromide. The receptor adopts a distorted conformation binding the anionic species out of the molecule plane.

More recently Hamilton and co-workers produced compounds **3-4** and demonstrated that these receptors adopt a planar and rigid conformation with the NH protons pointing inwards toward the macrocycle core.[20] Compound **3** was found to bind spherical anions such as iodide and chloride, and planar anions such as nitrate in a 2% DMSO-d_6/$CDCl_3$ solution. Upon addition of less than 0.5 equivalents of either iodide, chloride or nitrate anions, two receptor molecules coordinate one guest; and after addition of further anions a 1:1 complex is formed. Selectivity was observed for iodide over chloride (i.e. $K_{1\text{-iodide}} = 1.3\text{x } 10^5 M^{-1}$ and $K_{2\text{-iodide}} = 1.1\text{x } 10^4 M^{-1}$); the R substituents were shown not to affect the binding properties of the central core.

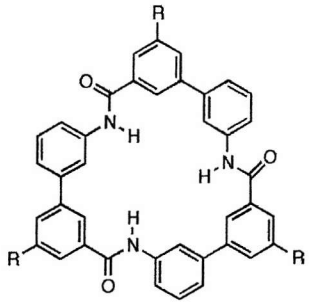

3 R = CO_2Et
4 R = NHBoc

Anslyn and co-workers reported the synthesis of the trigonal poly-amide box **5** that was found to be highly selective for nitrate anions.[21] Methyl red **6** is easily coordinated to receptor **5** in solution. Replacement of the methyl red, achieved upon addition of nitrate anions, leads to a dramatic change in the absorbance spectrum in acetonitrile:dichloromethane 25:75 solution. Therefore complex **5-6** behaves as an optical sensor for the detection of nitrate in solution.

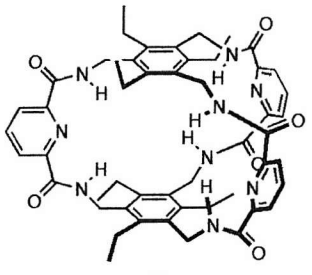

5

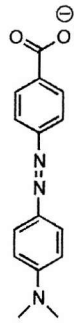

6

Urea and thiourea are particularly good coordinating groups especially towards carboxylates via the formation of two hydrogen bonds (Figure 1.6). Therefore receptors that incorporate these moieties can form strong complexes with carboxylate containing groups.

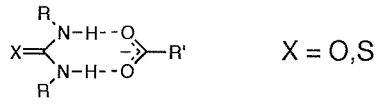

Figure 1.6: The binding motif of the interaction between (thio)urea group and a carboxylate.

In 1993, Hamilton and co-workers reported the synthesis of compounds **7** and **8** that proved to be efficient anion receptors for dicarboxylate anions (e.g. glutarate).[22] Bis-urea receptor **7** was found to bind strongly the bis-tetrabutylammonium glutarate in DMSO solution with a stability constant of $6.4x10^2\ M^{-1}$. The 1:1 host/guest complex stoichiometry (Scheme 1.1) was supported by the contemporaneous shift of the inner and outer urea NH resonances in the ^1H NMR spectrum upon addition of the anion, and confirmed by Job plot experiments.

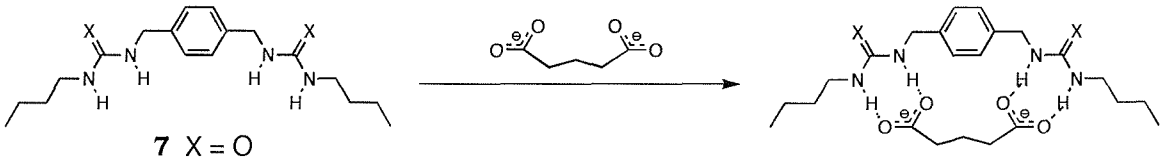

Scheme 1.1: The binding motif of the complex **7-8**/glutarate.

Wu and co-workers have synthesised a tripodal receptor containing naphthylurea.[23] Whilst the fluorescence spectrum of **9** showed a big enhancement in intensity upon addition of dihydrogenphosphate, a very small increase was observed for hydrogensulfate with no change for chloride or bromide. ^1H-NMR titration and fluorescence experiments, carried out in DMF, revealed a 1:1 stoichiometry and an association constant of $1.1x10^4\ M^{-1}$ for dihydrogenphosphate and $1.0x10^2 M^{-1}$ for hydrogensulfate.

Nam and co-workers appended two urea groups to *p-tert*-butylcalix[4]arene and, after oxidation with thallium trifluoroacetate, produced compound **10**.[24] This compound was found to bind hydrogensulfate selectively over other putative anionic guests such as

dihydrogenphosphate, chloride and acetate. This is due to an adjunctive hydrogen bond between the quinone and the OH proton of the hydrogensulfate anion. Electrochemistry studies confirmed this behaviour showing a considerable shift of 140mV for the quinone/semiquinone redox couple in the presence of hydrogensulfate (smaller shifts occurred with other anions). Surprisingly compound **11**, reported more recently by the same authors, did not show any selectivity among the considered anions.[25] The association constant, calculated using ^{1}H-NMR titration techniques in $CDCl_3$, were between 13000 and 17200M^{-1} for chloride, hydrogensulfate, dihydrogenphosphate and acetate. Bromide was the only anion to be bound with a lower stability constant (K_1 = 6340M^{-1}).

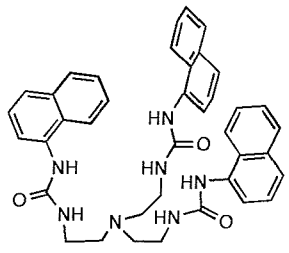

9

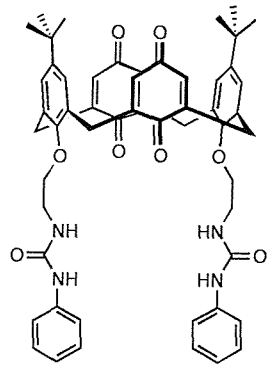

10

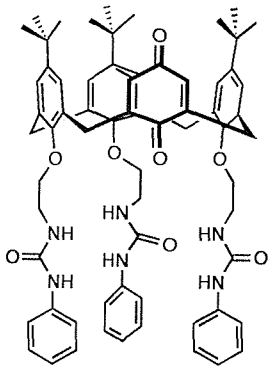

11

In 2001, Kilburn and co-workers reported the synthesis of a series of acyclic thiourea receptors, targeting the coordination of the carboxylate group of amino acid species.[26] The structure of one of these thiorea derivatives and the proposed complexation motif are shown (Figure 1.7). Compound **12** was found to be selective for a variety of amino acid derivatives revealing, for example, a 30:1 selectivity for *N*-Ac-L-Trp-CO_2^- over *N*-Ac-L-Ser-CO_2^- in $CDCl_3$. However moderate enantioselectivity was observed with slight preference for L-amino acids.

Anion coordination driven by simple electrostatic interactions with the receptor have been also reported in literature. In 1986 Schmidtchen reported the synthesis of the three macrocyclic quaternary ammonium salts **13-15**.[27] The decarboxylation rate of 6-nitrobenzisoxazole-3-carboxylate **16** in the presence of these receptors was investigated.

Kinetic studies revealed that compounds **13** and **15** consisting of 27-membered macrocycles are capable of coordinating compound **16** and catalysing the decarboxylation process showing in certain cases an enhancement of the reaction rate of 110 times. The rate, the binding constants and the dependence on the temperature suggest that the receptors encapsulate the guest species within the macrocycle cavity coordinating first the nitroaromatic moiety of **16**.

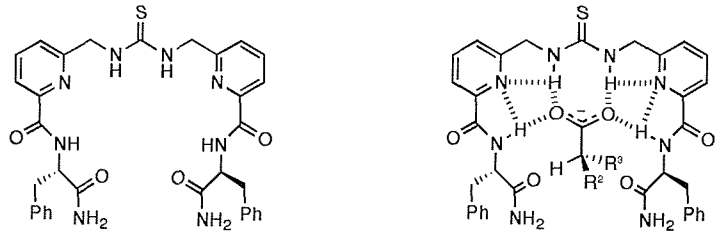

12 **12-guest**

Figure 1.7: Structure of the acyclic thiourea receptor **12** and proposed binging motif for the coordination of an amino acid guest.

The 21-membered macrocycle **14** proved to be too small to accommodate the guest species with this mode of association and therefore did not show any catalytic effect on the decarboxylation of compound **16**. In previous work the authors also reported the halide coordination properties of receptors **14-15**, highlighting the selectivity of **15** for iodide anions over the other halides in methanol/water (*v/v*, 95/5) solution ($\log K_{1\text{-Iodide}} = 5.0$, $\log K_{1\text{-Bromide}} = 3.9$).[28]

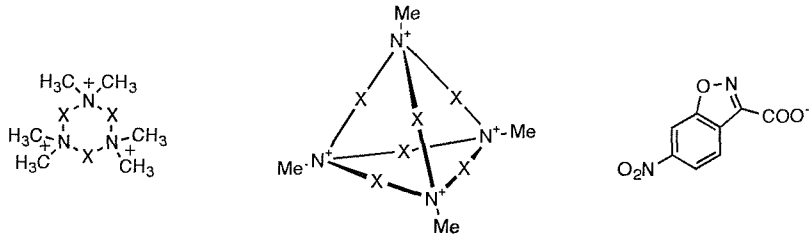

13 X = $(CH_2)_8$ **14** X = $(CH_2)_6$ **15** X = $(CH_2)_8$ **16**

Guanidinium and amidinium groups are extremely efficient coordinating groups for anions, as they combine the presence of two hydrogen bond donors and a delocalised positive charge.[29]

The simple bicyclic guanidinium **17** was found to behave as an efficient receptor for nitronate anions. Upon addition of aliquots of 2-nitropropanate to a DMSO solution of **17** (as the tetraphenylborate salt) a calorimetric titration curve was obtained consistent with the formation of a 1:1 complex (Scheme 1.2). Application of a one-site binding model revealed an association constant of $3200M^{-1}$ and an enthalpy of association of –2.9 $kcal{\cdot}mol^{-1}$.[30]

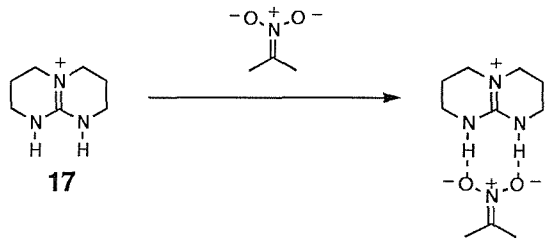

Scheme 1.2: Bicyclic guanidinium **17** coordinates the 2-nitropropanate with a 1:1 host:guest stoichiometry *via* the formation of two hydrogen bonds.

The pyrene functionalised monoguanidinium **18** has been synthesised by Nishizawa and co-workers and reported in 1999.[31] In the presence of pyrophosphate anions this molecule can form a 2:1 receptor to anion complex. A dramatic change in the fluorescence spectrum of this compound was observed, as a consequence of the close proximity of the two pyrene moieties in the receptor:anion complex (Scheme 1.3). Other anions such as hydrogensulfate, dihydrogenphosphate, acetate, thiocyanide, chloride and bromide, did not promote such aggregation phenomena and, therefore, did not lead to any change in the pyrene fluorescence.

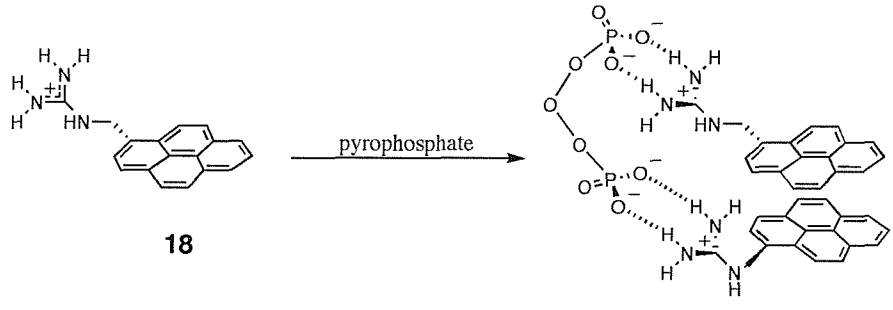

Scheme 1.3: Complexation of pyrophosphate anion by two molecules of the pyrene functionalised monoguanidinium **18**. The close proximity of the two host molecules leads to a dramatic change in the fluorescence spectrum of the pyrene.

A variety of steroidal guanidines, synthesised by functionalization of cholic acid, have recently been reported by Davis and co-workers.[32] Extraction experiments from an aqueous solution to chloroform revealed that these compounds can coordinate amino acid derivatives. In certain cases chiral discrimination was observed. Compound **19**, for example, was used to extract *N*-acetyl-α-amino acids from a racemic mixture with an extraction efficiency between 41 and 90%. It proved possible to enantioselectively extract the L and D isomers of the *N*-acetyl- alanine in a ratio of 10:1.

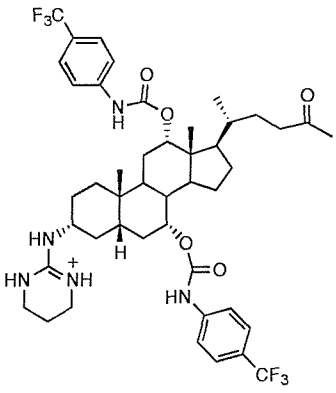

19

In addition to guanidinium and amidinium, the ammonium group is a good hydrogen bond donor and is also positively charged. Cryptand-like ammonium derivatives, first reported by Simmons and Park in 1968 were the first examples of synthetic anion receptors.[10] A variety of different length 1,(k+2)-diazabicyclo[k,l,m]alkanes have been synthesised and reacted with an appropriate acid. The resulting ammonium salts proved to be fluxional and the existence of different conformational isomers was supported by low temperature ^{1}H NMR experiments. As a matter of fact the ammonium groups can adopt three different conformations: in-in (both the NH groups point inward the macrocycle), out-out (both the NH groups point outward the macrocycle), and in-out (Figure 1.8) The diprotonated form of compound **20** has been crystallized and in the solid state the in-in and the out-out conformation have been isolated.[10] Evidence of encapsulation of chloride within the macrocycle cavity came from ^{1}H NMR investigations. The chloride salt of compound **20** proved to coordinate one of the two chloride counteranions, adopting an in-in conformation, whereas coordination of bromide was less favoured and binding of iodide was not detected at all.

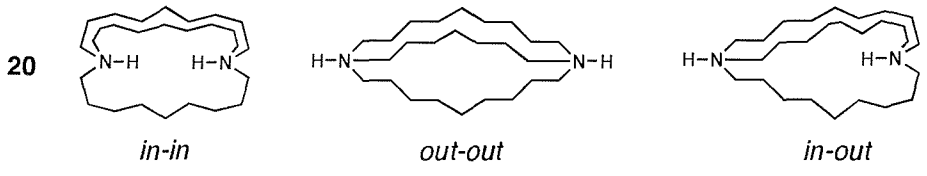

Figure 1.8: Conformational isomers attributed to compound **20**.

More recently Lehn and co-workers reported the synthesis of hexaaza-macrocycles **21** and **22** that proved to be efficient ditopic receptors for the coordination of

dicarboxylate species.[33] Modulation of the alkylic chain length revealed to be a powerful method to increase the selectivity of these receptors toward specific dicarboxylate guests.

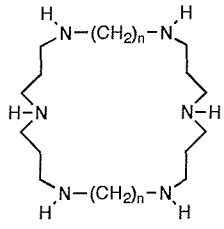

21 n = 7
22 n = 10

Indeed the hexaprotonated form of compound **21** was found to be selective for malonate and succinate in aqueous solution at room temperature. Under the same conditions **22**·**6H**$^+$ showed high selectivity for pimelate and suberate. Compound **21**·**6H**$^+$ binds preferentially the dianions *N*-acetyl-(L)-aspartate and *N*-acetyl-(L)-glutamate over the dipeptide *N*-acetyl-(L)-glutamylglycinate, whereas **22**·**6H**$^+$ behaves in the opposite way, in line with the different length of these receptors.

Bowman-James and co-workers recently reported the anion complexation study results of the polyprotonated forms of compounds **23** and **24**.[34] In accordance with X-ray, potentiometric and NMR studies, compound **23**·6H$^+$ did not show any potential as an anion receptor for monoanionic species such as nitrate and fluoride. However coordination of the divalent sulfate was found to be quite strong, with an association constant of 2.3×10^4 M $^{-1}$ (calculated for the encapsulation of the anion in the hexaprotonated ligand). Compound **24**·6H$^+$ proved to be a better receptor, showing association constant values greater than $1 \times 10^3 M^{-1}$ for both mono and divalent anionic species.

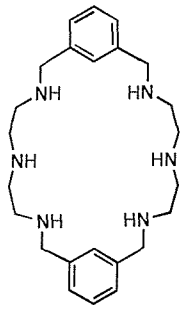

23

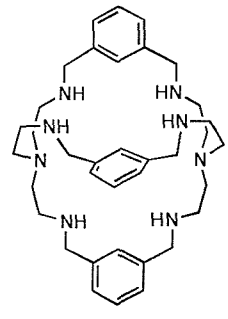

24

If a cation is bound to a receptor it can enhance the strength of the receptor/anion interaction. Inclusion of a cation binding group, can allow the molecule to act as an ion pair receptor that is capable of extracting inorganic salts in organic solvent.

Beer and co-workers recently reported the synthesis of ruthenium complexes featuring the presence of amide groups capable of coordinating anionic species.[35] He

found that the association constants, selectivity and stoichiometry of the anion complexes were strongly dependent upon the nature of the solvent. In fact compounds **25**, **26** and **28** proved to be selective for chloride over nitrate and acetate, binding with a 2:1 anion to receptor stoichiometry in a dichloromethane:methanol 9:1 solution.

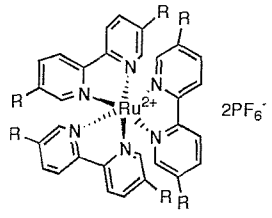

25 R = $CONHCH_2CH_2OMe$

26 R = $CONH(n\text{-}C_4H_9)$

27 R = $CONH(n\text{-}C_{12}H_{25})$

28 R = 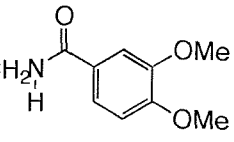

Anion binding properties of compound **27** were investigated in dichloromethane, producing association constants too high to be measured accurately. When the percentage volume of methanol was increased to 30%, the selectivity of receptors **25-28** for chloride is maintained but nitrate is bound with a 1:1 stoichiometry. With a higher concentration of methanol (50%), the stoichiometry is 1:1 for all the anions, and the selectivity of the receptor changes, binding nitrate more strongly than chloride. This behaviour has been explained as a consequence of the anion solvation energies in the different solvent mixtures. Solvation/desolvation phenomena plays an even more important role for compounds **27** and **28**. In fact the presence of more lipophillic groups in these receptors, require the anion to be highly desolvated before being complexed.

In 2001 Smith and co-workers reported the synthesis of two ion-pair receptors featuring the presence of a crown ether moiety and an isophthalic amide. Compound **29** was found to bind NaCl in water solution as a solvent separated ion-pair.[36] However the presence of Na^+ increased the **29**/chloride association constant by less than ten. The synthesis of compound **30** has been achieved to create a receptor with a smaller distance between the anion and cation binding sites. In fact ^{1}H-NMR titration experiments revealed that, in DMSO-d_6, **30** binds potassium chloride more tightly than free K^+ or Cl^-. A 300-fold enhancement in the affinity for chloride was observed in a $CDCl_3$:DMSO-d_6 85:15 solution in the presence of one molar equivalent of potassium tetraphenylborate.

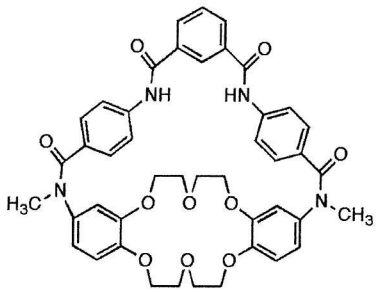

29

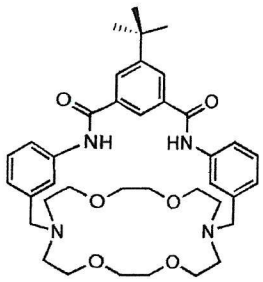

30

Finally compound **30** has been shown to be capable of coordinating one equivalent of potassium chloride in chloroform with the complex being stable enough to survive column chromatography using silica gel and weakly polar solvents.

1.3 Pyrrole and polypyrrole

1.3.1 Acyclic pyrrole derivatives

Pyrrole is a hydrogen bond donor suitable for anion coordination. Unlike amides that can self-associate via C=O···HN interactions, pyrrole alone does not contain a hydrogen bond acceptor and so does not 'compete with itself' for hydrogen bond formation to potential guests. Recently Gale and co-workers highlighted pyrrole's coordinating ability by crystallizing tetramethylammonium chloride from pyrrole (Figure 1.9).[37] The crystal structure reveals the complexation of one chloride anion by two molecules of pyrrole (N···Cl = 3.241Å). However, in solution, pyrrole binds anions very weakly[38] and therefore it must be functionalised with complementary groups to enhance its affinity toward anions.

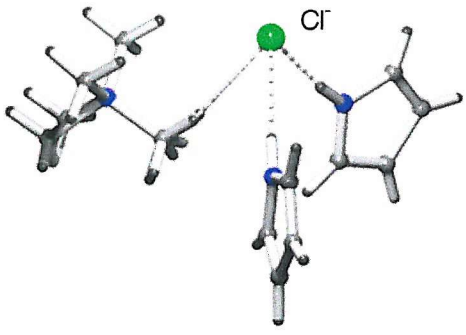

Figure 1.9: Crystal structure of the pyrrole/tetramethyl ammonium chloride complex.

Schmuck and co-workers produced a series of pyrrole guanidinium derivatives (**31** and **32**),[39,40] which proved to be excellent receptors for acetate. The interaction strength for the complex **31**/acetate was investigated by using ^{1}H-NMR titration experiments, in DMSO solution. However the stability constant was found to be too high to be accurately measured using this technique (K > 10^6 M^{-1}). Measuring the stability constant in more polar solvents (e.g. DMSO/water 50/50) led to a value of approximately 10^3 M^{-1}.[39] Although in solution a 1:1 stoichiometry was observed, the solid state revealed a two dimensional hydrogen bonding network, in which two molecules of receptor interact with one molecule of acetate (Figure 1.10).

31 **32**

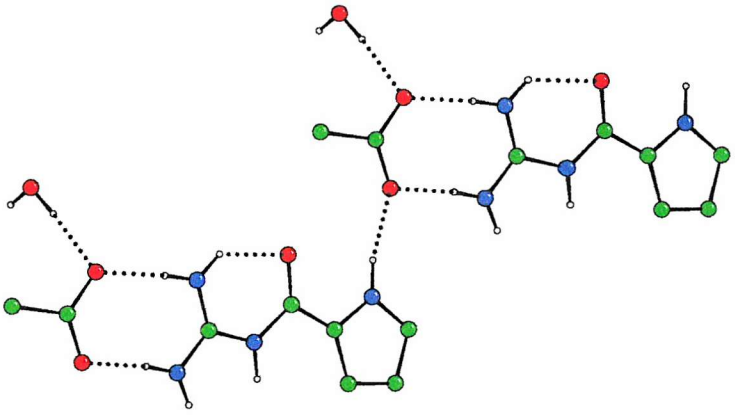

Figure 1.10: Crystal structure of the two dimensional network for the complex **31**/acetate complex

When pyrrole was functionalised with a guanidinium group in the 2-position and an ester in the 5-position (compound **32**), self-assembly was observed in DMSO solution.[41] Proton NMR experiments revealed a stability constant value of 673 M^{-1} for the dimerisation process. This value was found to be strongly dependent on the nature of the counteranion. In fact chloride promoted the self-assembly in DMSO solution whereas picrate anions seemed to inhibit it. Variable temperature ^{1}H-NMR experiments revealed that the association phenomena is an endothermic process driven by entropy.

Sessler and co-workers reported the synthesis of a variety of acyclic pyrrole receptors which act as optical sensors for anions.[42] Dipyrrolylquinoxaline **33** was investigated as receptor for a variety of anionic species including fluoride, chloride and dihydrogenphosphate. Addition of fluoride to either a DMSO or dichloromethane

solution of **33** led to a dramatic yellow to purple colour change, whereas treatment with other anions did not show any colour change. Moreover, in the presence of fluoride anions a quenching of the fluorescence was observed. This behaviour has been explained as a perturbation of the orbital overlap between the pyrrolic units and the quinoxaline in the presence of coordinated fluoride anion. Compound **34** was obtained reacting 3,4-difluoropyrrole in the place of simple pyrrole; this compound showed increased affinity and a higher selectivity for dihydrogenphosphate over chloride.[43] Addition of either fluoride or dihydrogenphosphate to a solution of **34** led to a colour change, whereas no change was observed upon addition of chloride in either DMSO or dichloromethane solution.

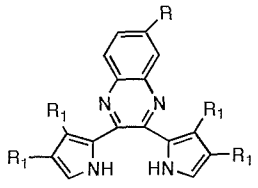

33 R=NO_2, R_1= H

34 R=H, R_1=F

1.3.2 Cyclic pyrrolic derivatives

Although the literature does not provide many examples of acyclic pyrrolic derivatives as anion receptors, pyrrole based macrocycles have been more widely used as a class of compounds for anion coordination.

Taking a simple example, Sessler has recently reported the synthesis of a bridged dipyrrole *ansa*-ferrocene **35**.[44] The complex's stoichiometry was found to be strongly dependent upon the nature of the anion. Whilst a 2:1 (anion to host) stoichiometry was observed in the case of fluoride, a 1:1 complex was formed in the presence of other anions such as chloride, bromide, hydrogensulfate and dihydrogenphosphate. ^{1}H-NMR titration experiments revealed that this macrocycle is selective for fluoride, chloride and dihydrogenphosphate over the other putative anions. Different selectivity has been observed by electrochemical measurements. Co-ordination of the different anionic species to the host can be detected through the cathodic shift in the ferrocene-ferrocenium redox couple. Compound **35** gave a greater response in the presence of dihydrogenphosphate (136mV) followed by fluoride and chloride (80 and 24 mV, respectively).

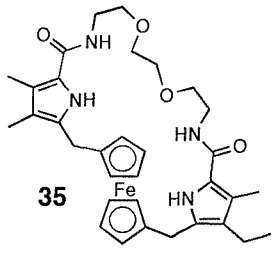

35

Sessler, Vögtle and co-workers reported the first example of a dipyrrole based [2]catenane **36**, synthesised from the appropriate bipyrrole acyl chloride and p-xylenediamine building blocks.[45] The anion binding properties of this compound have been investigated. ^{1}H, $^{13}C\{^{1}H\}$ and $^{19}F\{^{1}H\}$-NMR studies carried out in 1,1,2,2-tetrachloroethane-d_2 revealed that the receptor, upon addition of fluoride anions, changes its conformation in solution to accommodate the anionic guest. Surprisingly in this solvent the receptor complexed chloride and dihydrogenphosphate more strongly than fluoride, suggesting that, for these anions, the co-ordination may take place *between* the two rings of the catenane.

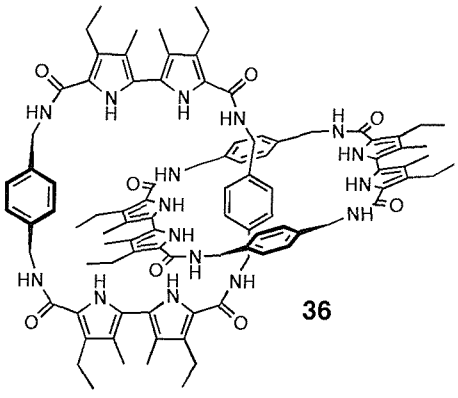

36

1.3.3 Calix[n]pyrroles

The acid catalysed condensation of pyrrole with a ketone leads to the formation of a tetrapyrrolic macrocycle, known as calix[4]pyrrole because of the structural similarity with calixarenes. The synthesis of these compounds has been well known from more than a century[46] and their cation complexation chemistry has been widely investigated.[47] However only in the last decade have these compounds been considered as possible anion receptors.

meso-Octamethylcalix[4]pyrrole **37** and other structurally similar calixpyrroles are able to coordinate a variety of anions including fluoride, chloride and dihydrogenphospate by the formation of four pyrrole-anion hydrogen bonds (Figure 1.11). Coordination of small neutral molecules such as DMSO and methanol has also been observed in the solid state and in solution.[38]

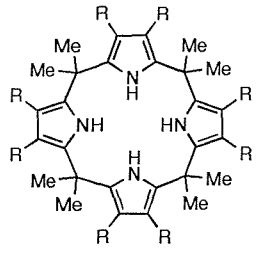

37 R = H

38 R = F

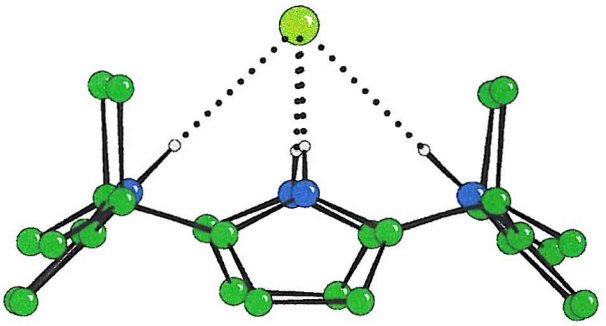

Figure 1.11: Crystal structure of *meso*-octamethylcalix[4]pyrrole **37**/chloride. The calixpyrrole assumes a *cone* conformation with the formation of four NH-fluoride hydrogen bounds.

As shown previously, the use of 3,4-difluoropyrrole leads to the formation of receptors in which the affinity for anions is increased. Compound **38**, for example proved to be a better receptor than **37** by showing an increased selectivity for chloride over dihydrogenphosphate. [43]

Reaction of pyrrole with *p*-hydroxy-acetophenone leads to the formation of compound **39** as a mixture of four isomers.[48,49] From this mixture the αααα isomer (the isomer in which the *meso* methyl groups point in the same direction) can be isolated by either column chromatography (due to the differing dipoles of the isomers) or crystallization from acetic acid. This compound showed increased selectivity for fluoride over other putative anions, and provides a suitable scaffold to which complementary functional groups can be appended.

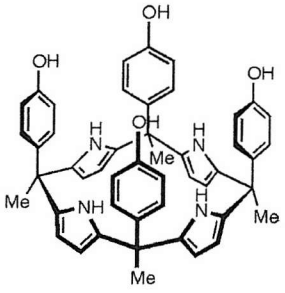

39 (αααα isomer)

Calix[4]pyrroles have been used as optical sensors for the detection of anions in solution. This has been achieved by linking either a fluorophore moiety (dansyl, Lisamine-rhodamine B, fluorescein), or a chromophore group (nitro benzene, dinitro benzene, anthraquinone, red methyl).[50] By way of example, calix[4]pyrrole **40** contains a fluorescent group linked to the macrocycle and displays a quenching of fluorescence upon addition of anionic species, with this effect being more pronounced for fluoride. Moreover the presence of the sulfonamide binding site increases the selectivity of the calix[4]pyrrole for dihydrogenphosphate and pyrophosphate over chloride in dichloromethane. Compound **41** acts as an optical anion sensor, showing a colour

transition from yellow to red distinguishable by the naked eye upon addition of fluoride anions in dichloromethane.

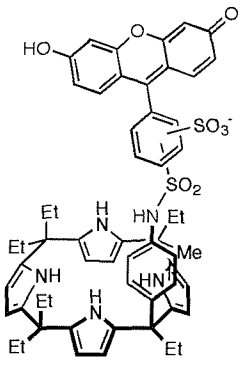

40

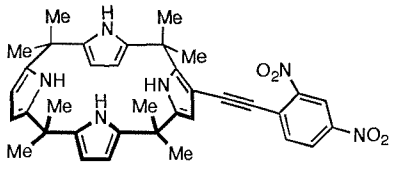

41

Calix[4]pyrrole modified silica gel proved to be suitable as a solid-phase HPLC support for the separation of anions. The calix[4]pyrrole based silica gel, called **Gel M** due to the silica linkage at the *meso* position, has been investigated as a new column material for the separation of anionic species.[51] This support was employed in the separation of 5'-adenosine monophosphate (AMP), 5'-adenosine diphosphate (ADP), 5'-adenosine triphosphate (ATP). The order of elution proved to be different from that obtained on neutral solid supports also used for anion separation. Moreover **Gel M** proved to an efficient support for the separation of different length oligonucleotides. As expected nucleotides containing the greatest number of phosphate groups were retained for longer. However separation of three oligonuclueotides of equal charge and length was achieved, confirming that the calix[4]pyrrole can also interact with the various nucleobases of which these oligonucleotides are formed.

Gel M

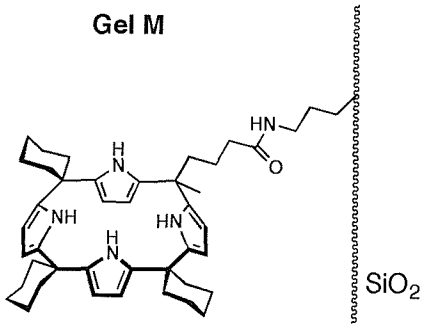

A higher order calixpyrrole has been synthesised in order to increase the number of coordinating groups and the macrocycle core size. Compounds **42** and **43** have been obtained as by-products in the synthesis of compound **38**.[52] The anion coordination properties of **42** have been investigated. Selectivity for chloride was observed, revealing an association constant of 41000M^{-1} in acetonitrile containing 0.5% D_2O (stability constant four times greater than the corresponding octafluoro-calix[4]pyrrole **38**).

The synthesis of calix[6]pyrroles has been recently reported in literature and the anion coordination properties of these compounds studied.[53,54] *meso*-dodecamethylcalix[6]pyrrole **44** was produced by Kohnke and co-workers by modifying the previously known furan-based analogue.[53] This compound proved to be selective for chloride and transport experiments from aqueous to dichloromethane solution confirmed this property (association constant ten times greater than the corresponding calix[4]pyrrole **37**). Selectivity for bigger anions has been also observed for compound **45** that showed a strong preference for iodide over the other halides.[54]

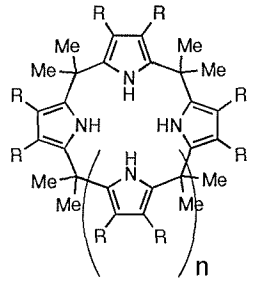

42 R = F, n = 2
43 R = F, n = 5
44 R = H, n = 3

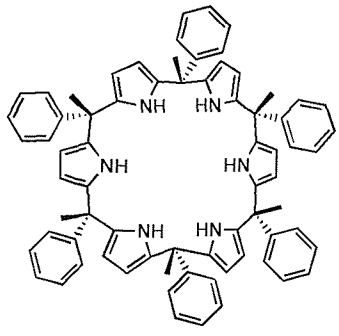

45

A cryptand-like calixpyrrole has been recently produced by Sessler and co-workers.[55] Compound **46** features three identical cavities and therefore is able to coordinate anions with 1:1, 1:2 and 1:3 receptor to anion stoichiometry. ^{1}H-NMR experiments carried out in dichloromethane-d_2 and THF-d_8 revealed that the stoichiometry is strongly dependent on the nature of the anion. Whilst fluoride is coordinated to six of the nine pyrrolic NH in a 1:1 complex, chloride is coordinated with a 2:1 receptor to anion stoichiometry, providing a stability constant of 3.08×10^6 M^{-1} in dichloromethane-d_2, for the formation of **46**$\cdot$Cl$^-$**46**.

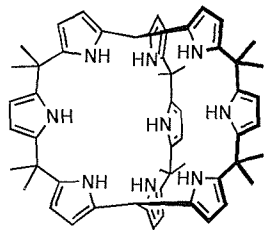

46

However two molecules of nitrate can coordinate one molecule of receptor with the stability constants K_1 and K_2 being 1740 and 420M^{-1} respectively in dichloromethane-d_2.

1.2.4 Sapphyrin and other higher order pyrrole based macrocycles

The first example of a synthetic pyrrole based anion receptor was sapphyrin, an expanded porphyrin first synthesised by Woodward and co-workers[56] which when diprotonated was found by Sessler and co-workers to be an excellent fluoride receptor (Figure 1.12).[57]

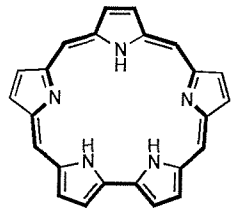

Figure 1.12: Structure of Sapphyrin.

The synthesis of sapphyrin derivatives (e.g. **47** and **48)** have been achieved by a variety of different methods, based on the condensation of linear polypyrroles under the appropriate conditions to afford the pentapyrrolic macrocycle.[57] It is planar, rigid, and features an aromatic 22 π-electron system. A complete structural and solution study for this class of compounds has been provided by Sessler and co-workers in two elegant papers.[58,59] The diprotonated form of sapphyrin **47** can interact with a variety of anionic species including fluoride, chloride, phosphate and carboxylate. However the binding motif that this compound reveals with fluoride is unique. In fact this anionic species is encapsulated in the macrocycle core, interacting with a pentagonal array of pyrrolic moieties within a ca. 5.5 Å diameter core (Figure 1.13a). Chloride is encapsulated by this receptor but the stoichiometry in the solid state is 2:1 anion to receptor and the crystal structure (Figure 1.13b) showed the anion placed ca. 1.8 Å above and below the macrocycle. Therefore the diprotonated form of sapphyrin represents a unique and selective anion receptor for fluoride, exhibiting a selectivity at least $\geq 10^3$ relative to either chloride or bromide in both methanol and dichloromethane solution.

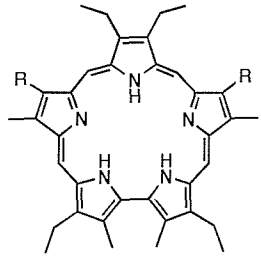

47 R = CH_2CH_3

48 R = $(CH_2)_2CH_2OH$

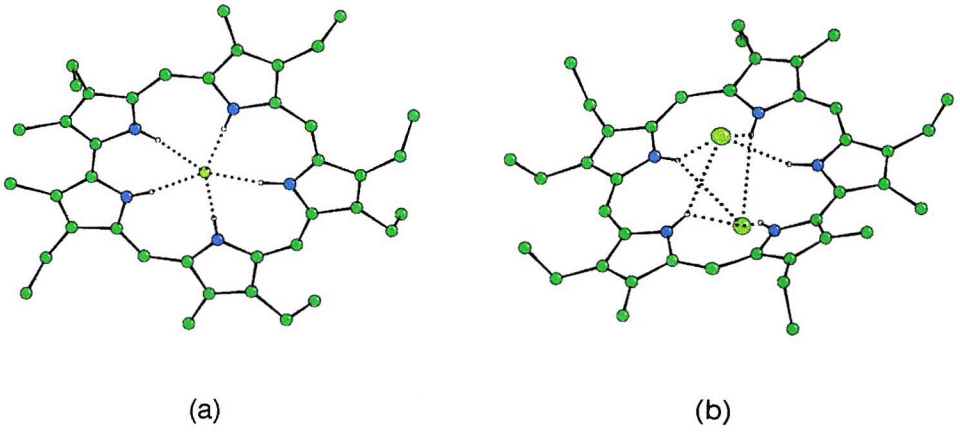

(a) (b)

Figure 1.13: Crystal structure of the diprotonated form of sappyrin in the presence of fluoride anion ((a) 1:1 complex) and chloride ((b) 1:2 complex)

Sessler, who can be considered the father of the pyrrole based anion receptors, encouraged by this selectivity decided to investigate the use of this compound as a carrier in the transport of fluoride.[60] A model three-phase H_2O-dichloromethane-H_2O bulk liquid membrane system was used for the investigation. Two aqueous solutions, containing different concentrations of fluoride were separated by a dichloromethane solution. In the absence of sapphyrin in the organic layer, slow uptake of fluoride was observed due to diffusion phenomena. In the presence of receptor **47** a considerable increase in the transport flux ϕ was observed, which was four times higher than in the absence of the diprotonated macrocycle, within a range of pH values.

Sapphyrin derivatives are also able to coordinate phosphate and its derivatives. Inspired by this possibility, in 1995 Sessler and co-workers produced the sapphyrin trimers **49, 50** and the tetramer **51**, and investigated their anion binding properties toward phosphorilated anionic species.[61]

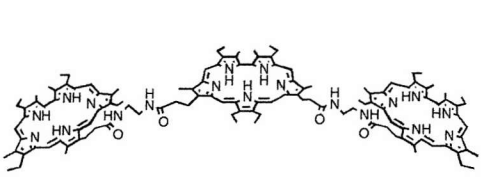

49

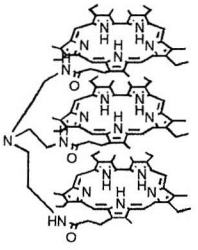

50

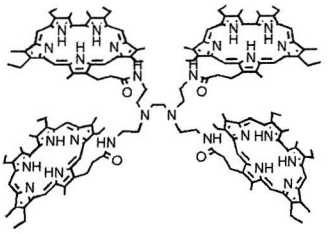

51

These receptors displayed two distinct Soret bands in the UV spectrum, clear sign of a considerable aggregation grade in solution. Addition of phosphate led to a dramatic change in the spectrum, with an increasing of the intensity of the Soret-like band with the higher wavelength maximum at the expense of the one at lower wavelength. This behaviour is due to the de-aggregation phenomena as consequence of the encapsulation of the anion. Once the coordination of phosphate was proved by these experiments, Sessler investigated the use of these receptors as carrier in the transport of phosphorylated nucleotides across bulk liquid membranes. Whilst compounds **49** and **50** proved to be efficient receptors for nucleotide diphosphate, they did not transport triphosphate. However, compound **51** was found to be an effective carrier for all the considered phosphorylated species.

In 1996 Sessler and co-workers reported the synthesis of a new lasalocid modified sapphyrin **52** and investigated the anion binding properties toward a variety of aromatic amino acids in their zwitterionic form.[62] H_2O-dichloromethane-H_2O U-tube transport experiments, showed that receptor **52** not only is highly selective for phenylalanine and tryptophan ($k_{t\text{-}L\text{-}Phe}$ = 20x10^{-5} mol cm^{-2} h^{-1}), but shows also a considerable discrimination grade among the different chiral homologues.

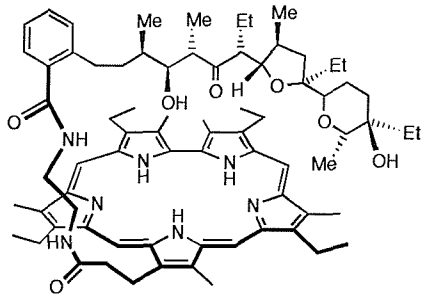

52

Sessler and co-workers recently reported the synthesis of more expanded pyrrole-based macrocycles.[63] [28]heptaphyrin (1.0.0.1.0.0.0) **53** and of [32]octaphyrin(1.0.0.0.1.0.0.0) **54** have been synthesised by direct oxidative ring closure of linear polypyrrolic species and crystallized in their diprotonated forms in the presence of sulfate and chloride anions respectively. In the solid-state compound **53** coordinates sulfate in the macrocycle core which is in a planar conformation (Figure 1.14a).

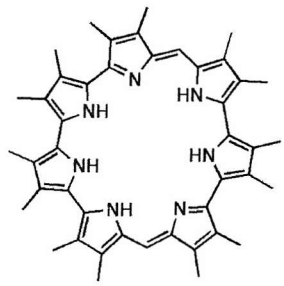

53

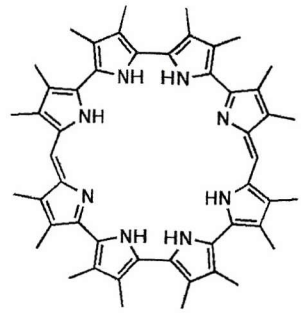

54

The seven hydrogen bond motif is reminiscent of the sulfate binding protein.[64] Compound **54** is larger and more flexible and therefore able to accommodate two chloride anions while deviating substantially from planarity (Figure 1.14b).

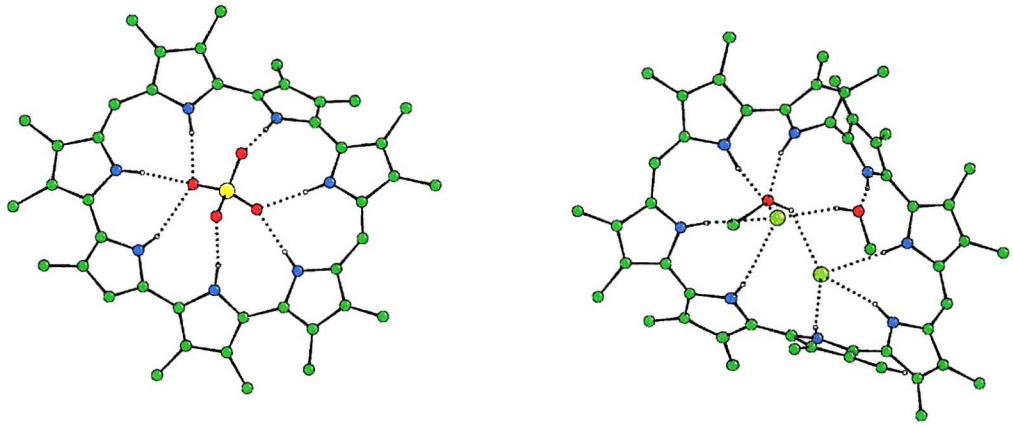

(a) (b)

Figure 1.14: Crystal structure of complexes (a) **53**/sulfate, and (b) **54**/2·chloride·2methanol.

1.4 Aim of the project

As shown throughout this chapter, the literature provides a wide variety of anion receptors that utilise coordinating groups such as amides, urea, amidinium, pyrrole, and other hydrogen bond donating groups. Nevertheless selectivity for a single anionic substrate represents the main target of many researchers and has rarely been achieved. For this reason, anion coordination chemistry is a field in continuous growth, and many

researchers employ considerable effort in designing and synthesising new and more selective anion receptors.

In this thesis, new anion receptors are reported and their complexation properties toward anionic species investigated. We focussed on three topics:

- Functionalization of the pyrrole with amide groups in the 2 and 5 positions in order to investigate whether simple pyrrolic clefts can behave as efficient anion receptors designed to bind oxo-anions via multiple hydrogen bonds.
- Deep cavity calix[4]pyrrole **39** was used as starting material and functionalised at the phenoxy position to achieve 'super-extended' cavity calix[4]pyrroles. The binding properties of these compounds toward anionic and cationic substrates was investigated.
- Finally the anion complexation and assembly properties of amidinium derivatized calix[4]arenes toward carboxylates species was investigated.

2. Pyrrolic amide receptors: simple anion coordinating agents

2.1 Introduction. Simple amide cleft as effective anion receptors

Pyrrole is a hydrogen bond donating moiety and, as we have seen, has been incorporated into a variety of anion receptors.[42,44] It does not contain a hydrogen bond acceptor and therefore is not inclined to promote self-assembly processes such as those observed for example in the case of amides. (Figure 2.1).

(a) (b)

Figure 2.1: In the absence of a hydrogen bond acceptor the pyrrole cannot self-assemble(a). Self-assembling phenomena are observed for amides (b).

In nature, pyrrole plays a role in the chemistry of anionic species. A class of tripyrrolic linear oligomers (the prodigiosins e.g. **55**), red pigments produced by micro-organisms like *Streptomyces* and *Serratia*, and some of its derivatives raise intralysosomal pH by inhibiting the lysosomal acidification driven by the vacuolar-type(V-)ATPase without inhibiting ATP hydrolysis (i.e. they transport HCl).[65]

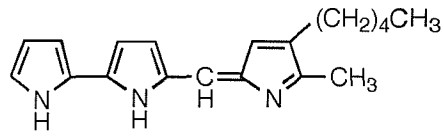

55

In the previous chapter it has been shown how functionalization of pyrrole can lead to the formation of efficient and sometimes selective anion receptors. Indeed the recent work of Schmuck,[39-41] Sessler[44] and Vögtle[45] supports the postulate that a wide variety of anion receptors can be produced upon functionalization of pyrrole with amide groups. Inspired by this idea as well as by the excellent results obtained by Crabtree on simple amide cleft anion coordination,[19] the synthesis of pyrrolic amide receptors have been one of the main aims of this project (Figure 2.2). A variety of compounds has been produced by introducing amide groups at the 2- and 5- position of pyrrole, and the anion binding properties of these receptors investigated by the use of ^{1}H NMR titration techniques.

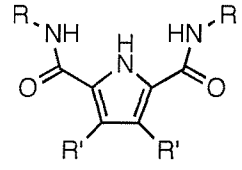

Figure 2.2: General structure of the pyrrolic amide receptors that have been produced by introducing amide groups at the 2- and 5- position of pyrrole.

2.2 3,4-Diphenyl pyrrole amide clefts

2.2.1 Synthesis and characterization

Two new pyrrole amide clefts **58** and **59**[66] have been synthesized (Scheme 2.1). 2,5-Dicarboxy-3,4-diphenyl pyrrole **56** was prepared following literature procedures[67] and was refluxed with an excess of thionyl chloride overnight in order to obtain the bis-acid chloride **57**. Upon reaction of **57** with 2.2 equivalents of either butylamine or aniline in the presence of triethylamine and DMAP, compounds **58** and **59** have been obtained in 18 and 47% yield respectively.

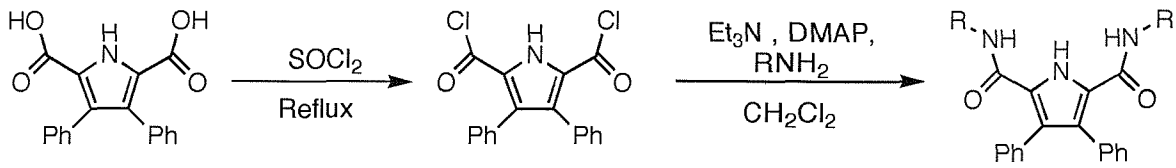

56 **57**

Scheme 2.1

The pyrrole monoamide clefts **61** and **62**[68] have been prepared in according to Scheme 2.2. The 3,4-diphenyl-5-methyl-2-carboxylic acid ethyl ester **60** was prepared using a modification of a method previously reported in literature and based on a Paal-Knorr reaction.[69,70] The characterization of this compound proved to be in good agreement with the published data.[71] Compound **61** was prepared by refluxing a methanol solution of **60** with an excess of butylamine (ca. 50 equiv.) in the presence of a catalytic amount of sodium cyanide,[72] and was isolated in 29% yield. Compound **60** was also converted to the 3,4-diphenyl-5-methyl-2-carboxylic acid phenyl amide **62** by reaction with an aluminum phenylamide derivative, prepared in situ by reaction of trimethyl aluminum and anilne,[73] in 17% yield.

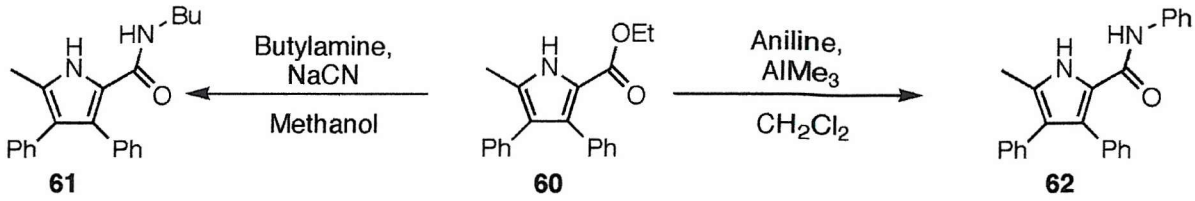

Scheme 2.2

X-ray quality single crystals of **58** have been obtained by slow evaporation of a dichloromethane/ethanol solution of this receptor. The crystal structure reveals the formation of dimers and polymers bridged by intramolecular hydrogen bonds (Figure 2.3). The dihedral angles formed between the phenyl rings and the pyrrolic plane are 129.4(3)° and 99.0(3)°. The amide moieties deviate from the pyrrole plane by 8.27(5)° and 45.8(5)° with the amide NH groups pointing backward in respect of the pyrrole NH (see Appendix for structure information).

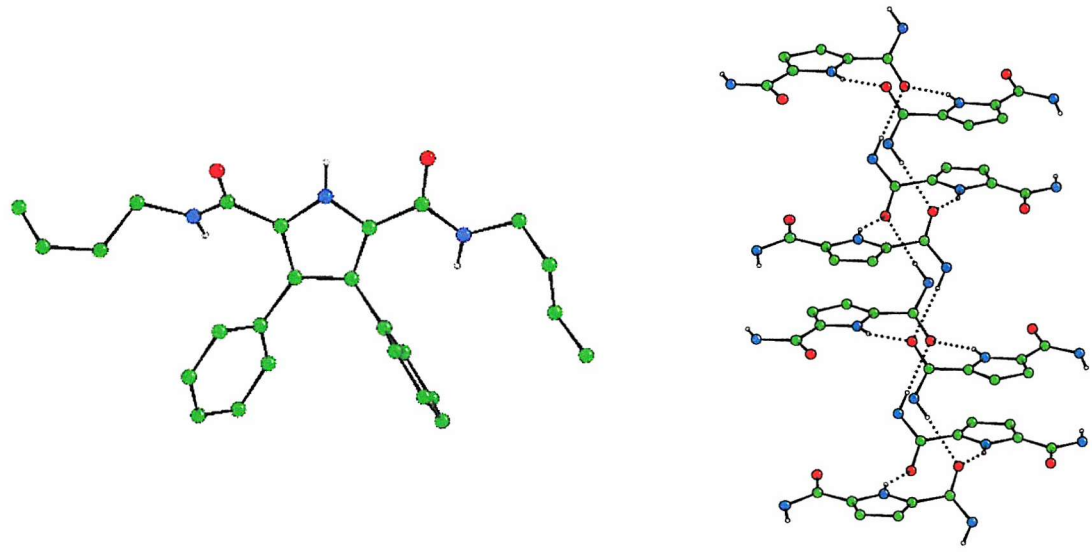

(a) (b)

Figure 2.3: (a) Crystal structure of receptor **58**; (b) in the solid state a dimer is formed via the formation of two hydrogen bonds between the pyrrolic NH and the carbonyl group (average $N_{pyrrole}\cdots OC$ distance 2.961(4)Å); a second hydrogen bond is formed between an amide group and the carbonyl group of two discrete dimer (average $N_{amide}\cdots OC$ distance 3.021(4)Å), leading to the formation of a polymer that extends long the *c* axis. Phenyl groups omitted for clarity.

In the dimer, two molecules are linked together via the formation of two hydrogen bonds between the pyrrolic NH and the carbonyl group (average $N_{pyrrole}\cdots OC$ distance 2.961(4)Å). The dimers are bridged into chains that extend along the *c* axis by the formation of hydrogen bonds between the carbonyl group and the amide NH of two discrete dimeric units (average $N_{amide}\cdots OC$ distance 3.021(4)Å).

Single crystals of **59** have been obtained by slow re-crystallization from a hot acetonitrile solution of this receptor. The crystal structure again revealed the formation of dimers. Compound **59** forms centrosymmetric dimers via both NH···O hydrogen bonds, and C—H···O hydrogen bonds (Figure 2.4) as has been recently observed by Schmuck and Lex in the crystal structure of the methyl 5-amidopyrrole-2-carboxylate.[74] The phenyl rings in the 3- and 4- position deviate from the pyrrole plane by 72.0(5)and 68.9(5)°. The dihedral angles formed between the amide CONH moieties and the pyrrole ring are 9.72 and 2.94°, and again the amide NH groups point backwards with respect to the pyrrole NH. The distance between the pyrrolic nitrogen and the carbonyl group is 3.238(4)Å whereas the length of the $C_{Arom.}\cdots O$ hydrogen bond 3.271(4)Å (see Appendix for structure information).

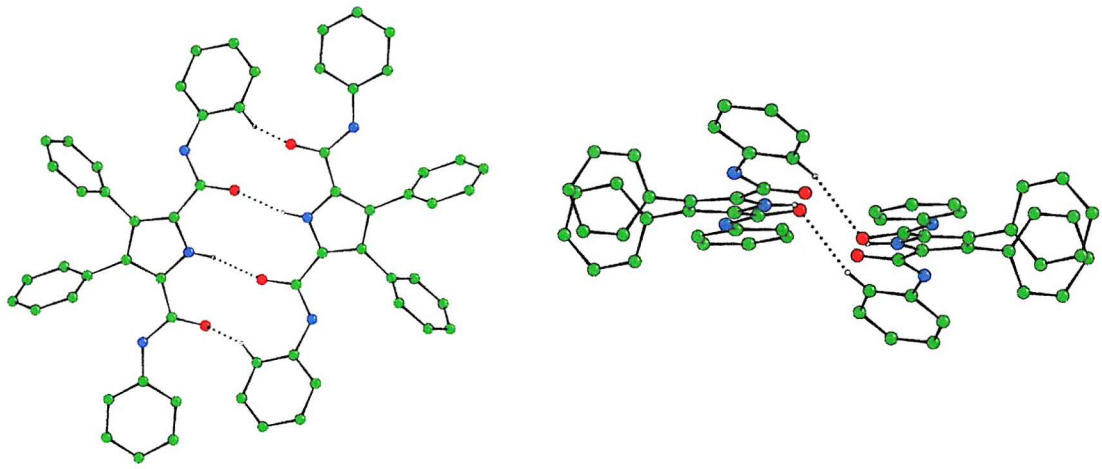

Figure 2.4: (a) Crystal structure of receptor **59**; the formation of the dimers is due to intramolecular hydrogen bonds between the pyrrolic NH and the carbonyl groups (distance $N_{pyrrole}\cdots OC = 3.238(4)$Å) and the one phenylic CH and the carbonyl (distance $C_{Arom}\cdots OC = 3.271(4)$Å). (b) side view.

X-ray quality single crystals of **59** have been obtained from a DMSO solution of the receptor. Interestingly in this case the receptor adopts a 'semi-cleft' conformation binding a molecule of DMSO via the formation of two hydrogen bonds between the solvent oxygen and both the pyrrolic NH and one of the amide NH groups (distances $N_{pyrrole}\cdots O = 2.757(4)$Å, $N_{amide}\cdots O = 2.831(4)$Å) (Figure 2.5). The dihedral angles formed between the phenyl groups attached at the 3- and 4- positions and the pyrrole plane are 109.10(5) and 111.11(5)°. The amide NH group that point toward the DMSO molecule shows a deviation from the pyrrole plane of 13.55(5)°. The second amide CONH moiety also deviates from planarity revealing a dihedral angle with the pyrrole ring of 5.42(5)° (see Appendix for structure information).

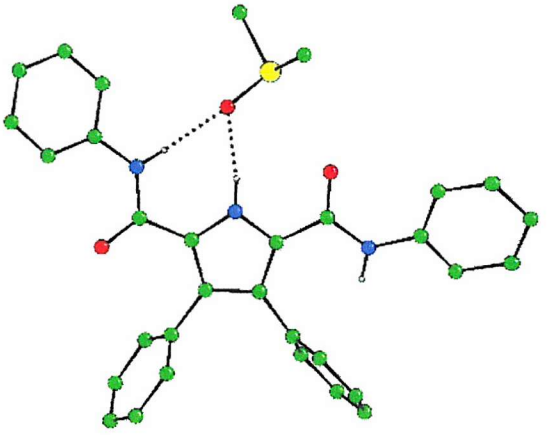

Figure 2.5: Crystal structure of the complex **59**/DMSO. The receptor adopts a 'semicleft like' conformation (Distance $N_{pyrrole}\cdots O = 2.757(4)$Å, $N_{amide}\cdots O = 2.831(4)$Å).

X-ray quality single crystals of compound **61** have been obtained by slow evaporation of a dichloromethane/methanol solvent mixture. The crystal structure (Figure 2.6) reveals the presence of a dimer in the solid state. Two molecules of **61** are linked together via the formation of two hydrogen bonds between the pyrrolic NH and the carbonyl group (CO··· N distance 2.766(6)Å), as previously observed for the bis-amide analogues. The dihedral angles formed between the phenyl rings and the pyrrole plane are 46.5(4) and 60.0(4)°. The

amide CONH moiety shows a deviation from planarity revealing a dihedral angle with the pyrrole plane of 6.63(5)° (see Appendix for structure information).

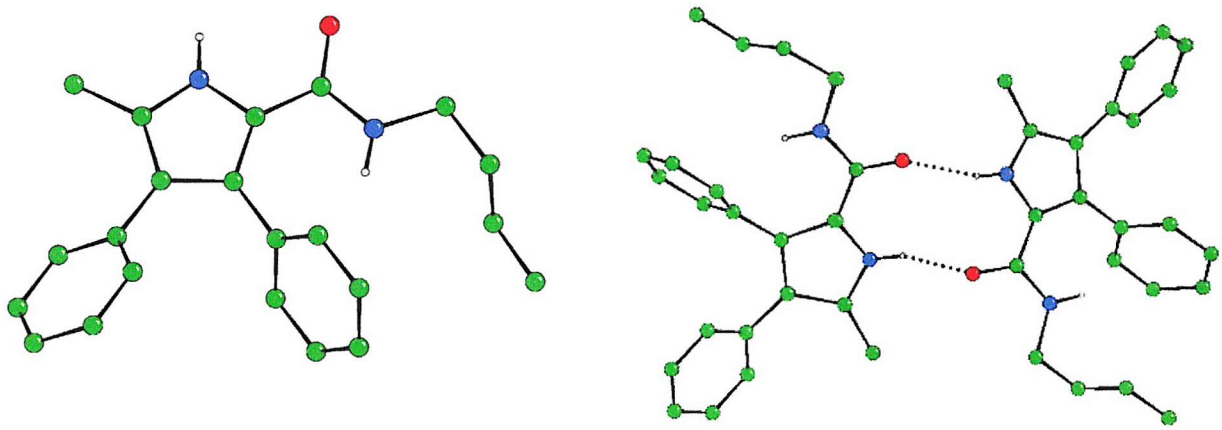

(a) (b)

Figure 2.6: (a) Crystal structure of receptor **61**. (b) The dimerization via the formation of two hydrogen bonds between the pyrrolic NH and the carbonyl group (CO···HN distance 2.766(6)Å).

Finally X-ray quality single crystals of compound **62** have been obtained by slow evaporation of a dichloromethane/acetonitrile solution. Again the crystal structure reveals the presence of dimers in the solid state (CO···N distance of 2.875(5)Å) (Figure 2.7). The phenyl rings attached at the 3- and 4- positions reveal a deviation from the pyrrole plane of 146.7(5) and 61.2(5)°. The amide moiety is almost co-planar with the pyrrole ring orientated with a dihedral angle of 6.5(5)° with the amide NH group pointing backwards with respect to the pyrrole NH group (see Appendix for structure information).

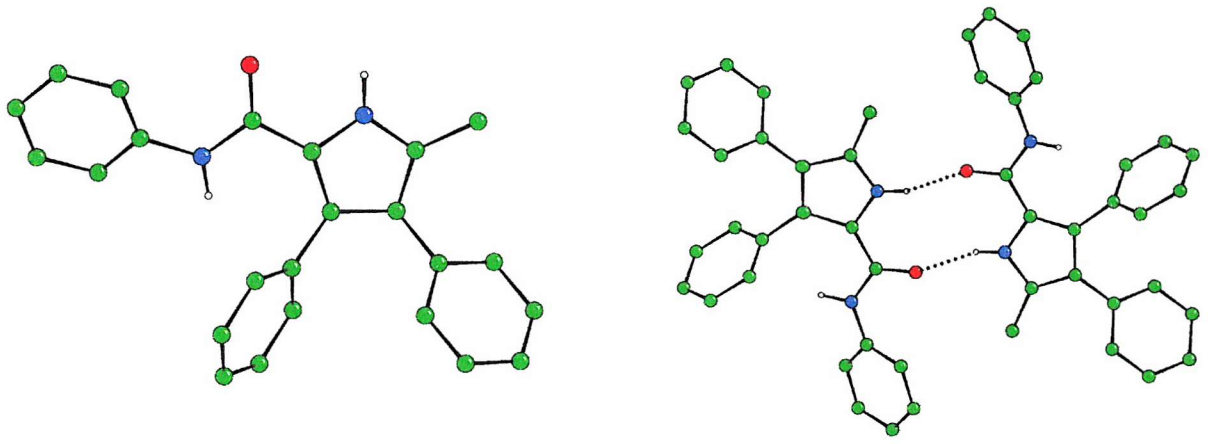

(a) (b)

Figure 2.7: (a) Crystal structure of receptor **62**. (b) The dimerization is due to the formation of a double hydrogen bond between the pyrrolic NH and the carbonyl group (CO···N distance 2.875(5)Å).

Although the pyrrole diamide clefts **58-59** and the pyrrole monoamide clefts **61-62** formed dimers and, in certain cases, polymers in the solid state, dilution studies revealed that this phenomenon does not occur in DMSO-d_6 solution.

2.2.2 Binding study results. Selectivity for oxanions

Proton NMR titration techniques have been used in order to investigate the anion binding properties of receptors **58-59** and **61-62**. Anions were added as their tetrabutylammonium salts, since this cation does not compete significantly with the anion binding site and therefore is considered a relatively 'innocent' counterion. Elaboration of the titration curves has been achieved by using appropriate software (e.g. EQNMR[75]). Job plot analyses have been carried out in order to investigate the stoichiometry of the receptor/anion complexes.

The anion complexation properties of receptors **58** and **61** have been investigated in acetonitrile-d_3 solution; however solubility problems forced the use of more polar DMSO-d_6 (0.5% water) for compound **59**. Unfortunately precipitation and crystallization processes

during the titration experiments on compound **62** did not allow any anion binding investigation for this receptor, even in DMSO solution.

Analysis of the NMR titration curves and Job plot profiles showed the formation of 1:1 complexes exclusively. Figure 2.8 shows the Job plot analysis for the complex **59**/$H_2PO_4^-$.

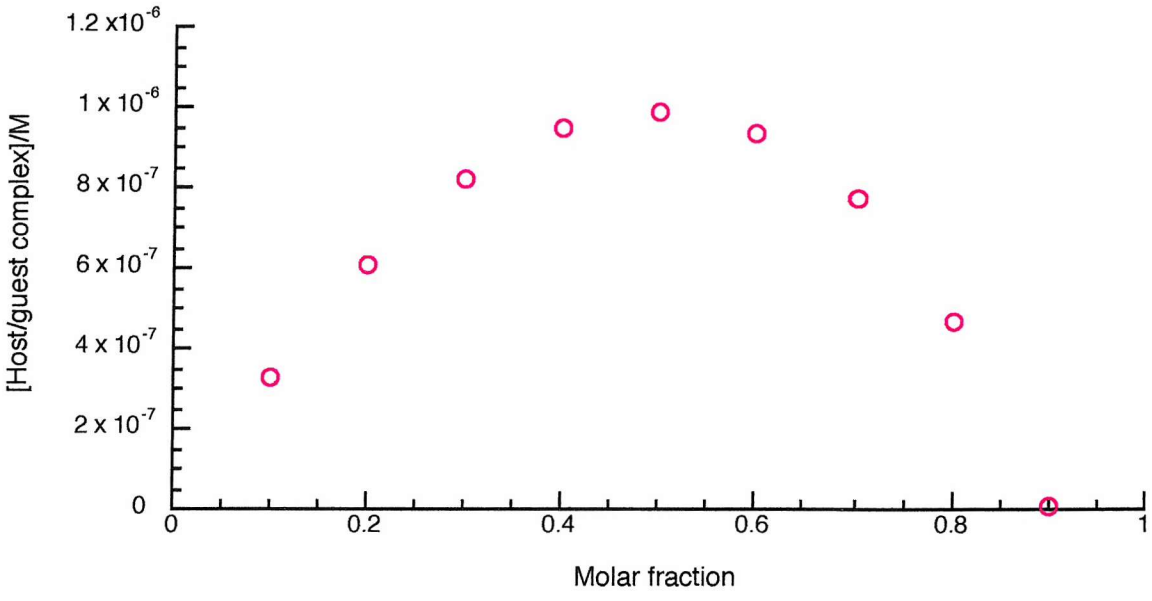

Figure 2.8: Job plot of the system compound **58**/$TBAH_2PO_4$. The peak at 0.5 indicates the 1:1 stoichiometry.

NMR titration experiments revealed the interesting anion complexation properties of both the pyrrolic diamides and monoamides clefts. A strong selectivity for oxanions over other anions such as fluoride, chloride and bromide was observed (Table 2.1). Receptor **58** coordinates benzoate with an association constant 30 times higher than that observed for the complexation of fluoride anions in acetonitrile solution. On the other hand, receptor **59** was found to bind dihydrogenphosphate selectively with a stability constant of 1450 M^{-1} in DMSO (0.5% water) solution (ca. 20 times higher than the association constant found for fluoride coordination).

Receptor **61** was found to bind benzoate selectively over the other anions in acetonitrile solution. Interestingly the presence of water in the solvent proved to have dramatic effects on the association constants of fluoride and chloride. Indeed, whilst fluoride is bound by receptor **58** more weakly than chloride in acetonitrile containing 0.03% water (Table 2.1), its

estimated association constant was found to be higher than chloride when the percentage of water was increased to 0.5% ($K_{1\text{-Fluoride}} = 37\ M^{-1}$, $K_{1\text{-Chloride}} = 12.5\ M^{-1}$).

Generally the association constants for the **61**/anion complexes were found to be much lower than those observed for the diamide analogue **58**. The results of the anion complexation studies are summarized in the Table 2.1.

	Receptor **58**[a]	Receptor **59**[b]	Receptor **61**[a]
Fluoride	85	74	134
Chloride	138	11	28
Bromide	< 10	< 10	<10
Dihydrogenphosphate	357	1450	89
Benzoate	2500	560	202

Table 2.1: Association constant of receptors **58**, **59** and **61** (M^{-1}) with various anionic guests at 25°C: the anions were added as their tetrabutylammonium salts. The errors were estimated to be < 15%. (a) NMR experiments carried out in acetonitrile (0.03% water). (b) NMR experiments carried out in DMSO (0.5% water).

2.2.2 The binding motif

Receptors **58** and **59** contain two amide NH and one pyrrolic NH group and therefore there are a number of possible binding motifs (Figure 2.9). A possible clarification of the binding mode may be hypothesized by comparison of the di- and monoamides clefts anion complexation strengths. In Figure 2.9 the most probable anion binding motifs for receptors **58** and **61** are summarized. The selectivity of compound **61** for benzoate suggests that the coordination of this anionic species is more likely to occur via the formation of two hydrogen bonds in according with the binding motif (ii). If coordination of the anionic guest was achieved through binding motif (i), fluoride would be expected to bind more strongly as it has a higher charge density than the carboxylate oxygen. However the association

constants for compound **61** and anions were all rather low and hence it is not possible to predict the binding mode.

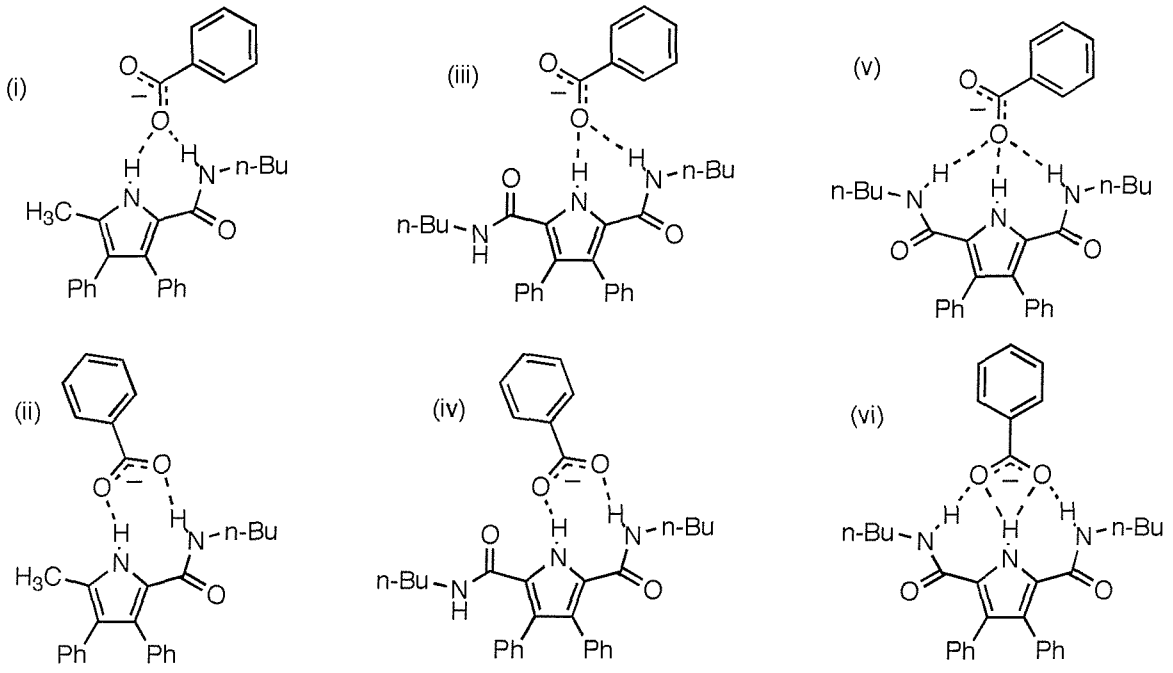

Figure 2.9: Representation of the possible binding motif for the benzoate complexation of benzoate by receptor **58** (iii-vi) and **61** (i-ii).

Perhaps more reliable predictions come from the comparison of the anion binding properties of the mono- and the diamide clefts. For example, compound **58** was found to bind benzoate 10 times more strongly than the monoamide cleft **61** in acetonitrile. This behavior leads to the hypothesis that all the NH groups of the receptor **58** must take part in the coordination of the anionic species, leaving either mode (v) or mode (vi) as the most likely candidates. A binding motif similar to (vi) has been observed in the solid state.[76] X-ray quality single crystals of the **58**/benzoate complex were obtained by slow evaporation of a dichloromethane solution of the receptor in the presence of an excess of tetrabutylammonium benzoate. The crystal structure reveals the receptor adopting a 'cleft' conformation and coordinating benzoate via the formation of three hydrogen bonds (Figure 2.10). One amide NH group is almost co-planar to the pyrrole ring at a dihedral angle of

5.63(5)°. The second amide group shows a deviation from the pyrrole plane of 34.95(6)°. The benzoate lies almost perpendicularly to the receptor with a deviation of 101.31(5)°. The pyrrole NH and the almost co-planar amide NH groups form two hydrogen bonds with one of the carboxylate oxygen (distances $N_{amide}\cdots O = 2.8638(4)$Å, $N_{pyrrole}\cdots O = 2.7710(4)$Å). The second amide NH group coordinates the remaining anion oxygen via the formation of a third hydrogen bond (distance $N\cdots O = 2.7915(6)$Å) (see Appendix for structure information).

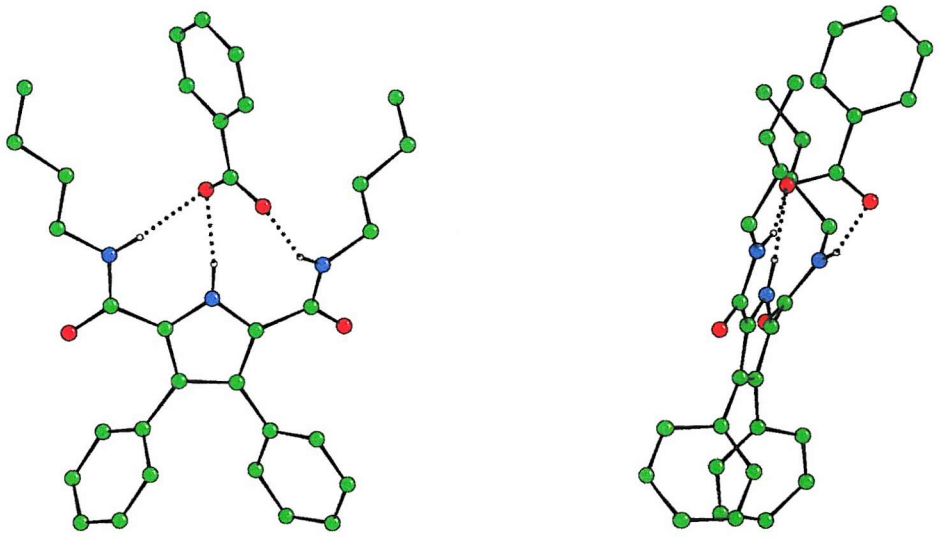

(a) (b)

Figure 2.10: (a) Crystal structure of the complex **58**/benzoate. The receptor adopts a 'cleft' conformation and coordinates the anion via the formation of three hydrogen bonds. One benzoate oxygen interacts with both the pyrrole and one of the amide NH groups via the formation of two hydrogen bonds (distances $N_{amide}\cdots O = 2.8638(4)$Å, $N_{pyrrole}\cdots O = 2.7710(4)$Å); the second carboxylate oxygen interact with the remaining amide group through the formation of the third hydrogen bond (distance $N\cdots O = 2.7915(6)$Å) . (b) Side view of the crystal structure.

2.3 Introducing electron withdrawing groups in the pyrrolic skeleton

Electron withdrawing groups have been introduced in the 3- and 4- positions of the pyrrole diamide clefts in order to increase the acidity of the NH groups present in these molecules and hence form stronger anion complexes. The literature provides a number of examples that demonstrate how introduction of electron withdrawing groups is not just an efficient method of increasing the affinity of a receptor for anions, but in certain cases can modulate the selectivity among different anions.[43]

2.3.1 Synthesis and characterization

Two pyrrole diamide clefts functionalized with chlorine atoms in the pyrrole 3- and 4-positions have been prepared.[77] 3,4-Dichloro-2,5-dicarboxylic acid ethyl ester **63** was obtained by literature methods.[70] A methanol solution of **63** was refluxed with 100 equivalents of n-butylamine in the presence of a catalytic amount of sodium cyanide[72] in order to obtain the 3,4-dichloro-2,5-dicarboxylic acid butyl amide **64** in 71% yield (Scheme 2.3).[77] The 3,4-dichloro-2,5-dicarboxylic acid phenyl amide **65** was prepared by reacting the ester **63** with two equivalents of an aluminum phenylamide (Scheme 2.3) prepared *in situ* by mixing trimethyl aluminum and aniline.[73] After crystallization from acetonitrile the desired compound was obtained in 11% yield.

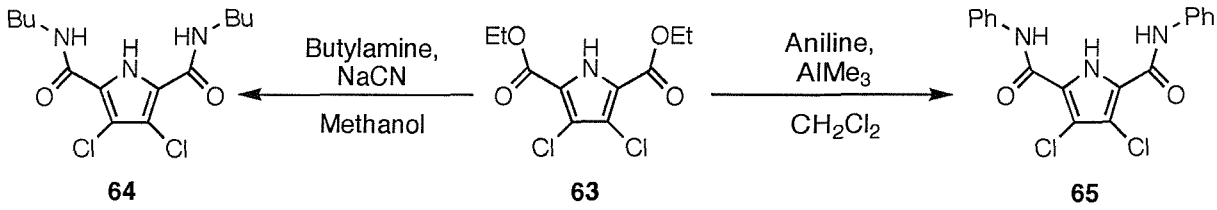

64 **63** **65**

Scheme 2.3: Synthesis of the dichloro pyrrole diamide clefts **64** and **65**.

Reaction of 4-nitro-, 3,5-dinitro and pentafluoro aniline with the 3,4-diphenyl-2,5-dicarboxylic acid chloride **57** led to the synthesis of three new pyrrole diamide clefts **66-68** (Scheme 2.4).[78]

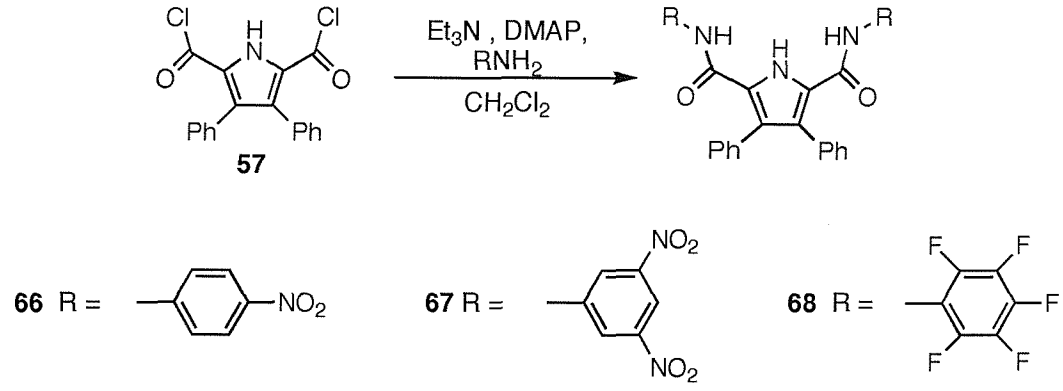

Scheme 2.4: Synthesis of the electron withdrawing groups functionalized pyrrole diamide clefts **66-68**.

Compound **66** was prepared by reacting the acid chloride **57** in dichloromethane with 2.2 equivalents of 4-nitroaniline in the presence of triethylamine and a catalytic amount of DMAP. Crystallization in the minimum amount of acetonitrile led to the desired compound in 43% yield. Similarly compound **67** was prepared by stirring compound **57** with 3,5-dinitroaniline and again purification of the desired compound was achieved by crystallization from acetonitrile (11% yield).

The 3,4-diphenyl-2,5-dicarboxylic acid pentafluoro-phenylamide **68** was prepared by reacting the acid chloride **57** in dichloromethane with 2.2 equivalents of pentafluoroaniline in the presence of triethylamine and a catalytic amount of DMAP. Crystallization from a minimum amount of acetonitrile led to the formation of a white crystalline solid corresponding to the desired compound in 28% yield.

X-ray quality single crystals of compound **66** were obtained by re-crystallization from a concentrated DMSO solution. The crystal structure revealed the presence of a molecule of solvent interacting with the receptor through the formation of two hydrogen bonds (Figure 2.11). Compound **66** adopts a 'semicleft' conformation binding the DMSO molecule via the formation of two hydrogen bonds with the pyrrolic NH and one of the two amide NH groups. The distance between the pyrrolic nitrogen and the DMSO oxygen was found to be 2.768(2)Å, whereas the amide nitrogen was found to be as close as 2.828(2)Å to the solvent

oxygen. The dihedral angles formed between the phenyl rings attached at the 3- and 4-position are 63.7(6) and 118.5(6)°. The amide NH groups that points toward the coordinated solvent deviates from the pyrrole plane by 8.6(5)°, whereas the second amide moiety shows a deviation from the pyrrole ring of 6.5(5)° (see Appendix for structure information).

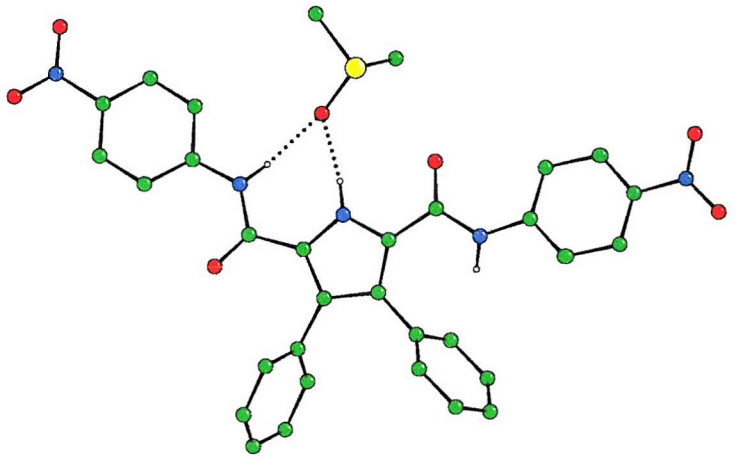

Figure 2.11: Crystal structure of receptor **66**. One molecule of solvent is coordinated to the receptor via the formation of two hydrogen bonds between the DMSO oxygen and both the pyrrolic and one amide NH ($N_{pyrrole}$···O = 2.768(2)Å, N_{amide}···O = 2.828(2)Å).

Compound **66** has also been crystallized by slow evaporation of a dilute acetonitrile solution. White crystals have been isolated and crystallographic analysis has been carried out. The crystal structure revealed the presence in the solid state of discrete molecules of the receptor and, in contrast to the structures obtained for the previous compounds, dimerisation does not occur and no solvent is coordinated to the receptor (Figure 2.12). However an intramolecular π-stacking interaction between two discrete monomers is observed. The molecule is highly planar with the amide moieties deviating from the pyrrole plane of 1.3(3) and 2.5(3)°. Moreover the dihedral angles formed between the phenyl rings attached at the amide nitrogens and the amide planes are just 1.74(5) and 6.37(5)° (see Appendix for

structure information). The π-stacking interaction between two molecules of receptor is due to the overlapping of the electron clouds of the phenyl rings attached at the amide nitrogens. The average distance between these aromatic residues proved to be 3.648(8)Å. The phenyl rings attached at the 3- and 4- position do not take part in the π-stacking interaction since they deviate from planarity (see Appendix for structure information).

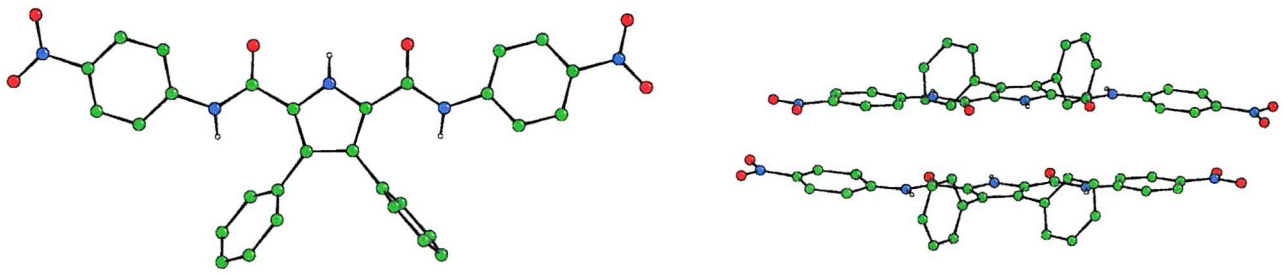

(a) (b)

Figure 2.12: (a) Crystal structure of the receptor **66**. (b) Side view of the π-stacking interaction.

X-ray quality crystals of receptor **67** were obtained by slow evaporation of a dichloromethane solution of the receptor. Crystallographic analysis revealed that in the solid state the receptor forms a sheet(Figure 2.13) via NH···ON hydrogen bonds (distance N···O = 3.8967(4)Å) (see Appendix for structure information).

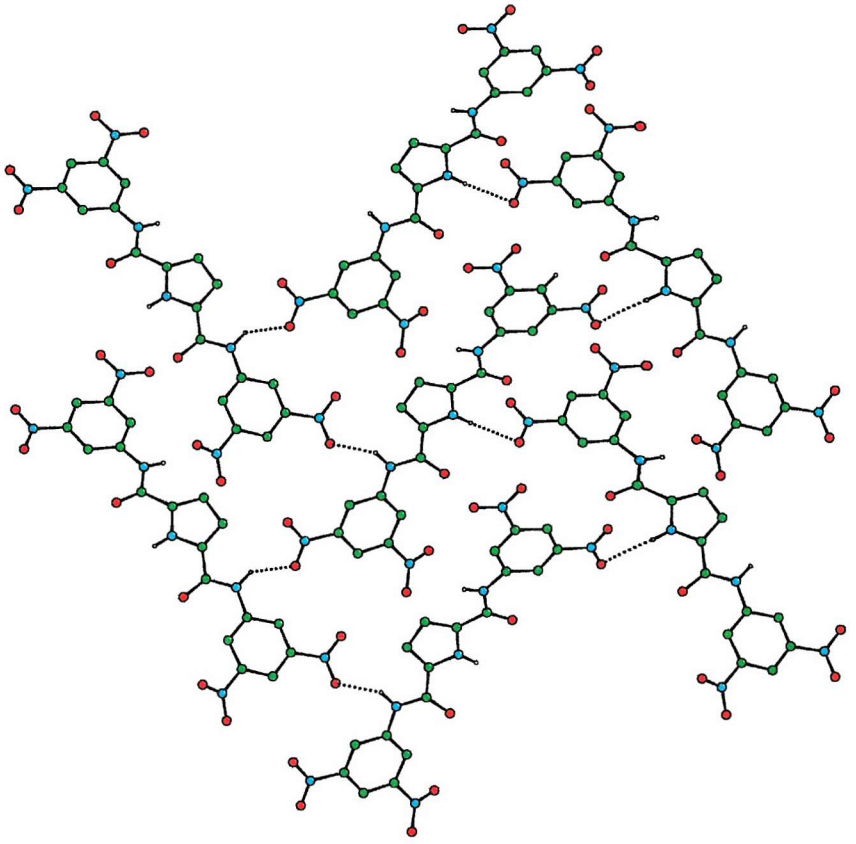

Figure 2.13: Crystal structure of receptor **67** (phenyl rings at the 3- and 4- positions of the pyrrole, omitted for clarity). NH···ON hydrogen bonds mediate the formation of a sheet (distance N···O = 3.8967(4)Å).

The dihedral angles formed between the phenyl rings attached at the 3- and 4- positions and the pyrrole plane are 68.46(6) and 120.70(7)°. The amide moieties deviate from the pyrrole plane of 12.25(4) and -14.08(4)° with the amide NH groups pointing backwards with the respect of the pyrrole NH group.

X-ray quality single crystals of **67** have also been obtained by re-crystallization of the receptor from a hot DMSO solution. The crystal structure revealed that in the solid state the receptor adopts a 'semicleft' conformation, and coordinates one molecule of DMSO via the formation of two hydrogen bonds (Figure 2.14). The amide moieties both deviate slightly from planarity: the amide NH involved in the solvent coordination deviates from the pyrrole plane of 6.20(5)°, whereas the second amide group shows a deviation of 6.75(5)°. The $N_{pyrrole}$···O distance was found to be 2.812(5)Å while the amide nitrogen proved to be 2.787(4)Å away from the DMSO oxygen (see Appendix for structure information).

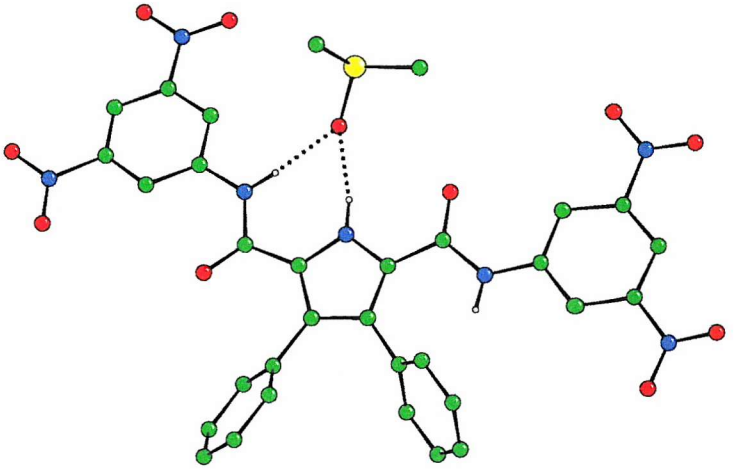

Figure 2.14: Crystal structure of the complex **67**/DMSO. The receptor adopts a 'semicleft' conformation and coordinates a molecule of solvent via the formation of two hydrogen bonds (distance $N_{pyrrole}\cdots O = 2.812(5)$Å, distance $N_{amide}\cdots O = 2.787$Å).

Finally X-ray quality single crystals of receptor **68** were obtained by slow evaporation of an acetonitrile solution of the receptor. The crystal structure reveals the presence of dimers in the solid state. In fact two molecules of the receptor are bound together via the formation of two hydrogen bonds between the pyrrolic NH and the carbonyl group (Figure 2.15). The amide moieties are almost co-planar to the pyrrole ring and show a deviation of 5.11(7) and 3.73(6)°. In the dimer the distance between the pyrrole nitrogen and the carbonyl group involved in the hydrogen bond is 2.968(5)Å(see Appendix for structure information).

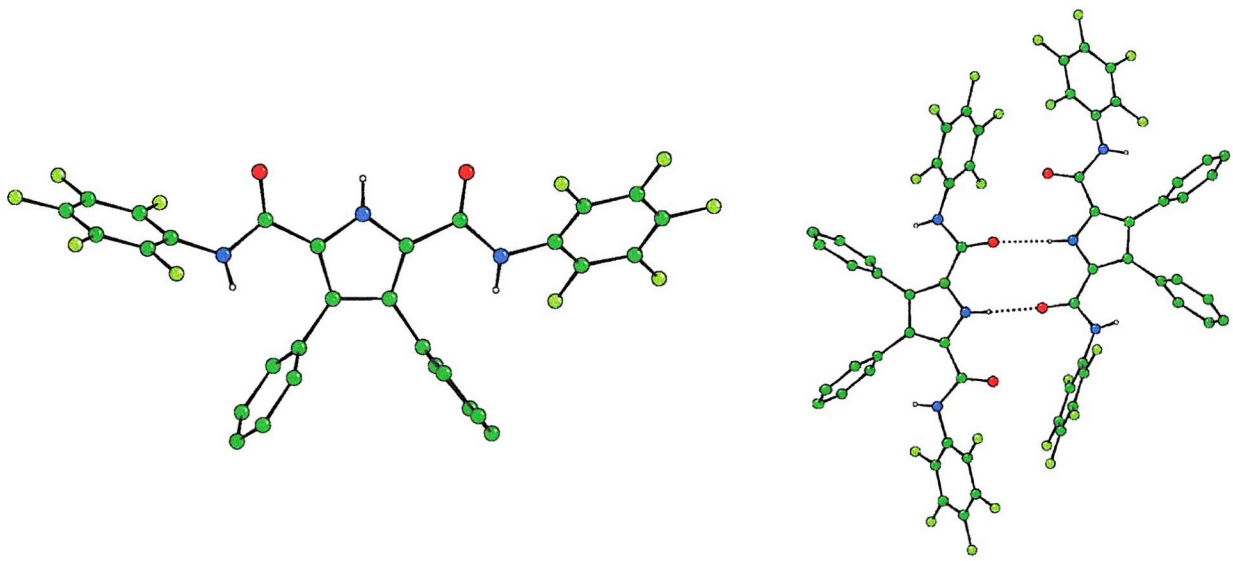

(a) (b)

Figure 2.15: (a) Crystal structure of compound **68**. (b) The structure reveals the presence of a dimer in the solid state. Two molecules of receptors are bound via the formation of two hydrogen bonds between the pyrrolic NH and the amide carbonyl ($N_{pyrrole}$···OC distance 2.968(5)Å).

2.3.2 Binding study results

2.3.2.1 3,4-Dichloro pyrrolic amides: pH switchable catenane precursors

Proton NMR titration techniques have been used in order to establish whether receptors **64-68** show an increased affinity for anions as a consequence of the presence of electron withdrawing groups attached to the pyrrole diamide cleft.[77] Evidence of an increased affinity of receptor **64** came from ^{1}H NMR experiments carried out in DMSO-d_6 solution with tetrabutylammonium chloride. Upon addition of this anionic species the NMR titration curve that was obtained was consistent with the formation of a 1:1 complex ($K_{Chloride}$ = 2013 M^{-1}) (Figure 2.16). This experiment confirmed the expected increase of the the 3,4-dichloro-pyrrolic diamide cleft affinity for anions ($K_{64/Chloride}$ = 20 x $K_{58/Chloride}$).

However unusual titration curves were obtained upon addition of fluoride, benzoate and dihydrogenphosphate to either a dichloromethane or an acetonitrile solution of the receptor

64. As a matter of fact, the amide NH resonance showed a downfield shift upon addition of 1.5-2 equivalents of the anionic species, followed by a upfield shift when the concentration of the anionic guest was increased (Figure 2.17).

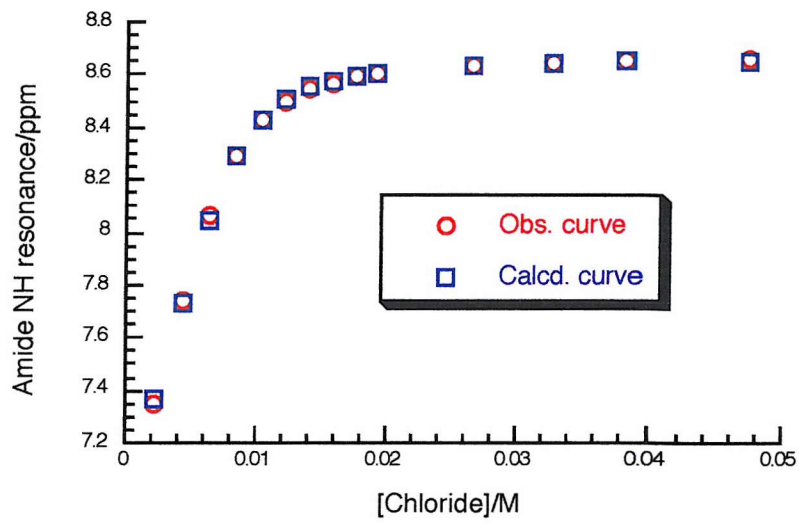

Figure 2.16: ^{1}H NMR titration curve obtained upon addition of discrete amounts of tetrabutylammonium chloride to an acetonitrile solution of receptor **64**. K_1 = 2013 M^{-1}, error < 7%.

Examination of the titration profiles of these receptors lead us to suppose that at least two different processes are occurring in solution.

Addition of aliquots of fluoride anions to a dichloromethane solution of receptor **65** gave a titration curve in which the two processes in solution were clearly identifiable (Figure 2.18). The amide NH resonance showed a downfield shift to 9.9 ppm after addition of the first equivalent of fluoride. Further addition of the anionic species caused an upfield shift that reached the plateau at 9.3 ppm after two equivalents of fluoride have been added.

Formation of a 2:1 anion to receptor complex was considered unlikely. First of all the presence of two anions within the coordination sphere of the receptor would not be thermodynamically favorable because of the electrostatic repulsion. Moreover any attempt to fit the titration curves by using a 2:1 (anion to receptor) fitting model proved to be unsuccessful.

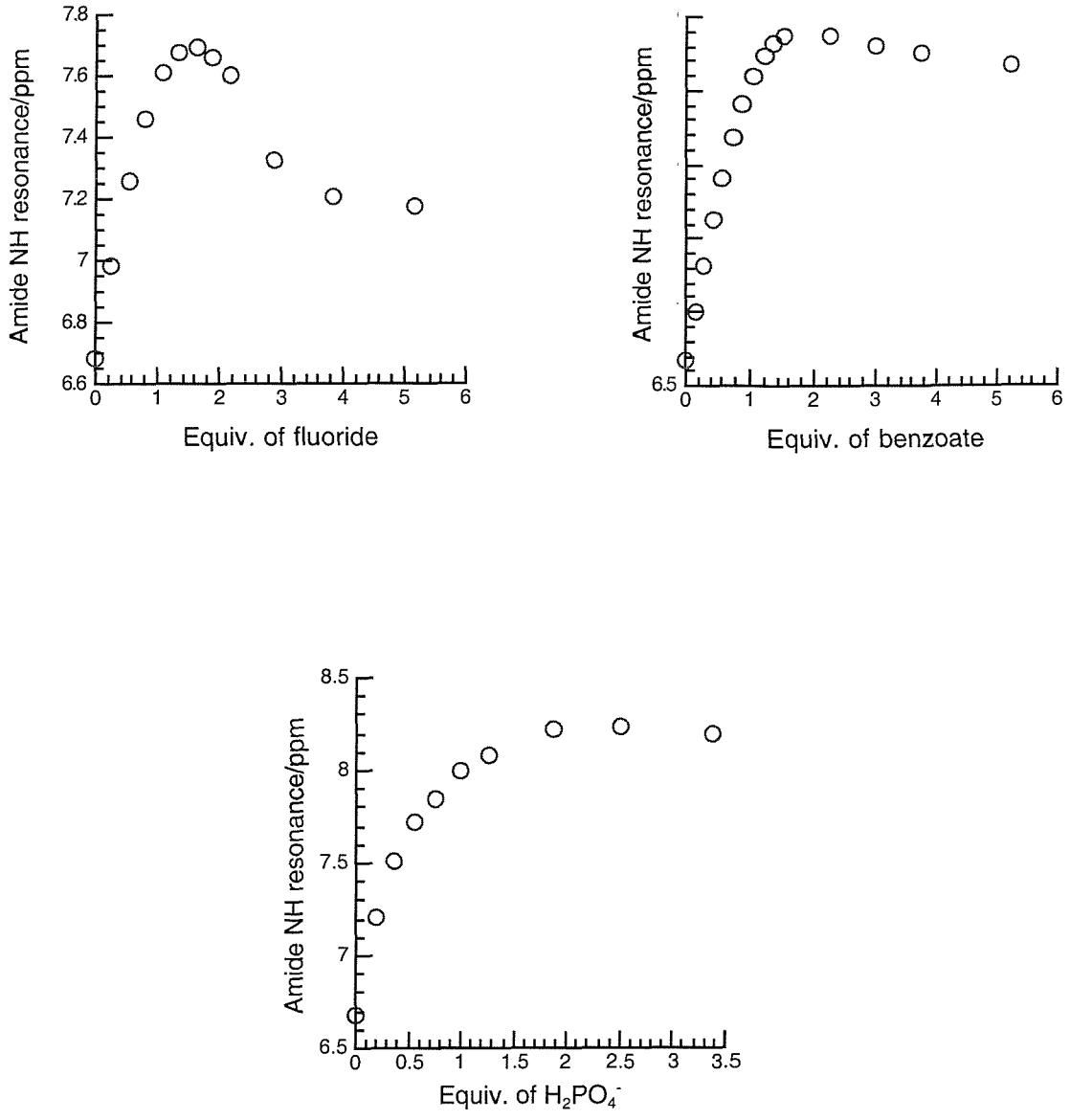

Figure 2.17: ^{1}H NMR titration curves obtained upon addition of fluoride, benzoate and dihydrogenphosphate (as tetrabutylammonium salts) to a dichloromethane solution of receptor **64**.

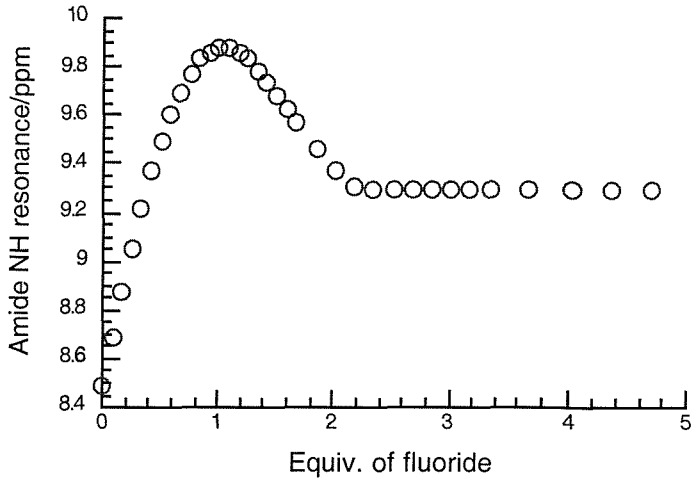

Figure 2.18: ^{1}H NMR titration curve obtained upon addition of tetrabutylammonium fluoride to a dichloromethane solution of receptor **65**. The plot shows two clearly identifiable processes occurring in solution.

When a solution of receptor **65** containing a five fold excess of tetrabutylammonium fluoride was subjected to negative electrospray mass spectrometry, the M^- peak was observed. This result suggested that the presence of two chlorine atoms in the 3- and 4-positions of the pyrrole may polarize the pyrrolic NH group enough that it is deprotonated by fluoride anions. As a consequence of this, the deprotonation process may interfere with the coordination of anions. Reaction of receptor **65** with one equivalent of tetrabutylammonium hydroxide led to the formation of a new species that was fully characterized. Negative electrospray mass spectrometry provided the same M^- peak that was observed for receptor **65** in the presence of an excess of fluoride. Interestingly the amide NH resonance of this new species in dichloromethane-d_2 solution was found to be 9.3 ppm, the same value observed for the amide NH resonance of compound **65** after addition of two equivalents of fluoride.

This results led to the conclusion that a possible explanation of the unusual NMR titration profile in dichloromethane-d_2 solution may come from the combination of the coordination and the deprotonation processes in the following manner: the initial downfield shift of the amide NH resonance is consistent with the coordination of the anionic species;

the upfield shift may be a consequence of the deprotonation of the pyrrole by fluoride. The coordinated anion is then released in solution by the deprotonated receptor, and from fluoride and hydrofluoric acid the anionic species HF_2^- may be generated.

Further evidence came from the solid state study. Slow evaporation of a dichloromethane solution of receptor **65** in the presence of an excess of tetrabutylammonium fluoride provided X-ray quality single crystals. The crystal structure (Figure 2.19) reveals no trace of fluoride anions and the receptor deprotonated at the pyrrolic NH. Interestingly in the solid state the deprotonated **65** dimerizes via the formation of 4 hydrogen bonds between the amide NH groups and the pyrrolic nitrogen. Two molecules of the deprotonated receptor lie perpendicularly to each other with the amide NH being at an average of 3.136(6)Å from the pyrrolic nitrogen. Additional π-H interactions between the phenyl hydrogen and the pyrrole ring have been observed and proved to be in a range of 2.4627(5)-2.6401(4)Å. The amide moieties are almost co-planar to the pyrrole ring showing a deviation of 0.98(6) and 2.36(6)° (see Appendix for structure information).

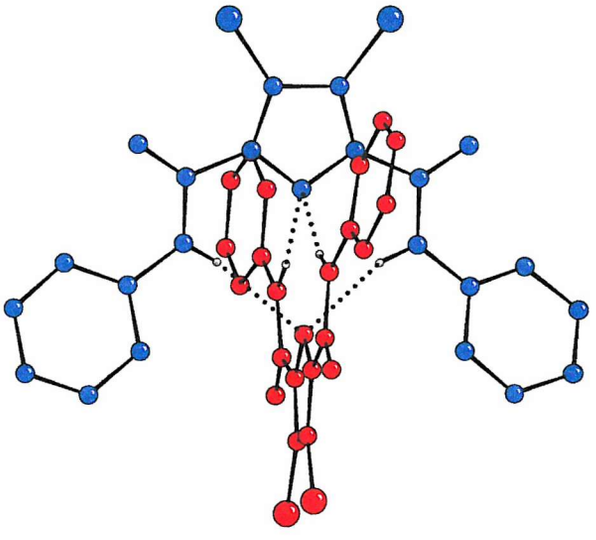

Figure 2.19: Crystal structure of the deprotonated receptor **65**. In the solid state the receptor dimerizes in the deprotonated form, via the formation of four hydrogen bonds between the amide NH groups and the deprotonated pyrrolic nitrogen (distances $N_{amide}\cdots N_{pyrrole}$ = 3.218(4), 3.130(4), 3.124(4), 3.072(4)Å).

Dilution studies carried out in dichloromethane-d_2 on the tetrabutylammonium salt of receptor **65** revealed a 0.1 ppm shift of the amide NH resonance (9.26 ppm to 9.34 ppm) in a range of concentration between 1 and 40mM. Elaboration of the dilution curve by using appropriate software (e.g. NMRDILL_Dimer, kindly provided by Prof. C.A. Hunter[79]) provided an association constant of $8.13M^{-1}$ (error < 2%).

This result is relevant for two reasons: first of all, the combination of 4 hydrogen bonds and 4 π-H interactions promotes the formation of an anionic dimer containing two negative charges so close to each other that otherwise would represent a thermodynamically unfavorable adduct. Secondly compound **65** represents a potential precursor for the synthesis of new interlocked materials.[80]

2.3.2.2 4-Nitrophenyl and 3,5-dinitrophenyl pyrrole amides: optical sensing of fluoride

Proton NMR titration experiments have been carried out on compounds **66-68** in DMSO-d_6 solution in order to compare the anion complexation properties of these receptors to the analogue **58**.[78] Compound **66** was found to bind benzoate twice as strongly as **58** (K_1 = 4150 M^{-1}), whereas fluoride was bound almost 15 times more strongly (K_1 = 1250 M^{-1}). The affinity toward anions was therefore improved however the selectivity for the oxoanions was lost. Surprisingly chloride coordination by receptor **66** was found to be less efficient, revealing a stability constant of 39 M^{-1}. The titration curve obtained for the system **66**/$H_2PO_4^-$ presented the same profile observed for compounds **64-65** (Figure 2.14) and therefore attempts to fit this curve with either a 1:1 or 2:1 fitting model proved to be unsuccessful. Upon addition of 10 equivalents of fluoride, benzoate or dihydrogenphosphate to a 0.2mM DMSO-d_6 (0.5% water) solution of **66** a yellow to orange colour change was observed. In addition a colourless to yellow color change was observed upon addition of the same anions to an acetonitrile suspension of this receptor (Figure 2.20a).

More interesting results came from NMR experiments carried out on compounds **67** and **68** in DMSO-d_6 (0.5% water) and acetonitrile-d_3 solution respectively. Upon addition of aliquots of chloride anions to solutions of these receptors, titration profiles were obtained consistent with the formation of 1:1 complexes (K_1 = 53 M^{-1} for the system **67**/chloride, K_1 =

19 M^{-1} for the system **68**/chloride). Addition of either fluoride or benzoate to a DMSO-d_6 (0.5% water) solution of **67** did not cause any shift of the amide NH resonance as it was observed for the other receptors, but rather the disappearance of this peak. Identical behavior was observed upon addition of fluoride, benzoate and dihydrogenphosphate to receptor **68** in acetonitrile-d_3 solution.

The most interesting feature of compound **67** is its colourimetric sensor properties. A yellow to orange colour change was observed upon addition of fluoride, benzoate and dihydrogenphosphate anions to a DMSO solution of **67**. Addition of the same anions to an acetonitrile suspension of **67** produced a colourless to yellow colour change. On the other hand no colour change was observed upon addition of either chloride or bromide to this receptor in either DMSO nor acetonitrile solution. These observations mirror the results obtained for receptor **66**. However upon addition of fluoride to an acetonitrile suspension of **67** the yellow solution rapidly turns to a dark blue colour (within 1 minute) (Figure 2.20b).

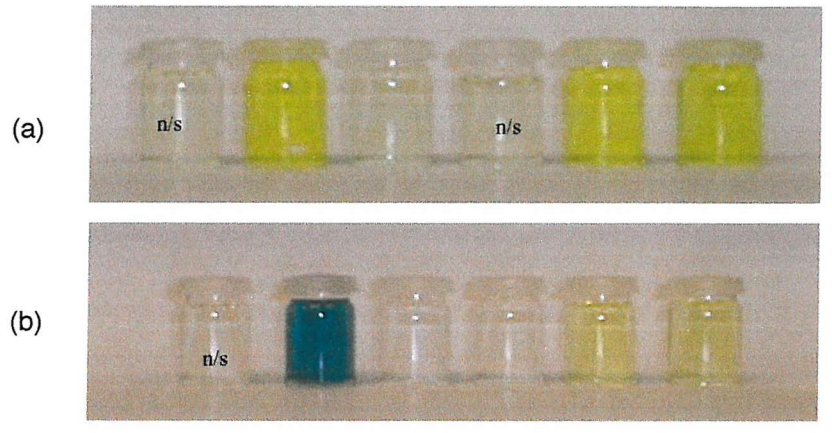

Figure 2.20: The vials contain 0.2mM acetonitrile solutions of receptors (a) **66** and (b) **67** in the presence of 10 equivalents of a various anions (as their tetrabutylammonium salts). Receptor **67** gives a highly selective optical response for fluoride anions (n/s = not soluble)

Therefore compound **67** behaves as a highly selective optical sensor for fluoride anions in acetonitrile solution. Further investigation has shown that the dark blue colour is observed also upon addition of fluoride to a DMSO solution of **67** when the temperature is increased to 80°C.

The reasons for this behaviour are still under investigation. Mass and UV/Vis spectroscopy support the idea that deprotonation may compete with the anion coordination process even though the pyrrole does not carry electron withdrawing groups. Negative electrospray mass spectrometry analysis carried out on receptor **67** in the presence of a variety of anionic species such as fluoride, chloride, benzoate and dihydrogenphosphate, showed that the M^- peak of the receptor is always present. However in the presence of an excess of fluoride the M^{2-} species was also observed. UV/Vis experiments carried out in acetonitrile revealed that a possible explanation of the **67**/fluoride deep blue colour can be due to a deprotonation process followed by coordination of the anionic species. In fact upon addition of 5 equivalents of sodium hydride to an acetonitrile suspension of the receptor a dark red solution was obtained. The UV/vis analysis of this solution revealed a peak at 488 nm (Figure 2.21). Addition of fluoride to this solution led to a red to deep blue colour change with the formation of a peak at 593 nm, whereas no colour change was observed upon addition of the other anions. If a 10 fold excess of fluoride is added to an acetonitrile suspension of **67** a similar spectrum featuring a peak at 598 nm is obtained, suggesting that a deptotonation process may be followed by the coordination of the anionic species (Figure 2.21).

Further evidence came from ^{1}H NMR titration experiments carried out on compound **67** in DMSO-d_6. Addition of aliquots of tetrabutylammonium fluoride to a solution of the receptor provided the titration profile that is shown in Figure 2.22. Upon addition of the first two equivalents of anion a curve is obtained that resembles that observed during the titration of compound **65** with fluoride in dichloromethane (Figure 2.18). Further addition of anion causes a downfield shift until the plateau is reached after addition of three equivalents of fluoride. This behaviour seems to be consistent with a three step process that may be hypothesized as follows: the first equivalent of fluoride is coordinated by the receptor; the second equivalent promotes the deprotonation process and, as observed for receptor **65**, HF_2^- may be generated; the third equivalent of fluoride is coordinated by the deprotonated receptor probably with the participation of the phenyl CH groups that in this receptor are particularly acidic because of the presence of the electron withdrawing groups attached to the phenyl ring.

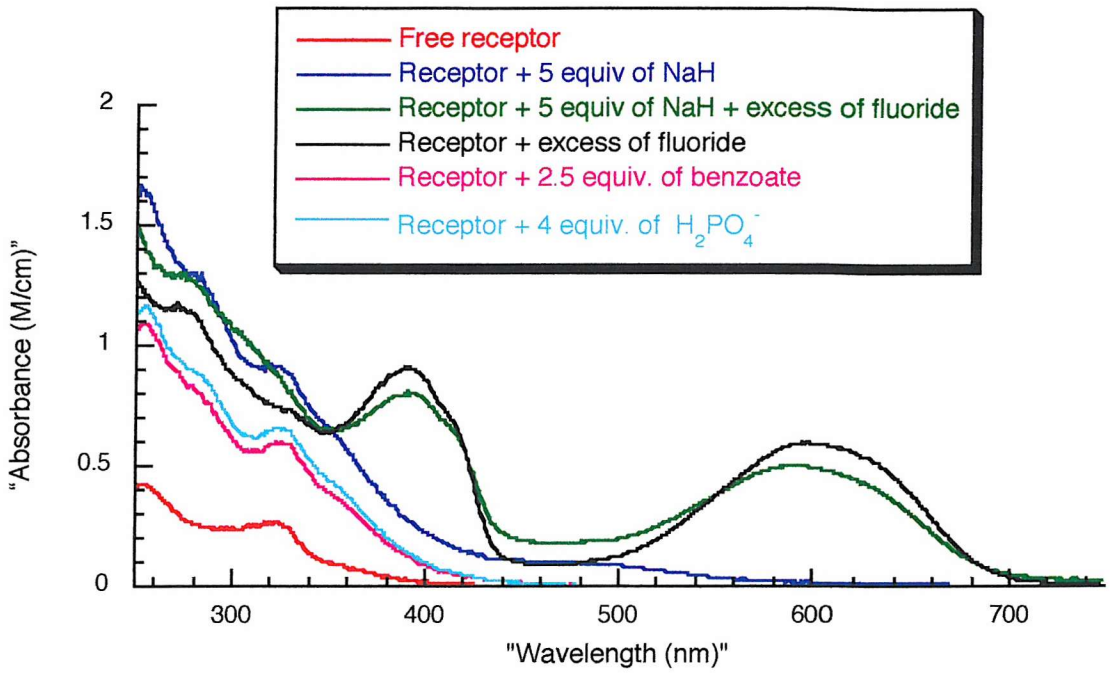

Figure 2.21: UV/Vis spectrum of receptor **67** (3.2mM) recorded in acetonitrile solution.

Crystallographic analysis provided a further proof for this theory. X-ray quality colourless single crystals have been isolated after evaporation of a blue dichloromethane/methanol solution of the receptor in the presence of an excess of fluoride. The structure reveals the receptor in a deprotonated form while coordinates an adventitious chloride anion (Figure 2.23), confirming the idea that compound **67** is able to coordinate an anionic host even if the deprotonation of the pyrrolic NH occurs.

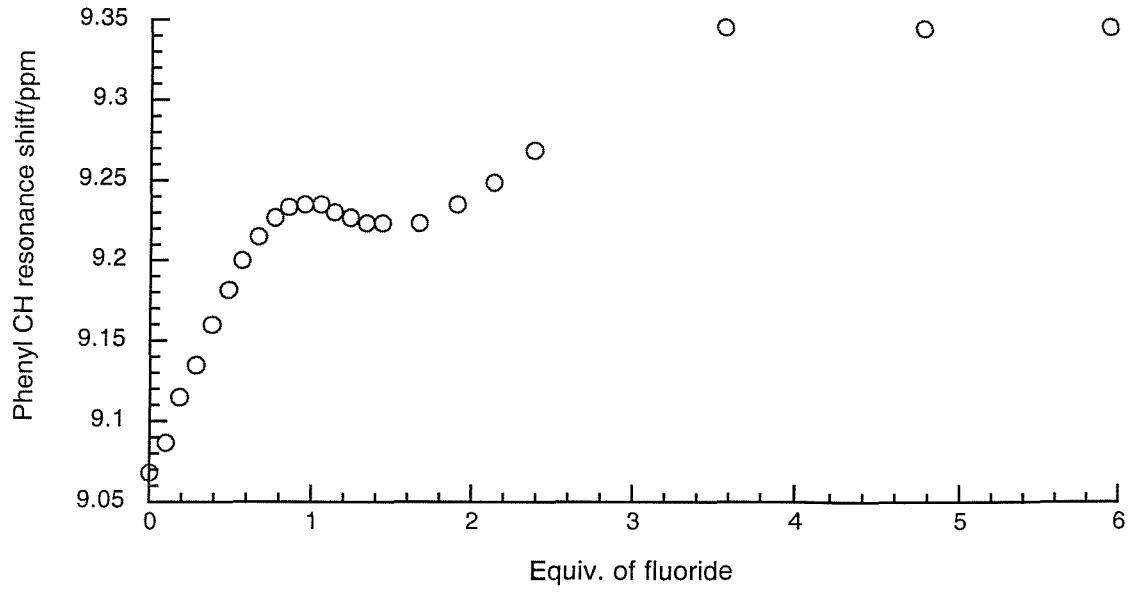

Figure 2.22: Proton NMR titration profile obtained by addition of aliquots of tetrabutylamonium fluoride to a DMSO-d_6 solution of receptor **67**.

In this structure the deprotonated receptor coordinates one chloride anion holding it between the two amide groups and two phenyl rings. The proximity of the chloride to the amide groups suggests that the negative charge may be localized on the pyrrolic nitrogen. The chloride is coordinated by the receptor via the formation of two hydrogen bonds with the amide NH groups (N_{amide}···Cl = 3.354(5) and 3.378(5)Å) and two hydrogen bonds with the phenylic CH groups ($C_{arom.}$···Cl = 3.350(4) and 3.374(4)Å). The phenyl rings attached at the 3- and 4- positions deviates from the pyrrole plane of 48.42(4) and 51.50(4)°. The amide moieties are almost co-planar to the pyrrole ring and give a deviation of 2.28(5) and 16.17(5)° (see Appendix for structure information). Therefore in the solid state compound **67** is relatively planar and the coordination of the chloride occurs without evident deviation from the receptor plane, in contrast with the observation reported by Crabtree on bromide coordination by simple phenyl diamide clefts.[8]

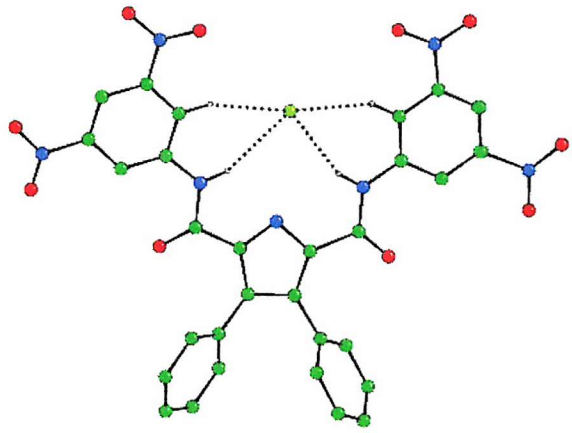

Figure 2.23: Crystal structure of the deprotonated receptor **67** with one chloride anion coordinated to it. The anionic species interact with the receptor via the formation of four hydrogen bonds two of which involve the amide NH groups (N···Cl = 3.354(5) and 3.378(5)Å) and two aromatic CH groups (C···Cl = 3.350(4) and 3.374(4)Å). The tetrabutylammonium counter cations have been omitted for clarity.

2.4 Introducing a cation binding site at the 2- and 5-positions of the pyrrole cleft

Introduction of a cation binding site in the scaffold of an anion receptor may result in the formation of a ion-pair coordinating agent. The simultaneous coordination of a cationic and an anionic species is extremely important when the extraction of an inorganic salt from aqueous to an organic solution is required. Coordination of a cationic species provides a powerful method of enhancing the interaction strength of the receptor for anions, due to the addition of an electrostatic component to the anion binding.

As shown in the previous chapter incorporation of a crown-ether moiety into an anion receptor structure can achieve both these targets.[36] Inspired by this idea, two new pyrrolic amide clefts have been synthesised that contain one or two 15-crown-5-ether moieties respectively.

2.4.1 Synthesis and characterization

Compound **69** was synthesised by reacting the pyrrole mono ester derivative **60**[70] with 4'-aminobenzo-15-crown-5-ether in the presence of $AlMe_3$[73] (Scheme 2.5).[81] Crystallization of the reaction mixture in the minimum amount of acetonitrile led to the isolation of the desired compound **69** in 28% yield.

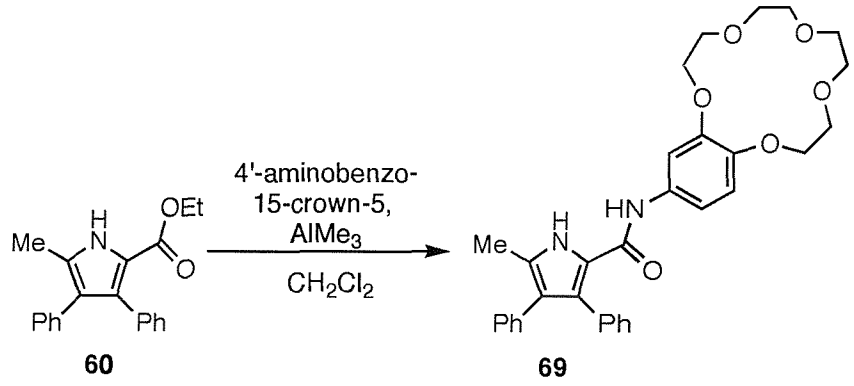

60 **69**

Scheme 2.5

The pyrrolic bis-amide cleft **70** has been synthesised by reaction of the diacid chloride **57** with 4'-aminobenzo-15-crown-5 in dichlromethane in the presence of triethyl amine and a catalytic amount of DMAP (Scheme 2.6). The desired compound was isolated in 33% yield by crystallization with acetonitrile.

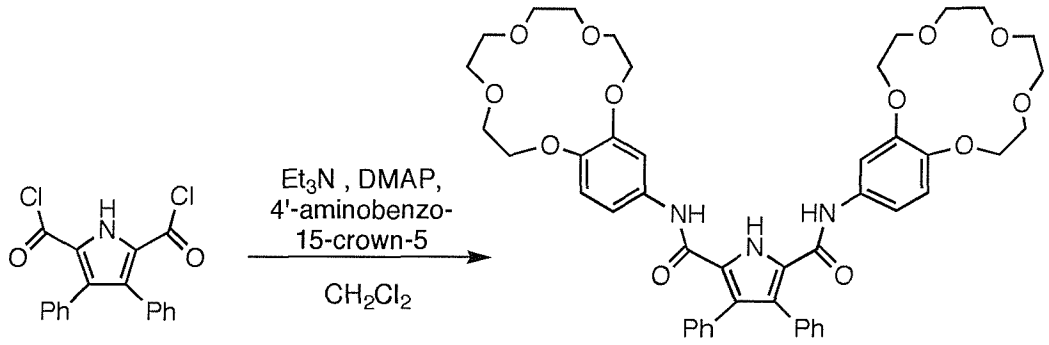

57 **70**

Scheme 2.6

Slow evaporation of a dilute acetonitrile solution of compound **69** led to the formation of X-ray quality single crystals. The crystal structure (Figure 2.24) revealed that the receptor

forms a dimer via the formation of two hydrogen bonds between the pyrrolic NH group and the carbonyl group. The NH···OC distance proved to be 2.814(5)Å. As observed for the two pyrrole monoamides **61** and **62**, the amide plane deviates slightly from the pyrrole ring showing a dihedral angle of just 9.71(7)Å (see Appendix for structure information).

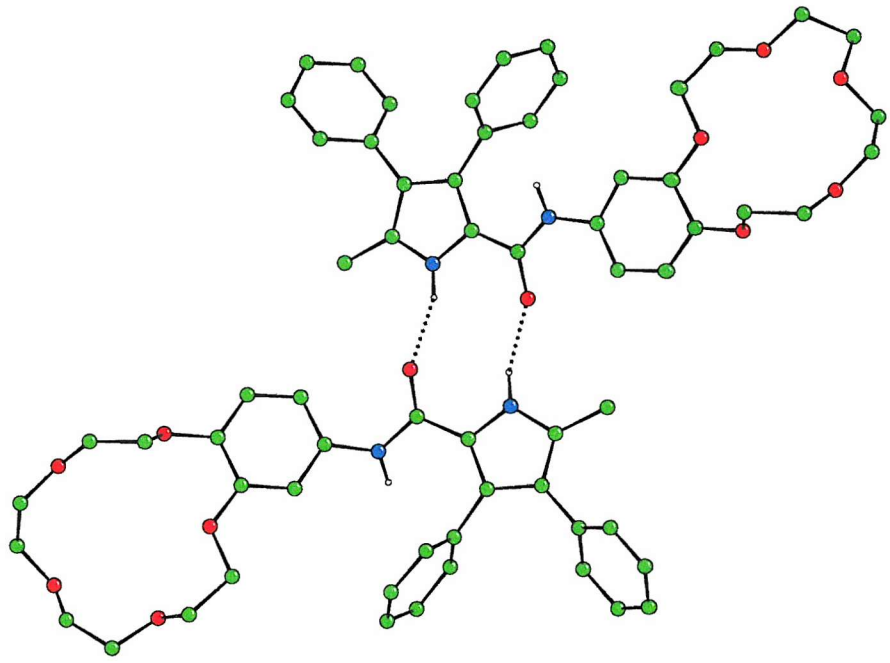

Figure 2.24: Crystal structure of a dimer of receptor **69** (distance $N_{pyrrole}$···OC = 2.814(5)).

2.4.2 Binding study results

Proton NMR titration experiments in DMSO-d_6 (0.5% water) have been performed in order to investigate the anion coordination properties of receptors **69** and **70** (Table 2.2).[81] All the titration curves were consistent with the formation of 1:1 complexes. Receptor **70** behaves similarly to its analogue **59**, and showed high selectivity for oxanions such as benzoate and dihydrogenphosphate. NMR titration experiments have been carried out on

receptor **69** in order to confirm the higher affinity of the bis-amide cleft for anions over the mono-amide cleft (Table 2.2).

Anion	Receptor **69**	Receptor **70**
Fluoride	(a)	< 10
Chloride	< 10	16
Benzoate	70	896.5
Dihydrogenphosphate	307	1880

Table 2.2: Association constant of receptors **69**, and **70** (M^{-1}) with various anionic guests at 25°C in DMSO-d_6 (0.5% water). The anions have been added as tetrabutylammonium salts. The errors were estimated to be < 15%. (a) disappearing of the amide NH resonance during the titration did not allow the calculation of the association constant.

The same experiments were carried out in the presence of one equivalent of either sodium or caesium for receptor **69** and two equivalents of either sodium or caesium for receptor **70**. Interestingly the presence of the cation did not enhance the anion coordination strength at all, instead a decrease of the association constant values was observed (Table 2.3). Only fluoride was bound to receptor **70** almost 5 times more strongly in the presence of caesium cations in DMSO solution.

Interestingly in some cases the metal ion seemed to compete with the anion binding site in the coordination of the anionic species. Addition of fluoride anions to a DMSO-d_6 (0.5% water) solution of receptor **70** in the presence of two equivalents of sodium tetraphenylborate with respect to the receptor gave an unusual titration curve. Addition of the first two equivalents of this anionic species did not cause any shift in the amide ^{1}H NMR resonance. However when the concentration of the anionic species was increased to 8 equivalents a 2 ppm shift was observed (Figure 2.25).

The same behaviour has recently been observed by Smith and co-workers during the investigation of the anion complexation properties of a simple urea based anion receptor in DMSO-d_6 solution in the presence of a 'non-innocent' metal ion such as sodium, potassium

or caesium. In this work, the authors explain the unusual titration profile as an effect of the high degree of the ion-pair aggregation in organic solvents.

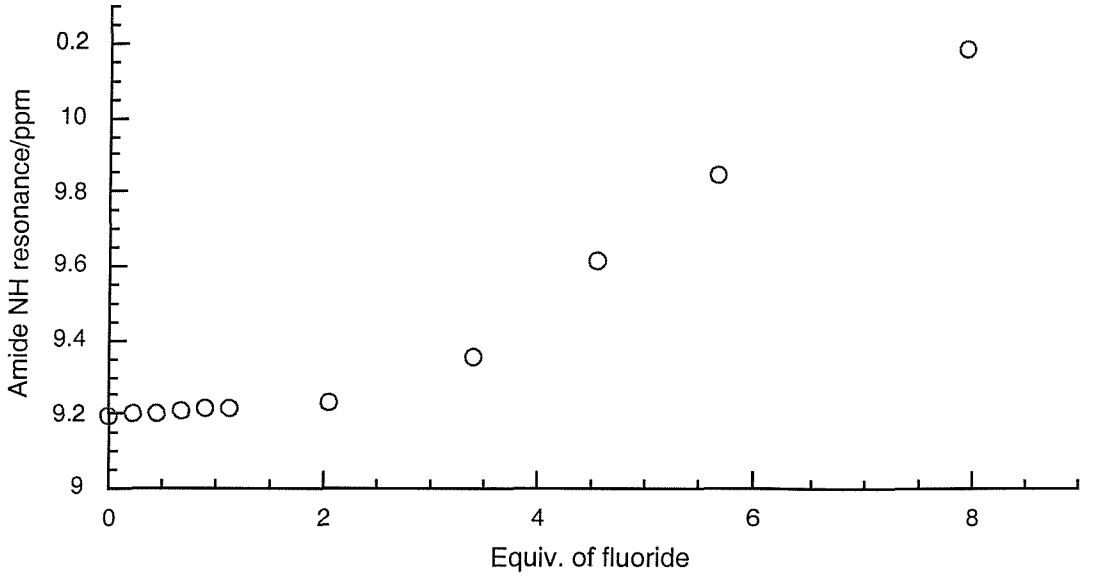

Figure 2.25: ^{1}H NMR titration curve obtained by adding discrete amounts of fluoride anions to a DMSO solution of receptor **70** in the presence of two equivalents of sodium tetraphenylborate.

In accordance with this theory the metal ion is able to stoichiometrically sequester the anion and therefore prevents the receptor/anion binding.[82] As a matter of fact, upon addition of tetrabutylammonium fluoride to a DMSO-d_6 solution containing **70** together with 2 equivalents of sodium tetraphenylborate, the first two equivalents of anion appear not to bind to the pyrrolic binding site. However further addition of fluoride produced a 'normal looking' curve. In accordance with this theory, ion-pair aggregation is less likely to occur if the anion and cation differ significantly in their size and charge. Indeed this is the case of the fluoride/caesium system, in which the presence of the cation does not seem to promote any ion-pair aggregation phenomena but instead increases the receptor's affinity for fluoride (Table 2.3).

Anion	Receptor **69** + 1eq of $Na^{+(c)}$	Receptor **69** + 1eq of $Cs^{+(c)}$	Receptor **70** + 2 eq. of $Na^{+(c)}$	Receptor **70** + 2 eq. of $Cs^{+(c)}$
Fluoride	(a)	(a)	(b)	307.5
Chloride	6.7	7.6	16.6	1.8
Benzoate	29.7	86.8	296.7	816.4
Dihydrogen phosphate	(b)	(b)	(b)	(b)

Table 2.3: Association constant of receptors **69** in the presence of sodium ions, and **70** the presence of sodium and cesium ions (M^{-1}) with various anionic guests at 25°C in DMSO-d_6. The anions have been added as tetrabutylammonium salt. The errors were estimated to be < 15%. (a) disappearance of the amide NH resonance during the titration did not allow the calculation of the association constant. (b) Sigmoidal titration curve. (c) Cation added as tetraphenylborate salt.

2.6 Conclusion

A series of pyrrolic mono (e.g. **61-62**) and bis-amide (e.g. **58-59**) receptors has been synthesised and their anion coordination properties investigated by the use of ^{1}H NMR titration techniques. These receptors proved to be efficient anion receptors and showed selectivity toward oxoanions such as benzoate and dihydrogenphosphate.

Upon functionalization of the pyrrolic clefts with electron withdrawing groups at the 3- and 4- positions two new anion receptors were obtained. The 3,4-dichloropyrrolic amide clefts bound chloride almost 200 times more strongly than the analogous 3,4-diphenyl pyrrole derivatives. However deprotonation processes often competed with the anion coordination process and led to the formation of dimers. Dilution studies revealed that self-assembly processes occur in solution.

A new highly selective fluoride optical sensor has been synthesised by functionalization of the pyrrole amide cleft with electron withdrawing nitro-groups. The colourless to dark blue colour change observed when **67** detects fluoride in acetonitrile solution may be of use in industrial fluoride sensors and a preliminary patent has been filed.

The synthesis of the 15-crown-5 pyrrole receptors **69** and **70** was performed in order to investigate the anion binding properties of these compounds in the presence of a metal ion coordinated to the crown-ether moiety. However the metal ion often seemed to compete with the pyrrolic binding site for the coordination of the anionic species, although fluoride coordination strength was increased by 5 times when receptor **70** was in the presence of 2 equivalents of caesium cations.

In conclusion the synthesis of pyrrole amide clefts proved to be successful in that:

- The high selectivity for oxoanions such as benzoate and dihydrogenphosphate was achieved.
- The formation of unusual anion dimers was achieved.
- The highly selective optical activity of the nitro derivatives toward fluoride.

3.Super-extended cavity calix[4]pyrroles: fluoride selective coordinating agents

3.1 Recent advances in the development of cyclic polypyrrole anion coordinating agents

The acid-catalyzed condensation of pyrrole with a ketone leads to the formation of tetrapyrrolic macrocycles[46] containing four pyrrole rings linked together by sp^3 hybridized carbon atoms carrying two alkyl or phenyl groups (Scheme 3.1).

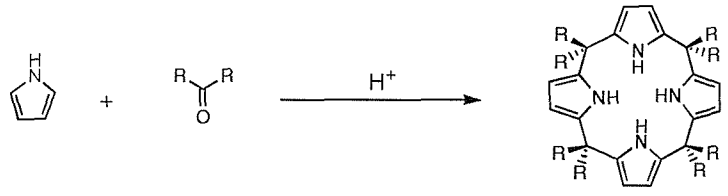

Scheme 3.1: General reaction for the synthesis of calix[4]pyrroles.

These macrocycles are strictly named porphyrinogens, as they are reduced precursors to porphyrins. However in this case the absence of hydrogen atoms in the *meso* positions, means that oxidation of these species to porphyrins does not occur readily. Moreover the

similarity of these compounds' structure to calix[4]arene has lead to them being known as calix[4]pyrroles due to their three dimensional conformational properties.

Free rotation of the pyrrolic moieties through the annulus of the macrocycle can occur allowing the receptor to adopt four possible conformations: cone, partial cone, 1,2-alternate and 1,3-alternate (Figure 3.1).[83]

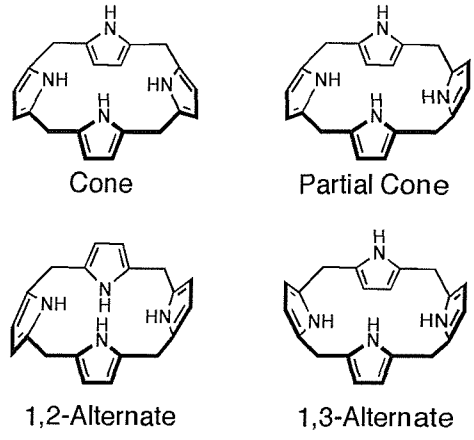

Figure 3.1: Possible conformation of a calix[4]pyrrole.

For a single pyrrole ring, solid state evidence has shown that the pyrrolic NH group can function as a hydrogen bond donor[37] although this is only a weak interaction when transferred to solution.[84] In contrast, calixpyrroles have proven to be effective and selective anion receptors in solution.[50]

The anion binding properties of the calix[4]pyrroles were reported for the first time by Sessler and co-workers in 1996.[84] Up until this point, these macrocycles were considered only to be good cation complexating agents.[47] *meso*-Octamethylcalix[4]pyrrole **37** was found to bind a variety of anions such as fluoride, chloride, and dihydrogenphosphate showing high selectivity for fluoride anions (Table 3.1).[84]

Anion added	Stability constant (M^{-1}) for compound **37**
Fluoride	17170 (± 900)
Chloride	350 (± 5.5)
Bromide	10 (± 0.5)
Iodide	< 10
Dihydrogenphosphate	97 (±3.9)
Hydrogensulfate	< 10

Table 3.1: Stability constant for **37** with anionic substrates in dichloromethane-d_2 at 298 K.

X-ray crystallographic analysis revealed a 1,3-alternate conformation for the free receptor in the solid state, whereas the cone conformation was observed for the chloride complex (Figure 3.2).[84] Proton NMR analysis showed that the cone conformation in the receptor/anion complex is maintained also in solution at low temperature.[84]

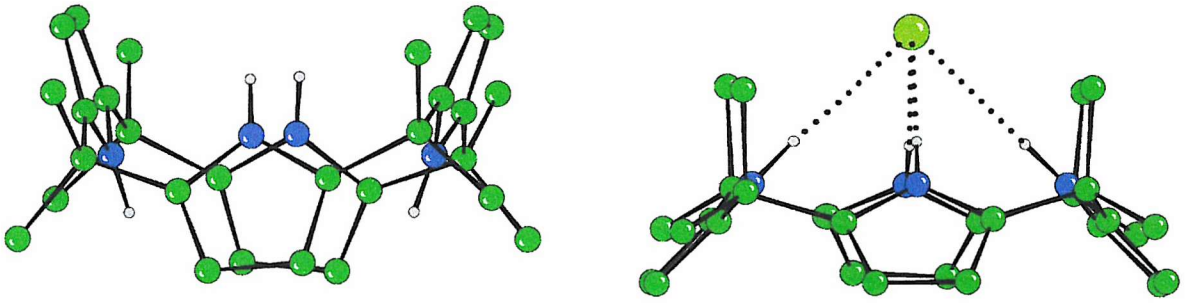

(a) (b)

Figure 3.2: Crystal structure of (a) free receptor **37** and (b) its chloride complex.

The facile preparation of these anion receptors from readily available starting materials encouraged many researchers to investigate calix[4]pyrrole chemistry.[38] In the last decade

new calix[4]pyrrole derivatives has been synthesized either by using a variety of different starting material or by *C*-rim functionalization of already known compounds.[38]

The recent development of the calix[4]pyrrole chemistry has been already highlighted in the previous chapter and therefore will not be discussed further in this chapter. However the synthesis and anion coordination properties of the *meso*-tetraphenoxy-calix[4]pyrrole **39** will be considered again, as it represents an important starting material in this project.

As reported previously, acid-catalyzed condensation of pyrrole with *p*-hydroxy-acetophenone leads to the formation of four calix[4]pyrrole isomers (Scheme 3.2).[48,49] The αααα isomer **39** can be isolated either by column chromatography or by crystallization from acetic acid. Slow crystallization from a hot acetic acid solution of compound **39** leads to the formation of single crystals suitable for X-ray analysis.[49] The crystal structure (Figure 3.3a) reveals the presence of a non-covalently linked trimer in which each monomer coordinates three molecules of acetic acid that act also as a bridges by the formation of a complicated network of hydrogen bonds.

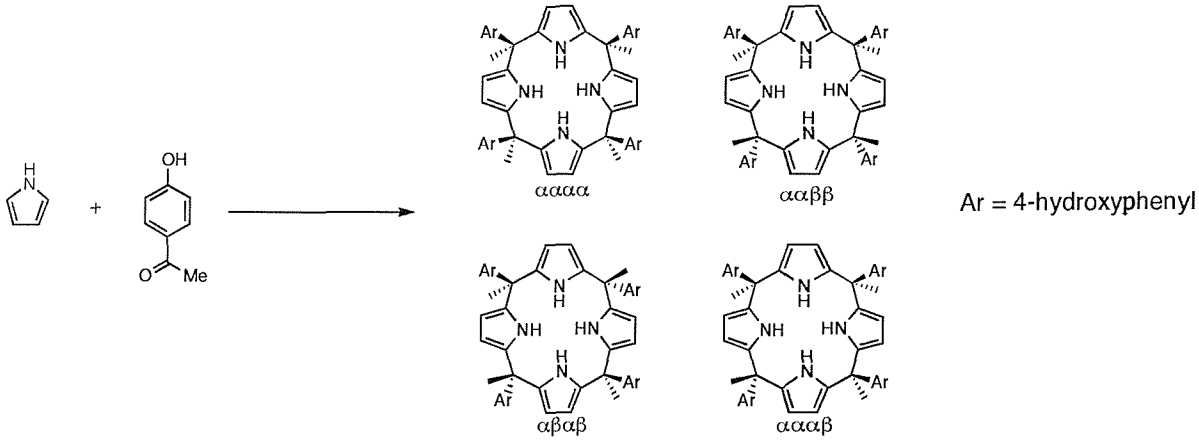

Scheme 3.2: Synthesis of the calix[4]pyrrole **39**.

X-ray quality crystals have been obtained also by slow evaporation of an ethanol solution of **39**.[48] Coordination of one molecule of solvent is observed in the solid state, with the receptor adopting a cone conformation (Figure 3.3b).

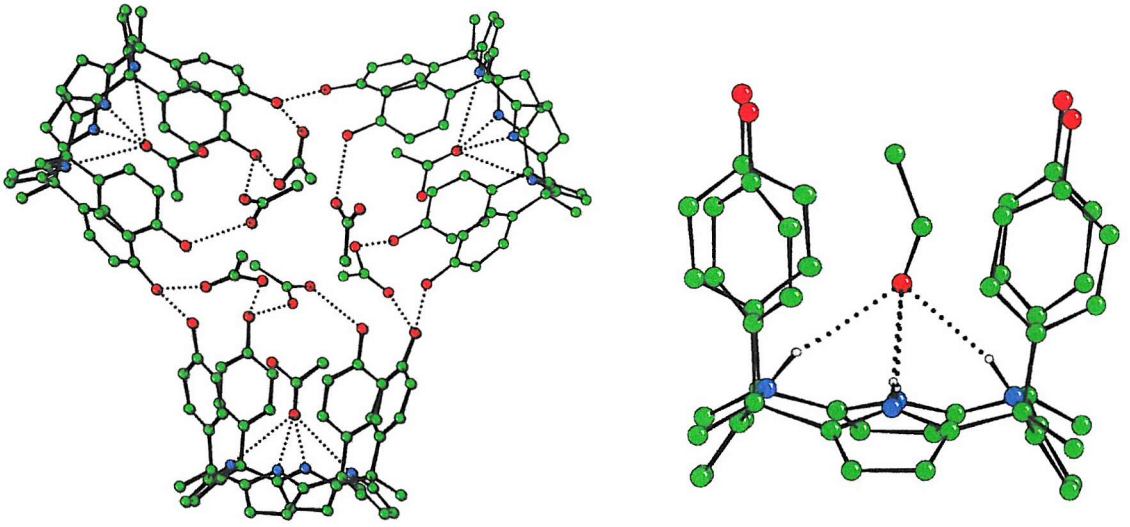

(a) (b)

Figure 3.3: Crystal structure of (a) the acetic acid complex of compound **39** and (b) its ethanol adduct.

The anion binding properties of compound **39** have been investigated.[48] This receptor was found to coordinate fluoride selectively over other anions such as chloride and phosphate. The selectivity for fluoride anions was found to be higher than the previously reported *meso*-octamethyl-calix[4]pyrrole **37** (Table 3.2).

Anion added	Calix[4]pyrrole **37**	Extended cavity calix[4]pyrrole **39**
Fluoride	> 10 000	>10 000
Chloride	> 5000	320
Dihydrogenphosphate	1300	500

Table 3.2: Stability constants for compounds **37** and **39** (M^{-1}) with anionic substrates in acetonitrile-d_3 (0.5% v/v D_2O) at 298 K.

For receptor **39**, the selectivity for dihydrogenphosphate over chloride is probably due to an interaction of the phenolic OH groups with the coordinated anion.

However compound **39** is not just a selective anion receptor. The presence of four phenoxy groups that can be easily functionalized, makes this molecule a particularly useful

starting material for the synthesis of more extended cavities calix[4]pyrroles. Indeed an analogy may be drawn between the structure of **39** and that of *p-tert*-butylcalix[4]arene[85] in that they both contain four phenol groups that are oriented in the same direction. There is much literature on the functionalisation of calix[4]arenes at the lower phenolic rim. For example, McKervey and co-workers reported the synthesis of lower rim ester functionalized calix[4]arene derivatives capable of coordinating metal ions such as sodium, potassium and caesium.[86] We decided to investigate whether tetra-ester and tetra-amide functionalized calix[4]pyrroles would function as receptors for cations in the oxygen rich region of the receptor and anions in the calixpyrrole and hence function as an ion-pair complexing agent. (Figure 3.4).

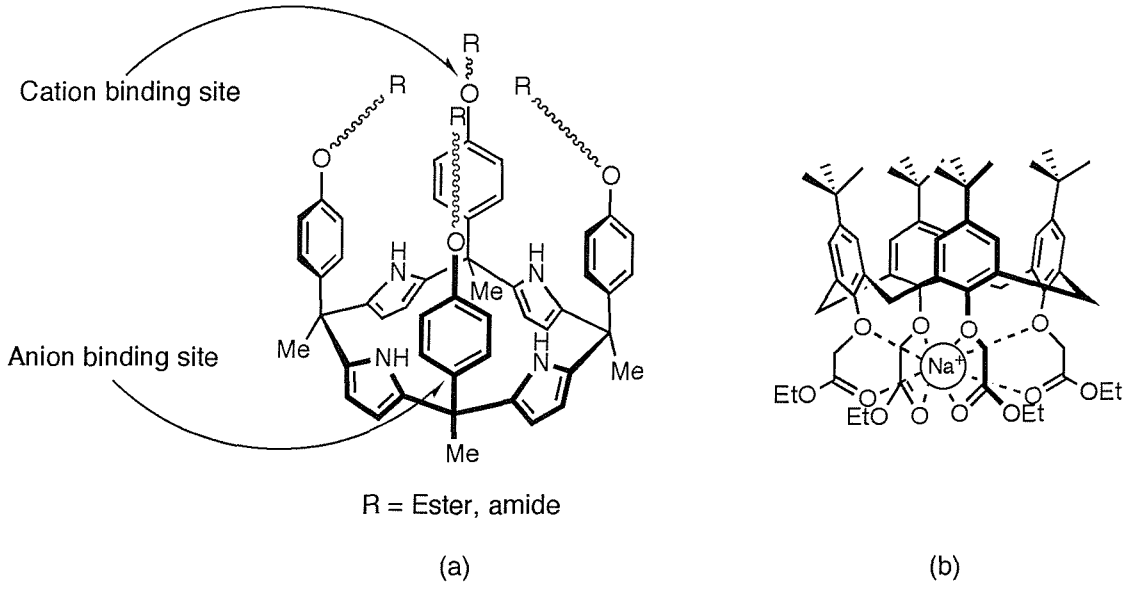

Figure 3.4: (a) Graphical representation of a calix[4]pyrrole featuring a cation binding site. (b) A tetra-ester calix[4]arene used for the coordination of cationic species.

3.2 Synthesis and characterization

Modification of the phenolic OH groups of compound **39** with ester and amide functional groups has been achieved using McKervey's methodology that was originally applied to calix[4]arenes. In addition an acetyl derivative have been produced (Scheme 3.3).

Compound **71**[87] was prepared by refluxing a freshly distilled acetone solution of **39**[48,49] in the presence of an excess of bromoethylacetate and potassium carbonate. After filtering off the inorganic components of the reaction, the desired product was re-crystallized from ethanol in 76.5% yield. Slow crystallization from hot DMSO led to the formation of X-ray quality single crystals. The crystal structure (Figure 3.5) shows the calix[4]pyrrole adopting a cone conformation. The N···N cross-ring separation was found to be 4.689(6) and 4.676(8)Å. The cavity formed by the *meso*-C atoms is an average 5.0542(6)Å in length and 7.1415(4)Å diagonally. One molecule of DMSO sits in the cavity forming four hydrogen bonds with the pyrrolic NH groups. The distance between the DMSO oxygen and the pyrrolic nitrogens is in the range of 2.934-3.004(9) Å (see Appendix for structure information).

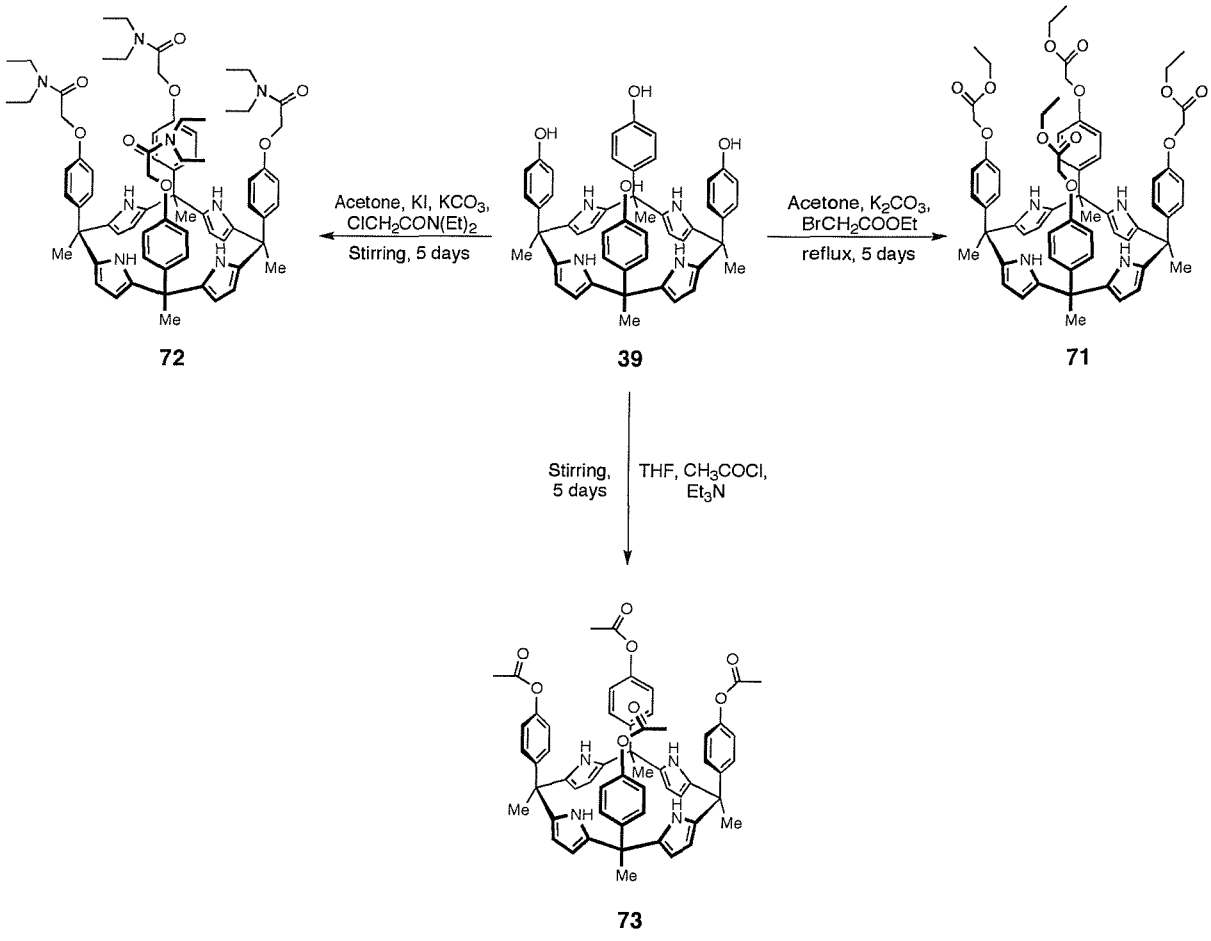

Scheme 3.3: Synthesis of the new 'super-extended' cavity calix[4]pyrrole derivatives **71-73**.

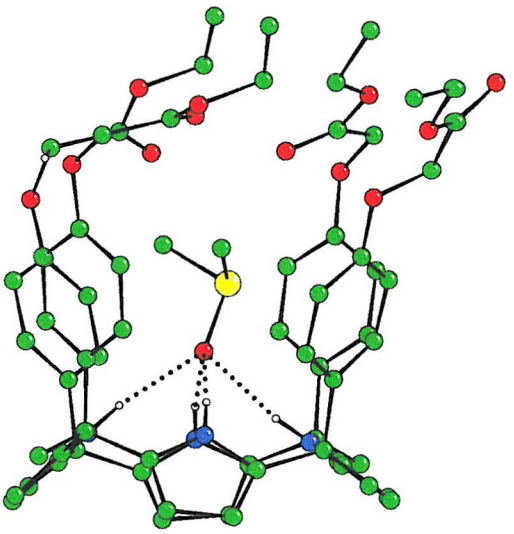

Figure 3.5: Crystal structure of the complex **71**/DMSO. The DMSO molecule sits inside the cavity and interacts with the macrocycle through the formation of four NH hydrogen bonds (distances N···O (Å): 3.004(8),2.992(4),2.934(7),2.965(8)).

The coordination of neutral molecules by calix[4]pyrrole derivatives has been already reported in literature.[38] For example, *meso*-octamethylcalix[4]pyrrole **37** was crystallized both from methanol and DMF.[84] The receptor was found to adopt a 1,3-alternate conformation with methanol, binding two molecules, one on each face of the macrocycle, whilst DMF was bound in a 1,2-alternate conformation, presumably due to π-stacking between the guest and macrocycle favoring this conformation (Figure 3.6).

The structure presented in Figure 3.5 is similar to the complex **39**/ethanol shown in Figure 3.3b. Interestingly, all the solid state X-ray crystallographic analyses of the extended cavity calixpyrroles show the macrocycle adopting a cone conformation with the pyrrole NH groups pointing into the phenolic cavity of the receptor when a neutral guest is bound.[48,49]

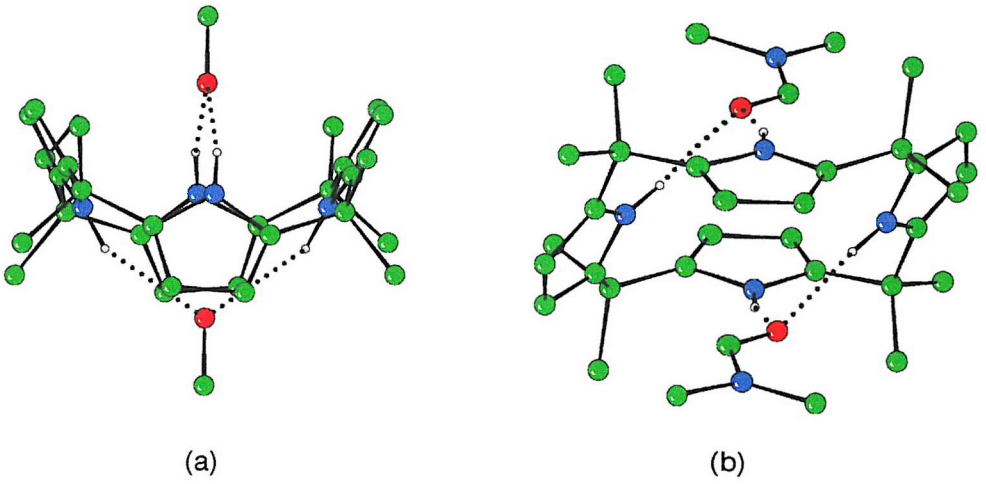

Figure 3.6: Crystal structure of (a) the methanol adduct of the *meso*-octamethylcalix[4]pyrrole **37** (1,3-alternate conformation) and (b) the **37**/2DMF complex (1,2-alternate conformation)

Compound **72**[87] was prepared by stirring calix[4]pyrrole **39** in freshly distilled acetone with 2-chloro-*N*,*N*-diethylacetamide in the presence of potassium iodide and potassium carbonate. After removing the inorganic residues by filtration and washing, **72** was re-crystallized from diethyl ether and obtained in 59% yield. X-ray quality single crystals were obtained by slow evaporation of an acetonitrile solution of **72**. As previously observed for derivative **71**, in the solid state the receptor adopts a cone conformation and reveals an N···N cross-ring distance of 4.737(5) and 4.723(3)Å. The cavity formed by the *meso*-C atoms is an average 5.047(4)Å in length and 7.137(7)Å diagonally. The receptor coordinates a molecule of solvent through the formation of four hydrogen bonds (Figure 3.7). The average distance between the acetonitrile nitrogen and the pyrrolic nitrogens was found to be 3.191(7) Å. A second molecule of acetonitrile sits within the four pyrrolic rings.[88] The distance between the methyl C atom of the solvent and the C atoms at the 3- and 4- position of the pyrrole rings was found to be an average of 3.9565(8)Å (see Appendix for structure information).

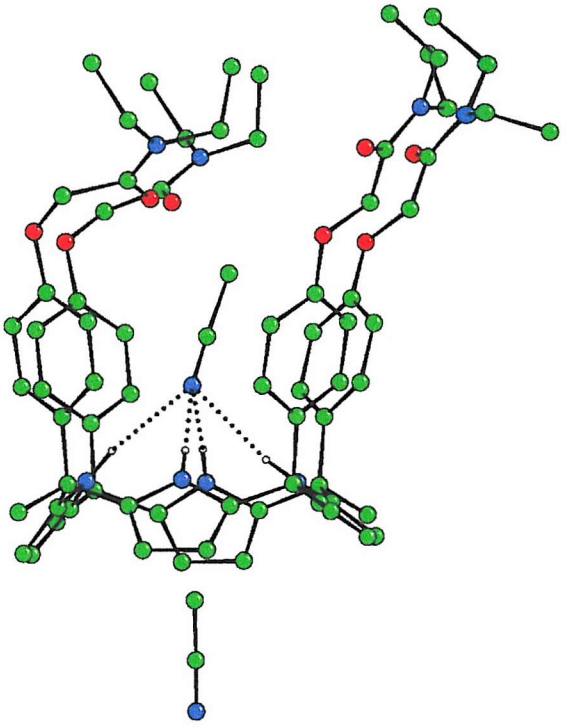

Figure 3.7: Crystal structure of the comeplex **72**/acetonitrile. One molecule of solvent sits inside the cavity and interacts with the macrocycle through the formation of four NH hydrogen bonds (average distance $N_{pyrrole}\cdots N_{acetonitrile}$ (Å): 3.191(7)). A second acetonitrile molecule is positioned within the four pyrrolic rings.

Finally the tetra-acetyl functionalized calix[4]pyrrole **73**[89] was prepared by stirring **39**, in freshly distilled THF, with a 4.1 fold excess of acetyl chloride in the presence of triethylamine. The desired compound was obtained by slow re-crystallization from hot methanol. X-ray suitable single crystals were obtained by slow re-crystallization from either acetonitrile or DMSO, affording three different crystal structures. In the solid-state, receptor **73** adopts a cone conformation in all the structures obtained. The acetonitrile complex (Figure 3.8) crystal structure proved to be highly symmetric (space groups P4/n). The N···N cross-ring separation was found to be 4.6789(6)Å whilst the cavity formed by the *meso*-C atoms proved to be 5.0453(3)Å in length and 7.1351(4)Å diagonally (see Appendix for structure information), representing therefore a perfect square. The receptor coordinates the solvent via the formation of four hydrogen bonds. The acetonitrile lies inside the cavity with the nitrogen being 3.2219(6)Å away from each pyrrole nitrogen.

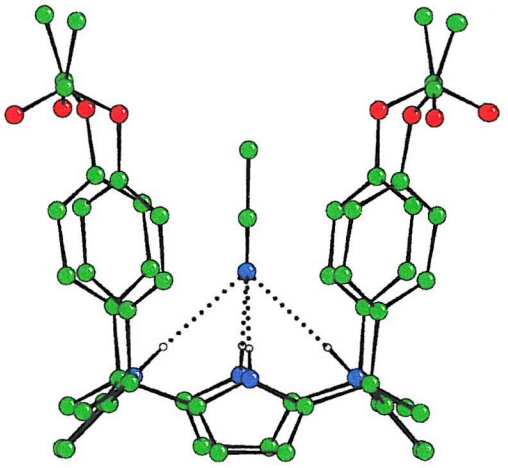

Figure 3.8: Crystal structure of the complex **73**/acetonitrile. The receptor adopts a cone conformation and coordinates a molecule of solvent through the formation of four hydrogen bonds (average distance $N_{pyrrole}—N_{acetonitrile}$ = 3.2219(5)Å)

From a concentrated DMSO solution two different crystals were collected corresponding to the DMSO complex and to the free receptor. Unfortunately both crystals were found to diffract poorly and therefore the obtained results were not suitable for publication (see Appendix for further details).

Figure 3.9 shows the DMSO complex in which the receptor adopts a cone conformation as previously observed for the others analogues calix[4]pyrroles. Again the solvent is coordinated by the receptor via the formation of four hydrogen bonds between the DMSO oxygen and the pyrrole nitrogens .

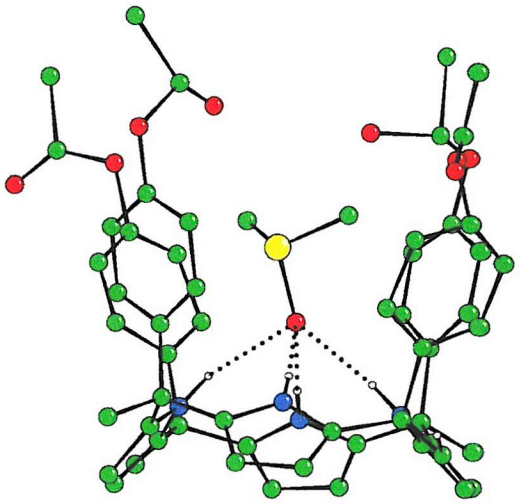

Figure 3.9: Crystal structure of the complex **73**/DMSO. Again the receptor encapsulates a molecule of solvent and coordinates it through the formation of four hydrogen bonds (average distance N···O = 2.9803(9)Å)

Finally the structure depicted in Figure 3.10 shows the receptor adopting a cone conformation also in the absence of a coordinated guest. This has not been observed previously for a calix[4]pyrrole derivative. Unfortunately the poor quality of the crystals did not allow a good refinement of the crystal structure (see Appendix for further information). Nevertheless the electron density map suggests that no guest is present within the hydrophobic cage of the calix[4]pyrrole. As a consequence of that, the postulate that the 'super-extended' calix[4]pyrrole **73** may adopt a cone conformation even in the absence of any coordinated species could be still acceptable.

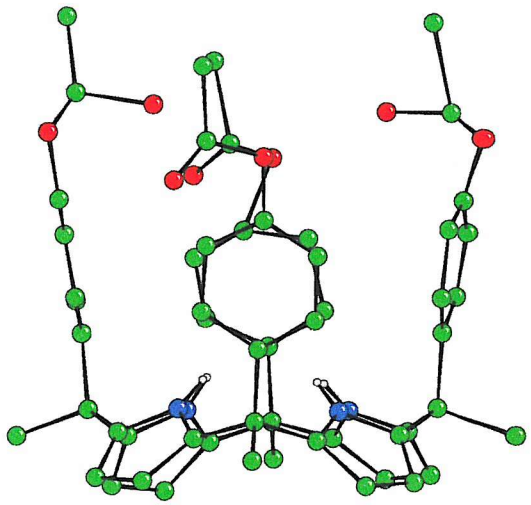

Figure 3.10: Crystal structure of receptor **73**. The structure reveals the macrocycle adopting a cone conformation even in the absence of any coordinated solvent.

3.3 Binding studies: a new fluoride only receptor in DMSO

Ester groups were appended to the phenolic OH rim of compound **39** in order to create a cation binding site and to exploit these new 'super-extended' cavity calix[4]pyrroles as ion-pair coordinating agents. Therefore the cation binding properties of compound **71** and **72** were investigated. These compounds, in spite of the structural similarity to the calix[4]arenes reported by McKervey (Figure 3.4), did not reveal any cation coordination. In fact, upon addition of a variety of metal ions such as Na^+, Li^+, K^+, Mg^{2+} and Ba^{2+} (as perchlorate salts) no change in the ^1H NMR spectrum was observed in DMSO-d_6 solution. The presence of a coordinated anionic species did not promote cation complexation. Indeed addition of the above cationic species to a DMSO-d_6 solution containing either compounds **71** or **72** and excess of tetrabutylammonium fluoride did not cause any shift of the proton resonances of these receptors. This was a discouraging however not unexpected result. The

resonances of these receptors. This was a discouraging however not unexpected result. The crystal structure of the 'super-extended' cavity calix[4]pyrroles reveal that the phenol groups diverge from the macrocycle, whereas in calix[4]arene, the OH groups converge at the lower rim of the macrocycle.

The anion binding properties of **71** and **72** were investigated using ^{1}H NMR titration techniques in a variety of deuteriated solvents.[87] The behviour of these receptors was studied firstly in acetonitrile-d_3. In this solvent *meso*-octamethylcalix[4]pyrrole **37** and the extended cavity calix[4]pyrrole **39** bind fluoride, chloride and phosphate showing high selectivity for fluoride (Table 3.2). Coordination of the anionic species is detected by following the shift of pyrrolic CH or NH resonances in the ^{1}H NMR upon addition of aliquots of anions, and the stability constants calculated using the appropriate software (e.g. EQNMR[75]). Compounds **71** and **72** did not show any interaction with dihydrogenphosphate, although interaction with fluoride and chloride was observed. Upon addition of these anionic species to an acetonitrile solution of **71** or **72**, new resonances appeared consistent with the formation of anion complexes with slow complexation/decomplexation kinetics relative to the NMR timescale. This has previously been observed for the *meso*-octamethylcalix[4]pyrrole **37** but only at low temperatures (-80°C)[90] and therefore represents unusual behavior.

Low solubility in less polar solvents such as dichloromethane or chloroform did not allow us to investigate the anion binding properties of the receptors in these solvents.

Investigation of the anion binding properties of these receptors in DMSO-d_6 solution revealed an unusual feature of the complexation properties of the 'super-extended' cavity calix[4]pyrroles **71-72**. In this solvent addition of 20 equivalents of chloride, bromide, iodide, dhidrogenphosphate and hydrogensulphate (as tetrabutylammonium salts) did not cause any change in the ^{1}H NMR spectrum of the receptors. Therefore no interaction at all was observed with these anions in DMSO-d_6 solution. However, upon addition of fluoride anions, new resonances were observed for the N*H*, Ar*H*, and pyrrole C*H* protons (Figure 3.11). In addition, coupling is observed between the pyrrolic NH protons and the coordinated fluoride anion (confirmed by ^{19}F{^{1}H} NMR spectroscopy) at room temperature with a coupling constant of 47 Hz for both compounds **71** and **72** (Figure 3.12a,b). A concentration profile of the free receptor and the host/anion complex during the ^{1}H NMR titration is shown in Figure 3.13. Because no shift was observed but rather the formation of

new resonances, the use of traditional software was not found to be suitable for the calculation of the stability constants.

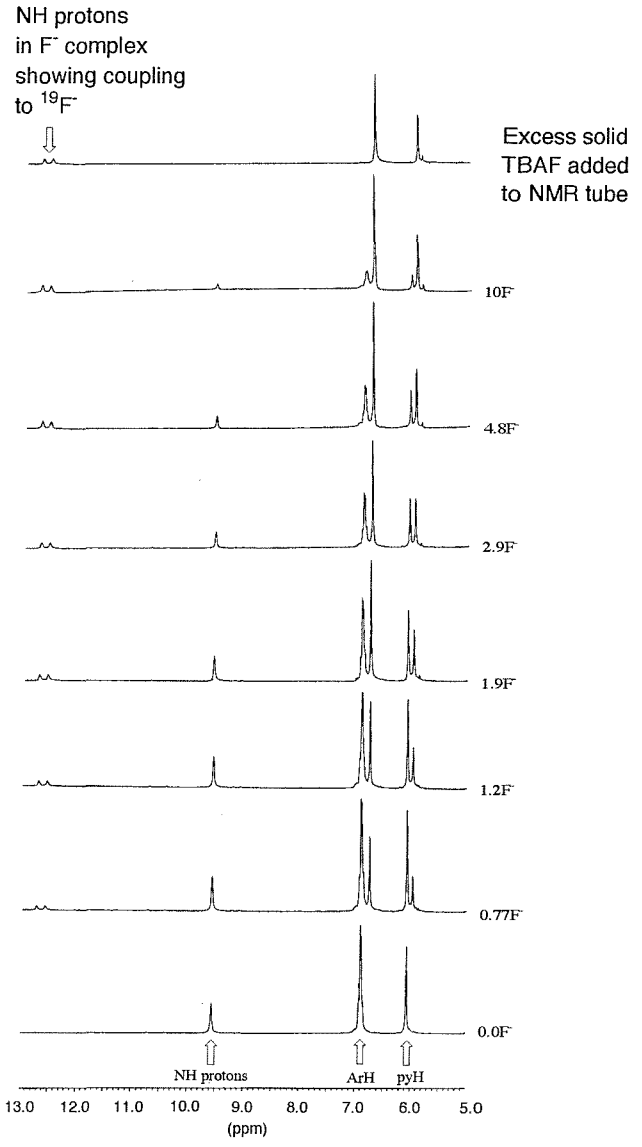

Figure 3.11:NMR titration of tetramide calix[4]pyrrole **72** with fluoride in DMSO-d_6.

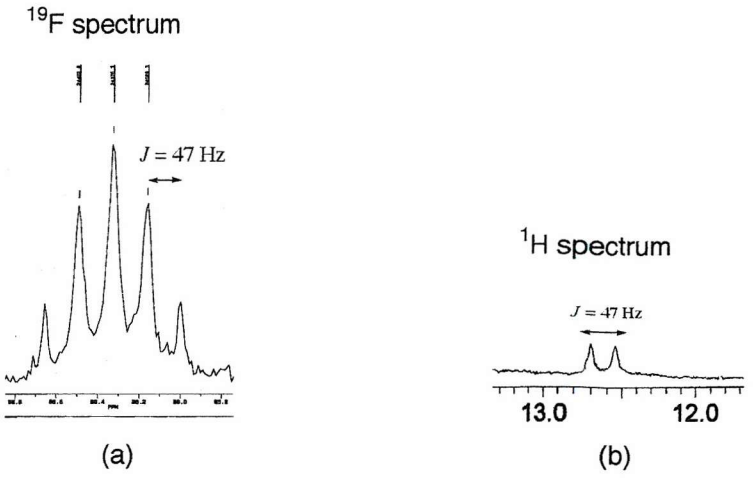

Figure 3.12: $^{19}F\{^{1}H\}$ NMR (a) and ^{1}H-NMR (b) spectra showing the coupling of the pyrrole NH groups with fluoride.

The concentration of the species during the titration has been calculated by using the intergration of the NH proton resonances as an indication of the relative populations of host and complex in solution. The stability constants (K_1= 36.0(±0.5)M^{-1} for the system **71**/fluoride, K_1= 47.3(±0.3)M^{-1} for the system **72**/fluoride) have been consequently calculated using the equation showed in Scheme 3.4.

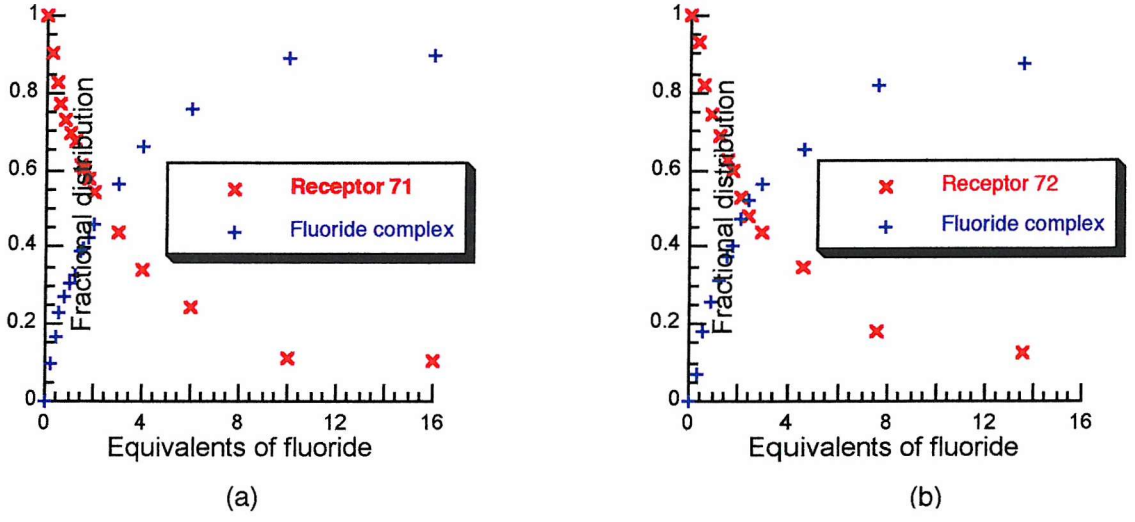

Figure 3.13 Concentration profile for (a) compound **71** and its fluoride complex and (b) compound **72** and its fluoride complex, during ^{1}H NMR titration in DMSO-d_6 at room temperature.

$$\text{Receptor} + \text{Fluoride} \rightleftharpoons \text{Complex}$$

$$K_1 = \frac{[\text{Complex}]}{[\text{Receptor}][\text{Fluoride}]}$$

Scheme 3.4: Calculation of the stability constant for slow kinetic complexation.

In order to understand the reasons of the fluoride only complexation observed in DMSO-d_6 and the slow complexation/decomplexation kinetics, the structurally simpler calix[4]pyrrole derivative **73** has been synthesized.

The cation coordination properties of this receptor were not found to be different from the previously studied macrocycles **71** and **72.** On the other hand, the anion binding properties of this receptor were found to be identical to those of compounds **71** and **72** i.e. the slow-exchange processes and high selectivity for fluoride in DMSO-d_6 solution were observed. In fact, addition of up to 100 equivalents of chloride, bromide, iodide, dihydrogenphosphate and hydrogensulphate did not cause any change in the ^{1}H NMR spectrum of compound **2.3** in DMSO-d_6 solution. However in this solvent, new resonances have been observed upon addition of 0.5 equivalents of fluoride anions, consistent with the formation of a 1:1 receptor/fluoride complex (Figure 3.14).[89]

A possible explanation for the observed slow kinetic complexation/decomplexation process is attributed to the structure of these 'super-extended' calix[4]pyrroles. The solid state evidence suggests that unlike other calixpyrroles, extended cavity calixpyrroles are locked in the cone conformation with the NH groups pointing into the phenolic cavity. This would be consistent with the stereic interactions present in the macrocycle. Therefore a hydrophobic cage is formed around the anion binding site. This means that the fluoride must be highly desolvated before being coordinated by the receptor; moreover the hydrophobic cage permits the solvent to approach the anion from one direction only and not to directly interfere with the hydrogen bonding interactions therefore the subsequent decomplexation process is slow (Figure 3.15).

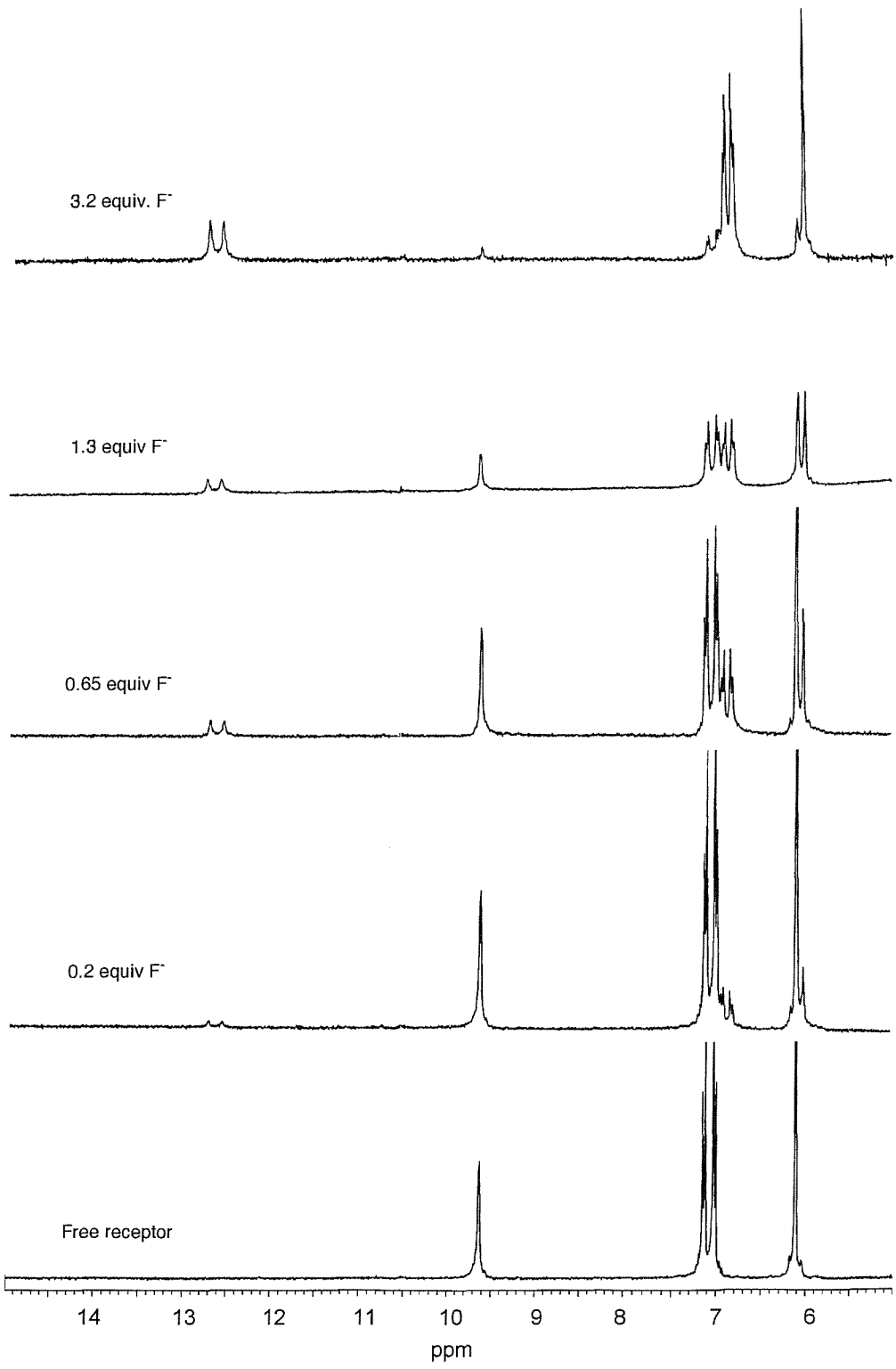

Figure 3.14: NMR titration of receptor **73** with TBA fluoride. The formation of new peaks supports the idea of a slow kinetic complexation/decomplexation process. A further evidence comes from the doublet at ca. 13 ppm due to the coupling of the pyrrolic NH with the fluoride. This behaviour has been previously observed only at low temperature.

Support for this theory comes from ^{1}H NMR titration experiments performed on the parent extended cavity calix[4]pyrrole **39** and *meso*-octamethylcalix[4]pyrrole **37** in DMSO-d_6 solution. In this solvent compound **39** was found to bind both fluoride *and* chloride with slow complexation/decomplexation kinetics relative to the NMR timescale. However, a resonance shift was observed for compound **37** upon addition of the same putative anionic guests (K_1 = 1060 M^{-1} for the system **37**/fluoride, K_1= 1025M^{-1} for the system **37**chloride).

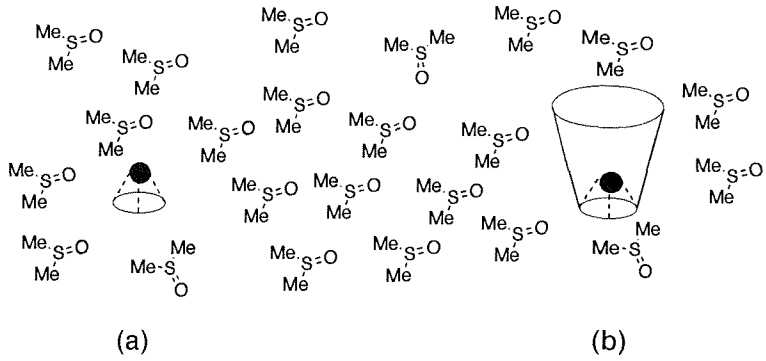

Figure 3.15: Two different approaches for the coordination of an anion to a calix[4]pyrrole. (a) In calixpyrroles such as compound **37**, fluoride is exposed to the bulk solvent. (b) In fixed walls calixpyrroles such as compound **73**, fluoride is partially shielded from the bulk solvent

In order to investigate these systems further, free energy simulations were performed on the complexes of compound **73** by Dr. Jonathan Essex and Mr Chris Woods at the University of Southampton.[89] In this work, the receptor was solvated with a periodic cubic box of solvent (Figure 3.16).

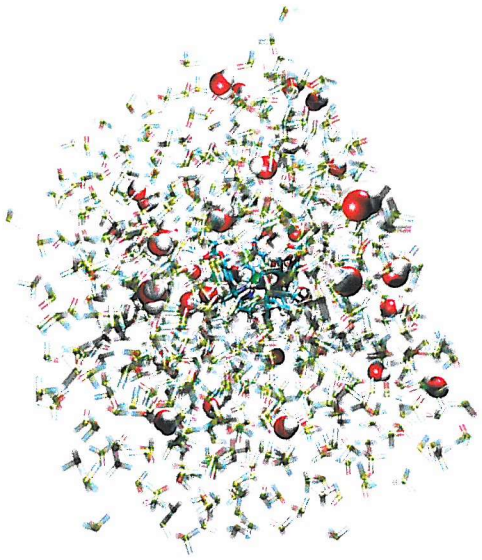

Figure 3.16: System consists of calixpyrrole **73** plus halide ion solvated in a 30 Å cubic box of MeCN or DMSO solvent, with 40 H_2O molecules randomly placed.

Either a box of DMSO/H_2O, or MeCN/H_2O was used. These simulations calculated the relative free energies of each of the fluoride, chloride and bromide complexes (Table 3.3). The results reproduce the experimental observation that the fluoride forms a more stable complex than the other halides.

System	DMSO/H_2O	MeCN/H_2O
Fluoride	-11.8 ± 0.6	-14.3 ± 1.8
Chloride	-0.6 ± 0.4	-0.9 ± 1.5
Bromide	0.0	0.0

Table 3.3: Relative binding free energies of the halide complexes (kcal mol^{-1}) for receptor **73**.

Initial analysis suggests that this is due to the electrostatic interactions in the calix ring. The electrostatic potential on a slice through the centre of the complex was calculated. This reveals a small positive pocket near the four N-H groups. The structures obtained from the simulations show that the fluoride ion sits lower in the ring, and fits into this pocket (Figure

3.17a). The other halides are larger, so sit higher in the cavity and fall outside this pocket (Figure 3.17b). This is seen in the average electrostatic interaction energies between the halide ion and selected atoms in the complex.

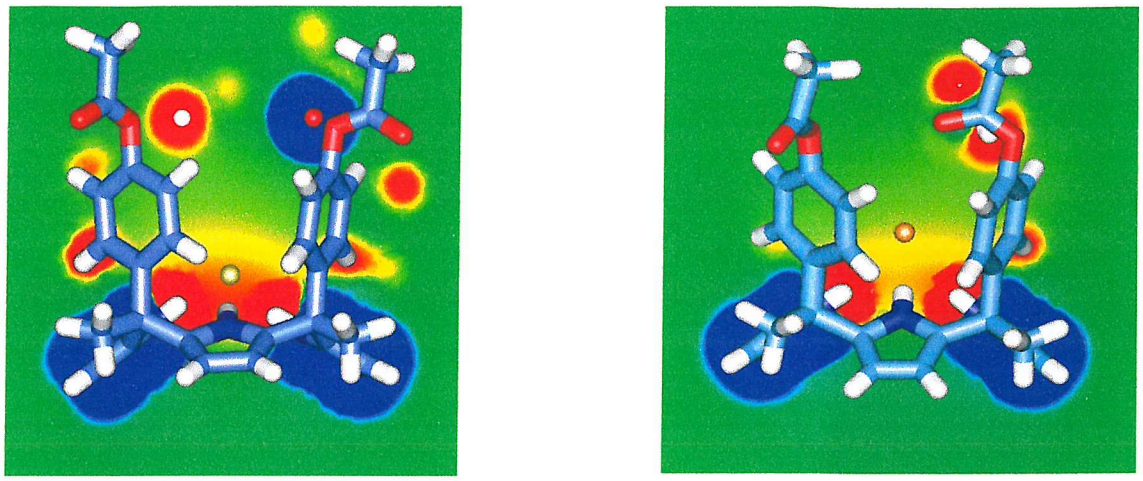

(a) (b)

Figure 3.17: Electrostatic potential on a slice through the centre of the calixpyrrole **73** (red = +ve, blue = -ve). (a) The fluoride is small enough to fit in the calix[4]pyrrole pocket, whereas chloride (b) can not fit in the macrocycle cavity.

These results were confirmed by solid-state studies. Slow evaporation of a dichloromethane solution of compound **73** in the presence of an excess of fluoride (as tetrabutylammonium salt) led to the formation of X-ray quality single crystals. The structure shown in Figure 3.18, reveals the receptor coordinating the guest fluoride anion in a cone conformation. The N···N cross-ring distances (4.600(7) and 4.591(8)Å) are smaller than those observed for the both the DMSO or the acetonitrile complexes, reflecting the smaller radius of fluoride and hence the need for the pyrrole rings to adopt a more distorted conformation. The cavity formed by the *meso*-C atoms is an average of 5.058(7)Å in length and 7.1525(4)Å diagonally (see appendix A for crystallographic table). The fluoride sits inside the cavity of the receptor very close to the pyrrolic NH groups, interacting through the formation of four hydrogen bonds (distance $N_{pyrrole}$-F^- = 2.734(7) Å).

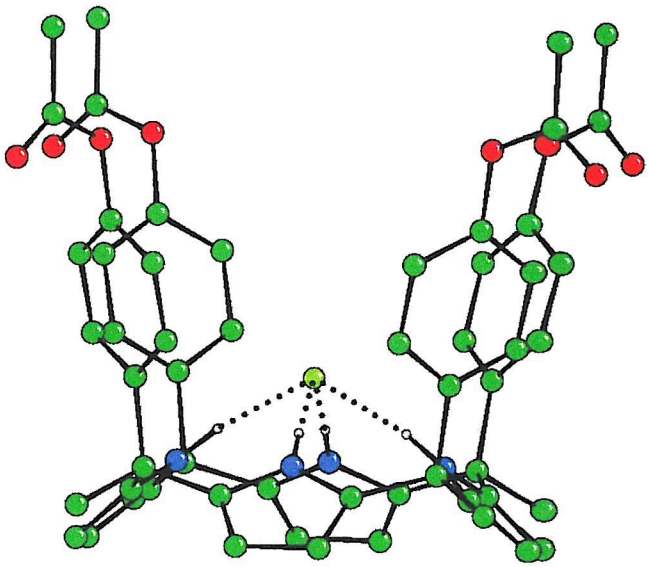

Figure 3.18: Crystal structure of the complex **73**/fluoride. The receptor adopts a cone conformation and coordinates the anionic guest species through the formation of four hydrogen bonds ($N_{pyrrole}$-F^- = 2.734(7) Å).

3.4 Conclusions

The synthesis of three novel 'super-extended' cavity calix[4]pyrrole has been achieved by functionalization of the known αααα-tetra-phenoxy-calix[4]pyrrole **39**. These compounds exhibit novel anion binding behaviour. The crystal structures of these receptors reveal that they adopt a cone conformation interacting with a molecule of solvent as previously observed for extended cavities calix[4]pyrrole (e.g. compound **39**). However the cone conformation has been observed in the solid state also in the absence of any either anionic or neutral coordinated species.

The anion complexation studies of these compounds provided even more interesting results. In both acetonitrile-d_3 or DMSO-d_6 compounds **71-73** showed slow complexation/decomplexation process at room temperature. Similar behaviour has been observed for other calix[4]pyrrole derivatives only in dichloromethane solution at very low temperatures (-80°C). Moreover in DMSO-d_6 solution these new 'super-extended' cavity calix[4]pyrroles were found to bind fluoride selectively, even in the presence of 100

equivalents of other putative anionic guests such as chloride, bromide, iodide, dihydrogenphosphate and hydrogensulphate. This is novel behaviour and may provide the basis in the future for a new generation of fluoride sensors that are insensitive to the presence of other anionic species.

4 Bis-amidinium calix[4]arene derivatives: new receptors for bis-carboxylates

4.1 Introduction

Calixarenes are [1n]metacyclophanes that acquired their name due to the resemblance of the shape of one of the smallest members of their family to a Greek vase called a calix crater. The name was initially chosen to apply specifically to the phenol-derived cyclic oligomers, but has subsequently taken on a more generic aspect and is now applied to a wide variety of structurally related types of compounds (such as the calixpyrroles, calixindoles,[91] calixfurans,[53] etc.).

The first step along the path of the calixarenes synthesis was taken by Zinke[92] and co-workers, who continued the previous work of Baeyer[93] and Baekeland[94] on the condensation of phenol and formaldehyde. Heating *p-tert*-butylphenol with formaldehyde in the presence of sodium hydroxide, Zinke was able to isolate a crystalline product that he later showed was the cyclic tetramer shown in Scheme 4.1. However the synthetic methodology reported by Zinke was improved throughout the last century, by Cornforth[95,96] (1950s) and Gutsche (1970s).[97]

The ready availability of the calixarenes from cheap starting materials has been an important factor in the rapid escalation of research in this field during the last decades.

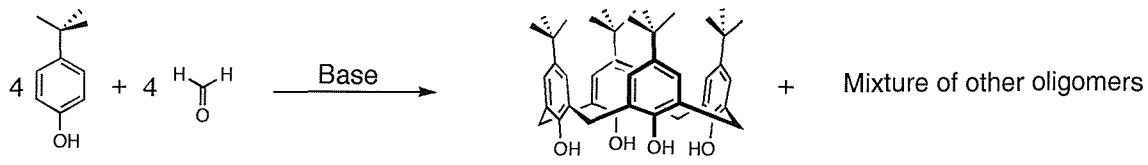

Scheme 4.1: Synthesis of the *p-tert*-Butylcalix[4]arene.

p-tert-Butylcalix[4]arene is obtained from the basic catalysed condensation of *p-tert*-butylphenol and formaldehyde (Scheme 4.1). In fact heating *p-tert*-butylphenol with formaldehyde in the presence of sodium hydroxide corresponding to 0.045 equivalents with the respect of the phenol, results in a thick viscous product called 'precursor'. After refluxing this precursor in diphenyl-ether the *p-tert*-butylcalix[4]arene is recrystallized from toluene in 50% yield.[97] The use of the correct amount of base proved to be a key factor. As a matter of fact, increasing the concentration of sodium hydroxide causes the yield of the calix[4]arene to fall leaving the cyclic hexamer as the major product (Figure 4.1).[98]

The nature of the base proved to have a significant effect. As a way of example, when potassium hydroxide is used in the above procedure the *p-tert*-butylcalix[6]arene is isolated in 80-85% yield.[85] The penta-, hepta- and octa-mer have been synthesized by changing the reaction conditions such as the solvent, the temperature and again the base. The synthesis of the *p-tert*-butylcalix[8]arene was achieved by using xylene as the solvent and sodium hydroxide as the base in 60-65% yield.[85] If the reaction is carried out in tetralin and in the presence of potassium *tert*-butoxide the cyclic pentamer was isolated in 5% yield.[99] The cyclic heptamer was prepared by using dioxane as the solvent and sodium hydroxide as the base in 6% yield.[100]

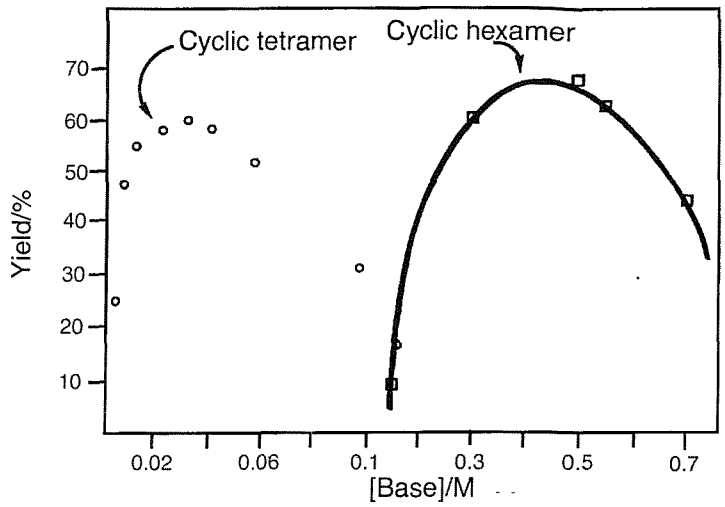

Figure 4.1: Effect of the concentration of sodium hydroxide in the synthesis of *p-tert*-butylcalix[4]arene.

Gutsche also carried out a detailed structural study on calix[4]arenes revealing that these macrocycles can adopt four different conformations: cone, partial cone, 1,2-alternate and 1,3 alternate[101] (Figure 4.2). ^{1}H-NMR has been a powerful technique in distinguishing these conformers. Indeed the ^{1}H NMR pattern of the methylene protons proved to be distinctive for the different conformations adopted by the calixarene (Table 4.1).

Cone	One pair of doublets
Partial cone	Two pairs of doublets (ratio 1:1) or one pair of doublets and one singlet (ratio 1:1)
1,2-Alternate	One singlet and two doublets (ratio 1:1)
1,3-Alternate	One singlet

Table 4.1: ^{1}H NMR pattern of the methylenic proton of calix[4]arenes in various conformations.

Although calix[4]arenes feature a high conformation mobility, freezing one particular conformation has been possible in a variety of ways. Since conformational inversion in the caixarene involves the rotation of the phenyl rings in a direction that brings the hydroxy groups through the annulus, replacement of the OH groups with bulky moieties proved to be useful in locking the macrocycle in a certain conformation. As an example ester and ether derivatized *p-tert*-butylcalix[4]arenes (e.g. **74**) were found to adopt a cone conformation in

the solid state,[102] whereas the tetra acetate derivative **75** was revealed to be locked in a partial cone conformation.[103]

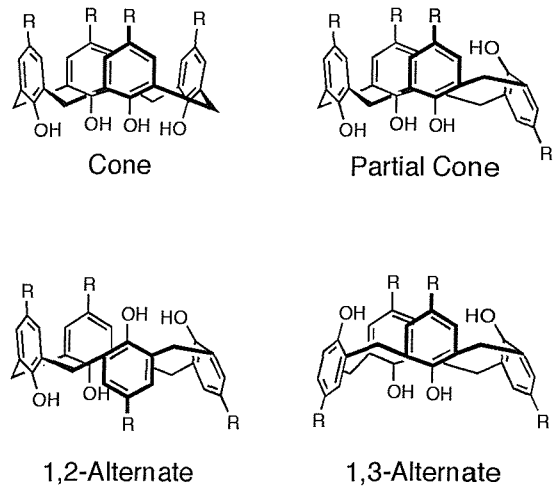

Figure 4.2: Representation of the calix[4]arene conformation.

Conformational freezing *via* upper rim functionalization has also been achieved. In 1985 Bohmer and co-workers reported the synthesis of a series of calix[4]arenes bridged on the upper rim (e.g. **76**) that were locked in a cone conformation between –63 and +182°C.[104]

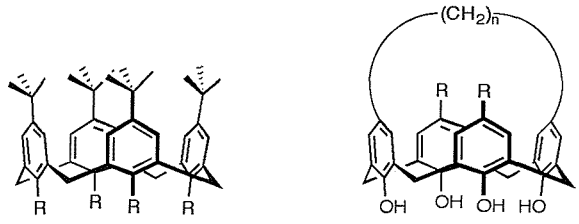

74 R = OCO_2Et

75 R = $OCOCH_3$

76

Finally intramolecular hydrogen bonds can force the calixarene scaffold to adopt a certain conformation. For example, the *p-tert*-butylcalix[4]arene adopts a cone conformation at 20 °C in chloroform. However the resonance arising from the methylene groups appears

as a singlet in the same solvent at temperatures above ca. 60°C, consistent with the compound adopting a 1,3-alternate conformation. This conformational fluxionality proved to be more evident in more polar solvents such as acetonitrile. These results are consistent with the formation of a hydrogen bond network between the hydroxy groups at the lower rim of the calix[4]arene (Figure 4.3).[105] Evidence for the formation of intramolecular hydrogen bond comes from the unusually low frequency of the stretching vibration of the OH groups in the IR spectrum of the *p-tert*-butylcalix[4]arene.

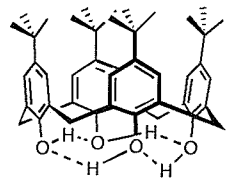

Figure 4.3: Hydrogen bond network within the calix[4]arene lower rim.

Calixarenes provide convenient scaffolds from which a variety of groups can be appended. As a consequence they have been functionalized and investigated for uses such as catalysts[106] and as biomimics[107]; moreover the growing interest for these compounds in the industrial field is attested by an increasing number of patents describing calixarenes.[108]

Functionalised calixarenes have been used also as receptors for cations,[86] anions,[109] and neutral guests.[110]

Cameron and Loeb have synthesised calix[4]arenes **77**, **78** and **79** (Scheme 4.2) containing amide groups with a different number of electron withdrawing chloro-substituents at the 1 and 3 position of the upper rim.[111] The spatial arrangements of the amide groups makes these molecules selective for Y-shaped anions such as carboxylate over tetrahedral anions such as ReO_4^- and phosphate.

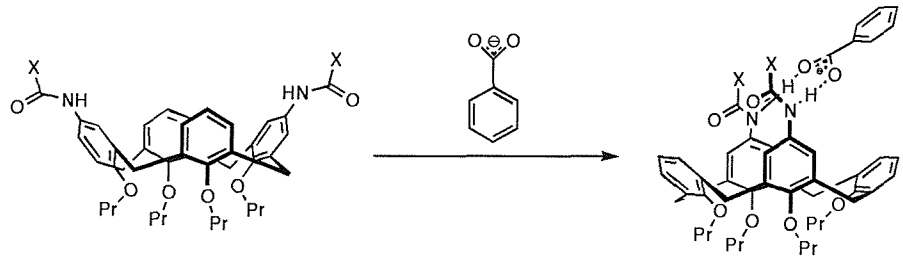

77 X = CH_2Cl
78 X = $CHCl_2$
79 X = CCl_3

Scheme 4.2: Pinched cone motif of a calix[4]arene derivative.

The strong binding of the anionic species is attributed to the calixarene adopting a 'pinched cone' conformation with the calixarene rings attached to the two amide groups becoming parallel, so allowing the amide groups to align in a complementary manner to the carboxylate guest.

Functionalization of the lower rim of *p-tert*-butylcalix[4]arene with either four or two (thio)urea groups, results in a class of receptors selective for spherical anions that are bound exclusively through hydrogen bonding.[112] For example compound **80** shows its highest selectivity for chloride in $CDCl_3$ ($K_{ass.}$ Cl^- = 7.1x10^3 M^{-1}).

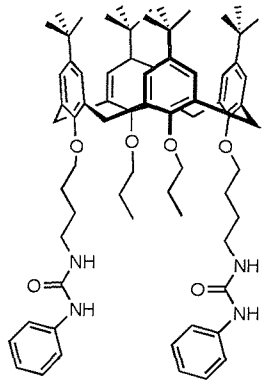

80

Beer and co-workers have prepared lower rim substituted calix[4]arene bis-pyridinium receptors (**81a,b**) that were shown to bind a variety of anionic guest species.[113] Proton NMR studies in DMSO-d_6 solution revealed **81a** and **81b** to complex dihydrogenphosphate,

chloride, bromide, and hydrogensulphate anions with a 1:2 receptor to anion stoichiometry with **81a** exhibiting selectivity for dihydrogenphosphate (K_1 = 45225 M^{-1}).

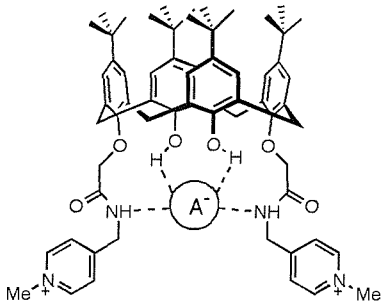

81a

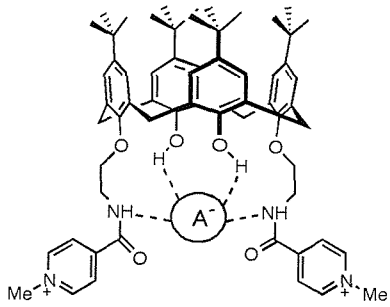

81b

Ungaro and co-workers produced a series of calix[4]arene based ditopic receptors containing an anion binding urea or thiourea group at the upper rim in addition to cation binding amide groups at the lower rim (**82a,b** and **83**).[114]

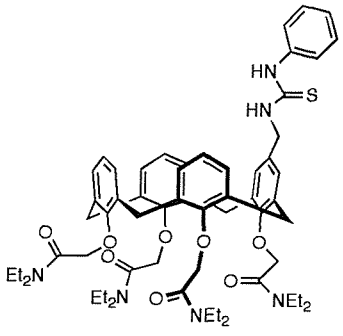

82a X = S
82b X = O

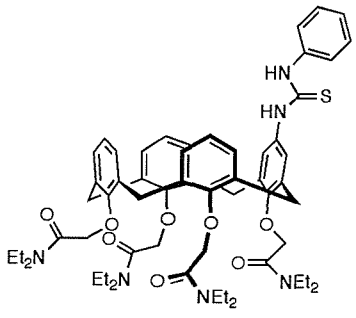

83

Quantitative binding studies in DMSO-d_6 with compound **83** showed that sodium complexation at the lower rim increases the efficiency but decreases the selectivity of anion binding at the top of the calixarene. Compound **82a** contains a methylene group as a spacer between the thiourea and the calixarene. As a consequence of that, the addition of sodium ions had little effect on the anion coordination ability of the receptor, since the lack of conjugation did not allow the positive charge to influence the acidity of the urea NH groups.

Amidinium groups have been attached to the lower rim of calix[4]rene in order to produce templates capable of coordinating carboxylate anions. Gale has reported the synthesis of the chloride salts of calix[4]arenes **84** and **85** and showed by UV-vis spectroscopy that anions such carboxybenzo[15]crown-5 assemble at the lower rim.[115]

The investigation of the anion coordination properties of compound **84** and **85** toward a series of mono- and bis- carboxylate anions has been one of the target of our research.

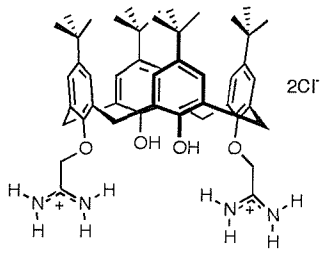

84

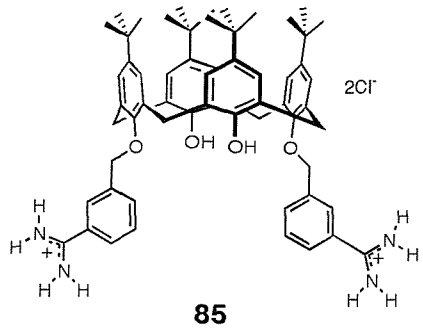

85

4.2 Synthesis and characterization

Bis-amidinium calix[4]arenes **84** and **85** have been prepared in according with literature.[115] *p-tert*-Butylcalix[4]arene was previously reacted with bromoacetonitrile[116] and α-bromo-*m*-tolunitrile[115] to afford compound **86** and **87** respectively (Scheme 4.3). These compounds have then been reacted with alkylchloroaluminium amides prepared in situ from $AlMe_3$ and NH_4Cl in according with the Garigipati methodology[117] in order to obtain the chloride salts of the calix[4]arenes amidinium derivatives **84** and **85**. Anion metathesis was achieved by reacting these compounds with $AgPF_6$ followed by Sephadex® gel chromatography purification, in order to obtain compounds **88** and **89** (Scheme 4.3). Hexafluorophosphate has been chosen as counteranion since it does not bind to the anion binding site of the receptors and therefore is considered relatively 'innocent'.

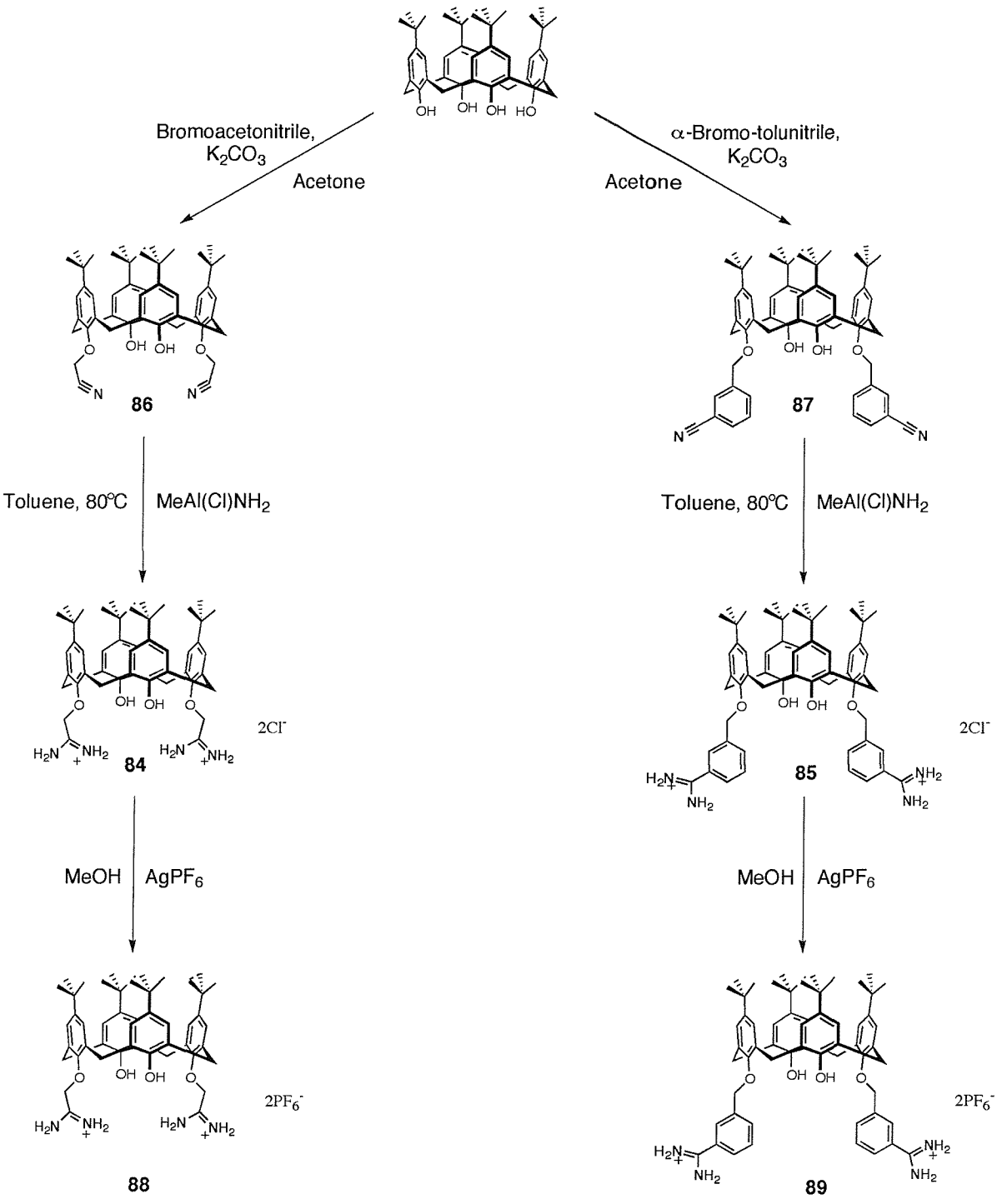

Scheme 4.3: Synthesis of the bis-amidinium calix[4]arenes **88** and **89.**

Crystallization of compounds **88** and **89** from a variety of solvents such as DMSO, acetonitrile, dichloromethane and methanol proved to be unsuccessful. However yellow crystals of the picrate salt of compound **88** have been obtained by dissolving an excess of

sodium picrate in an ethanol solution of **88** followed by filtration and slow evaporation (work carried out in collaboration with Prof. A.H. White and Dr. B. Skelton at UWA and Dr M.I. Ogden at Curtin).[118] The crystal structure was consistent with the formation of a 1:2 receptor:picrate complex in a unit cell where ~2.25 molecules of ethanol were also present (Figure 4.4). In the crystal structure receptor **88** adopts a distorted cone conformation and hosts a molecule of ethanol solvent, oriented with the methyl group into the cavity (see Appendix for structure information). A hydrogen bonding network is formed between the phenolic OH groups and the amidinium moieties (average O···N distance 2.811(6)Å). The picrate anions are coordinated to each of the two amidinium groups *via* the formation of a hydrogen bond motif that resembles the one observed in the picrate salt of L-arginine.[119]

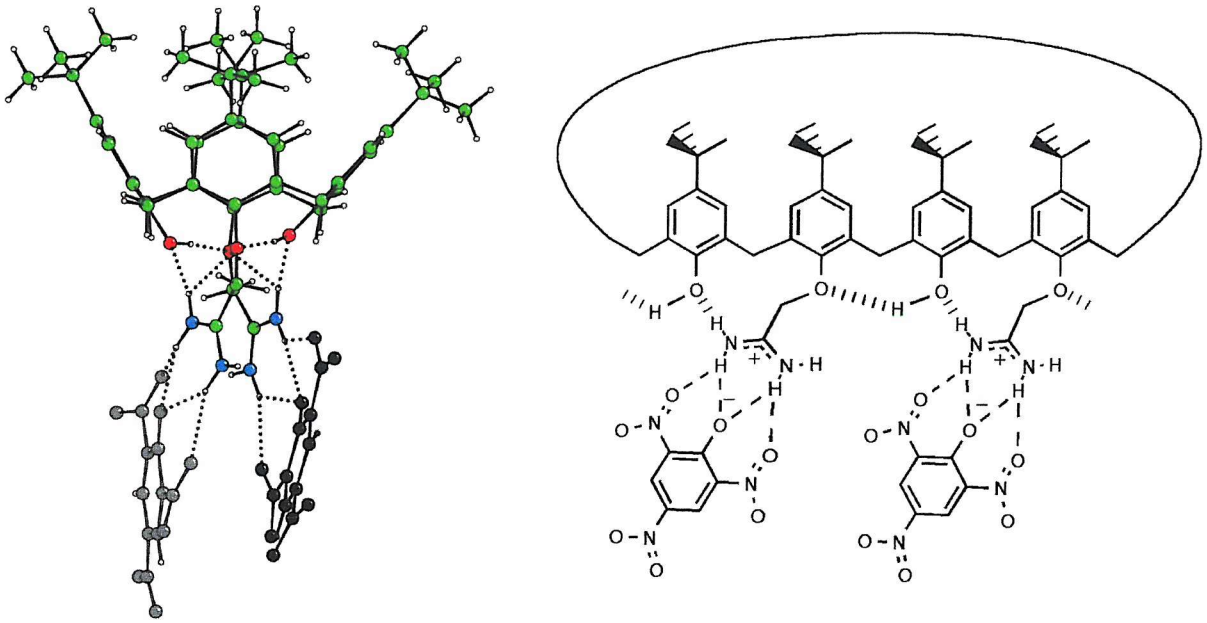

Figure 4.4*:* Hydrogen bonding array between the bis acetoamidinium calix[4]arene **88** and two molecules of picrate.

Slow crystallization of compound **88** from a methanol solution led to the formation of single crystals suitable for X-ray crystallographic analysis. However the crystal structure revealed the presence of an unexpected guest.[120]

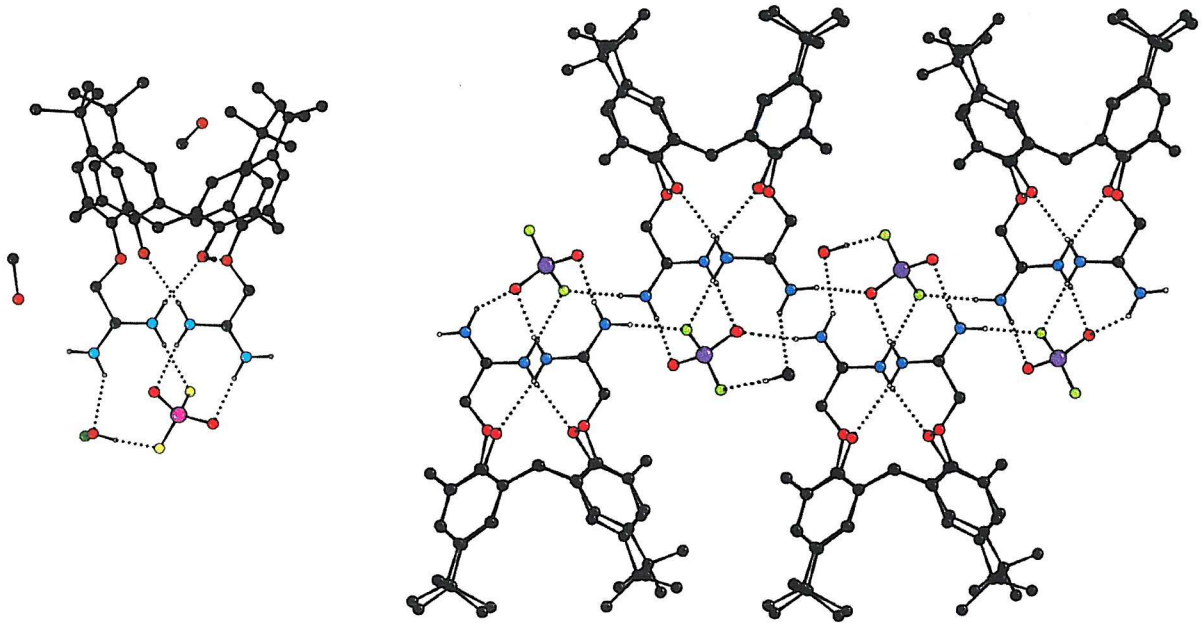

Figure 4.5: Crystal structure of the complex **88**/$PF_2O_2^-$. The difluorophosphinate anion is coordinated by the amidinium groups of the calixarene forming a pseudo one-dimensional hydrogen bond network.

Figure 4.5 shows a molecule of difluorophosphinate ($PF_2O_2^-$), a known hydrolysis product of the hexafluorophosphate, coordinated to a molecule of the bis-amidinium calix[4]arene **88**. It was subsequently found that this anion was present as an impurity in the silver hexafluorophosphate. In fact an old batch (ca. 3 years old) of this reagent was used on one occasion to achieve the metathesis of the chloride salt **88**. $^{31}P\{^1H\}$ NMR spectroscopy revealed two resonances in a sample of the silver hexafluorophsphate consistent with the presence of both hexafluorophosphate and difluorophosphinate anions (Figure 4.6). However the latter anion was not detected by negative electrospray mass spectroscopy.

In the solid state the bis-amidinium calix[4]arene **88** adopts a cone conformation, revealing the formation of one intramolecular hydrogen bond between the phenolic oxygens at the lower rim (see Appendix for structure information). Moreover each amidinium moiety forms a hydrogen bond with the phenolic oxygen (average N···O distance 3.018(10)Å) as was observed previously for the picrate salt. The amidinium arms are consequently twisted round into an offset parallel configuration. The difluorophosphinate anion is coordinated to one amidinium group *via* the formation of two hydrogen bonds between the anion oxygens and the amidinic NH groups. (average NH···O 2.788(11)Å). One fluorine interacts with the

second amidinium moiety through the formation of one hydrogen bond (distance NH···F 2.791(11)). Two molecules of methanol coordinate the fluorine and the amidinium NH groups ($OH_{methanol}$···F = 2.747(2)Å, $OH_{methanol}$···$NH_{amidinium}$ = 2.906(1)Å) that are not involved in the formation of the complex **88**/$PF_2O_2^-$. The difluorophosphinate anions also form a second hydrogen bond to an adjacent calixarene molecule so forming chains of calixarenes in the solid state (Figure 4.5b).[120]

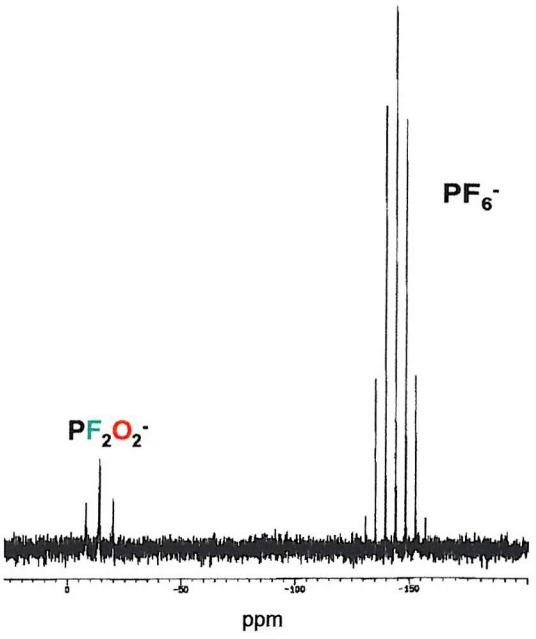

Figure 4.6: $^{31}P\{^1H\}$ NMR of the silver hexafluorophosphate used to prepare compound **88**. The triplet is attributed to the presence of traces of difluorophosphinate anions.

Coordination of the difluorophosphinate anion was an unexpected result however it represents an important achievement. The literature provides a variety of crystal structures featuring the presence of this anion. In most cases, the anion was found to be coordinated through one or both the oxygens to a metal centre,[121] although crystal structures of the free anion have been also elucidated.[122] However, to the best of our knowledge, this is the first occurrence of difluorophosphinate in a complex hydrogen bond network, and suggests that this anionic species may play an important role in promoting anion-directed assemblies in the solid state. The absence of difluorophosphinate anion in the batch of **88**·PF_6 that was used in the anion coordination studies was confirmed by IR measurements.

4.3 Binding studies results. The discovery of multiple equilibria in solution

The anion complexation properties of the two bis-amidinium calix[4]arenes **88** and **89** have been investigated using ^{1}H NMR titration techniques in DMSO-d_6.[118] The high affinity of the amidinium cation for the carboxylate anion has been previously discussed. Therefore the coordination of a variety of aliphatic and aromatic carboxylate anions by **88** and **89** has been investigated. Different aliphatic dicarboxylate species such as malonate, succinate, glutarate, adipate and pimelate have been used in order to investigate whether the chain length of these dicarboxylate anions could influence the type of interaction observed.

Moreover the possibility of an anion-directed assembly of receptors **88** and **89** (Figure 4.7) made these compounds very interesting substrates to work on.

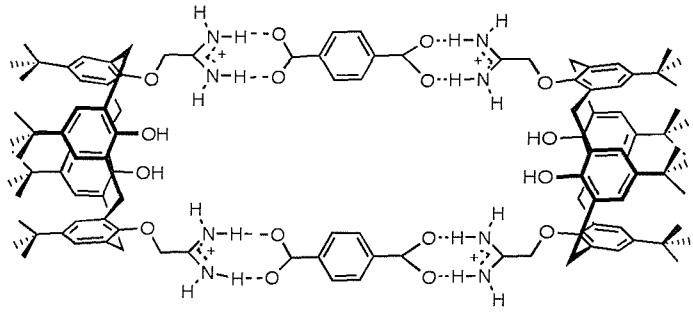

Figure 4.7: An hypothetical example of self-assembling promoted by an anionic species.

The anion coordination properties of compound **88** have been investigated with carboxylates. Upon addition of acetate anions (as the tetrabutylammonium salt) to a DMSO-d_6 solution of this receptor a titration curve was obtained that was consistent with the formation of a 2:1 anion to receptor complex (K_1 = 990M^{-1}, K_2 = 960 M^{-1}, errors<12%) (Figure 4.8). The 2:1 stoichiometry, confirmed by Job Plot experiments, showed that the two amidinium groups bind independently two acetate anions with similar stability constant values.[118]

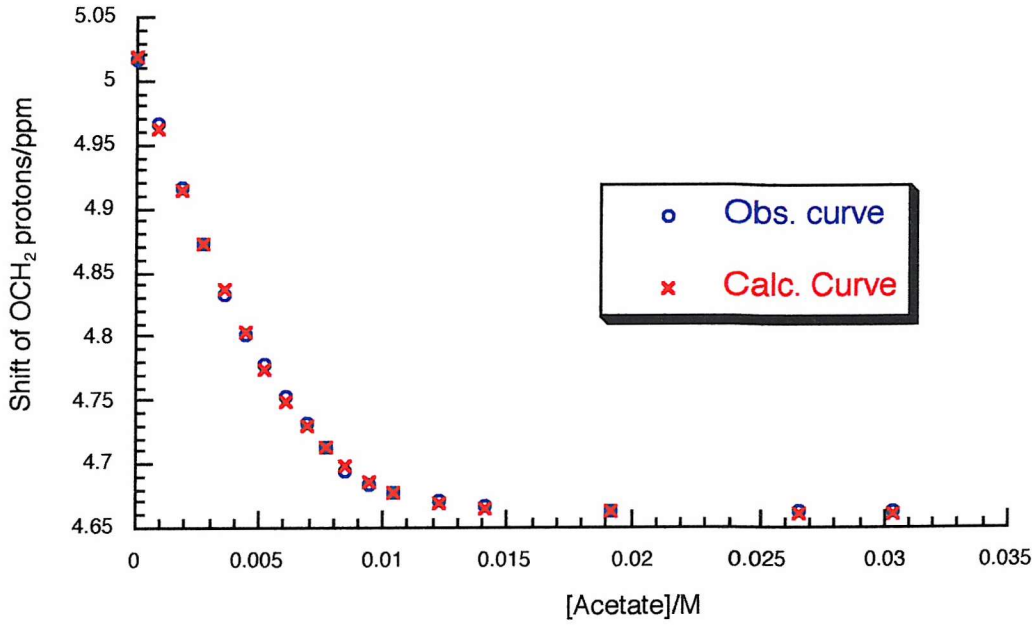

Figure 4.8: Titration curve for the complexation of compound **88** by tetrabutylammononoium acetate. The fitting model is consistent with the formation of a 2:1 anion to receptor stoichiometry.

Addition of malonate, succinate, glutarate, adipate and suberate (as their tetrabutylammonium salts, see chapter 5 for synthesis details) also gave evidence of the formation of a 2:1 complex, however the 2:1 model did not fit any of the titration curves. The titration profiles showed a 'stall' after addition of approximately one equivalent of anion that proved to be more evident as the dicarboxylate chain length increased (Figure 4.9). This behaviour has been attributed to the presence of multiple equilibria in solution. Indeed the crystal structure of compound **88** as both picrate and difluorophosphinate salt, shows the amidinium moieties oriented in a parallel but divergent manner because of the hydrogen bond interactions to the lower rim of the calixarene. Therefore the longer dicarboxylate anion could initially form a lower-rim bridged 1:1 complex that, upon addition of a further amount of anion may break and direct the system to the formation of a 2:1 complex (Scheme 4.4). However malonate is possibly too short to form a bridged 1:1 complex and therefore the titration curve does not show any 'stall'.

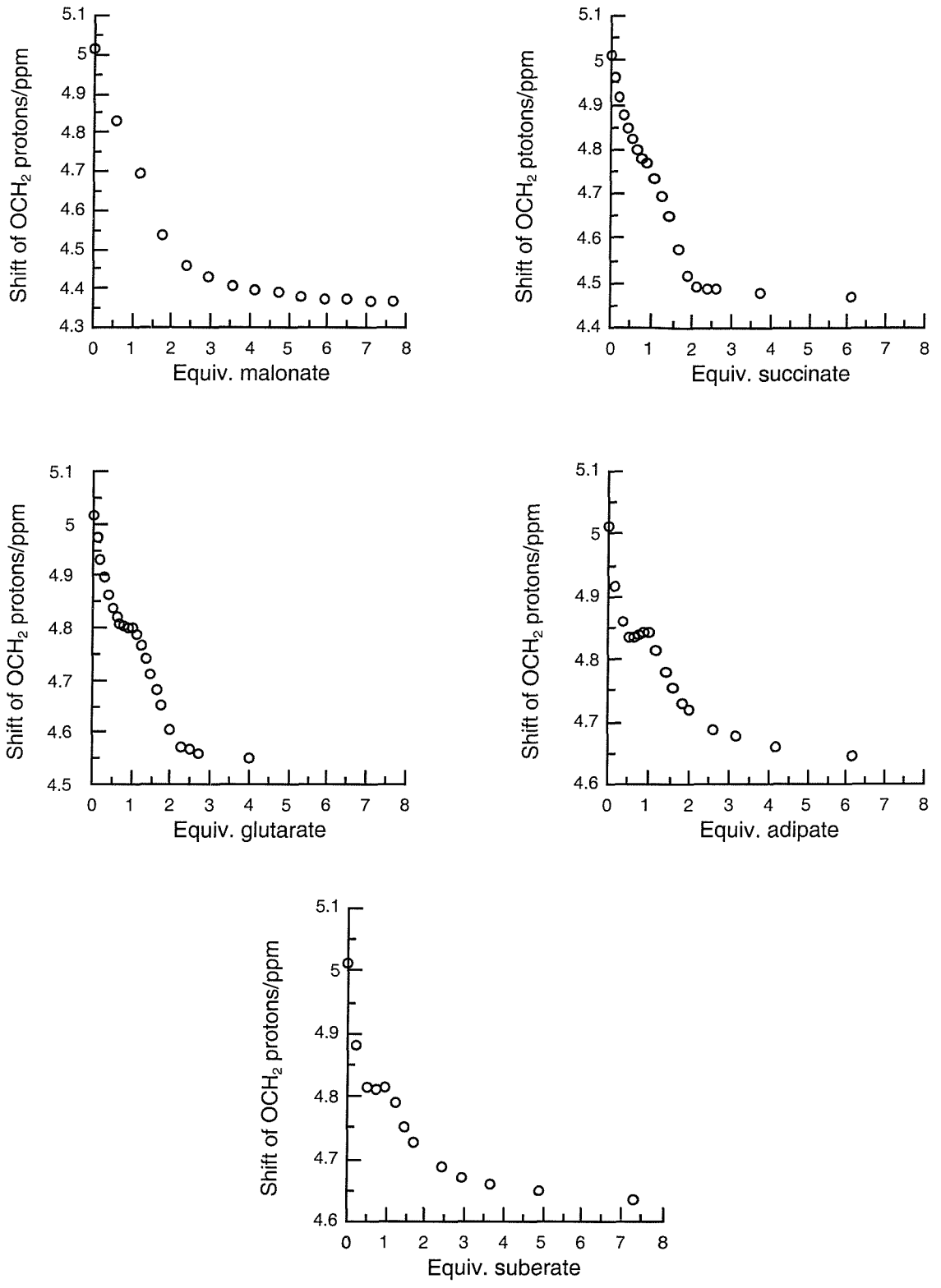

Figure 4.9: Addition of different length aliphatic dicarboxylate anions to a DMSO-d_6 solution of **88** produced a more marked 'stall' as chain length increased.

The anion binding properties of **88** toward aromatic dicarboxylate was also investigated. Addition of isophthalate anion to a DMSO solution of **88** provided a similar titration curve than the one observed for aliphatic dicarboxylate anions. Solubility problems did not allow any investigation of the complexation properties of **88** toward terephthalate anions.

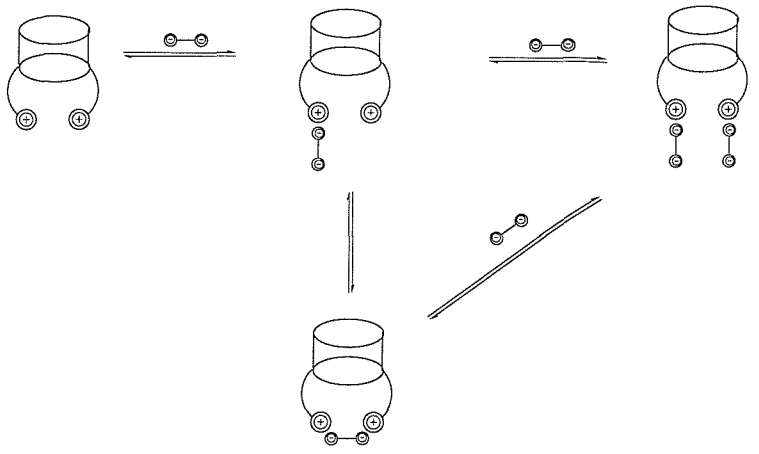

Scheme 4.4: Graphical representation of the multiple equilibria in solution for dicarboxylate complexes of receptor **88**.

In compound **89** the amidinium moieties are far from the lower rim of the calixarene and therefore their orientation is not constricted by the formation of intramolecular hydrogen bonds. Upon addition of acetate, malonate, succinate, glutarate, adipate and pimelate titration curves have been obtained consistent with the formation of 2:1 anion to receptor complexes. Proof of such stoichiometry came from Job plot analysis (Figure 4.10). Although the titration curves did not show any 'stall', a satisfying fit with a 2:1 model could not be achieved, suggesting multiple equilibria in solution.

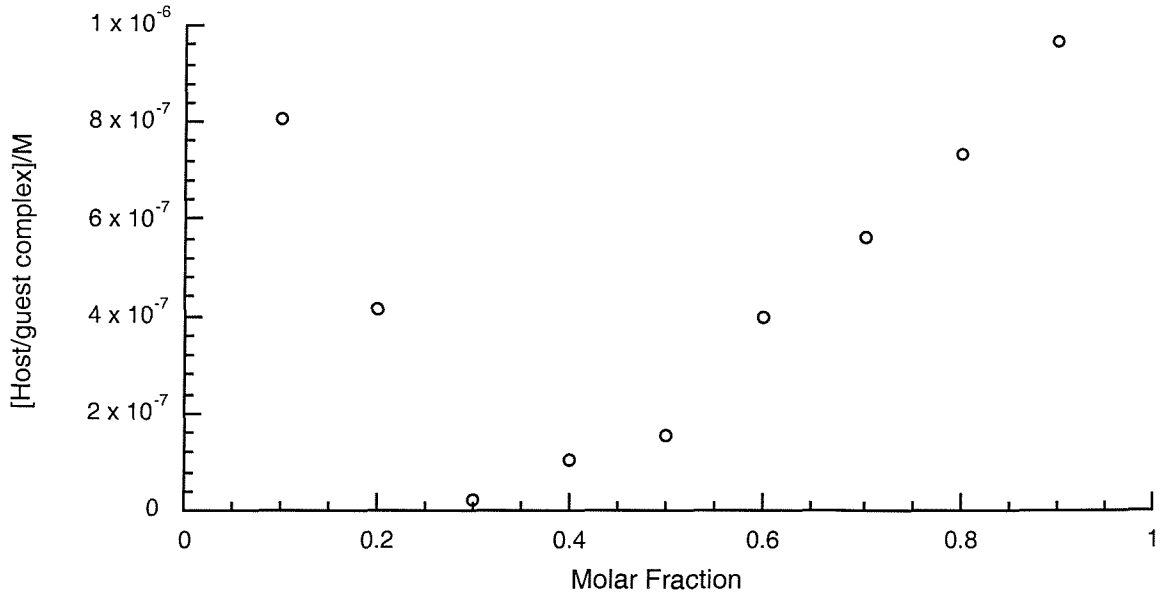

Figure 4.10: Job plot analysis of the system **89**/malonate. The minimum point at 0.3 suggest the formation of a 2:1 anion to receptor complex.

Further evidence of multiple equilibria in solution came from the investigation of the complexation properties of receptor **89** toward isophthalate anion. Addition of this guest to a DMSO-d_6 solution of **89** produced an unusual titration curve (Figure 4.11). Upon addition of less than one equivalent of anion, the benzamidinium protons *para* to the amidinium group showed an up-field shift. However further addition of isophthalate produced a reverse down-field shift. This behaviour may be attributed to the formation of a bridged 1:1 complex at low concentration of anion, followed by the formation of a 2:1 complex at higher anion/receptor ratio (Figure 4.12). However the bridged 1:1 complex may represent a high energy adduct as the receptor adopts a constricted distorted conformation. Among the considered anions the isophthalate is probably the one that structurally is more suitable for the formation of the 1:1 complex, revealing the most marked evidence. Indeed addition of terephthalate anions did not show any shift direction change but rather a continuous down-field shift.[118]

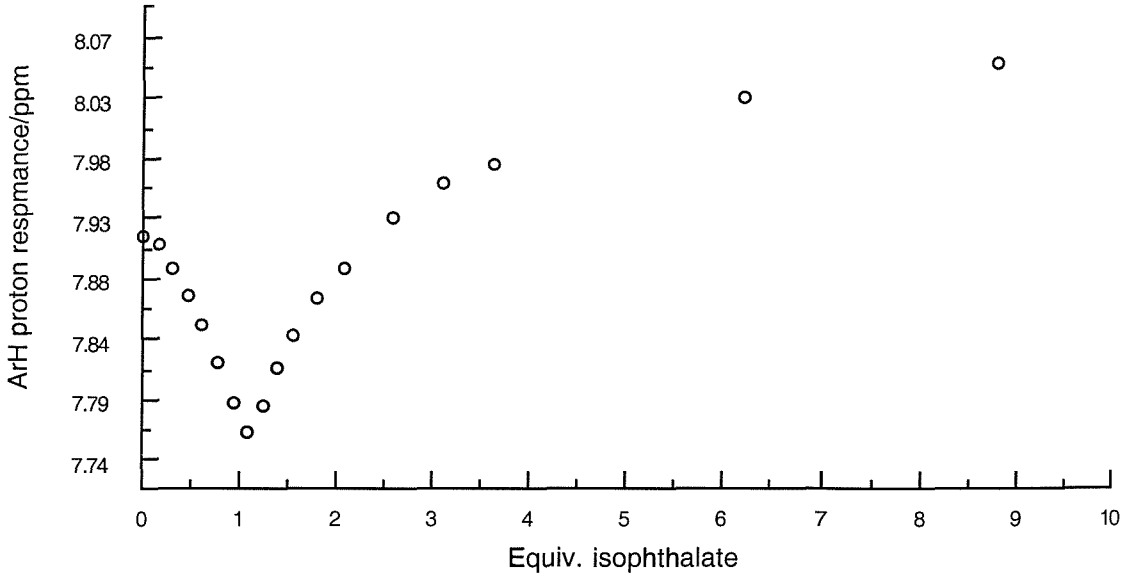

Figure 4.11: ^{1}H NMR titration curve of receptor **89** with isophthalate anions.

Evidence of the presence of different interactions between the anion and the receptors came from the solid-state study. The malonate salt of **89** was prepared by adding an aqueous solution of sodium malonate to an ethanol solution of the receptor. After removing the solvent the salt was obtained by extraction in dichloromethane.

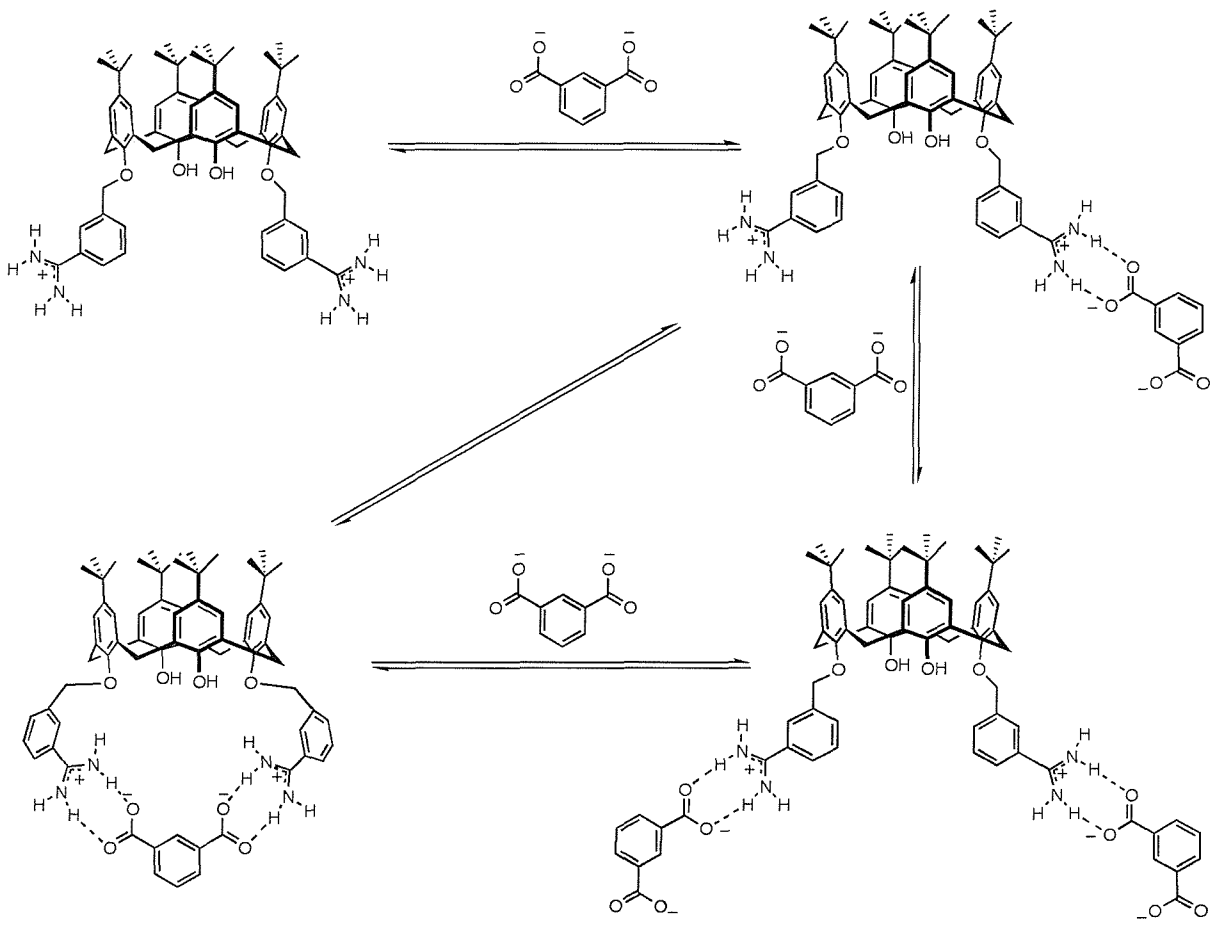

Figure 4.12: Multiple equilibria in solution during the NMR titration of the bis-amidinium calix[4]arenes **89**.

Slow evaporation of an ethanol/dichloromethane (50/50 v/v) of the malonate salt produced single crystals suitable for X-ray analysis. The crystal structure (Figure 4.13), is consistent with the formulation of the complex **89**·$(CH_2(COO^-)_2)$·4EtOH·H_2O (see Appendix for structure information).[118]

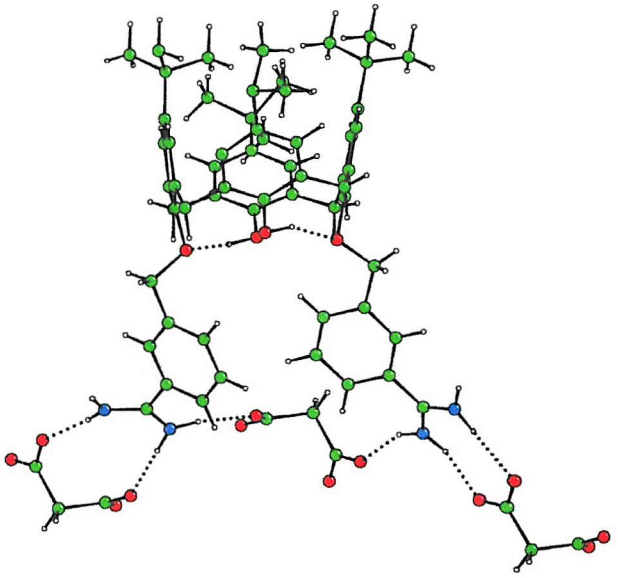

Figure 4.13: Crystal structure of the malonate salt of **89**. The structure points out the multiple interaction modes between receptor **89** and the malonate anions.

In this crystal structure the calixarene adopts a significantly distorted cone conformation revealing dihedral angles relative to the methylene-C_4 plane for ring 1-4 of 77.5(2), 47.7(2), 86.5(2) and 44.8(2)° respectively. This structure shows three different binding motifs between the receptor and the coordinated malonate anion. One is the expected amidinium/carboxylate bond due to the electrostatic interaction and the formation of two hydrogen bonds between these moieties. A second binding mode is a bridged coordination in which one oxygen of each carboxylate group interacts with one amidinic NH group through the formation of two hydrogen bonds. In addition two oxygens belonging to two different carboxylate groups within the same molecule of malonate are bound to one amidinium group interacting again through the formation of two hydrogen bonds. The last binding motif is probably unique for the malonate and is due to the short chain length of this dicarboxylate anion. The cation, anion and water are linked together in the solid state through the formation of an extended hydrogen bond network shown in Figure 4.14.

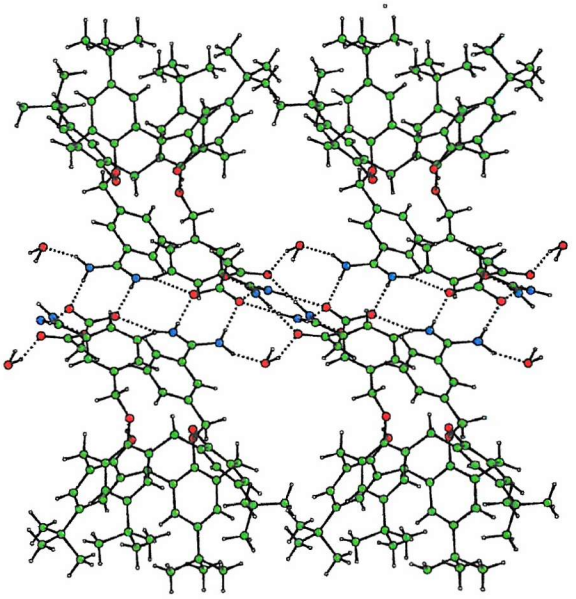

Figure 4.14: A complicated hydrogen bond network leads to an extended packing of molecule of **89** mediated by malonate anions and water (diagram viewed down the *a* axis; ethanol molecules excluded for clarity).

Therefore the solid state structure revealed that the bis-amidinium derivative **89** is able to coordinate dicarboxylate anions with a variety of binding motifs. Consequently ^{1}H NMR titration techniques do not represent a suitable method for the determination of the stability constant, since neither a pure 1:1 nor 1:2 complex is formed.

4.3 Conclusions

Anion complexation studies have been carried out on bis-amidinium calix[4]arenes **88** and **89**, in order investigate whether these compounds could behave as efficient receptors toward carboxylate and dicarboxylate anions. ^{1}H NMR titration techniques have been used to obtain the stability constant values and Job plot analysis to determine the stoichiometry of the host/guest complex. Although determination of the stability constants could not be achieved in all cases, the NMR experiments proved to be useful in elucidating the processes occurring in solution. Unusual titration curves have been obtained consistent with multiple equilibria. A possible process is the formation of bridged 1:1 complexes at low

concentration of dicaboxylate anions followed by the formation of a 2:1 complex when the concentration was further increased.

Moreover X-ray crystallographic analysis always revealed the presence of extended hydrogen bonds network and the co-existence of a variety of binding motifs between the receptors and the anion.

5. *Experimental*

5.1 Solvent and Reagent Pre-treatment

Where necessary solvents were purified prior to use. Dichloromethane was distilled over calcium hydride. Toulene was distilled from sodium. Tetrahydrofuran and diethyl ether were distilled from sodium using benzophenone as an indicator. Anhydrous acetonitrile (water < 0.003%) was acquired from Fluka. Triethylamine was distilled from KOH and stored under nitrogen in the presence of an excess of KOH pellets. Thionyl chloride was distilled from 10% (w/w) triphenyl phosphite and stored under nitrogen. Unless otherwise stated on the text, commercial grade chemicals were used without further purification. Reagents prepared in accordance with literature are so referenced. All the synthesis have been performed under nitrogen.

5.2 Instrumental methods

NMR spectra were recorded on Bruker AM300, AC300 and DPX400 spectrometers. Operating frequency have been used of 300 MHz for proton analyses, 75 MHz for ^{13}C analyses, 161 MHz for ^{31}P (referenced to H_3PO_4) and 376 MHz for ^{19}F (referenced to C_6F_6), Ultra-violet/Visible spectra were recorded on a Perkin Elmer Lambda 6 spectrometer. Low resolution mass spectra were recorded on Micromass Platform single quadrupole mass spectrometer (in acetonitrile), whereas high resolution mass spectra were performed on VG 70-SE Normal geometry double focusing mass spectrometer (in dichloromethane) by the Mass Spectrometry service at the University of Southampton. Elemental analyses were carried out at the University of Strathclyde and by Medac Ltd. Melting points were recorded in open capillaries on a Gallenkamp melting point apparatus and are uncorrected.

Proton NMR titrations have been carried out by addition of discrete aliquots of a 0.1 M solution of the anion (as the tetrabutylammonium salt) to a 0.01 M solution of the considered receptor in deutereted solvent. Elaboration of the observed data by using an appropriate software (e.g. EQNMR[75]) allowed the calculation of the stability constant.

5.3 Syntheses

5.3.1 Syntheses included in chapter 2

3,4-Diphenyl-1H-pyrrole-2,5-dicarboxylic acid butylamide (58): 3,4-Diphenylpyrrole-2,5-dicarboxylic acid **56**[67] (1g, 3.2 mmol) was refluxed in thionyl chloride (25mL) overnight to obtain the acid chloride. The excess of thionyl chloride was removed by rigorous drying under high vacuum. After dissolving the resulting acid chloride in dichloromethane (30mL), triethylamine(711mg, 7.04mmol) and DMAP (10mg, 0.08mmol) were added followed by butylamine (528mg, 7.04mmol). The reaction was stirred for 48 hours leading to a red suspension. The solvent was removed *in vacuo* and the residue purified by column chromatography (dichloromethane:methanol 95:5) to yield compound **58** (240mg,18%). ^{1}H NMR (DMSO-d_6, 300 MHz) δ 0.91 (t, J = 7.26, 6H, CH_3), 1.23 (m, 4H, CH_2CH_3), 1.37 (m, 4H, CH_2), 3.20 (m, 4H, NCH_2), 7.10 (t, J = 5.46, 2H, Arom.), 7.18 (m, 4H, Arom.), 7.30 (m, 4H, Arom. + obscured amide CONH, 2H), 12.03 (s, 1H, NH). ^{13}C{^{1}H} NMR (DMSO-d_6, 75 MHz) δ 13.7, 19.9, 31.2, 39.0, 124.1, 125.7, 128.1, 128.9, 130.9, 133.6, 160.4. MS (ES$^+$) 418 (M + H$^+$), 440 (M + Na$^+$), 857 (2M+ Na$^+$), 1274 (3M + Na$^+$), 1290 (M + K$^+$). HRMS (ES$^+$): 440.23 (M + Na$^+$), Δ = 0.4 ppm. Anal. calcd. for $C_{26}H_{31}N_3O_2 \cdot {}^2/_3\, H_2O$: C, 72.70; H, 7.59; N, 9.78. Found: C, 72.82; H, 7.37; N, 9.75. Mp: 162^{0}C (decom.).

3,4-Diphenyl-1H-pyrrole-2,5-dicarboxylic acid phenylamide (59): 3,4-Diphenylpyrrole-2,5-dicarboxylic acid **56**[67] (1g, 3.2 mmol) was refluxed in thionyl chloride (25mL) overnight to obtain the acid chloride. The excess thionyl chloride was removed by

rigorous drying under high vacuum. After dissolving the resulting acid chloride in dichloromethane (30mL), triethylamine(711mg, 7.04mmol) and DMAP (10mg, 0.08mmol) were added followed by aniline (654mg, 7.04mmol). The reaction was stirred for 48 hours leading to a red suspension. The solvent was removed *in vacuo* and the residue was crystallized in acetonitrie to yield compound **59** (687mg, 47%). ^{1}H NMR (DMSO-d_6, 300 MHz) δ 7.15 (t, J = 7.29, 2H, Ar), 7.34 (m, 14H, Ar), 7.55 (d, J = 8.19, 4H, Ar), 9.37 (s, 2H, CONH), 12.67 (s, 1H, NH). ^{13}C{^{1}H} NMR (DMSO-d_6, 75 MHz) δ119.3, 123.5, 124.7, 126.8, 127.2, 127.8, 128.7, 130.5, 133.7, 138.5, 158.6. MS (ES$^+$) 480 (M + Na$^+$), 937 (2M+ Na$^+$), 1394 (3M + Na$^+$), 1413 (3M+K$^+$). HRMS (ES$^+$): 480 (M + Na$^+$), Δ = 1.1 ppm. Anal. calcd. for $C_{30}H_{23}N_3O_2 \cdot {}^1/_3\ H_2O$: C, 77.73; H, 5.15; N, 9.07. Found: C, 77.90; H, 4.76; N, 8.80. Mp: 206^{0}C (decom.).

5-Methyl-3,4-diphenyl-1H-pyrrole-2-carboxylic acid ethyl ester (60): The method reported in literature was found to be unsuccessful for a large scale synthesis.[69] A modification of another methodology[70] led to the desired compound. Ethyl benzoyl acetate (49.3g, 0.256mol) was dissolved in acetic acid (100mL) and cooled in an ice bath. A solution of sodium nitrite (21.25g, 0.307mol) in water (32mL) was added dropwise and the solution allowed to stand overnight. Phenyl methyl ketone (34.5g, 0.256mol) was added followed by portionwise addition of zinc powder (36.5g, 0.557mol). The resulting orange suspension was then heated at 120^{0}C for 30 minutes. After cooling to at 50^{0}C the solution was poured into 300mL of ice/water, and stirred for 1 hour. The water was decanted and addition of ethanol (200mL) led to a white solid that was collected by filtration, washed twice with ethanol (30mL) and dried *in vacuo* (14.8g, 18.9%). The compound gave characterisation in accordance with literature.[71]

5-Methyl-3,4-diphenyl-1H-pyrrole-2-carboxylic acid butylamide (61): 5-Methyl-3,4-diphenyl-1H-pyrrole-2-carboxylic acid ethyl ester **60**[70,71] (1g, 3.3mmol) , butylamine (13g, 0.18mol) and sodium cyanide[72] (18mg, 3mmol) were dissolved in dry methanol (20mL) and refluxed for 5 days. The solvent was removed *in vacuo* and the residue purified by column chromatography (dichloromethane:methanol 95:5) (320mg, 29%). ^{1}H NMR (CD_2Cl_2, 300 MHz) δ 0.83 (t, 3H, J = 7.29, CH_2CH_3), 1.13 (m, 2H, CH_2CH_3), 1.29 (m, 2H, $CH_2CH_2CH_3$),

2.39(s, 3H, C*H*$_3$), 3.25 (m, 2H, NHC*H*$_2$), 5.52 (s, 1H, CONH), 7.07-7.42 (m, 10H, arom.), 11.17 (s, 1H, NH). $^{13}C\{^1H\}$ NMR (CD_2Cl_2, 75 MHz) δ 12.26, 13.97, 20.41, 31.86, 39.32, 121.36, 126.12, 128.12, 128.35, 129.31, 130.64, 131.52, 135.87, 136.23, 162.11. MS (ES^+) 333 (M + H^+), 374 (M^+ + CH_3CN), 396 (M + CH_3CN + Na^+), 665 (2M + H^+), 687 (2M + Na^+). HRMS (ES^+): 355.18 (M + Na^+), Δ = 0.9 ppm. Anal. calcd for $C_{22}H_{24}N_2O{\cdot}2.5H_2O$: C, 78.42; H, 7.33; N, 8.31. Found: C, 78.68; H, 7.12; N, 8.31. Mp: 158°C (decomp.)

5-Methyl-3,4-diphenyl-1H-pyrrole-2-carboxylic acid phenylamide (62): Aniline (305mg, 3.3mmol) was dissolved in freshly distilled dichloromethane (10mL) and a 2M solution of trimethyl aluminum in hexane[73] (1.65mL, 3.3mmol) was added dropwise. After stirring for 30 minutes, 5-methyl-3,4-diphenyl-1H-pyrrole-2-carboxylic acid ethyl ester **60**[70,71] (1g, 3.3mmol) was added and the solution refluxed for 3 days. The solution was washed carefully with HCl 2M (20mL) and the phases were separated. The aqueous solution was washed with 20mL of dichloromethane and the organic phases were joined, dried over $MgSO_4$, and filtered off. The solvent was removed *in vacuo* and crystallization in acetonitrile led to the wanted compound (200mg, 17%). ^1H NMR (DMSO-d_6, 300 MHz) δ 2.38 (s, 3H, CH_3), 7.09-7.43 (m, 15H, arom.), 8.20 (s, 1H, CONH), 11.92 (s, 1H, NH). $^{13}C\{^1H\}$ NMR (CD_2Cl_2, 75 MHz) δ 11.65, 118.59, 120.80, 122.15, 122.96, 125.53, 126.93, 127.12, 127.15, 127.81, 128.27, 128.72, 129.00, 129.65, 130.76, 134.76, 134.90,138.54. MS (ES^+) 353 (M + H^+), 705 (2M + H^+). HRMS (ES^+): 375.15 (M + Na^+), Δ = 0.5 ppm. Anal. calcd for $C_{24}H_{20}N_2O{\cdot}CH_2Cl_2{\cdot}0.5{\cdot}H_2O$: C, 67.27; H, 5.19; N, 6.28. Found: C, 67.65; H, 5.55; N, 6.01. Mp: 212°C (decom.).

3,4-Dichloro-1*H*-pyrrole-2,5-dicarboxylic acid bis-butylamide (64): 3,4-Dichloro-1*H*-pyrrole-2,5-dicarboxylic acid diethyl ester **63**[70] (1g, 3.57mmol) was dissolved in methanol (20mL) and butylamine (36mL, 0.36mol) was added together with a catalytic quantity of NaCN (10mg, 0,2mmol).[72] The red solution was refluxed for 4 days. After removing the solvent *in vacuo* a red oil was obtained that was purified by column chromatography (dichloromethane/methanol 97/3) (0.816g, 71%). ^1H NMR ($CDCl_3$, 300 MHz) δ 0.97 (t, 6H, *J* = 7.29, CH_3), 1.42 (m, 4H, CH_3CH_2), 1.61 (m, 4H, NCH_2CH_2), 3.47 (m, 4H, NCH_2), 6.71 (broad s, 2H, CONH), 10.18 (s, 1H, NH). $^{13}C\{^1H\}$ NMR ($CDCl_3$, 75 MHz) δ 13.8, 20.2, 31.6, 39.5, 111.3, 122.6, 158.2 MS (ES^+) 334 (M + H^+), 375 (M + H^+ +

CH_3CN), 669 (2M + H^+) 691 (2M + Na^+), 732 (2M + CH_3CN + Na^+). HRMS (ES^+): 334 (M + H^+), Δ = 0.3 ppm. Anal calcd. for $C_{14}H_{21}Cl_2N_3O_2$: C, 50.31; H, 6.33; N,12.57. Found: C, 50.17; H, 6.23 ; N, 12.20. Mp: 141°C

3,4-Dichloro-1*H*-pyrrole-2,5-dicarboxylic acid bis-phenylamide (65): Aniline (0.65mL, 7mmol) was mixed with dichloromethane (20mL) and trimethyl aluminium (2M hexane solution, 3.5mL, 7mmol) was added dropwise.[73] 3,4-Dichloro-1*H*-pyrrole-2,5-dicarboxylic acid diethyl ester **63**[70] (1g, 3.57mmol) was added to the resulting yellow solution and the misture was refluxed for 5 days. After cooling down the solution was neutralized with HCl 2M until effervescence ceased. The phases were separated and the water solution washed with dichloromethane (30mL). The organic fractions were joined together and the solvent was removed under vacuum. A brown solid formed that was purified by crystallization in acetonitrile (20mL) (150mg, 11%). ^1H NMR ($CDCl_3$, 300 MHz) δ 7.18 (t, 2H, *J* = 7.29, Arom.), 7.38 (m, 4H, Arom.), 7.62 (d, 4H, *J* = 8.19, Arom.), 8.49 (s, 2H, CONH), 10.55 (s, 1H, NH). $^{13}C\{^1H\}$ NMR ($CDCl_3$, 75 MHz) δ 120.6, 123.2, 125.4, 129.5, 137.0, 155.8. MS (ES^-) 372 (M^-), 486 (M + TFA^-), 747 (M--M^-). HRMS (ES^+): 372 (M^-), Δ = 2.3 ppm. Anal. calcd. for $C_{18}H_{13}Cl_2N_3O_2 \cdot H_2O$: C, 55.12; H, 3.85; N, 10.71 . Found C, 55.44; H, 3.88 ; N, 10.53. Mp: 221°C (decom.)

3,4-Dichloro-pyrrolate-2,5-dicarboxylic acid bis-phenylamide tetrabutylammonium (65$^-$TBA$^+$): 3,4-Dichloro-1*H*-pyrrole-2,5-dicarboxylic acid bis-phenylamide **65** (54.2, 0.14mmol) was dissolved in methanol (10mL). Tetrabutylamonium hydroxide 0.1M isopropanol/methanol solution (1.454mL) was added and the solution was stirred for 10 min. After removing the solvent under vacuum the wanted compound was dried by using a high vacuum pump for 12 hours (quantitative yield). ^1H NMR (CD_2Cl_2, 300 MHz) δ 0.93 (t, 12H, *J* = 7.62, CH_3), 1.33 (m, 8H, CH_2CH_3), 1.45 (m, 8H, $^+NCH_2CH_2$), 2.96 (m, 8H, $^+NCH_2$), 7.02 (t, 2H, *J* = 7.62, Arom.), 7.31 (t, *J* = 7.62, 4H, Arom.), 7.72 (d, 4H, *J* = 7.62, Arom.), 9.30 (s, 2H, CONH). $^{13}C\{^1H\}$ NMR ($CDCl_3$, 75 MHz) δ 13.8, 20.1, 24.2, 59.1, 119.5, 122.9, 129.3, 140.3, 162.2. MS (ES^-) 372 (M^-), 988 (2M^- + TBA^+). HRMS (ES^-): 372 (M^-), Δ = 1.2 ppm. Anal. calcd. for $C_{34}H_{48}Cl_2N_4O_2 \cdot H_2O$: C, 64.44; H, 7.95; N, 8.84. Found: C, 64.20; H, 8.00; N, 8.44. Mp: 136°C.

3,4-Diphenyl-1*H*-pyrrole-2,5-dicarboxylic acid bis-[(4-nitro-phenyl)-amide] (66): 3,4-Diphenyl-1*H*-pyrrole-2,5-dicarboxylic acid **56**[67] (1.0g , 3.3mmol) was suspended in $SOCl_2$ (20mL) and refluxed overnight. The reaction was allowed to cool and the excess of $SOCl_2$ was removed *in vacuo*. A brown solid formed that was dissolved in dichloromthane (30mL) and Et_3N (0.74g , 7.3mmol) and DMAP (5mg, 0.04mmol) were added. After addition of 4-nitro-aniline (0.98g, 7.15mmol), the mixture was stirred at room temperature for 72 hours. The solvent was removed *in vacuo* and acetonitrile (20mL) was added to the red solid. A pale yellow compound crystallized, that was collected and washed with acetonitrile (2x5mL). After drying 770mg of the desired compound was obtained (43.3%). ^{1}H NMR (DMSO-d_6, 300 MHz) δ 7.26-7.35 (m, 10H, Arom.), 7.85 (d, 4H, J = 9.1 Hz, NHCCH), 8.33 (d, J = 9.1 Hz, NO_2CCH), 10.19 (s, 2H, NH), 12.91 (s, 1H, NH). ^{13}C{^{1}H} NMR (DMSO-d_6, 75 MHz) δ 119.1, 125.0, 126.9, 127.8, 128.1, 130.5, 133.2, 142.4, 144.8, 159.3. MS (ES^+) 1095 ($2M+H^+$). HRMS (ES^-): 546 (M^-), Δ = 0.7 ppm. Anal. calcd. for $C_{30}H_{21}N_5O_6 \cdot {}^1/_2H_2O$: C, 64.74; H, 3.98; N, 12.58. Found: C, 64.80; H, 3.75; N, 12.27. Mp: >320^{0}C.

3,4-Diphenyl-1*H*-pyrrole-2,5-dicarboxylic acid bis-[(3,5-dinitro-phenyl)-amide] (67): 3,4-Diphenyl-1*H*-pyrrole-2,5-dicarboxylic acid **56**[67] (1.5g, 4.9mmol) was suspended in $SOCl_2$ (25mL) and refluxed overnight. The reaction was allowed to cool and the excess of $SOCl_2$ was removed in *vacuo*. A brown solid formed that was dissolved in dichloromethane (50mL) and Et_3N (1.21g, 12mmol) and DMAP (5mg, 0.04mmol) were added. After addition of 3,5-dinitro-aniline (1.88g, 10mmol), the mixture was stirred at room temperature for 72 hours. The solvent was removed *in vacuo* and acetonitrile (100mL) was added. A white solid corresponding to the wanted compound slowly crystallized from the hot acetonitrile solution. The solid was collected, washed with acetonitrile (2x10mL) and dried *in vacuo* (348mg, 11.1%). ^{1}H NMR (DMSO-d_6, 300 MHz) δ 7.26-7.33 (m, 10H, Arom.), 8.63 (s, 2H, Arom.), 9.13 (s, 4H , Arom.), 11.29 (s, 2H, CONH), 13.34 (s, 1H, NH). ^{13}C{^{1}H} NMR (DMSO-d_6, 75 MHz) δ 112.5, 118.8, 126.7, 127.5, 130.1, 130.7, 133.4, 141.4, 148.2, 159.2 . MS (ES^-) 636 (M^-), 672 ($M + Cl^-$), 749 ($M^- + TFA$). HRMS (ES^-): 636 (M^-), Δ = 2.1 ppm.

Anal. calcd. for $C_{30}H_{19}N_7O_{10}$: C, 56.52; H, 3.00; N, 15.38. Found: C , 56.20; H, 2.62; N, 15.35. Mp: >320^{0}C.

3,4-Diphenyl-1*H*-pyrrole-2,5-dicarboxylic acid bis-pentafluorophenyl-amide (68): 3,4-Diphenyl-1*H*-pyrrole-2,5-dicarboxylic acid **56**[67] (1g, 3.2mmol) was suspended in $SOCl_2$ (20mL) and refluxed overnight. The reaction was allowed to cool and the excess of $SOCl_2$ was removed in *vacuo*. A brown solid formed that was dissolved in dichloromethane (50mL) and Et_3N (0.68g, 6.7mmol) and DMAP (5mg, 0.04mmol) were added. After addition of pentafluoro-aniline (1.23g, 6.7mmol), the mixture was stirred at room temperature for 72 hours. The solution was washed with water (50mL) and the organic layer was dried on $MgSO_4$. After removing the dichloromethane *in vacuo*, acetonitrile (100mL) was added to the residue. A white crystalline solid corresponding to the desired compound was collected and washed with acetonitrile (2x20mL) providing a yield of 28%. ^{1}H NMR (acetonitrile-d_3, 300 MHz) δ 6.89 (s, 2H, CONH) 7.26-7.37 (m, 10H, Arom.), 10.40 (s, 1H, NH). ^{13}C{^{1}H} NMR (DMSO-d_6) δ 122.9, 126.3, 127.1, 128.0, 129.9, 132.4, 135.4, 137.9, 140.8, 143.3, 158.2. MS (ES$^+$) 638 (M + H$^+$), 679 (M + CH_3CN), 1275 (2M + H$^+$). HRMS (ES$^+$) not performed due to solubility problems. Anal. calcd. for $C_{30}H_{13}F_{10}N_3O_2$: C, 56.53; H, 2.06; N, 6.59. Found: C, 56.81; H, 2.21; N 6.39. Mp: 244^{0}C.

5-Methyl-3,4-diphenyl-1*H*-pyrrole-2-carboxylic acid -(benzo-15crown-5)-amide (69): 4'-aminobenzo-15-crown-5 (835mg, 2.9mmol) was dissolved in CH_2Cl_2 (15mL) and a 2M hexane solution of trimethyl aluminum[73] (1.47mL, 2.9mmol) was added dropwise. After stirring for 30 minutes 5-methyl-3,4-diphenyl-1*H*-pyrrole-2-carboxylic acid ethyl ester **60**[70,71] (900mg, 2.9mmol) was added and the mixture stirred for 3 days. The solution was carefully quenched with 2M HCl solution (20mL) and the phases were separated. The water solution was extracted with CH_2Cl_2 (50mL) and the organic phases were joined, dried on $MgSO_4$ and filtered off. The solvent was removed *in vacuo* and acetonitrile (5mL) was added to the residue leading to the wanted compound as a white and crystalline sold (448mg, 28%). ^{1}H NMR (DMSO-d_6, 300 MHz) δ 2.37 (s, 3H, CH_3), 3.75-4.09 (m, 16H, OCH_2), 6.37 (dd, 1H, J_1 = 7.9, J_2 = 1.8, Arom.), 6.72 (d, 1H, J = 9Hz, Arom.), 7.06 (d, 1H, J = 6.3, Arom.), 7.12-7.43 (m, 10H, Arom), 9.70 (s, 1H, pyrr. NH) (amidic NH hidden in the

aromatic area). $^{13}C\{^1H\}$ NMR (CD_2Cl_2, 75 MHz) δ 12.47, 69.22, 69.86, 70.03, 70.77, 70.89, 71.29, 106.59, 111.80,115.18, 121.50, 126.43, 128.47, 128.62, 129.59, 130.02, 130.61, 131.80, 132.94, 135.70, 149.90, 159.56. MS (ES^+) 565 ($M+Na^+$), 1108 ($2M+Na^+$). HRMS (ES^+): 565.13 ($M+Na^+$), Δ= 1.6 ppm. Anal. calcd for $C_{46}H_{51}N_3O_{12} \cdot {}^1/_3H_2O \cdot {}^1/_3CH_2Cl_2$: C, 67.31; H, 6.17; N, 4.86. Found: C, 67.15; H, 5.97; N, 4.95. Mp: 212°C (decom.).

3,4-Diphenyl-1*H*-pyrrole-2,5-dicarboxylic acid bis-(benzo-15crown-5)-amide (70): 3,4-Diphenyl-1*H*-pyrrole-2,5-dicarboxylic acid **56**[67] (1.0g, 3.3mmol) was suspended in $SOCl_2$ (20mL) and refluxed overnight. The reaction was allowed to cool and the excess of $SOCl_2$ was removed in *vacuo*. A brown solid formed that was dissolved in dichloromethane (30mL) and Et_3N (0.74g, 7.3mmol) and DMAP (5mg, 0.04mmol) were added. After addition of 4'-aminobenzo-15-crown-5, the mixture was stirred at room temperature for 72 hours. The solution was then washed with water (3*50mL), dried on $MgSO_4$, and filtered off. The solvent was removed again in *vacuo* and the brown solid was recrystallized in acetonitrile (20mL). A pale yellow solid was filtered off and washed with acetonitrile (2*20mL) leading to the wanted compound as a white and crystalline solid (yield: 0.89g, 33%). ^1H NMR (DMSO-d_6, 300 MHz) δ 3.69-4.10 (m, 32H, OCH_2), 6.98 (d, 2H, J = 8.2Hz, Arom.), 7.03 (d, 2H, J = 8.2Hz, Arom.), 7.22(s, 2H, Arom.), 7.26-7.36 (m, 10H, Arom.), 9.21 (s, 2H, CONH), 12.54 (s, 1H, NH). $^{13}C\{^1H\}$ NMR (CD_2Cl_2, 75 MHz) δ 69.20, 69.79, 69.94, 69.98, 70.72, 70.84, 71.32, 106.57, 111.89, 115.01, 125.31, 126.81, 129.09, 129.64, 131.71, 132.30, 133.66, 146.24, 149.83, 158.18. MS (ES^+) 442 ($M+2Na^+$), 860 ($M+Na^+$). HRMS (ES^+) : 860 ($M + Na^+$), Δ = 3.8 ppm. Anal. calcd. for $C_{46}H_{51}N_3O_{12} \cdot H_2O$: C, 64.55; H, 6.24; N, 4.91. Found: C, 64.40; H, 6.23; N, 4.91.Mp : 187°C.

5.3.2 Syntheses included in chapter 3

5,10,15,20-Tetra-(4-ethoxycarbonylmethoxy-phenyl)-5,10,15,20-tetramethyl-calix[4]pyrrole (71): αααα–5,10,15,20-Tetra-(4-hydroxy-phenyl)-5,10,15,20-tetramethyl-calix[4]pyrrole **39**[48,49] (1.52g, 2.1mmol) and K_2CO_3 (1.76g, 12.7mmol) were suspended in of fresh distilled acetone (150ml) and stirred for 2 hours. $BrCH_2COOEt$ (3.12g, 18.7mmol) was added and the suspension was refluxed for 5 days. After cooling the solution was filtered off to eliminate the excess of K_2CO_3, and the solvent was removed *in vacuo*. An orange oil was obtained that was dissolved in dichloromethane (50mL) and washed with water (3x20mL). The organic phase was dried with $MgSO_4$, filtered off and the solvent removed again. An orange oil formed that was triturated with ethanol (50 ml). An orange solid was collected, washed with ethanol (3x10mL) and dried *in vacuo* (1.55g, 68.4%). ^1H NMR (DMSO-d_6, 300 MHz) δ 1.31 (t, 12H, J = 6.93, CH_3), 1.83 (s, 12H, CCH_3), 4.24 (q, 8H, J = 6.93, OCH_2), 4.78 (s, 12H, OCH_2CO), 6.06 (s, 8H, Pyrr.), 6.86 (d, 8H, J = 8.46, Arom.), 6.96 (d, 8H, J = 8.46, Arom.), 9.55 (s, 4H, NH). $^{13}C\{^1H\}$ NMR ($CDCl_3$, 75 MHz) δ 14.57, 30.39, 44.78, 62.00, 66.06, 105.71, 114.79, 129.82, 138.91, 143.06, 157.50, 169.94. MS (ES^+) 1084.8 ($M+H^+$), 1106.7 ($M+Na^+$), 1122 ($M+K^+$). Anal. calcd. for $C_{64}H_{68}N_4O_{12}\cdot 3CH_2Cl_2$: C, 60.05; H, 5.57; N, 4.18. Found: C, 59.66 ; H, 5.60; N, 4.24. Mp: 193^{0}C (decom.)

5,10,15,20-Tetra-(4-diethylcarbamoylmethoxy-phenyl)-5,10,15,20-tetramethyl-calix[4]pyrrole (72): αααα–5,10,15,20-Tetra-(4-hydroxy-phenyl)-5,10,15,20-tetramethyl-calix[4]pyrrole **39**[48,49] (1g, 1.4mmol) and K_2CO_3 (1.55g, 11.2mmol) were suspended in fresh distilled acetone (120ml) and stirred for 2 hours. KI (1.8g, 10.8mmol) and $ClCH_2CON(C_2H_5)_2$ (1.63g, 10.8mmol) were added and the suspension was stirred for 5 days. A colour change from orange to white was observed. The solvent was removed *in vacuo* and a pale orange solid formed that was suspended in 50ml of dichloromethane. The suspension was filtered off and the organic solution was washed with water (3x20ml). After drying on $MgSO_4$ and filtering, the solvent was removed again *in vacuo*. The orange oil that formed was re-crystallized from diethyl ether. A white crystalline solid was obtained that was

collected, washed with diethyl ether (2x10mL) and dried *in vacuo* (800mg, 59%). ^{1}H NMR (DMSO-d_6, 300 MHz) δ 1.09 (t, 12H, J = 6.96, CH_3), 1.24 (t, 12H, J = 6.96, CH_3), 1.84 (s, 12H, CCH_3), 3.37 (m, 16H, CH_2), 4.76 (s, 8H, OCH_2CO), 6.06 (s, 8H, Pyrr.), 6.88 (m, 16H, Arom.), 9.56 (s, 4H, NH). ^{13}C{^{1}H} NMR (DMSO-d_6, 75 MHz) δ 12.39, 13.70, 30.97, 43.06, 65.57, 104.03, 113.80, 127.40, 136.95, 142.11, 156.43, 165.70. MS (ES^+) 1193.2 ($M+H^+$), 1215.1 ($M+Na^+$). Anal. calcd. for $C_{72}H_{88}N_8O_8 \cdot 2CH_2Cl_2 \cdot 4H_2O$: C, 61.51; H, 7.21; N, 7.86. Found: C, 61.88 ; H, 7.54; N, 7.57. Mp: 223^{0}C (decom.)

5,10,15,20-Tetra-(4-acetoxyphenyl)-5,10,15,20-tetramethyl-calix[4]pyrrole (73): αααα–5,10,15,20-Tetra-(4-hydroxy-phenyl)-5,10,15,20-tetramethyl-calix[4]pyrrole **39**[48,49] (3g, 4.0mmol) acetyl chloride (1.27g, 16.3mmol) and triethylamine (3.27g, 32.3mmol) were dissolved in freshly distilled THF (300mL) and stirred for 5 days. The solvent was removed *in vacuo*, and methanol was added. The brown suspension was heated and after cooling a white crystalline solid formed that was collected, washed with methanol (3x20mL) and dried *in vacuo* (2g, 55%). ^{1}H NMR (DMSO-d_6, 300 MHz) δ 1.90 (s, 12H, CCH_3), 2.33 (s, 12H, $COCH_3$), 6.11 (s, 8H, Pyrr.), 7.02 (d, 8H, J = 5.9, Arom.), 7.13 (d, 8H, J = 5.9, Arom.), 9.63 (s, 4H, NH). ^{13}C{^{1}H} NMR (DMSO-d_6, 75 MHz) δ 20.61, 31.2, 104.94, 121.68, 127.92, 137.20, 147.79, 149.27, 169.23. MS (ES^+) 909 ($M+H^+$), 932 ($M+Na^+$). HRMS (ES^+): 931.36 ($M + Na^+$), Δ = 1.9 ppm. Anal. calcd. for $C_{56}H_{52}N_4O_8 \cdot 3.5H_2O$: C, 69.19; H, 6.12; N, 5.76. Found: C, 69.18; H, 6.15; N, 5.88. Mp: 261^{0}C (decom.)

5.3.3 Syntheses included in chapter 4

Preparation of the tetrabutyl ammonium salts of the bis-carboxylic acids presented in chapter 4: the same procedure has been employed to synthesize these salts. 2.1 equivalents of TBAOH (1M methanol solution) were added to 1gr of each acid and the solvent was removed; an oil was obtained that was dried *in vacuo*, heating with an oil bath at 100°C. A white solid was obtained that was stirred for 4 hours in diethyl ether. The compound was filtered off, washed with ether (2x30mL) and dried using a high vacuum pump. The correct soichiometry of the salts was checked by the integration of the ^{1}H NMR spectrum peaks.

Preparation of the hexafluorophosphate salts of 88 and 89: **84** (350 mg, 0.42 mmol) or **85** (432mg, 0.44 mmol)[115] was dissolved in methanol (30mL). $AgPF_6$ (223 mg, 0.88 mmol) was added resulting in the formation of a white precipitate (AgCl). The white suspension was stirred for 30 minutes and allowed to stand for 2 hours. The AgCl was removed by filtration through a glass fibre filter (Millipore AP15), and the brown solution reduced *in vacuo*. The residue was purified by column filtration with methanol through Sephadex® LH-20 (240mg of **88** (54%) or 280mg of **89** (53%) were obtained.).

For **88**: ^{1}H NMR (DMSO-d_6, 300 MHz) δ 1.22 (s, 18H, CH_3), 1.29 (s, 18H, CH_3), 3.67 (d, 4H, J = 12.7, $ArCH_2Ar$), 4.14 (d, 4H, J = 12.7, $ArCH_2Ar$), 5.01 (s, 4H, OCH_2), 7.32 (s, 4H, Arom.), 7.36 (s, 4H, Arom.), 9.14 (b s, 8H, NH_2). $^{13}C\{^1H\}$ NMR (CD_3OD, 75 MHz) δ 31.4, 31.9, 32.2, 34.8, 35.2, 126.9, 127.7, 134.1, 145.1, 149.2, 149.9, 151.0, 168.5. MS (ES^+) 761.3 ($M + H^+$). MS (ES^-) 144 (PF_6^-). Anal. calcd. for $C_{48}H_{66}F_{12}N_4O_4P_2$: C 54.75, H 6.32, N 5.32, Found: C 53.49, H 6.60, N 4.92.[123] Mp: 176^{0}C (decom.).

For **89**: ^{1}H NMR (DMSO-d_6, 300 MHz) δ : 1.21 (s, 18H, CH_3), 1.28 (s, 18H, CH_3), 4.20 (d, 4H, J = 12.7, $ArCH_2Ar$), 5.20 (s, 4H, OCH_2), 7.23 (s, 4H, ArH), 7.26 (s, 4H, ArH), 7.64 (d, 2H, J = 8.2, Arom.), 7.94 (d, 2H, J = 8.2, Arom.), 7.64 (s, 2H, Arom.), 8.24 (s, 2H, OH), 8.30 (d, 2H, J = 8.2, Arom.). $^{13}C\{^1H\}$ NMR (DMSO-d_6, 75 MHz) δ 30.8, 31.4, 33.6, 34.0, 77.1, 125.4, 125.7, 127.2, 127.4, 127.9, 128.3, 129.4, 132.9, 137.6, 141.6, 147.4, 149.4, 149.9, 165.4. MS (ES^+) 913.5 ($M + H^+$). MS (ES^-) 144 (PF_6^-). Anal. calcd. for $C_{60}H_{74}F_{12}N_4O_4P_2$: C 59.8, H 6.19, N 4.65. Found: : C 58.01, H 6.35, N 4.63.[123] Mp: 234^{0}C

Appendix: crystal data.

A1. Introduction

The crystal structures presented in the chapters 2 and 3, and the crystal structure of the complex **88**/$PF_2O_2^-$ were solved by the EPSRC Crystallographic Service (Dr. S. Coles, Dr. M.E. Light, Prof. M.B. Hursthouse). The crystal structures of the complexes **88**/2·$C_6H_2N_3O_7^-$ and **89**·$(CH_2(COO^-)_2)$·4EtOH·H_2O reported in chapter 4 was solved by Prof. A.H. White and Dr. B. Skelton at UWA and Dr M.I. Ogden at Curtin. The refinement of the structures and the fractional coordinates are reported here for the sake of completeness and so that the structures may be regenerated from the text of this thesis if necessary.

A.2 Crystal data

3,4-diphenyl-1H-pyrrole-2,5-dicarboxylic acid butylamide

Identification code	**(58)**
Empirical formula	$C_{26}H_{31}N_3O_2$
Formula weight	417.54
Temperature	150(2) K
Wavelength	0.71073 Å
Crystal system	Monoclinic
Space group	*Cc*
Unit cell dimensions	a = 25.5294(5) Å b = 18.9718(5) Å β = 103.111(2)° c = 9.7130(2) Å
Volume	4581.75(18) Å^3
Z	8 (2 Molecules in asymmetric unit)
Density (calculated)	1.211 Mg / m^3
Absorption coefficient	0.077 mm^{-1}
F(000)	1792
Crystal	Colourless block
Crystal size	0.20 × 0.10 × 0.10 mm^3
θ range for data collection	3.04 – 23.26°
Index ranges	$-28 \le h \le 28$, $-21 \le k \le 21$, $-10 \le l \le 10$
Reflections collected	18454
Independent reflections	6361 [R_{int} = 0.0810]
Completeness to θ = 23.26°	99.7 %
Max. and min. transmission	0.9923 and 0.9847
Refinement method	Full-matrix least-squares on F^2
Data / restraints / parameters	6361 / 20 / 560
Goodness-of-fit on F^2	1.082
Final *R* indices [$F^2 > 2\sigma(F^2)$]	*R1* = 0.0567, *wR2* = 0.1438
R indices (all data)	*R1* = 0.0709, *wR2* = 0.1555
Absolute structure parameter	Not reliably determined
Extinction coefficient	0.0024(6)
Largest diff. peak and hole	0.667 and –0.410 e Å^{-3}

Table A.1: Structure and refinement data.

Atom	*x*	*y*	*z*	U_{eq}
Molecule 1				
N1	2074(2)	13048(2)	1320(4)	36(1)
N2	2002(1)	11142(2)	1157(3)	24(1)
N3	1621(1)	9544(2)	2466(3)	26(1)
O1	2543(1)	12278(2)	299(3)	35(1)
O2	1780(1)	9661(1)	272(3)	26(1)
C1	1229(2)	15101(3)	1019(8)	73(2)
C2	1633(2)	14521(2)	1544(6)	50(1)
C3	1899(2)	14258(2)	428(5)	49(1)
C4	2309(2)	13690(2)	899(6)	45(1)
C5	2183(2)	12394(2)	932(4)	24(1)
C6	1862(2)	11825(2)	1327(4)	22(1)
C7	1641(2)	10697(2)	1518(4)	23(1)
C8	1688(2)	9917(2)	1368(4)	21(1)
C9	1578(2)	8774(2)	2438(5)	36(1)
C10	1027(2)	8511(2)	2566(5)	45(1)
C11	811(3)	7771(4)	2070(8)	91(2)
C12	1196(3)	7301(5)	2560(8)	98(2)
C13	1387(2)	11812(2)	1791(4)	20(1)
C14	1250(2)	11093(2)	1927(4)	24(1)
C15	1035(2)	12430(2)	1956(4)	24(1)
C16	1061(2)	12764(2)	3242(5)	30(1)
C17	716(2)	13312(2)	3348(5)	38(1)
C18	346(2)	13545(2)	2174(5)	39(1)
C19	317(2)	13220(2)	883(5)	40(1)
C20	657(2)	12665(2)	774(5)	33(1)
C21	735(2)	10845(2)	2262(4)	23(1)
C22	414(2)	10360(2)	1404(4)	28(1)
C23	−71(2)	10162(3)	1682(5)	36(1)
C24	−233(2)	10433(2)	2837(5)	34(1)
C25	89(2)	10913(2)	3720(5)	34(1)
C26	581(2)	11103(2)	3443(5)	29(1)
Molecule 2				
N4	2682(2)	3078(2)	4877(4)	35(1)
N5	2678(1)	1157(2)	4663(3)	21(1)
N6	3032(2)	−431(2)	3258(3)	25(1)
O3	2138(1)	2264(2)	5512(3)	32(1)
O4	2913(1)	−320(1)	5506(2)	25(1)
C27	3329(3)	4381(4)	8852(6)	81(2)
C28	3158(2)	4188(3)	7296(5)	56(1)

Table A.2: Continued Overleaf

C29	2604(2)	3838(2)	6929(4)	41(1)
C30	2399(2)	3667(2)	5355(5)	39(1)
C31	2512(2)	2407(2)	4999(4)	25(1)
C32	2838(2)	1846(2)	4541(4)	24(1)
C33	3043(2)	714(2)	4271(4)	19(1)
C34	2984(2)	−54(2)	4384(4)	20(1)
C35	3054(2)	−1203(2)	3280(4)	28(1)
C36	3624(2)	−1473(2)	3436(5)	31(1)
C37	3639(2)	−2266(2)	3571(4)	27(1)
C38	4213(2)	−2570(2)	4060(5)	37(1)
C39	3313(2)	1840(2)	4081(4)	24(1)
C40	3444(2)	1124(2)	3908(4)	22(1)
C41	3662(2)	2451(2)	3965(4)	26(1)
C42	3592(2)	2858(2)	2743(5)	36(1)
C43	3933(2)	3424(3)	2679(5)	46(1)
C44	4347(2)	3589(3)	3826(5)	45(1)
C45	4416(2)	3206(2)	5033(5)	40(1)
C46	4079(2)	2637(2)	5102(4)	33(1)
C47	3940(2)	869(2)	3551(4)	22(1)
C48	4253(2)	340(2)	4337(5)	30(1)
C49	4730(2)	109(2)	4024(5)	33(1)
C50	4910(2)	428(2)	2932(5)	37(1)
C51	4612(2)	949(3)	2160(5)	35(1)
C52	4135(2)	1171(2)	2446(4)	28(1)

Table A.2: Atomic coordinates [$\times 10^4$], equivalent isotropic displacement parameters [$Å^2 \times 10^3$] and site occupancy factors. U_{eq} is defined as one third of the trace of the orthogonalized U^{ij} tensor.

3,4-diphenyl-1H-pyrrole-2,5-dicarboxylic acid butylamide (TBA benzoate complex)

Identification code	**[58·Benzoate]TBA**
Empirical formula	$C_{49}H_{72}N_4O_4$
Formula weight	781.11
Temperature	120(2) K
Wavelength	0.71073 Å
Crystal system	Monoclinic
Space group	$P2_1/n$
Unit cell dimensions	a = 10.0782(2) Å
	b = 26.9772(7) Å β = 106.0400(10)°
	c = 17.7925(6) Å
Volume	4649.1(2) Å^3
Z	4
Density (calculated)	1.116 Mg / m^3
Absorption coefficient	0.070 mm^{-1}
F(000)	1704
Crystal	Colourless Block
Crystal size	0.20 × 0.08 × 0.06 mm^3
θ range for data collection	3.02 – 25.03°
Index ranges	$-11 \le h \le 10$, $-32 \le k \le 31$, $-20 \le l \le 21$
Reflections collected	35158
Independent reflections	7892 [R_{int} = 0.1039]
Completeness to θ = 25.03°	96.2 %
Max. and min. transmission	0.9958 and 0.9861
Refinement method	Full-matrix least-squares on F^2
Data / restraints / parameters	7892 / 0 / 521
Goodness-of-fit on F^2	0.926
Final R indices [$F^2 > 2\sigma(F^2)$]	$R1$ = 0.0535, $wR2$ = 0.0920
R indices (all data)	$R1$ = 0.1441, $wR2$ = 0.1145
Extinction coefficient	0.0017(3)
Largest diff. peak and hole	0.195 and –0.203 e Å^{-3}

Table A.3:. Crystal data and structure refinement.

Atom	x	y	z	U_{eq}
O1	4674(2)	2034(1)	−186(1)	34(1)
O2	3884(2)	1417(1)	3422(1)	35(1)
N1	5567(2)	1289(1)	245(1)	31(1)
N2	4953(2)	1465(1)	1687(1)	25(1)
N3	5632(2)	979(1)	3176(1)	27(1)
C1	7629(3)	20(1)	−1121(2)	51(1)
C2	6800(3)	497(1)	−1203(2)	37(1)
C3	6702(3)	700(1)	−424(2)	34(1)
C4	5797(3)	1155(1)	−504(2)	30(1)
C5	4977(2)	1722(1)	341(2)	25(1)
C6	4720(2)	1816(1)	1108(1)	23(1)
C7	4290(2)	2247(1)	1393(1)	23(1)
C8	4266(2)	2150(1)	2177(1)	22(1)
C9	4673(2)	1659(1)	2338(1)	22(1)
C10	4692(3)	1341(1)	3023(2)	25(1)
C11	5621(3)	584(1)	3731(1)	29(1)
C12	4776(3)	139(1)	3343(2)	32(1)
C13	4851(3)	−300(1)	3882(2)	36(1)
C14	4022(3)	−742(1)	3475(2)	44(1)
C15	3935(2)	2736(1)	995(1)	22(1)
C16	4635(3)	3163(1)	1324(1)	27(1)
C17	4265(3)	3623(1)	997(2)	29(1)
C18	3170(3)	3668(1)	337(2)	28(1)
C19	2459(3)	3250(1)	−1(2)	30(1)
C20	2844(2)	2788(1)	325(1)	26(1)
C21	3965(2)	2509(1)	2733(2)	22(1)
C22	4800(3)	2536(1)	3499(2)	27(1)
C23	4556(3)	2878(1)	4018(2)	29(1)
C24	3487(3)	3212(1)	3786(2)	29(1)
C25	2645(3)	3198(1)	3029(2)	27(1)
C26	2879(2)	2848(1)	2506(2)	24(1)
O3	5824(2)	527(1)	1398(1)	32(1)
O4	7591(2)	645(1)	2449(1)	38(1)
C27	6988(3)	418(1)	1846(2)	26(1)
C28	7692(3)	−42(1)	1640(2)	29(1)
C29	8993(3)	−181(1)	2101(2)	41(1)
C30	9640(3)	−594(1)	1906(2)	52(1)
C31	9007(3)	−870(1)	1264(2)	54(1)
C32	7716(3)	−742(1)	800(2)	44(1)
C33	7060(3)	−326(1)	992(2)	35(1)

Table A.4: Continued Overleaf

N4	4804(2)	6850(1)	1636(1)	23(1)
C34	5281(3)	6354(1)	1404(2)	27(1)
C35	4242(3)	5936(1)	1298(2)	32(1)
C36	4645(3)	5518(1)	837(2)	37(1)
C37	3642(3)	5084(1)	721(2)	47(1)
C38	4419(3)	6797(1)	2397(1)	27(1)
C39	5586(3)	6642(1)	3100(1)	34(1)
C40	5091(3)	6611(1)	3835(2)	44(1)
C41	4113(4)	6192(1)	3831(2)	74(1)
C42	5979(2)	7215(1)	1712(2)	25(1)
C43	5805(3)	7713(1)	2063(2)	29(1)
C44	7001(3)	8055(1)	2070(2)	33(1)
C45	6938(3)	8537(1)	2505(2)	35(1)
C46	3512(2)	7029(1)	1020(1)	23(1)
C47	3579(2)	6983(1)	182(1)	27(1)
C48	2349(3)	7236(1)	−378(2)	35(1)
C49	1002(3)	6962(1)	−470(2)	46(1)

Table A.4: Atomic coordinates [$\times 10^4$], equivalent isotropic displacement parameters [$Å^2 \times 10^3$] and site occupancy factors. U_{eq} is defined as one third of the trace of the orthogonalized U^{ij} tensor.

3,4-Diphenyl-1H-pyrrole-2,5-dicarboxylic acid phenylamide

Identification code	**(59)**	
Empirical formula	$C_{30}H_{23}N_3O_2$	
Formula weight	457.51	
Temperature	150(2) K	
Wavelength	0.71073 Å	
Crystal system	Triclinic	
Space group	P-1	
Unit cell dimensions	a = 9.4890(9) Å	α = 91.483(3)°
	b = 9.4925(9) Å	β = 88.321(3)°
	c = 27.4534(5) Å	γ = 73.520(4)°
Volume	2368.7(3) Å^3	
Z	4	
Density (calculated)	1.283 Mg / m^3	
Absorption coefficient	0.082 mm^{-1}	
F(000)	960	
Crystal	Colourless prism	
Crystal size	0.10 × 0.08 × 0.03 mm^3	
θ range for data collection	3.07 – 23.26°	
Index ranges	$-10 \le h \le 10$, $-10 \le k \le 10$, $-28 \le l \le 30$	
Reflections collected	12778	
Independent reflections	6387 [R_{int} = 0.0863]	
Completeness to θ = 23.26°	93.5 %	
Max. and min. transmission	0.9976 and 0.9919	
Refinement method	Full-matrix least-squares on F^2	
Data / restraints / parameters	6387 / 0 / 632	
Goodness-of-fit on F^2	1.016	
Final R indices [$F^2 > 2\sigma(F^2)$]	$R1$ = 0.0622, $wR2$ = 0.1249	
R indices (all data)	$R1$ = 0.1269, $wR2$ = 0.1625	
Extinction coefficient	0.0027(9)	
Largest diff. peak and hole	0.236 and –0.299 e Å^{-3}	

Table A.5: Structure and refinement data

Atom	*x*	*y*	*z*	U_{eq}
Molecule A				
N1	8970(4)	7086(3)	1297(1)	30(1)
N2	7309(3)	8280(3)	155(1)	24(1)
N3	7679(3)	8730(3)	−1150(1)	30(1)
O1	6577(3)	7651(3)	1084(1)	35(1)
O2	5648(3)	9428(3)	−630(1)	34(1)
C1	7607(5)	6798(4)	2049(2)	32(1)
C2	7651(5)	6302(5)	2519(2)	40(1)
C3	8973(5)	5622(5)	2723(2)	38(1)
C4	10259(5)	5429(5)	2450(2)	38(1)
C5	10239(5)	5924(5)	1980(2)	35(1)
C6	8905(4)	6609(4)	1780(2)	26(1)
C7	7879(5)	7502(4)	979(2)	26(1)
C8	8363(4)	7736(4)	484(2)	24(1)
C9	9717(4)	7441(4)	243(2)	26(1)
C10	9464(4)	7791(4)	−250(2)	23(1)
C11	7944(4)	8339(4)	−294(2)	23(1)
C12	6980(4)	8882(4)	−702(2)	26(1)
C13	7117(4)	8963(4)	−1621(2)	29(1)
C14	8129(5)	8538(5)	−2010(2)	39(1)
C15	7686(5)	8713(5)	−2485(2)	40(1)
C16	6214(5)	9300(5)	−2574(2)	38(1)
C17	5206(5)	9723(4)	−2185(2)	37(1)
C18	5639(4)	9576(4)	−1708(2)	30(1)
C19	11222(4)	6867(4)	434(1)	22(1)
C20	11836(4)	7768(4)	710(2)	29(1)
C21	13279(5)	7284(5)	851(2)	33(1)
C22	14118(5)	5865(5)	726(2)	35(1)
C23	13510(5)	4956(5)	460(2)	41(1)
C24	12069(4)	5436(4)	314(2)	31(1)
C25	10662(4)	7686(4)	−622(1)	23(1)
C26	11571(4)	8605(4)	−578(2)	29(1)
C27	12740(4)	8475(4)	−904(2)	33(1)
C28	13031(4)	7432(4)	−1278(2)	32(1)
C29	12153(5)	6507(5)	−1328(2)	39(1)
C30	10986(4)	6621(4)	−998(2)	31(1)
Molecule B				
N4	6928(3)	4187(3)	−3613(1)	27(1)
N5	8251(3)	2299(3)	−4777(1)	24(1)
N6	8581(3)	2367(3)	−6091(1)	29(1)

Table A.6: Continued Overleaf

O3	7601(3)	1743(3)	−3828(1)	32(1)
O4	9401(3)	476(3)	−5578(1)	33(1)
C31	6727(4)	2948(4)	−2847(1)	26(1)
C32	6372(4)	3098(5)	−2351(2)	32(1)
C33	5858(4)	4451(5)	−2120(2)	33(1)
C34	5677(4)	5695(5)	−2382(2)	34(1)
C35	6010(4)	5573(4)	−2876(2)	31(1)
C36	6539(4)	4213(4)	−3111(1)	24(1)
C37	7416(4)	3033(5)	−3935(1)	24(1)
C38	7711(4)	3409(4)	−4441(1)	21(1)
C39	7426(4)	4733(4)	−4680(1)	23(1)
C40	7785(4)	4371(4)	−5181(2)	24(1)
C41	8309(4)	2838(4)	−5229(1)	21(1)
C42	8837(4)	1794(4)	−5642(2)	24(1)
C43	8687(4)	1627(4)	−6551(2)	27(1)
C44	7915(5)	2440(5)	−6923(2)	41(1)
C45	7954(5)	1811(5)	−7384(2)	47(1)
C46	8744(5)	355(5)	−7481(2)	40(1)
C47	9505(5)	−434(5)	−7109(2)	35(1)
C48	9495(4)	196(4)	−6650(2)	28(1)
C49	6892(4)	6268(4)	−4478(2)	26(1)
C50	7794(5)	6864(5)	−4197(2)	34(1)
C51	7344(5)	8319(5)	−4033(2)	39(1)
C52	5979(5)	9195(5)	−4149(2)	47(1)
C53	5072(5)	8623(5)	−4425(2)	46(1)
C54	5513(4)	7159(4)	−4595(2)	35(1)
C55	7635(4)	5502(4)	−5560(1)	22(1)
C56	8566(4)	6391(4)	−5565(2)	29(1)
C57	8387(5)	7496(4)	−5891(2)	30(1)
C58	7269(5)	7733(4)	−6220(2)	33(1)
C59	6325(4)	6871(4)	−6216(2)	28(1)
C60	6504(4)	5762(4)	−5884(2)	27(1)

Table A.6: Atomic coordinates [$\times 10^4$], equivalent isotropic displacement parameters [$Å^2 \times 10^3$] and site occupancy factors. U_{eq} is defined as one third of the trace of the orthogonalized U^{ij} tensor.

3,4-Diphenyl-1H-pyrrole-2,5-dicarboxylic acid phenylamide (DMSO complex)

Identification code	**(59)·DMSO**
Empirical formula	$C_{32}H_{29}N_3O_3S$
Formula weight	535.64
Temperature	120(2) K
Wavelength	0.71073 Å
Crystal system	Monoclinic
Space group	$P2_1/n$
Unit cell dimensions	a = 9.6860(2) Å
	b = 18.6429(4) Å β = 104.503(5)°
	c = 15.5603(3) Å
Volume	2720.27(10) Å^3
Z	4
Density (calculated)	1.308 Mg / m^3
Absorption coefficient	0.158 mm^{-1}
F(000)	1128
Crystal	Colourless Needle (cut)
Crystal size	0.10 × 0.02 × 0.02 mm^3
θ range for data collection	2.92 – 24.70°
Index ranges	$-11 \le h \le 11, -21 \le k \le 21, -18 \le l \le 18$
Reflections collected	19625
Independent reflections	4605 [R_{int} = 0.1853]
Completeness to θ = 24.70°	99.2 %
Max. and min. transmission	0.9968 and 0.9844
Refinement method	Full-matrix least-squares on F^2
Data / restraints / parameters	4605 / 0 / 355
Goodness-of-fit on F^2	0.995
Final R indices [$F^2 > 2\sigma(F^2)$]	$R1$ = 0.0616, $wR2$ = 0.1249
R indices (all data)	$R1$ = 0.1302, $wR2$ = 0.1500
Extinction coefficient	0.0042(7)
Largest diff. peak and hole	0.297 and –0.335 e Å^{-3}

Table A.7: Structure and refinement data

Atom	x	y	z	U_{eq}
C1	3299(4)	−1150(2)	3653(2)	26(1)
C2	3646(4)	−1387(2)	4529(2)	30(1)
C3	3674(4)	−926(2)	5225(2)	29(1)
C4	3334(4)	−216(2)	5048(2)	30(1)
C5	2989(4)	36(2)	4187(2)	24(1)
C6	2989(4)	−426(2)	3480(2)	20(1)
C7	2628(4)	−427(2)	1831(2)	21(1)
C8	2651(4)	53(2)	1073(2)	19(1)
C9	2446(4)	−116(2)	181(2)	20(1)
C10	2727(4)	514(2)	−255(2)	20(1)
C11	3106(4)	1045(2)	392(2)	20(1)
C12	3486(4)	1816(2)	391(2)	22(1)
C13	3842(4)	2814(2)	−617(2)	23(1)
C14	4560(4)	3293(2)	24(2)	23(1)
C15	4918(4)	3967(2)	−241(2)	26(1)
C16	4559(4)	4165(2)	−1123(2)	27(1)
C17	3837(4)	3691(2)	−1757(3)	31(1)
C18	3471(4)	3014(2)	−1506(2)	27(1)
C19	2010(4)	−820(2)	−265(2)	21(1)
C20	642(4)	−1083(2)	−378(2)	24(1)
C21	241(4)	−1725(2)	−827(2)	27(1)
C22	1210(4)	−2116(2)	−1153(2)	26(1)
C23	2587(4)	−1861(2)	−1040(2)	25(1)
C24	2981(4)	−1210(2)	−606(2)	24(1)
C25	2605(4)	616(2)	−1220(2)	21(1)
C26	1268(4)	680(2)	−1809(2)	23(1)
C27	1142(4)	869(2)	−2689(2)	26(1)
C28	2355(4)	983(2)	−2991(2)	30(1)
C29	3673(4)	898(2)	−2426(3)	35(1)
C30	3805(4)	714(2)	−1543(2)	30(1)
C31	4569(4)	2601(2)	3179(2)	29(1)
C32	2475(4)	2254(2)	3951(2)	29(1)
N1	2721(3)	−110(2)	2626(2)	24(1)
N2	3048(3)	759(1)	1188(2)	21(1)
N3	3451(3)	2113(2)	−412(2)	25(1)
O1	2551(3)	−1087(1)	1717(2)	29(1)
O2	3836(3)	2153(1)	1096(2)	29(1)
O3	3190(3)	1388(1)	2811(2)	31(1)
S1	2878(1)	2180(1)	2899(1)	25(1)

Table A.8 : Atomic coordinates [$\times 10^4$], equivalent isotropic displacement parameters [$Å^2 \times 10^3$] and site occupancy factors. U_{eq} is defined as one third of the trace of the orthogonalized U^{ij} tensor.

5-Methyl-3,4-diphenyl-1H-pyrrole-2-carboxylic acid butylamide

Identification code	**(61)**	
Empirical formula	$C_{22}H_{24}N_2O$	
Formula weight	332.43	
Temperature	120(2) K	
Wavelength	0.71073 Å	
Crystal system	Triclinic	
Space group	P-1	
Unit cell dimensions	a = 13.9643(3) Å	α = 117.534(3)°
	b = 16.0644(3) Å	β = 91.766(4)°
	c = 16.0895(3) Å	γ = 115.390(6)°
Volume	2770.69(9) Å^3	
Z	6 (3 Molecules in asymmetric unit)	
Density (calculated)	1.195 Mg / m^3	
Absorption coefficient	0.074 mm^{-1}	
F(000)	1068	
Crystal	Colourless Needle	
Crystal size	0.30 × 0.02 × 0.02 mm^3	
θ range for data collection	2.92 – 23.26°	
Index ranges	$-15 \le h \le 15$, $-17 \le k \le 17$, $-17 \le l \le 17$	
Reflections collected	18333	
Independent reflections	7850 [R_{int} = 0.2117]	
Completeness to θ = 23.26°	98.7 %	
Max. and min. transmission	0.9985 and 0.9783	
Refinement method	Full-matrix least-squares on F^2	
Data / restraints / parameters	7850 / 0 / 683	
Goodness-of-fit on F^2	0.822	
Final R indices [$F^2 > 2\sigma(F^2)$]	$R1$ = 0.0963, $wR2$ = 0.2303	
R indices (all data)	$R1$ = 0.1859, $wR2$ = 0.3068	
Extinction coefficient	0.0052(17)	
Largest diff. peak and hole	0.455 and −0.403 e Å^{-3}	

Table A.9: Structure and refinement data

Atom	*x*	*y*	*z*	U_{eq}
Molecule 1				
O1	3903(3)	5262(3)	23(3)	41(1)
N1	5916(4)	6438(4)	1411(3)	25(1)
N2	3237(4)	6247(4)	1047(4)	37(1)
C1	7846(5)	7017(5)	2176(4)	30(2)
C2	6842(5)	7140(4)	2190(4)	23(1)
C3	6656(5)	7925(5)	2891(4)	24(1)
C4	5544(5)	7662(5)	2503(4)	24(1)
C5	5122(4)	6719(4)	1583(4)	21(1)
C6	4049(5)	6029(5)	834(4)	26(2)
C7	2155(5)	5650(5)	340(4)	36(2)
C8	1539(5)	6269(5)	688(4)	33(2)
C9	1179(5)	6331(5)	1585(5)	37(2)
C10	530(6)	6927(6)	1925(6)	63(2)
C11	7451(5)	8877(5)	3848(4)	22(1)
C12	8017(5)	8758(5)	4465(4)	28(2)
C13	8789(5)	9641(5)	5350(4)	35(2)
C14	8970(5)	10672(5)	5637(5)	34(2)
C15	8420(5)	10813(5)	5047(4)	29(2)
C16	7639(5)	9924(5)	4160(4)	25(2)
C17	4974(5)	8278(4)	2968(4)	24(2)
C18	4586(5)	8275(5)	3747(4)	30(2)
C19	4000(5)	8810(5)	4135(5)	37(2)
C20	3788(5)	9329(5)	3745(5)	36(2)
C21	4194(5)	9350(5)	2973(5)	41(2)
C22	4768(5)	8821(5)	2600(5)	32(2)
Molecule 2				
O2	580(3)	3690(3)	1352(3)	41(1)
N3	−1608(4)	2112(4)	275(3)	30(1)
N4	1188(4)	2569(4)	451(4)	34(1)
C23	−3654(5)	1243(5)	−299(5)	38(2)
C24	−2599(5)	1239(5)	−382(4)	28(2)
C25	−2368(5)	476(5)	−1076(4)	25(2)
C26	−1185(5)	918(5)	−823(4)	25(2)
C27	−753(5)	1943(5)	21(4)	28(2)
C28	376(5)	2796(5)	654(4)	30(2)
C29	2358(5)	3340(5)	977(5)	41(2)
C30	3063(5)	2971(5)	355(5)	35(2)
C31	2972(5)	1919(5)	177(5)	39(2)
C32	3684(6)	1579(6)	−452(5)	53(2)

Table A.10: Continued Overleaf

C33	−3191(5)	−552(5)	−1982(4)	30(2)
C34	−4232(5)	−1226(5)	−1963(5)	32(2)
C35	−5031(5)	−2098(5)	−2829(5)	38(2)
C36	−4818(5)	−2350(5)	−3716(5)	38(2)
C37	−3781(5)	−1715(5)	−3746(5)	38(2)
C38	−2978(5)	−822(5)	−2885(4)	29(2)
C39	−571(5)	388(5)	−1352(4)	25(1)
C40	−589(5)	−455(5)	−1307(4)	32(2)
C41	14(5)	−940(5)	−1765(5)	38(2)
C42	667(5)	−557(5)	−2273(4)	32(2)
C43	699(5)	286(5)	−2341(4)	28(2)
C44	84(5)	754(5)	−1874(4)	30(2)
Molecule 3				
O3	8143(3)	3880(3)	1527(3)	37(1)
N5	10190(4)	5156(4)	2953(3)	26(1)
N6	7412(4)	4733(4)	2603(4)	33(1)
C45	12151(5)	5875(5)	3716(5)	37(2)
C46	11053(5)	5792(5)	3778(4)	26(2)
C47	10681(5)	6248(4)	4568(4)	25(2)
C48	9531(4)	5859(4)	4181(4)	21(1)
C49	9257(5)	5174(5)	3161(4)	26(2)
C50	8244(5)	4547(5)	2370(4)	26(2)
C51	6283(5)	4071(5)	1942(4)	36(2)
C52	5499(5)	4278(5)	2538(4)	31(2)
C53	5636(5)	5402(5)	2967(5)	37(2)
C54	4878(5)	5606(6)	3603(5)	48(2)
C55	11294(4)	6935(4)	5614(4)	23(1)
C56	12367(5)	7826(5)	5968(4)	32(2)
C57	12926(5)	8455(5)	6954(5)	39(2)
C58	12449(5)	8234(5)	7611(5)	37(2)
C59	11372(5)	7355(5)	7271(5)	33(2)
C60	10821(5)	6710(5)	6281(4)	29(2)
C61	8783(5)	6112(5)	4750(4)	22(1)
C62	8946(5)	7157(5)	5285(4)	32(2)
C63	8237(5)	7377(5)	5813(4)	32(2)
C64	7339(5)	6551(5)	5831(4)	34(2)
C65	7183(5)	5516(5)	5307(4)	32(2)
C66	7899(5)	5300(5)	4791(4)	31(2)

Table A.10: Atomic coordinates [$\times 10^4$], equivalent isotropic displacement parameters [$Å^2 \times 10^3$] and site occupancy factors. U_{eq} is defined as one third of the trace of the orthogonalized U^{ij} tensor.

5-Methyl-3,4-diphenyl-1H-pyrrole-2-carboxylic acid phenylamide

Identification code	**(62)**	
Empirical formula	$C_{24.50}H_{21}ClN_2O$	
Formula weight	394.88	
Temperature	120(2) K	
Wavelength	0.71073 Å	
Crystal system	Monoclinic	
Space group	*C2/c*	
Unit cell dimensions	a = 31.911(6) Å	α = 90°
	b = 5.8971(12) Å	β = 110.83(3)°
	c = 22.306(5) Å	γ = 90°
Volume	3923.3(14) Å^3	
Z	8	
Density (calculated)	1.337 Mg / m^3	
Absorption coefficient	0.213 mm^{-1}	
F(000)	1656	
Crystal	Needle; colourless	
Crystal size	0.20 × 0.05 × 0.02 mm^3	
θ range for data collection	3.52 – 27.06°	
Index ranges	$-40 \le h \le 38$, $-6 \le k \le 7$, $-25 \le l \le 28$	
Reflections collected	10903	
Independent reflections	3959 [R_{int} = 0.1303]	
Completeness to θ = 27.06°	91.3 %	
Absorption correction	Semi–empirical from equivalents	
Max. and min. transmission	0.9958 and 0.9586	
Refinement method	Full-matrix least-squares on F^2	
Data / restraints / parameters	3959 / 0 / 260	
Goodness-of-fit on F^2	0.991	
Final R indices [$F^2 > 2\sigma(F^2)$]	*R1* = 0.0764, *wR2* = 0.1453	
R indices (all data)	*R1* = 0.2031, *wR2* = 0.1944	
Extinction coefficient	0.0009(3)	
Largest diff. peak and hole	0.269 and –0.326 e Å^{-3}	

Table A.11: Structure and refinement data

Atom	x	y	z	U_{eq}
C25	0	1861(12)	7500	61(2)
Cl1	337(1)	234(3)	7206(1)	78(1)
C1	856(1)	1699(7)	5343(2)	30(1)
C2	1229(1)	2959(7)	5698(2)	28(1)
C3	1085(1)	4528(7)	6072(2)	29(1)
C4	631(2)	4156(7)	5938(2)	30(1)
C5	306(1)	5199(7)	6203(2)	36(1)
C6	771(2)	−161(7)	4875(2)	31(1)
C7	1108(1)	−2339(7)	4205(2)	30(1)
C8	861(1)	−4338(7)	4130(2)	33(1)
C9	883(2)	−5918(7)	3681(2)	38(1)
C10	1152(2)	−5564(8)	3319(2)	41(1)
C11	1399(2)	−3600(7)	3408(2)	38(1)
C12	1377(2)	−1982(7)	3841(2)	36(1)
C13	1697(1)	2743(7)	5711(2)	28(1)
C14	1937(1)	738(7)	5926(2)	30(1)
C15	2380(2)	587(7)	5967(2)	35(1)
C16	2588(2)	2407(7)	5802(2)	35(1)
C17	2353(2)	4370(8)	5589(2)	36(1)
C18	1909(2)	4554(7)	5538(2)	31(1)
C19	1360(1)	6128(7)	6562(2)	28(1)
C20	1189(1)	8234(7)	6651(2)	29(1)
C21	1444(2)	9716(7)	7123(2)	32(1)
C22	1872(2)	9151(7)	7512(2)	34(1)
C23	2051(2)	7075(7)	7429(2)	33(1)
C24	1799(1)	5595(7)	6960(2)	32(1)
N1	500(1)	2440(6)	5503(2)	33(1)
N2	1109(1)	−655(6)	4659(2)	31(1)
O1	407(1)	−1153(5)	4686(2)	43(1)

Table A.12: Atomic coordinates [$\times 10^4$], equivalent isotropic displacement parameters [$Å^2 \times 10^3$] and site occupancy factors. U_{eq} is defined as one third of the trace of the orthogonalized U^{ij} tensor.

3,4-Dichloro- pyrrolate-2,5-dicarboxylic acid bis-phenylamide (dimer)

Identification code	**[(65)]$^{2-}$·2TBA**
Empirical formula	$C_{68}H_{96}Cl_4N_8O_4$
	$2C_{18}H_{12}N_3Cl_2O_2 \cdot 2C_{16}H_{36}N$
Formula weight	1231.33
Temperature	120(2) K
Wavelength	0.71073 Å
Crystal system	Monoclinic
Space group	*Pn*
Unit cell dimensions	a = 13.2385(4) Å
	b = 16.9228(5) Å β = 99.944(2)°
	c = 15.0678(4) Å
Volume	3324.96(17) Å^3
Z	2
Density (calculated)	1.230 Mg / m^3
Absorption coefficient	0.231 mm^{-1}
F(000)	1320
Crystal	Colourless Block
Crystal size	0.15 × 0.15 × 0.10 mm^3
θ range for data collection	3.00 – 25.03°
Index ranges	$-15 \le h \le 14$, $-20 \le k \le 20$, $-17 \le l \le 17$
Reflections collected	19094
Independent reflections	10094 [R_{int} = 0.0588]
Completeness to θ = 25.03°	99.1 %
Max. and min. transmission	0.9773 and 0.9662
Refinement method	Full-matrix least-squares on F^2
Data / restraints / parameters	10094 / 2 / 766
Goodness-of-fit on F^2	0.988
Final R indices [$F^2 > 2\sigma(F^2)$]	*R1* = 0.0476, *wR2* = 0.0868
R indices (all data)	*R1* = 0.0819, *wR2* = 0.0984
Absolute structure parameter	–0.05(4)
Extinction coefficient	0.0034(4)
Largest diff. peak and hole	0.325 and –0.226 e Å^{-3}

Table A.13: Crystal and refinement data

Atom	x	y	z	U_{eq}
C1	5584(3)	7204(2)	8172(2)	28(1)
C2	6223(3)	7400(2)	8973(3)	34(1)
C3	5885(3)	7880(2)	9597(3)	32(1)
C4	4909(3)	8178(2)	9411(2)	30(1)
C5	4266(3)	7998(2)	8615(2)	26(1)
C6	4604(3)	7513(2)	7979(2)	24(1)
C7	4162(3)	7099(2)	6365(2)	22(1)
C8	3246(3)	6968(2)	5673(2)	21(1)
C9	1614(3)	6916(2)	5102(2)	20(1)
C10	2146(3)	6759(2)	4400(2)	22(1)
C11	3186(3)	6799(2)	4761(2)	21(1)
C12	507(3)	6955(2)	5090(2)	21(1)
C13	−733(3)	7263(2)	6134(2)	24(1)
C14	−773(3)	7635(2)	6952(3)	31(1)
C15	−1714(3)	7755(2)	7216(3)	36(1)
C16	−2609(3)	7513(2)	6676(3)	36(1)
C17	−2555(3)	7130(2)	5879(3)	33(1)
C18	−1617(3)	6996(2)	5595(3)	26(1)
C53	8669(3)	4658(2)	7210(2)	24(1)
C54	8850(3)	5524(2)	7433(2)	26(1)
C55	8872(3)	5667(2)	8438(2)	29(1)
C56	7832(3)	5581(2)	8713(3)	36(1)
C57	7453(3)	4901(2)	5774(2)	21(1)
C58	6516(3)	4822(2)	6223(2)	28(1)
C59	5589(3)	5114(2)	5589(2)	32(1)
C60	4597(3)	5052(2)	5950(3)	31(1)
C61	8170(3)	3583(2)	6112(2)	23(1)
C62	9057(3)	3023(2)	6360(3)	33(1)
C63	8695(3)	2174(2)	6306(3)	32(1)
C64	8006(4)	1956(2)	6990(3)	41(1)
C65	9280(3)	4701(2)	5751(2)	24(1)
C66	9122(3)	4563(2)	4741(2)	30(1)
C67	10089(3)	4742(2)	4369(2)	29(1)
C68	9847(3)	4810(2)	3343(2)	35(1)
N1	3922(2)	7340(2)	7177(2)	23(1)
N2	2288(2)	7045(2)	5876(2)	20(1)
N3	264(2)	7175(2)	5906(2)	21(1)
N8	8407(2)	4461(2)	6212(2)	21(1)
O1	5042(2)	6996(2)	6237(2)	30(1)
O2	−134(2)	6817(1)	4423(2)	27(1)
Cl1	4173(1)	6684(1)	4154(1)	31(1)

Table A.14: Continued Overleaf

Cl2	1646(1)	6583(1)	3279(1)	30(1)
C19	1557(3)	4836(2)	8058(2)	26(1)
C20	1589(3)	4046(2)	7860(3)	36(1)
C21	1886(3)	3799(2)	7060(3)	34(1)
C22	2159(3)	4357(2)	6478(3)	29(1)
C23	2142(3)	5146(2)	6680(3)	27(1)
C24	1844(3)	5402(2)	7477(2)	23(1)
C25	1663(3)	6607(2)	8390(2)	25(1)
C26	1636(3)	7470(2)	8308(2)	23(1)
C27	1679(3)	8631(2)	7675(2)	23(1)
C28	1421(3)	8755(2)	8521(2)	27(1)
C29	1401(3)	8029(2)	8923(2)	25(1)
C30	1835(3)	9215(2)	6991(2)	25(1)
C31	2467(3)	9330(2)	5531(2)	23(1)
C32	2867(3)	8891(2)	4897(2)	33(1)
C33	3259(4)	9251(2)	4207(3)	43(1)
C34	3249(4)	10057(2)	4139(3)	41(1)
C35	2845(3)	10501(2)	4753(3)	37(1)
C36	2459(3)	10146(2)	5452(3)	32(1)
N4	1826(2)	6222(2)	7623(2)	25(1)
N5	1801(2)	7841(2)	7543(2)	22(1)
N6	2125(2)	8913(2)	6226(2)	27(1)
O3	1548(2)	6265(2)	9079(2)	34(1)
O4	1712(2)	9929(2)	7102(2)	38(1)
Cl3	1095(1)	7874(1)	9975(1)	42(1)
Cl4	1175(1)	9640(1)	9021(1)	43(1)
C37	9860(4)	8963(2)	4256(3)	42(1)
C38	9584(4)	9606(3)	4868(3)	58(2)
C39	9196(5)	9354(3)	5634(3)	81(2)
C40	8942(5)	9973(3)	6275(3)	62(2)
C41	8133(4)	8898(2)	3292(3)	38(1)
C42	7770(4)	8133(2)	3648(3)	38(1)
C43	6666(4)	8199(3)	3816(3)	45(1)
C44	5903(4)	8341(3)	2967(3)	47(1)
C45	9639(3)	8230(2)	2840(2)	31(1)
C46	9129(4)	8106(2)	1872(3)	36(1)
C47	9439(3)	7328(2)	1497(2)	31(1)
C48	8851(4)	7177(2)	562(3)	42(1)
C49	9480(4)	9706(2)	2807(3)	41(1)
C50	10596(5)	9868(3)	2762(4)	72(2)
C51	10756(5)	10608(3)	2237(4)	81(2)
C52	10471(8)	10531(5)	1330(5)	158(4)
N7	9272(3)	8946(2)	3302(2)	32(1)

Table A.14: Atomic coordinates [$\times 10^4$], equivalent isotropic displacement parameters [$Å^2 \times 10^3$] and site occupancy factors. U_{eq} is defined as one third of the trace of the orthogonalized U^{ij} tensor.

3,4-Diphenyl-1*H*-pyrrole-2,5-dicarboxylic acid bis-[(4-nitro-phenyl)-amide]

Identification code	**66**
Empirical formula	$C_{45}H_{31.50}N_{7.50}O_9$
Formula weight	821.28
Temperature	120(2) K
Wavelength	0.71073 Å
Crystal system	Orthorhombic
Space group	*Pbcn*
Unit cell dimensions	a = 32.285(2) Å
	b = 11.8982(6) Å
	c = 19.8475(11) Å
Volume	7624.2(8) Å^3
Z	8
Density (calculated)	1.431 Mg / m^3
Absorption coefficient	0.102 mm^{-1}
F(000)	3408
Crystal	Colourless Plate
Crystal size	0.06 × 0.04 × 0.02 mm^3
θ range for data collection	3.22 – 25.02°
Index ranges	$-38 \le h \le 38$, $-14 \le k \le 13$, $-19 \le l \le 23$
Reflections collected	40433
Independent reflections	5946 [R_{int} = 0.4075]
Completeness to θ = 25.02°	88.3 %
Max. and min. transmission	0.9980 and 0.9939
Refinement method	Full-matrix least-squares on F^2
Data / restraints / parameters	5946 / 0 / 555
Goodness-of-fit on F^2	0.958
Final R indices [$F^2 > 2\sigma(F^2)$]	*R1* = 0.0941, *wR2* = 0.1043
R indices (all data)	*R1* = 0.3726, *wR2* = 0.1634
Largest diff. peak and hole	0.303 and –0.318 e Å^{-3}

Table A.15: Crystal and refinement data

Atom	x	y	z	U_{eq}
C1	−2008(3)	7512(8)	4566(4)	31(2)
C2	−2072(3)	8639(7)	4641(4)	30(2)
C3	−1738(3)	9362(7)	4575(4)	31(2)
C4	−1346(3)	8921(7)	4448(4)	25(2)
C5	−1282(3)	7778(7)	4363(4)	32(2)
C6	−1620(3)	7072(7)	4416(4)	40(3)
C7	−605(3)	9473(8)	4317(4)	30(3)
C8	−324(3)	10450(7)	4261(4)	28(2)
C9	−351(3)	11609(7)	4287(4)	23(2)
C10	52(3)	12026(6)	4157(3)	20(2)
C11	309(3)	11115(7)	4069(4)	21(2)
C12	756(3)	10903(8)	3931(4)	21(2)
C13	1429(3)	11908(9)	3786(4)	33(3)
C14	1682(3)	10977(7)	3752(4)	32(2)
C15	2102(3)	11107(8)	3678(4)	37(3)
C16	2265(3)	12170(9)	3657(4)	35(3)
C17	2017(3)	13124(7)	3674(4)	37(3)
C18	1599(3)	12989(7)	3745(4)	33(2)
C19	189(2)	13227(7)	4145(4)	23(2)
C20	351(2)	13719(7)	4722(4)	34(2)
C21	499(2)	14805(7)	4702(5)	41(3)
C22	486(2)	15402(7)	4108(5)	40(3)
C23	323(2)	14924(7)	3538(4)	32(2)
C24	175(2)	13823(6)	3555(4)	27(2)
C25	−728(2)	12283(7)	4421(5)	24(2)
C26	−885(3)	13036(7)	3941(4)	32(2)
C27	−1245(3)	13629(7)	4075(4)	35(2)
C28	−1457(3)	13503(7)	4669(5)	38(3)
C29	−1307(3)	12751(7)	5147(4)	38(3)
C30	−943(3)	12150(6)	5008(4)	29(2)
C31	6772(3)	4165(7)	2829(4)	32(3)
C32	7186(3)	4379(7)	2885(4)	30(3)
C33	7313(3)	5469(8)	2992(4)	28(2)
C34	7036(3)	6355(7)	3069(4)	30(2)
C35	6620(2)	6125(7)	3007(3)	27(2)
C36	6488(3)	5032(8)	2879(4)	26(2)
C40	5489(2)	2683(7)	2577(4)	23(2)
C41	5814(3)	2534(7)	2124(4)	30(2)
C42	6088(3)	1647(8)	2189(4)	39(3)
C43	6032(3)	861(7)	2709(5)	37(3)
C44	5700(3)	989(7)	3134(4)	30(2)

Table A.16: Continued Overleaf

C45	5432(2)	1882(7)	3084(4)	32(2)
N1	−2355(2)	6725(7)	4648(3)	39(2)
N2	−1015(2)	9698(5)	4414(3)	30(2)
N3	74(2)	10171(5)	4130(3)	24(2)
N4	1001(2)	11851(5)	3898(3)	28(2)
N5	2719(3)	12299(7)	3615(3)	38(2)
N6	7758(2)	5711(7)	3017(4)	40(2)
N7	6069(2)	4757(5)	2801(3)	28(2)
N8	5000	5465(7)	2500	26(3)
O1	−2699(2)	7128(5)	4772(3)	51(2)
O2	−2294(2)	5717(5)	4563(3)	56(2)
O3	−464(2)	8526(5)	4268(3)	32(2)
O4	885(2)	9954(4)	3868(3)	31(2)
O5	2927(2)	11430(5)	3592(3)	57(2)
O6	2868(2)	13255(5)	3609(3)	56(2)
O7	7999(2)	4893(5)	3022(3)	52(2)
O8	7875(2)	6688(5)	3038(3)	45(2)
O9	5751(2)	6446(5)	2621(3)	33(2)
C37	5737(3)	5426(8)	2653(4)	25(2)
C38	5342(3)	4799(7)	2557(4)	26(2)
C39	5219(2)	3670(7)	2532(4)	22(2)

Table A.16. Atomic coordinates [$\times 10^4$], equivalent isotropic displacement parameters [$Å^2 \times 10^3$] and site occupancy factors. U_{eq} is defined as one third of the trace of the orthogonalized U^{ij} tensor.

3,4-Diphenyl-1*H*-pyrrole-2,5-dicarboxylic acid bis-[(4-nitro-phenyl)-amide] (DMSO complex)

Identification code	**(66)·DMSO**	
Empirical formula	$C_{36}H_{36}N_5O_9S_3$	
Formula weight	778.88	
Temperature	120(2) K	
Wavelength	0.71073 Å	
Crystal system	Triclinic	
Space group	P-1	
Unit cell dimensions	a = 11.0659(2) Å	α = 84.4620(10)°
	b = 12.0400(2) Å	β = 81.3330(10)°
	c = 15.9608(4) Å	γ = 64.3060(10)°
Volume	1893.21(7) Å^3	
Z	2	
Density (calculated)	1.366 Mg / m^3	
Absorption coefficient	0.256 mm^{-1}	
F(000)	814	
Crystal	Yellow Plate	
Crystal size	0.30 × 0.15 × 0.05 mm^3	
θ range for data collection	3.08 – 25.03°	
Index ranges	$-13 \le h \le 13$, $-11 \le k \le 14$, $-18 \le l \le 18$	
Reflections collected	19454	
Independent reflections	6390 [R_{int} = 0.0621]	
Completeness to θ = 25.03°	95.4 %	
Max. and min. transmission	0.9873 and 0.9272	
Refinement method	Full-matrix least-squares on F^2	
Data / restraints / parameters	6390 / 0 / 488	
Goodness-of-fit on F^2	1.022	
Final R indices [$F^2 > 2\sigma(F^2)$]	*R1* = 0.0452, *wR2* = 0.1118	
R indices (all data)	*R1* = 0.0675, *wR2* = 0.1222	
Extinction coefficient	0.0058(12)	
Largest diff. peak and hole	0.463 and –0.365 e Å^{-3}	

Table A.17: Crystal and refinement data

Atom	*x*	*y*	*z*	U_{eq}
C1	5433(2)	6784(2)	10174(1)	23(1)
C2	4948(2)	6469(2)	9526(1)	23(1)
C3	5586(2)	6455(2)	8712(2)	24(1)
C4	6699(2)	6732(2)	8548(1)	20(1)
C5	7195(2)	7013(2)	9214(1)	22(1)
C6	6541(2)	7046(2)	10031(2)	24(1)
C7	8225(2)	7084(2)	7327(1)	20(1)
C8	8442(2)	7061(2)	6391(1)	18(1)
C9	7926(2)	6677(2)	5785(1)	18(1)
C10	8425(2)	7024(2)	4979(1)	18(1)
C11	9240(2)	7586(2)	5120(1)	18(1)
C12	10027(2)	8078(2)	4485(1)	18(1)
C13	11785(2)	8877(2)	4351(1)	19(1)
C14	11913(2)	9091(2)	3473(1)	23(1)
C15	12818(2)	9558(2)	3099(2)	24(1)
C16	13563(2)	9826(2)	3600(2)	23(1)
C17	13451(2)	9628(2)	4472(2)	24(1)
C18	12563(2)	9149(2)	4843(2)	22(1)
C19	7033(2)	6023(2)	5943(1)	19(1)
C20	7492(3)	4849(2)	6337(1)	24(1)
C21	6643(3)	4262(2)	6513(2)	31(1)
C22	5345(3)	4823(3)	6286(2)	36(1)
C23	4897(3)	5971(3)	5878(2)	35(1)
C24	5736(2)	6569(2)	5706(2)	26(1)
C25	8148(2)	6727(2)	4166(1)	18(1)
C26	8537(2)	5500(2)	3991(2)	22(1)
C27	8248(2)	5192(2)	3253(2)	27(1)
C28	7562(2)	6108(2)	2682(2)	26(1)
C29	7157(3)	7334(2)	2853(2)	27(1)
C30	7452(2)	7644(2)	3587(1)	23(1)
C31	11897(3)	7221(2)	8038(2)	34(1)
C32	12272(3)	9188(3)	7349(2)	41(1)
C33	11456(3)	6187(3)	279(2)	36(1)
C34	10533(3)	7206(4)	1790(2)	61(1)
N1	4725(2)	6861(2)	11035(1)	29(1)
N2	7266(2)	6698(2)	7698(1)	22(1)
N3	9239(2)	7590(2)	5978(1)	18(1)
N4	10914(2)	8394(2)	4797(1)	20(1)
N5	14496(2)	10348(2)	3205(1)	30(1)
O1	3933(2)	6381(2)	11195(1)	40(1)
O2	4954(2)	7401(2)	11561(1)	54(1)
O3	8834(2)	7461(2)	7723(1)	26(1)

Table A.18: Continued Overleaf

O4	9871(2)	8188(2)	3733(1)	27(1)
O5	15098(2)	10643(2)	3672(1)	38(1)
O6	14638(2)	10471(2)	2427(1)	41(1)
O7	11130(2)	8164(2)	6555(1)	27(1)
O8	8870(2)	7157(2)	811(1)	44(1)
S1	11045(1)	8590(1)	7435(1)	24(1)
S2	10164(1)	6318(1)	1135(1)	35(1)
S3A	2499(1)	9287(1)	10097(1)	26(1)
O9A	1865(2)	8900(3)	9514(2)	70(1)
C35A	3489(3)	9969(3)	9493(2)	39(1)
C36A	1287(3)	10576(3)	10647(2)	42(1)
S3B	1803(2)	9888(2)	9639(2)	33(1)
O9B	1865(2)	8900(3)	9514(2)	70(1)
C35B	3489(3)	9969(3)	9493(2)	39(1)
C36B	1287(3)	10576(3)	10647(2)	42(1)

Table A.18: Atomic coordinates [$\times 10^4$], equivalent isotropic displacement parameters [$Å^2 \times 10^3$] and site occupancy factors. U_{eq} is defined as one third of the trace of the orthogonalized U^{ij} tensor.

3,4-Diphenyl-1*H*-pyrrole-2,5-dicarboxylic acid bis-[(3,5-dinitro-phenyl)-amide]

Identification code	**(67)**
Empirical formula	$C_{30}H_{19}N_7O_{10}$
Formula weight	637.52
Temperature	120(2) K
Wavelength	0.71073 Å
Crystal system	Monoclinic
Space group	$P2_1/c$
Unit cell dimensions	a = 20.3034(11) Å
	b = 10.1636(5) Å $\quad\beta$ = 104.057(2)°
	c = 13.4570(6) Å
Volume	2693.8(2) Å^3
Z	4
Density (calculated)	1.572 Mg / m^3
Absorption coefficient	0.122 mm^{-1}
F(000)	1312
Crystal	Colourless Prism
Crystal size	0.10 × 0.04 × 0.03 mm^3
θ range for data collection	3.04 – 25.03°
Index ranges	$-24 \le h \le 24$, $-12 \le k \le 12$, $-16 \le l \le 15$
Reflections collected	17978
Independent reflections	4716 [R_{int} = 0.0965]
Completeness to θ = 25.03°	99.3 %
Max. and min. transmission	0.9964 and 0.9879
Refinement method	Full-matrix least-squares on F^2
Data / restraints / parameters	4716 / 0 / 425
Goodness-of-fit on F^2	0.928
Final R indices [$F^2 > 2\sigma(F^2)$]	$R1$ = 0.0550, $wR2$ = 0.1074
R indices (all data)	$R1$ = 0.1256, $wR2$ = 0.1308
Extinction coefficient	0.0021(5)
Largest diff. peak and hole	0.266 and −0.281 e Å^{-3}

Table A.19: Crystal and refinement data

Atom	x	y	z	U_{eq}
C1	−4067(1)	10375(3)	−2050(2)	27(1)
C2	−4399(2)	11556(3)	−2127(2)	28(1)
C3	−4280(2)	12483(3)	−1355(2)	29(1)
C4	−3824(2)	12116(3)	−466(2)	28(1)
C5	−3486(1)	10928(3)	−319(2)	26(1)
C6	−3603(1)	10051(3)	−1136(2)	27(1)
C7	−2676(2)	8457(3)	−489(2)	26(1)
C8	−2433(1)	7157(3)	−705(2)	24(1)
C9	−2619(1)	6255(3)	−1505(2)	26(1)
C10	−2161(1)	5188(3)	−1269(2)	25(1)
C11	−1706(2)	5484(3)	−348(2)	26(1)
C12	−1064(2)	4869(3)	234(2)	29(1)
C13	−264(2)	3073(3)	31(2)	27(1)
C14	178(1)	3106(3)	1000(2)	27(1)
C15	699(1)	2206(3)	1217(2)	25(1)
C16	813(1)	1269(3)	543(2)	27(1)
C17	360(2)	1260(3)	−405(2)	27(1)
C18	−163(2)	2143(3)	−679(2)	29(1)
C19	−3178(1)	6361(3)	−2445(2)	26(1)
C20	−3682(2)	5396(3)	−2666(2)	29(1)
C21	−4203(2)	5487(3)	−3540(2)	32(1)
C22	−4234(2)	6531(3)	−4199(2)	33(1)
C23	−3743(2)	7490(3)	−3996(2)	31(1)
C24	−3214(2)	7402(3)	−3130(2)	28(1)
C25	−2155(1)	3967(3)	−1873(2)	26(1)
C26	−2270(1)	2750(3)	−1461(2)	28(1)
C27	−2209(2)	1589(3)	−1963(2)	33(1)
C28	−2039(2)	1627(3)	−2897(2)	35(1)
C29	−1937(2)	2824(3)	−3328(2)	35(1)
C30	−1994(1)	3985(3)	−2816(2)	31(1)
N1	−4916(1)	11836(3)	−3074(2)	35(1)
N2	−3704(1)	13051(3)	394(2)	38(1)
N3	−3290(1)	8820(2)	−1100(2)	28(1)
N4	−1883(1)	6659(2)	−17(2)	27(1)
N5	−823(1)	3901(2)	−292(2)	31(1)
N6	1168(1)	2197(2)	2247(2)	29(1)
N7	428(1)	217(2)	−1136(2)	31(1)
O1	−5032(1)	10999(2)	−3753(2)	43(1)
O2	−5216(1)	12890(2)	−3132(2)	43(1)
O3	−3700(1)	14222(2)	191(2)	59(1)

Table A.20: Continued Overleaf

O4	−3616(1)	12602(2)	1256(2)	44(1)
O5	−2339(1)	9170(2)	178(2)	35(1)
O6	−772(1)	5250(2)	1078(2)	36(1)
O7	1067(1)	2968(2)	2890(2)	37(1)
O8	1639(1)	1413(2)	2405(2)	37(1)
O9	892(1)	−576(2)	−854(2)	38(1)
O10	4(1)	177(2)	−1961(2)	37(1)

Table A.20: Atomic coordinates [$\times 10^4$], equivalent isotropic displacement parameters [$Å^2 \times 10^3$] and site occupancy factors. U_{eq} is defined as one third of the trace of the orthogonalized U^{ij} tensor.

3,4-Diphenyl-1*H*-pyrrole-2,5-dicarboxylic acid bis-[(3,5-dinitro-phenyl)-amide] (DMSO complex)

Identification code	**(67)·DMSO**	
Empirical formula	$C_{34}H_{31}N_7O_{12}S_2$	
Formula weight	793.78	
Temperature	120(2) K	
Wavelength	0.71073 Å	
Crystal system	Triclinic	
Space group	*P*–1	
Unit cell dimensions	a = 8.608(5) Å	α = 67.786(5)°
	b = 15.212(5) Å	β = 84.475(5)°
	c = 15.257(5) Å	γ = 73.886(5)°
Volume	1776.8(13) Å^3	
Z	2	
Density (calculated)	1.484 Mg / m^3	
Absorption coefficient	0.225 mm^{-1}	
F(000)	824	
Crystal	Colourless Plate	
Crystal size	0.15 × 0.10 × 0.02 mm^3	
θ range for data collection	3.16 – 25.03°	
Index ranges	$-10 \le h \le 10$, $-18 \le k \le 18$, $-18 \le l \le 18$	
Reflections collected	19499	
Independent reflections	6028 [R_{int} = 0.1126]	
Completeness to θ = 25.03°	96.3 %	
Max. and min. transmission	0.9955 and 0.9670	
Refinement method	Full-matrix least-squares on F^2	
Data / restraints / parameters	6028 / 0 / 501	
Goodness-of-fit on F^2	0.909	
Final *R* indices [$F^2 > 2\sigma(F^2)$]	*R1* = 0.0559, *wR2* = 0.0998	
R indices (all data)	*R1* = 0.1424, *wR2* = 0.1242	
Extinction coefficient	0.0025(6)	
Largest diff. peak and hole	0.297 and –0.310 e Å^{-3}	

Table A.21: Structure and refinement data

Atom	x	y	z	U_{eq}
C1	1869(4)	4926(3)	1351(3)	23(1)
C2	499(4)	5698(3)	1105(3)	22(1)
C3	−24(5)	6250(3)	184(3)	24(1)
C4	934(4)	5971(3)	−500(3)	22(1)
C5	2313(4)	5204(3)	−308(3)	22(1)
C6	2797(4)	4680(3)	632(3)	22(1)
C7	5198(4)	3451(3)	369(3)	21(1)
C8	6454(4)	2562(3)	902(3)	20(1)
C9	6793(4)	2024(3)	1852(3)	21(1)
C10	8279(4)	1314(3)	1905(3)	20(1)
C11	8788(4)	1438(3)	978(3)	20(1)
C12	10223(4)	844(3)	665(3)	21(1)
C13	11846(4)	761(3)	−742(3)	22(1)
C14	12037(5)	1309(3)	−1689(3)	24(1)
C15	13384(4)	976(3)	−2157(3)	23(1)
C16	14575(4)	121(3)	−1734(3)	23(1)
C17	14315(4)	−401(3)	−809(3)	22(1)
C18	12992(4)	−119(3)	−298(3)	21(1)
C19	5763(4)	2147(3)	2660(3)	23(1)
C20	6320(5)	2406(3)	3331(3)	27(1)
C21	5333(5)	2555(3)	4060(3)	33(1)
C22	3782(5)	2440(3)	4127(3)	33(1)
C23	3222(5)	2180(3)	3474(3)	30(1)
C24	4212(5)	2026(3)	2748(3)	25(1)
C25	9112(4)	569(3)	2797(3)	22(1)
C26	10704(4)	483(3)	2988(3)	25(1)
C27	11446(5)	−205(3)	3829(3)	32(1)
C28	10599(6)	−810(3)	4483(3)	38(1)
C29	9007(6)	−725(3)	4313(3)	35(1)
C30	8266(5)	−23(3)	3475(3)	28(1)
C31	7663(5)	5259(3)	4853(3)	41(1)
C32	9243(5)	3597(3)	4584(3)	45(1)
C33	7290(7)	2044(4)	7351(4)	59(2)
C34	5679(6)	3761(5)	7450(4)	67(2)
N1	−469(4)	5927(3)	1879(3)	30(1)
N2	413(4)	6506(2)	−1489(2)	26(1)
N3	4153(4)	3873(2)	920(2)	25(1)
N4	7654(3)	2207(2)	379(2)	19(1)
N5	10493(4)	1152(2)	−291(2)	24(1)
N6	13551(4)	1585(3)	−3156(2)	29(1)
N7	15525(4)	−1327(2)	−309(3)	24(1)

Table A.22: Continued Overleaf

O1	52(3)	5475(2)	2690(2)	34(1)
O2	−1755(3)	6564(2)	1662(2)	39(1)
O3	−786(4)	7208(2)	−1671(2)	39(1)
O4	1190(3)	6215(2)	−2095(2)	36(1)
O5	5147(3)	3793(2)	−492(2)	28(1)
O6	11102(3)	112(2)	1232(2)	30(1)
O7	12495(4)	2339(2)	−3523(2)	42(1)
O8	14744(4)	1290(2)	−3580(2)	43(1)
O9	16663(3)	−1620(2)	−767(2)	34(1)
O10	15345(3)	−1748(2)	539(2)	32(1)
O11	6356(3)	3780(2)	5339(2)	35(1)
O12	8331(3)	2750(2)	8434(2)	27(1)
S1	7234(1)	4352(1)	4524(1)	34(1)
S2	7681(1)	3080(1)	7437(1)	27(1)

Table A.22 Atomic coordinates [$\times 10^4$], equivalent isotropic displacement parameters [$Å^2 \times 10^3$] and site occupancy factors. U_{eq} is defined as one third of the trace of the orthogonalized U^{ij} tensor.

3,4-Diphenyl-1*H*-pyrrolate-2,5-dicarboxylic acid bis-[(3,5-dinitro-phenyl)-amide] (chloride complex)

Identification code	**(67$^{\cdot\cdot}$Cl^{-})·2TBA^{+}**	
Empirical formula	$C_{62}H_{90}ClN_9O_{10}$	
Formula weight	1156.88	
Temperature	120(2) K	
Wavelength	0.71069 Å	
Crystal system	Triclinic	
Space group	P-1	
Unit cell dimensions	a = 13.408(5) Å	α = 73.042(5)°
	b = 15.847(5) Å	β = 74.733(5)°
	c = 17.023(5) Å	γ = 68.046(5)°
Volume	3159.9(18) Å^3	
Z	2	
Density (calculated)	1.216 Mg / m^3	
Absorption coefficient	0.123 mm^{-1}	
F(000)	1244	
Crystal	Colourless plate	
Crystal size	0.06 × 0.04 × 0.01 mm^3	
θ range for data collection	3.07 – 25.02°	
Index ranges	$-15 \le h \le 15$, $-18 \le k \le 18$, $-17 \le l \le 18$	
Reflections collected	19191	
Independent reflections	8690 [R_{int} = 0.2915]	
Completeness to θ = 25.02°	78.0 %	
Max. and min. transmission	0.9988 and 0.9926	
Refinement method	Full-matrix least-squares on F^2	
Data / restraints / parameters	8690 / 378 / 700	
Goodness-of-fit on F^2	0.830	
Final R indices [$F^2 > 2\sigma(F^2)$]	*R1* = 0.1330, *wR2* = 0.1941	
R indices (all data)	*R1* = 0.4834, *wR2* = 0.2967	
Extinction coefficient	0.0015(5)	
Largest diff. peak and hole	0.646 and –0.278 e Å^{-3}	

Table A.23: Structure and refinement data

Atom	x	y	z	U_{eq}
Cl1	4148(4)	6478(3)	1889(3)	77(2)
O1	534(10)	3343(9)	2169(8)	93(4)
O2	−660(9)	4568(8)	1563(7)	77(4)
O3	−118(11)	7557(9)	811(8)	96(5)
O4	1313(11)	7688(8)	1067(9)	90(5)
O5	3580(7)	2970(7)	2800(6)	60(3)
O6	7712(7)	4187(6)	3443(6)	51(3)
O7	5347(10)	8639(7)	1167(8)	78(4)
O8	6360(9)	9271(9)	1471(9)	95(4)
O9	9387(10)	7339(8)	2853(7)	76(4)
O10	9478(9)	5917(8)	3521(7)	75(4)
N1	167(12)	4184(11)	1888(9)	64(4)
N2	759(16)	7226(11)	1083(10)	91(6)
N3	3400(8)	4534(7)	2398(7)	47(3)
N4	5297(9)	4191(7)	2922(7)	44(3)
N5	6455(9)	5345(7)	2721(7)	43(3)
N6	6053(12)	8590(9)	1494(9)	68(4)
N7	9070(10)	6661(12)	3067(9)	58(4)
C1	1807(8)	4350(5)	2158(6)	58(5)
C2	832(7)	4741(6)	1851(6)	54(4)
C3	472(6)	5689(7)	1498(6)	51(4)
C4	1087(8)	6245(5)	1454(6)	57(5)
C5	2062(7)	5853(6)	1761(6)	44(4)
C6	2422(6)	4905(7)	2113(6)	50(4)
C7	3918(13)	3609(12)	2722(10)	53(5)
C8	4978(12)	3432(11)	2982(9)	50(4)
C9	5796(11)	2602(9)	3208(8)	39(4)
C10	6656(11)	2847(9)	3339(8)	43(4)
C11	6321(12)	3815(10)	3111(9)	45(4)
C12	6911(12)	4433(10)	3122(10)	45(4)
C13	6845(7)	6096(6)	2584(6)	44(4)
C14	6297(6)	6955(7)	2128(6)	53(4)
C15	6654(7)	7714(5)	1986(5)	53(4)
C16	7559(8)	7614(6)	2300(6)	55(5)
C17	8107(6)	6755(7)	2756(6)	46(4)
C18	7751(7)	5996(5)	2898(5)	51(4)
C19	5861(8)	1611(5)	3272(6)	47(4)
C20	5050(6)	1260(6)	3791(6)	55(4)
C21	5143(7)	335(7)	3879(5)	60(5)
C22	6048(8)	−239(5)	3448(6)	60(5)
C23	6859(7)	112(6)	2930(6)	61(5)
C24	6766(7)	1037(6)	2841(5)	47(4)
C25	7700(6)	2162(6)	3559(6)	36(4)

Table A.24: Continued Overleaf

C26	7701(6)	1382(7)	4200(5)	51(4)
C27	8684(8)	713(5)	4379(5)	55(4)
C28	9667(6)	825(6)	3917(6)	68(5)
C29	9666(6)	1605(7)	3276(6)	63(5)
C30	8683(8)	2274(5)	3097(5)	53(4)
N8	5213(10)	2177(8)	653(8)	55(4)
C31	4715(11)	1599(9)	1418(9)	48(4)
C32	4115(11)	1012(9)	1328(9)	46(4)
C33	3764(11)	439(9)	2136(9)	59(5)
C34	2891(12)	992(11)	2727(10)	75(5)
C35	6097(11)	1573(10)	100(10)	58(4)
C36	7133(11)	1020(10)	494(9)	56(4)
C37	8030(13)	400(11)	−47(11)	80(5)
C38	7670(30)	−320(20)	−270(20)	276(17)
C39	5613(12)	2802(10)	927(9)	57(5)
C40	6090(12)	3459(10)	229(9)	60(5)
C41	6500(12)	4035(10)	597(10)	66(5)
C42	7517(12)	3442(10)	998(10)	72(5)
C43	4374(12)	2747(10)	114(10)	68(5)
C44	3327(11)	3433(10)	517(9)	59(5)
C45	2455(13)	3883(11)	−52(11)	79(6)
N9	7986(9)	3028(8)	5779(8)	47(3)
C46	1863(14)	3184(11)	−11(11)	102(7)
C47	8991(10)	2683(9)	5143(9)	43(4)
C48	10097(10)	2419(9)	5401(9)	51(4)
C49	11023(10)	2032(9)	4718(9)	47(4)
C50	12104(11)	1649(10)	5030(10)	69(5)
C51	7897(11)	3959(9)	5902(8)	46(4)
C52	7847(11)	4737(9)	5091(9)	52(4)
C53	7572(11)	5664(9)	5309(9)	51(4)
C54	8453(11)	5753(9)	5679(9)	59(5)
C55	7042(11)	3075(10)	5439(9)	53(4)
C56	5906(11)	3571(10)	5873(10)	61(5)
C57	5023(11)	3500(10)	5504(9)	55(5)
C58	4916(12)	2528(10)	5717(9)	65(5)
C59	8042(12)	2375(10)	6623(10)	61(5)
C60	8181(12)	1372(9)	6674(9)	57(5)
C61	8435(12)	775(11)	7506(10)	74(5)
C62	9579(12)	649(10)	7628(10)	74(5)

Table A.24: Atomic coordinates [$\times 10^4$], equivalent isotropic displacement parameters [$Å^2 \times 10^3$] and site occupancy factors. U_{eq} is defined as one third of the trace of the orthogonalized U^{ij} tensor.

3,4-Diphenyl-1*H*-pyrrole-2,5-dicarboxylic acid bis-pentafluorophenyl-amide

Identification code	**(68)**
Empirical formula	$C_{30}H_{13}F_{10}N_3O_2$
Formula weight	637.43
Temperature	120(2) K
Wavelength	0.71073 Å
Crystal system	Orthorhombic
Space group	*Pbcn*
Unit cell dimensions	a = 30.5621(10) Å
	b = 9.6116(2) Å
	c = 17.5716(4) Å
Volume	5161.7(2) Å^3
Z	8
Density (calculated)	1.641 Mg / m^3
Absorption coefficient	0.154 mm^{-1}
F(000)	2560
Crystal	Colourless Block
Crystal size	0.15 × 0.02 × 0.01 mm^3
θ range for data collection	2.91 – 25.02°
Index ranges	$-21 \le h \le 36$, $-9 \le k \le 11$, $-20 \le l \le 20$
Reflections collected	15365
Independent reflections	4515 [R_{int} = 0.1234]
Completeness to θ = 25.02°	99.1 %
Max. and min. transmission	0.9985 and 0.9773
Refinement method	Full-matrix least-squares on F^2
Data / restraints / parameters	4515 / 0 / 458
Goodness-of-fit on F^2	0.897
Final R indices [$F^2 > 2\sigma(F^2)$]	$R1$ = 0.0541, $wR2$ = 0.0966
R indices (all data)	$R1$ = 0.1608, $wR2$ = 0.1272
Largest diff. peak and hole	0.274 and –0.328 e Å^{-3}

Table A.25: Structure and refinement data

Atom	x	y	z	U_{eq}
C1	3289(1)	9124(5)	−606(2)	32(1)
C2	2854(2)	9417(5)	−733(2)	37(1)
C3	2544(1)	8615(5)	−377(2)	39(1)
C4	2667(1)	7524(5)	71(2)	35(1)
C5	3107(1)	7220(4)	173(2)	28(1)
C6	3425(1)	8048(5)	−160(2)	26(1)
C7	4094(1)	7660(4)	603(2)	24(1)
C8	4578(1)	7536(4)	529(2)	24(1)
C9	4854(1)	7556(4)	−96(2)	24(1)
C10	5287(1)	7371(4)	185(2)	25(1)
C11	5256(1)	7247(4)	966(2)	22(1)
C12	5582(1)	7012(5)	1573(2)	27(1)
C13	6356(1)	6487(5)	1806(2)	27(1)
C14	6523(1)	7473(5)	2294(2)	28(1)
C15	6881(1)	7188(5)	2740(2)	30(1)
C16	7081(1)	5901(5)	2696(2)	32(1)
C17	6917(1)	4909(5)	2229(2)	31(1)
C18	6560(1)	5197(5)	1783(2)	28(1)
C19	4734(1)	7734(5)	−908(2)	22(1)
C20	4644(1)	6610(6)	−1366(3)	32(1)
C21	4500(1)	6762(6)	−2107(3)	36(1)
C22	4445(1)	8084(6)	−2405(3)	32(1)
C23	4542(1)	9215(6)	−1964(3)	34(1)
C24	4686(1)	9058(5)	−1225(2)	29(1)
C25	5684(1)	7350(5)	−306(2)	24(1)
C26	5931(2)	8535(5)	−417(2)	34(1)
C27	6298(2)	8525(6)	−881(3)	38(1)
C28	6417(2)	7320(6)	−1244(3)	39(1)
C29	6173(2)	6118(6)	−1156(3)	35(1)
C30	5806(2)	6147(5)	−681(2)	32(1)
N1	3879(1)	7764(4)	−82(2)	28(1)
N2	4822(1)	7353(4)	1170(2)	24(1)
N3	6001(1)	6778(4)	1313(2)	34(1)
O1	3910(1)	7672(3)	1211(2)	34(1)
O2	5494(1)	7000(3)	2245(2)	32(1)
F1	3590(1)	9930(3)	−955(1)	49(1)
F2	2735(1)	10485(3)	−1170(2)	58(1)
F3	2115(1)	8883(3)	−475(2)	60(1)
F4	2363(1)	6706(3)	402(1)	52(1)
F5	3214(1)	6101(3)	581(1)	39(1)
F6	6341(1)	8738(3)	2331(1)	37(1)

Table A.26: Continued Overleaf

F7	7045(1)	8173(3)	3205(1)	41(1)
F8	7435(1)	5642(3)	3128(1)	48(1)
F9	7104(1)	3636(3)	2195(1)	42(1)
F10	6411(1)	4219(3)	1298(1)	42(1)

Table A.26: Atomic coordinates [$\times 10^4$], equivalent isotropic displacement parameters [$Å^2 \times 10^3$] and site occupancy factors. U_{eq} is defined as one third of the trace of the orthogonalized U^{ij} tensor.

5-Methyl-3,4-diphenyl-1*H*-pyrrole-2-carboxylic acid -(benzo-15-crown-5)-amide

Identification code	**(69)**	
Empirical formula	$C_{32}H_{31.50}N_2O_6$	
Formula weight	540.09	
Temperature	120(2) K	
Wavelength	0.71073 Å	
Crystal system	Monoclinic	
Space group	$P2_1/n$	
Unit cell dimensions	a = 9.0934(18) Å	$\alpha = 90°$
	b = 36.865(7) Å	$\beta = 92.70(3)°$
	c = 16.608(3) Å	$\gamma = 90°$
Volume	5561.4(19) Å^3	
Z	8	
Density (calculated)	1.290 Mg / m^3	
Absorption coefficient	0.089 mm^{-1}	
F(000)	2284	
Crystal	Plate; colourless	
Crystal size	0.14 × 0.10 × 0.01 mm^3	
θ range for data collection	2.96 – 24.94°	
Index ranges	$-10 \le h \le 10, -43 \le k \le 43, -19 \le l \le 19$	
Reflections collected	47013	
Independent reflections	8960 [R_{int} = 0.1535]	
Completeness to θ = 24.94°	92.2 %	
Absorption correction	Semi–empirical from equivalents	
Max. and min. transmission	0.9991 and 0.9876	
Refinement method	Full-matrix least-squares on F^2	
Data / restraints / parameters	8960 / 18 / 774	
Goodness-of-fit on F^2	1.003	
Final R indices [$F^2 > 2\sigma(F^2)$]	$R1$ = 0.0822, $wR2$ = 0.1679	
R indices (all data)	$R1$ = 0.2408, $wR2$ = 0.2277	
Extinction coefficient	0.0000(3)	
Largest diff. peak and hole	0.639 and –0.466 e Å^{-3}	

Table A.27: Structure and refinement data

Atom	x	y	z	U_{eq}
C1	446(6)	−3032(2)	1379(3)	45(2)
C2	100(6)	−3381(2)	927(3)	55(2)
C3	529(6)	−2967(2)	2204(3)	49(2)
C4	309(6)	−3237(2)	2844(3)	47(2)
C5	1064(7)	−3564(2)	2853(4)	77(2)
C6	816(8)	−3825(2)	3428(4)	88(2)
C7	−146(8)	−3763(2)	4024(4)	68(2)
C8	−888(7)	−3436(2)	4022(3)	59(2)
C9	−673(6)	−3177(2)	3438(3)	48(2)
C10	797(6)	−2587(2)	2304(3)	44(2)
C11	958(6)	−2386(2)	3077(3)	42(2)
C12	2186(6)	−2420(2)	3572(3)	44(2)
C13	2406(7)	−2206(2)	4254(3)	56(2)
C14	1360(7)	−1960(2)	4458(3)	55(2)
C15	123(7)	−1924(2)	3970(4)	71(2)
C16	−92(6)	−2130(2)	3284(3)	71(2)
C17	898(5)	−2439(2)	1535(3)	40(2)
C18	1236(6)	−2080(2)	1241(3)	42(2)
C19	2167(7)	−1474(2)	1751(3)	55(2)
C20	2300(8)	−1294(2)	1036(3)	77(2)
C21	2756(8)	−934(2)	1060(3)	78(2)
C22	3060(7)	−752(2)	1770(3)	55(2)
C23	2902(6)	−936(2)	2488(3)	43(2)
C24	2473(6)	−1304(2)	2481(3)	47(2)
C25	3031(6)	−926(1)	3936(3)	42(2)
C26	3439(6)	−665(2)	4587(3)	45(2)
C27	2616(6)	−114(2)	5184(3)	52(2)
C28	2077(9)	243(2)	4864(4)	87(2)
O4	2779(9)	488(2)	4481(4)	46(4)
C29	2801(10)	496(2)	3632(4)	97(3)
C30	3935(13)	276(4)	3302(5)	61(5)
O4'	3506(12)	249(3)	4215(6)	60(5)
C29'	2801(10)	496(2)	3632(4)	97(3)
C30'	4449(18)	559(5)	3092(8)	55(6)
O5	4000(6)	291(1)	2463(3)	80(1)
C31	4811(17)	−63(5)	2691(11)	79(7)
C31'	5007(12)	132(3)	2083(8)	48(5)
C32	4903(7)	−306(2)	2062(4)	60(2)
C33	4583(6)	3229(2)	6570(3)	40(1)
C34	4837(6)	3575(2)	6126(3)	53(2)

Table A.28: Continued Overleaf

C35	4519(5)	3160(2)	7390(3)	38(1)
C36	4573(6)	3443(2)	8025(3)	43(2)
C37	3561(6)	3726(2)	7991(3)	60(2)
C38	3550(7)	3995(2)	8567(4)	74(2)
C39	4550(8)	3984(2)	9205(4)	63(2)
C40	5555(8)	3706(2)	9261(3)	65(2)
C41	5571(6)	3436(2)	8672(3)	54(2)
C42	4305(5)	2784(2)	7487(3)	37(1)
C43	4171(6)	2579(1)	8259(3)	36(1)
C44	5390(6)	2496(2)	8734(3)	49(2)
C45	5297(7)	2279(2)	9417(3)	59(2)
C46	3956(7)	2150(2)	9620(3)	48(2)
C47	2700(6)	2236(2)	9158(3)	43(2)
C48	2817(6)	2460(1)	8489(3)	38(1)
C49	4193(5)	2633(2)	6720(3)	37(1)
C50	4025(5)	2260(2)	6407(3)	38(1)
C51	3595(5)	1635(2)	6908(3)	37(1)
C52	3229(6)	1463(2)	7618(3)	42(2)
C53	2703(6)	1107(2)	7603(3)	40(2)
C54	2562(6)	924(2)	6874(3)	39(1)
C55	2964(6)	1093(2)	6190(3)	45(2)
C56	3487(6)	1447(2)	6190(3)	42(2)
C57	525(7)	523(2)	6985(4)	60(2)
C58	339(10)	245(3)	7612(9)	64(4)
C58'	180(20)	146(7)	7024(17)	55(8)
C59	398(9)	−334(3)	8033(5)	142(4)
C60	1501(10)	−399(2)	8709(4)	101(3)
C61	2272(11)	−51(3)	9832(6)	124(3)
C62	2597(11)	271(2)	10243(4)	126(4)
C63	1992(8)	837(2)	9657(3)	69(2)
C64	2459(7)	1099(2)	9031(3)	62(2)
N1	677(4)	−2715(1)	986(2)	45(1)
N2	1782(5)	−1845(2)	1808(2)	57(1)
N3	4372(4)	2909(1)	6176(2)	38(1)
N4	4050(4)	2000(1)	6979(2)	43(1)
O1	1057(4)	−1996(1)	514(2)	49(1)
O2	3165(4)	−749(1)	3184(2)	47(1)
O3	2368(4)	−387(1)	4592(2)	63(1)
O6	3418(5)	−389(1)	1760(2)	61(1)
O7	3845(4)	2199(1)	5679(2)	43(1)
O8	2091(4)	567(1)	6854(2)	47(1)
O9	847(5)	−105(1)	7434(3)	73(1)

Table A.28: Continued Overleaf

O10	1511(17)	−92(2)	9160(4)	100(5)
O10'	2600(40)	−176(6)	9312(15)	48(11)
O11	3038(5)	559(1)	9743(2)	77(1)
O12	2309(4)	926(1)	8266(2)	52(1)

Table A.28: Atomic coordinates [$\times 10^4$], equivalent isotropic displacement parameters [$Å^2 \times 10^3$] and site occupancy factors. U_{eq} is defined as one third of the trace of the orthogonalized U^{ij} tensor.

5,10,15,20-Tetra-(4-ethoxycarbonylmethoxy-phenyl)-5,10,15,20-tetramethyl-calix[4]pyrrole (DMSO complex)

Identification code	**71·DMSO**	
Empirical formula	$C_{68}H_{80}N_4O_{14}S_2$	
Formula weight	1241.48	
Temperature	150(2) K	
Wavelength	0.71073 Å	
Crystal system	Monoclinic	
Space group	$P2_1/n$	
Unit cell dimensions	a = 15.455(3) Å	α = 90°
	b = 25.235(5) Å	β = 111.40(3)°
	c = 17.345(4) Å	γ = 90°
Volume	6298(2) Å^3	
Z	4	
Density (calculated)	1.309 Mg / m^3	
Absorption coefficient	0.154 mm^{-1}	
F(000)	2640	
Crystal	Plate; colourless	
Crystal size	0.17 × 0.15 × 0.02 mm^3	
θ range for data collection	2.94 – 27.50°	
Index ranges	$-20 \le h \le 18$, $-29 \le k \le 32$, $-22 \le l \le 22$	
Reflections collected	63231	
Independent reflections	14294 [R_{int} = 0.1142]	
Completeness to θ = 27.50°	98.8 %	
Absorption correction	Semi–empirical from equivalents	
Max. and min. transmission	0.9969 and 0.9735	
Refinement method	Full-matrix least-squares on F^2	
Data / restraints / parameters	14294 / 0 / 816	
Goodness-of-fit on F^2	0.954	
Final R indices [$F^2 > 2\sigma(F^2)$]	$R1$ = 0.0591, $wR2$ = 0.1123	
R indices (all data)	$R1$ = 0.1567, $wR2$ = 0.1430	
Extinction coefficient	0.00048(17)	
Largest diff. peak and hole	0.285 and –0.295 e Å^{-3}	

Table A.29: Structure and refinement data.

Atom	x	y	z	U_{eq}
S1	6734(1)	1460(1)	7903(1)	27(1)
S2	644(1)	1191(1)	6282(1)	34(1)
S2'	113(4)	1503(2)	5744(4)	50(2)
O1	5743(1)	−511(1)	8735(1)	42(1)
O2	5994(1)	302(1)	9903(1)	57(1)
O3	6719(2)	−285(1)	10908(1)	63(1)
O4	3028(1)	1309(1)	5074(1)	30(1)
O5	3247(1)	2130(1)	6174(1)	51(1)
O6	3118(1)	1566(1)	7123(1)	41(1)
O7	5296(1)	2884(1)	8246(1)	39(1)
O8	5592(1)	1891(1)	8900(1)	46(1)
O9	5834(1)	2198(1)	10169(1)	43(1)
O10	8453(1)	1142(1)	11361(1)	38(1)
O11	8167(1)	1729(1)	13088(1)	48(1)
O12	8816(1)	960(1)	12938(1)	35(1)
O13	7358(1)	1272(1)	7444(1)	29(1)
O14	714(1)	1171(1)	5449(1)	47(1)
N1	9131(1)	644(1)	8007(1)	25(1)
N2	7474(1)	538(1)	6130(1)	24(1)
N3	7396(1)	1852(1)	5991(1)	24(1)
N4	9038(1)	1944(1)	7838(1)	24(1)
C1	9996(2)	860(1)	8419(1)	24(1)
C2	10626(2)	514(1)	8316(2)	28(1)
C3	10132(2)	81(1)	7839(2)	28(1)
C4	9209(2)	166(1)	7659(1)	24(1)
C5	8372(2)	−168(1)	7164(1)	25(1)
C6	8705(2)	−738(1)	7099(2)	34(1)
C7	7667(2)	−216(1)	7602(2)	27(1)
C8	6716(2)	−271(1)	7156(2)	32(1)
C9	6098(2)	−364(1)	7552(2)	36(1)
C10	6421(2)	−409(1)	8405(2)	33(1)
C11	7357(2)	−355(1)	8862(2)	30(1)
C12	7963(2)	−262(1)	8456(2)	29(1)
C13	6042(2)	−627(1)	9590(2)	42(1)
C14	6245(2)	−137(1)	10129(2)	42(1)
C15	6891(3)	117(2)	11548(2)	91(1)
C16	6660(3)	−83(2)	12213(3)	116(2)
C17	7939(2)	59(1)	6298(2)	25(1)
C18	7948(2)	−129(1)	5566(2)	27(1)
C19	7469(2)	238(1)	4937(2)	26(1)
C20	7183(2)	650(1)	5296(1)	23(1)

Table A.29: Continued Overleaf

C21	6644(2)	1148(1)	4911(1)	24(1)
C22	6376(2)	1110(1)	3965(2)	30(1)
C23	5715(2)	1189(1)	5051(1)	24(1)
C24	5253(2)	742(1)	5170(2)	28(1)
C25	4366(2)	776(1)	5189(2)	29(1)
C26	3934(2)	1263(1)	5100(2)	25(1)
C27	4388(2)	1714(1)	4998(2)	28(1)
C28	5265(2)	1675(1)	4963(1)	26(1)
C29	2912(2)	1205(1)	5833(2)	30(1)
C30	3121(2)	1692(1)	6378(2)	33(1)
C31	3264(2)	2003(1)	7708(2)	50(1)
C32	3208(3)	1775(2)	8482(2)	80(1)
C33	7215(1)	1646(1)	5210(1)	22(1)
C34	7564(2)	1997(1)	4805(2)	27(1)
C35	7952(2)	2428(1)	5345(2)	29(1)
C36	7830(2)	2334(1)	6074(2)	23(1)
C37	8117(2)	2659(1)	6862(2)	26(1)
C38	8294(2)	3235(1)	6661(2)	34(1)
C39	7359(2)	2687(1)	7243(2)	26(1)
C40	6417(2)	2647(1)	6769(2)	29(1)
C41	5753(2)	2704(1)	7126(2)	31(1)
C42	6016(2)	2813(1)	7958(2)	30(1)
C43	6949(2)	2861(1)	8441(2)	32(1)
C44	7604(2)	2797(1)	8081(2)	29(1)
C45	5494(2)	2827(1)	9106(2)	40(1)
C46	5653(2)	2254(1)	9361(2)	36(1)
C47	5934(2)	1655(1)	10475(2)	48(1)
C48	5876(2)	1669(1)	11311(2)	57(1)
C49	9006(2)	2441(1)	7494(2)	25(1)
C50	9860(2)	2661(1)	7864(2)	28(1)
C51	10428(2)	2296(1)	8455(2)	29(1)
C52	9899(2)	1855(1)	8430(1)	25(1)
C53	10139(2)	1355(1)	8946(2)	25(1)
C54	11170(2)	1387(1)	9520(2)	34(1)
C55	9580(2)	1309(1)	9523(1)	25(1)
C56	9539(2)	824(1)	9895(2)	30(1)
C57	9151(2)	777(1)	10488(2)	33(1)
C58	8801(2)	1224(1)	10741(2)	30(1)
C59	8803(2)	1708(1)	10368(2)	31(1)
C60	9194(2)	1743(1)	9763(2)	30(1)
C61	8444(2)	1588(1)	11848(2)	34(1)
C62	8444(2)	1433(1)	12686(2)	33(1)
C63	8917(2)	812(1)	13783(2)	42(1)
C64	9207(2)	251(1)	13917(2)	51(1)

Table A.30: Continued Overleaf

C65	5591(2)	1271(1)	7247(2)	41(1)
C66	6904(2)	981(1)	8689(2)	35(1)
C67	−521(2)	1053(1)	6153(2)	41(1)
C68	636(2)	1864(1)	6537(2)	59(1)

Table A.30: Atomic coordinates [$\times 10^4$], equivalent isotropic displacement parameters [$Å^2 \times 10^3$] and site occupancy factors. U_{eq} is defined as one third of the trace of the orthogonalized U^{ij} tensor.

5,10,15,20-Tetra-(4-diethylcarbamoylmethoxy-phenyl)-5,10,15,20-tetramethyl-calix[4]pyrrole

Identification code	**(72)·CH_3CN**
Empirical formula	$C_{80}H_{100}N_{12}O_8$
Formula weight	1357.72
Temperature	150(2) K
Wavelength	0.71073 Å
Crystal system	Orthorhombic
Space group	$P2_12_12_1$
Unit cell dimensions	a = 11.1764(3) Å
	b = 22.9910(7) Å
	c = 28.9180(10) Å
Volume	7430.7(4) Å^3
Z	4
Density (calculated)	1.214 Mg / m^3
Absorption coefficient	0.080 mm^{-1}
F(000)	2912
Crystal	Colourless cut needle
Crystal size	0.20 × 0.15 × 0.08 mm^3
θ range for data collection	2.93 – 23.26°
Index ranges	$-12 \le h \le 12$, $-23 \le k \le 25$, $-32 \le l \le 32$
Reflections collected	20396
Independent reflections	10130 [R_{int} = 0.0841]
Completeness to θ = 23.26°	98.6 %
Absorption correction	Empirical
Max. and min. transmission	0.9941 and 0.9843
Refinement method	Full-matrix least-squares on F^2
Data / restraints / parameters	10130 / 0 / 906
Goodness-of-fit on F^2	0.949
Final R indices [$F^2 > 2\sigma(F^2)$]	$R1$ = 0.0666, $wR2$ = 0.1242
R indices (all data)	$R1$ = 0.1607, $wR2$ = 0.1548
Absolute structure parameter	Not reliably determined
Extinction coefficient	0.0013(2)
Largest diff. peak and hole	0.262 and −0.225 e Å^{-3}

Table A.31: Structure and refinement data

Atom	x	y	z	U_{eq}
O5	5077(3)	1659(2)	7449(2)	46(1)
O1	10967(3)	−1419(2)	7647(2)	48(1)
O4	11625(4)	2446(2)	8444(2)	53(1)
N3	8596(4)	−806(2)	5668(2)	34(1)
O6	7169(4)	1350(2)	7840(2)	50(1)
O2	11748(4)	−2037(2)	8341(2)	53(1)
N1	8574(4)	1247(2)	5715(2)	37(1)
N4	10665(3)	217(3)	5770(2)	36(1)
C1	9661(5)	1444(3)	5554(2)	33(2)
N7	7409(4)	2195(2)	8229(2)	41(2)
N2	6450(3)	210(2)	5598(2)	31(1)
O3	11025(3)	1859(2)	7709(2)	49(1)
C49	6107(5)	1375(3)	6074(2)	34(2)
N5	12561(5)	−1280(3)	8720(2)	54(2)
C25	10777(5)	−970(3)	6249(2)	31(2)
N6	12692(5)	1726(2)	8775(2)	44(1)
C19	11275(6)	710(3)	5658(2)	33(2)
C21	5574(5)	1749(3)	5299(2)	40(2)
C5	6355(5)	1299(3)	5563(2)	37(2)
C9	6067(4)	−278(3)	5361(2)	32(2)
C6	6071(5)	699(3)	5382(2)	29(2)
C50	6722(5)	1760(3)	6344(2)	39(2)
C39	11560(5)	1195(3)	7080(2)	39(2)
C55	5675(5)	2073(3)	7728(2)	41(2)
C41	10166(5)	1979(3)	6978(2)	38(2)
C20	10839(5)	1318(3)	5791(2)	34(2)
C42	10083(5)	1846(3)	6516(2)	32(2)
C15	10853(5)	−875(3)	5730(2)	32(2)
C4	7657(5)	1438(3)	5443(2)	33(2)
C47	12837(5)	2085(3)	9195(2)	46(2)
C26	10122(5)	−1421(3)	6443(2)	37(2)
C37	10747(5)	1394(3)	6324(2)	31(2)
C28	10907(5)	−1230(3)	7197(2)	38(2)
C30	11474(5)	−638(3)	6554(2)	39(2)
C10	6354(5)	−887(3)	5532(2)	35(2)
C22	5551(5)	−1320(3)	5265(2)	40(2)
C11	7653(5)	−1034(3)	5417(2)	35(2)
C35	12897(6)	−1665(3)	9101(2)	57(2)
C32	12015(6)	−1517(3)	8357(2)	45(2)
C27	10169(5)	−1551(3)	6910(2)	38(2)
C8	5453(5)	−88(3)	4982(2)	40(2)

Table A.32: Continued Overleaf

C3	8168(6)	1751(3)	5098(2)	44(2)
C59	6940(6)	2759(3)	8373(2)	49(2)
C38	11466(5)	1076(3)	6611(2)	40(2)
C23	11786(5)	−1303(3)	5542(2)	46(2)
C44	12031(6)	1958(3)	8422(2)	43(2)
C12	8135(6)	−1383(3)	5080(2)	48(2)
C16	11274(5)	−268(3)	5621(2)	32(1)
C2	9402(5)	1756(3)	5161(2)	40(2)
C7	5461(5)	537(3)	4998(2)	39(2)
C14	9676(5)	−1022(3)	5503(2)	36(2)
C43	11894(6)	1587(3)	7998(2)	43(2)
C53	4828(5)	1192(3)	6738(2)	40(2)
C61	6092(5)	−954(3)	6044(2)	30(2)
C40	10931(5)	1661(3)	7261(2)	38(2)
C13	9404(5)	−1370(3)	5138(2)	51(2)
C17	12278(5)	−73(3)	5405(2)	39(2)
C24	11765(5)	1765(3)	5619(2)	41(2)
C57	8561(6)	2001(3)	8417(2)	48(2)
C51	6437(6)	1868(3)	6807(2)	42(2)
C56	6809(5)	1837(3)	7939(2)	39(2)
C18	12279(5)	545(3)	5432(2)	43(2)
C60	6073(5)	2735(3)	8777(2)	54(2)
C45	13155(6)	1130(3)	8798(3)	53(2)
C54	5121(5)	1083(3)	6286(2)	41(2)
C52	5476(6)	1587(3)	7004(2)	38(2)
C29	11519(5)	−760(3)	7023(2)	44(2)
C48	11765(6)	2045(3)	9505(2)	71(2)
C31	11752(6)	−1120(3)	7948(2)	51(2)
C36	11846(6)	−1816(3)	9397(2)	62(2)
C58	8497(7)	1792(3)	8905(3)	77(2)
C33	12934(8)	−670(4)	8749(3)	91(3)
C46	14488(6)	1098(3)	8707(3)	67(2)
C34	12365(12)	−368(4)	9155(3)	172(5)
N10	8320(4)	179(3)	6421(2)	47(1)
C75	8490(5)	204(3)	6811(3)	47(2)
C65	6479(6)	−1417(3)	6784(2)	41(2)
C62	5145(5)	−677(3)	6245(2)	36(2)
C66	6739(5)	−1334(3)	6330(2)	38(2)
C63	4832(5)	−749(3)	6702(2)	43(2)
C76	8761(5)	245(4)	7314(2)	75(2)
C64	5511(6)	−1122(3)	6978(2)	45(2)
O7	5123(4)	−1173(2)	7434(2)	48(1)
O8	7284(4)	−885(2)	7793(2)	53(1)

Table A.32: Continued Overleaf

C68	6907(5)	−1368(3)	7904(2)	39(2)
C67	5704(5)	−1584(3)	7725(2)	53(2)
C74	8154(6)	240(4)	8562(3)	99(3)
C73	9441(9)	293(5)	8496(3)	98(3)
N9	10433(7)	356(5)	8453(4)	161(4)
N8	7482(4)	−1725(2)	8193(2)	42(1)
C70	8703(6)	−1391(3)	8865(3)	68(2)
C69	8676(5)	−1562(3)	8363(2)	49(2)
C72	6120(5)	−2243(3)	8754(2)	51(2)
C71	6994(6)	−2292(3)	8344(2)	48(2)
N12	3255(5)	203(3)	7714(2)	57(2)
C79	4276(6)	206(3)	7704(2)	52(2)
C78	8894(6)	232(4)	4779(2)	67(2)
C80	5573(5)	195(4)	7698(3)	91(3)
C77	9028(6)	398(4)	4325(3)	80(3)
N11	9127(6)	546(4)	3936(3)	130(4)

Table A.32: Atomic coordinates [$\times 10^4$], equivalent isotropic displacement parameters [$Å^2 \times 10^3$] and site occupancy factors. U_{eq} is defined as one third of the trace of the orthogonalized U^{ij} tensor.

5,10,15,20-Tetra-(4-acetoxyphenyl)-5,10,15,20-tetramethyl-calix[4]pyrrole

Identification code	**73**	
Empirical formula	$C_{64}H_{67}N_4O_{16}S_2$	
Formula weight	1212.34	
Temperature	150(2) K	
Wavelength	0.71073 Å	
Crystal system	Monoclinic	
Space group	$P2_1/n$	
Unit cell dimensions	a = 11.114(2) Å	α = 90°
	b = 25.406(5) Å	β = 99.69(3)°
	c = 21.293(4) Å	γ = 90°
Volume	5926(2) Å^3	
Z	4	
Density (calculated)	1.359 Mg / m^3	
Absorption coefficient	0.165 mm^{-1}	
F(000)	2556	
Crystal	Plate; colourless	
Crystal size	0.25 × 0.10 × 0.04 mm^3	
θ range for data collection	2.93 – 23.85°	
Index ranges	$-12 \le h \le 12$, $-28 \le k \le 28$, $-24 \le l \le 24$	
Reflections collected	24170	
Independent reflections	9040 [R_{int} = 0.0853]	
Completeness to θ = 23.85°	98.8 %	
Absorption correction	Semi–empirical from equivalents	
Max. and min. transmission	0.9934 and 0.9600	
Refinement method	Full-matrix least-squares on F^2	
Data / restraints / parameters	9040 / 60 / 828	
Goodness-of-fit on F^2	2.718	
Final R indices [$F^2 > 2\sigma(F^2)$]	$R1$ = 0.1996, $wR2$ = 0.4524	
R indices (all data)	$R1$ = 0.2504, $wR2$ = 0.4713	
Extinction coefficient	0.016(9)	
Largest diff. peak and hole	1.572 and –0.934 e Å^{-3}	

Table A.33: Structure and refinement data

Atom	x	y	z	U_{eq}
S1	2838(10)	1354(4)	1994(5)	67(3)
S2	1760(20)	−655(7)	2528(11)	153(7)
O1	7140(30)	409(10)	3410(20)	132(16)
O2	5360(50)	169(17)	2640(50)	290(50)
O3	5940(30)	635(11)	300(19)	101(11)
O4	7580(30)	861(13)	−93(17)	106(11)
O3'	5050(60)	750(20)	−150(30)	180(20)
O4'	3440(90)	860(30)	−1200(30)	230(20)
C23'	4520(90)	810(50)	−900(40)	220(50)
C24'	5000(70)	230(40)	−1090(50)	240(60)
O5	−350(60)	400(30)	1010(30)	160(30)
O6	1680(70)	250(20)	1290(30)	200(20)
O7	790(40)	498(11)	4152(17)	50(10)
O8	140(60)	330(20)	3150(30)	140(18)
C51	350(70)	170(30)	3690(30)	100(30)
C52	50(90)	−360(20)	3870(40)	130(30)
O7'	1580(60)	510(20)	4330(20)	21(15)
O8'	2110(60)	630(30)	5350(30)	50(20)
C51'	1810(80)	330(30)	4940(40)	30(20)
C52'	1690(90)	−200(30)	4980(40)	40(20)
O9	3271(17)	1888(7)	2232(8)	34(5)
O10	3810(20)	1287(8)	2383(10)	50(6)
O11	1280(30)	−646(14)	3152(16)	107(11)
O12	2280(50)	−820(20)	1960(30)	190(20)
N1	5245(18)	2648(8)	2059(9)	23(5)
N2	2510(20)	2653(10)	1179(10)	40(6)
N3	1290(20)	2598(9)	2480(11)	36(6)
N4	3970(20)	2584(8)	3366(9)	30(5)
C1	6190(20)	2616(10)	3229(12)	31(6)
C2	7380(30)	2824(12)	3619(14)	43(8)
C3	6340(30)	2012(11)	3234(14)	39(7)
C4	6970(30)	1770(12)	2807(18)	55(9)
C5	7230(30)	1237(14)	2880(20)	80(13)
C6	6860(40)	950(17)	3350(30)	95(17)
C7	6220(40)	1175(15)	3750(20)	76(14)
C8	5970(30)	1704(14)	3716(15)	54(9)
C9	6160(130)	20(50)	2870(60)	270(40)
C10	7080(80)	−530(30)	2860(40)	200(30)
C11	6020(20)	2842(9)	2563(11)	24(6)
C12	6620(20)	3259(10)	2340(13)	34(7)
C13	6150(30)	3312(10)	1675(12)	32(7)

Table A.34: Continued Overleaf

C14	5310(20)	2922(9)	1516(11)	25(6)
C15	4620(30)	2770(10)	877(11)	32(7)
C16	5110(30)	3100(12)	358(13)	48(8)
C17	4870(40)	2182(12)	730(13)	53(10)
C18	4070(40)	1887(13)	316(15)	72(12)
C19	4560(30)	1338(12)	157(14)	47(8)
C20	5590(40)	1190(20)	420(20)	90(15)
C21	6330(50)	1474(15)	770(30)	98(18)
C22	6020(40)	1963(13)	960(20)	66(11)
C23	6900(60)	551(19)	−10(40)	140(30)
C24	7080(80)	−60(20)	−110(50)	250(60)
C25	3260(30)	2892(12)	810(12)	40(8)
C26	2520(30)	3217(13)	396(13)	49(9)
C27	1340(30)	3165(14)	525(14)	58(10)
C28	1320(30)	2813(15)	1004(13)	54(9)
C29	300(30)	2607(14)	1308(14)	53(9)
C30	−900(30)	2806(18)	933(18)	85(14)
C31	240(30)	1988(15)	1278(18)	63(11)
C32	−200(30)	1694(17)	1734(17)	62(10)
C33	−330(40)	1170(20)	1680(20)	83(14)
C34	−70(40)	950(20)	1140(30)	96(17)
C35	370(40)	1195(17)	634(18)	89(15)
C36	530(40)	1715(19)	735(16)	82(14)
C37	270(90)	230(30)	1130(30)	110(30)
C38	240(80)	−430(30)	1060(40)	190(30)
C39	420(30)	2791(13)	1994(16)	46(8)
C40	−230(30)	3144(15)	2260(20)	70(12)
C41	190(30)	3174(13)	2900(20)	63(11)
C42	1130(20)	2836(10)	3048(13)	33(7)
C43	1880(30)	2665(10)	3682(13)	36(7)
C44	1330(30)	2949(12)	4212(16)	57(10)
C45	1670(30)	2062(10)	3796(12)	32(7)
C46	570(30)	1852(12)	3606(14)	44(8)
C47	330(50)	1319(15)	3737(19)	65(11)
C48	1080(50)	1030(20)	4030(30)	78(14)
C49	2220(60)	1196(18)	4273(16)	110(20)
C50	2580(30)	1775(12)	4154(13)	50(9)
C53	3210(30)	2807(11)	3750(12)	33(7)
C54	3890(30)	3135(13)	4162(14)	53(9)
C55	5110(40)	3130(13)	4037(14)	59(10)
C56	5140(30)	2775(11)	3547(12)	35(7)
C57	4120(50)	1070(15)	1810(20)	99(17)
C58	2690(40)	992(11)	2694(15)	58(10)

Table A.34: Continued Overleaf

C59	2460(70)	−340(30)	3190(40)	180(40)
C60	1860(40)	−1264(14)	2728(19)	77(12)
O99	−1570(20)	4439(8)	3279(16)	81(9)
C98	4970(30)	−260(17)	4170(18)	69(11)
C99	4620(30)	−120(18)	4748(16)	75(12)
O2S	8460(70)	640(30)	4510(40)	280(40)

Table A.34: Atomic coordinates [$\times 10^4$], equivalent isotropic displacement parameters [$Å^2 \times 10^3$] and site occupancy factors. U_{eq} is defined as one third of the trace of the orthogonalized U^{ij} tensor.

5,10,15,20-Tetra-(4-acetoxyphenyl)-5,10,15,20-tetramethyl-calix[4]pyrrole (DMSO complex)

Identification code	**73·DMSO**	
Empirical formula	$C_{63}H_{67}N_5O_{13}S_{2,50}$	
Formula weight	1182.37	
Temperature	150(2) K	
Wavelength	0.71073 A	
Crystal system	Monoclinic	
Space group	$P2_1/n$	
Unit cell dimensions	a = 11.095(2) Å	a= 90°
	b = 25.388(5) Å	b= 99.90(3)°
	c = 21.257(4) Å	c= 90°
Volume	5899(2) A^3	
Z	4	
Density (calculated)	1.331 Mg/m^3	
Absorption coefficient	0. 177 mm^{-1}	
F(O00)	2496	
Crystal	Needle; colourless	
Crystal size	0.5 x 0.1 X 0.1 mm^3	
θ range for data collection	2.93 - 27.50°	
Index ranges	-14≤h≤14, -32≤k:≤32, -27 ≤*l*≤27	
Reflections collected	87854	
Independent reflections	13431 [R_{int} = 0. 146 1]	
Completeness to 0 = 27.50'	99.2%	
Absorption correction	Semi-empirical from equivalents	
Max. and min. transmission	0.993 and 0.518	
Refinement method	Full-matrix least-squares on F^2	
Data 1 restraints 1 parameters	13431/84 / 821	
Goodness-of-fit on F2	2.381	
Final R indices [P > 2a(P)]	R*1* = 0. 1927, wR2 = 0.4343	
R indices (all data)	R*1* = 0.3199, wR2 = 0.4613	
Largest diff. peak and hole	1.462 and -1.289 e $Å^{-3}$	

Table A.35: Structure and refinement data

Atom	*x*	*y*	*z*	U_{eq}
S1	7870(30)	1350(10)	1995(12)	67(8)
S2	6740(90)	-650(20)	2520(30)	130(30)
S3	6530(60)	5590(30)	6620(50)	220(30)
01	-340(110)	4550(60)	6050(60)	150(50)
02	1650(160)	4750(60)	6210(80)	230(60)
03	1150(90)	4490(20)	9240(40)	110(30)
04	1920(170)	4340(60)	10400(70)	100(50)
04'	100(200)	4680(70)	8080(90)	150(90)
05	7090(90)	4590(30)	8330(50)	130(40)
06	5400(180)	4820(60)	7660(150)	400(200)
07	5460(140)	4290(50)	5050(80)	200(30)
08	7540(110)	4140(50)	4870(60)	170(50)
09	8780(70)	1290(30)	2390(30)	90(20)
010	8300(40)	1888(17)	2231(19)	33(12)
011	6340(130)	-610(50)	3140(90)	100(50)
012	7500(200)	-840(80)	1960(100)	150(60)
013	5750(150)	5890(70)	6040(80)	270(100)
014	7300(190)	5750(70)	6020(90)	250(70)
NI	2500(50)	2350(20)	6160(30)	39(16)
N2	1290(50)	2400(20)	7480(30)	41(16)
N3	4000(50)	2420(20)	8360(20)	31(14)
N4	5250(50)	2350(20)	7050(20)	27(13)
C1	3260(70)	2100(30)	5800(30)	38(18)
C2	2510(80)	1770(40)	5390(40)	60(30)
C3	1320(70)	1820(40)	5520(40)	60(30)
C4	1340(80)	2180(40)	5990(40)	60(20)
C5	320(70)	2390(40)	6300(40)	60(30)
C6	-930(80)	2190(50)	5920(50)	100(40)
C7	270(80)	3000(40)	6260(50)	70(30)
C8	540(100)	3270(50)	5730(50)	100(50)
C9	390(130)	3780(50)	5650(50)	120(60)
C10	-20(120)	4060(50)	6100(70)	100(50)
C11	-280(90)	3850(50)	6650(60)	80(40)
C12	-200(80)	3300(50)	6710(50)	80(30)
C13	370(150)	4760(50)	6060(60)	90(40)
C14	600(300)	5470(120)	6180(160)	320(140)
C15	420(60)	2200(40)	6980(40)	50(30)
C16	-210(80)	1840(40)	7250(50)	80(30)
C17	200(80)	1830(30)	7890(50)	70(30)
C18	1150(70)	2180(30)	8050(40)	41(19)
C19	1890(60)	2350(30)	8680(30)	35(17)
C20	1360(90)	2060(30)	9210(40)	60(30)

Table A.36: Continued Overleaf

C21	1710(70)	2940(30)	8800(30)	37(18)
C22	620(80)	3170(30)	8610(40)	50(20)
C23	410(110)	3690(40)	8760(50)	70(30)
C24	1290(140)	3980(40)	9090(60)	70(30)
C25	2390(150)	3770(40)	9290(50)	90(40)
C26	2620(80)	3240(30)	9160(40)	50(20)
C27	1660(170)	4650(70)	9970(120)	70(60)
C28	1700(300)	5240(80)	10000(110)	130(110)
C27'	400(300)	4800(110)	8600(200)	130(120)
C28'	200(200)	5380(80)	8970(140)	120(90)
C29	3220(70)	2200(30)	8740(30)	37(18)
C30	3920(80)	1860(30)	9150(40)	60(20)
C31	5130(80)	1870(30)	9030(40)	50(20)
C32	5170(60)	2220(30)	8540(30)	34(17)
C33	6200(60)	2380(30)	8230(30)	33(17)
C34	7400(70)	2160(30)	8610(40)	50(20)
C35	6370(60)	2980(30)	8210(40)	40(19)
C36	6990(70)	3220(30)	7780(50)	60(30)
C37	7230(90)	3750(40)	7820(60)	90(30)
C38	6880(110)	4060(40)	8260(80)	100(40)
C39	6280(100)	3830(40)	8720(60)	80(40)
C40	6010(70)	3290(30)	8690(40)	50(20)
C41	6900(700)	4890(110)	7930(130)	600(80)
C42	7200(200)	5500(80)	7810(110)	230(90)
C43	6030(60)	2150(30)	7550(30)	31(16)
C44	6610(60)	1730(30)	7330(40)	41(19)
C45	6140(60)	1670(30)	6660(30)	37(18)
C46	5310(60)	2070(30)	6510(30)	29(16)
C47	4600(70)	2220(30)	5860(30)	34(17)
C48	5120(80)	1900(30)	5340(30)	50(20)
C49	4870(110)	2810(30)	5710(40)	60(30)
C50	6040(100)	3040(30)	5940(50)	70(30)
C51	6450(110)	3510(40)	5820(60)	80(30)
C52	5740(110)	3720(60)	5460(50)	90(40)
C53	4590(120)	3660(30)	5150(40)	80(40)
C54	4020(110)	3100(40)	5310(40)	80(30)
C55	6300(200)	4390(50)	5220(100)	160(40)
C56	7000(200)	5050(70)	5000(200)	500(300)
C57	9110(120)	1040(40)	1800(50)	100(40)
C58	7700(90)	990(30)	2670(40)	60(30)
C59	7400(400)	-320(80)	2900(200)	210(70)
C60	6860(110)	-1280(40)	2710(50)	20(30)
C61	7400(300)	4900(130)	6700(200)	400(300)
C62	5060(190)	5290(120)	6180(170)	400(300)

Table A.36: Continued Overleaf

C63	4940(140)	5240(60)	9270(80)	130(50)
C64	5500(500)	5700(200)	9000(200)	400(200)
N5	4780(120)	5020(150)	9790(60)	320(150)

Table A.36: Atomic coordinates [$\times 10^4$], equivalent isotropic displacement parameters [$Å^2 \times 10^3$] and site occupancy factors. U_{eq} is defined as one third of the trace of the orthogonalized U^{ij} tensor.

5,10,15,20-Tetra-(4-acetoxyphenyl)-5,10,15,20-tetramethyl-calix[4]pyrrole (acetonitrile complex)

Identification code	**73·CH_3CN**	
Empirical formula	$C_{62}H_{61}N_7O_8$	
Formula weight	1032.18	
Temperature	150(2) K	
Wavelength	0.71073 Å	
Crystal system	Tetragonal	
Space group	*P4/n*	
Unit cell dimensions	a = 11.3723(16) Å	$\alpha = 90°$
	b = 11.3723(16) Å	$\beta = 90°$
	c = 21.020(4) Å	$\gamma = 90°$
Volume	2718.4(8) $Å^3$	
Z	2	
Density (calculated)	1.261 Mg / m^3	
Absorption coefficient	0.084 mm^{-1}	
F(000)	1092	
Crystal	Plate; colourless	
Crystal size	0.10 × 0.10 × 0.03 mm^3	
θ range for data collection	3.19 – 27.50°	
Index ranges	$-13 \le h \le 13$, $-14 \le k \le 14$, $-25 \le l \le 27$	
Reflections collected	23657	
Independent reflections	3120 [R_{int} = 0.0917]	
Completeness to θ = 27.50°	99.6 %	
Absorption correction	Semi–empirical from equivalents	
Max. and min. transmission	0.9975 and 0.9916	
Refinement method	Full-matrix least-squares on F^2	
Data / restraints / parameters	3120 / 6 / 187	
Goodness-of-fit on F^2	1.018	
Final R indices [$F^2 > 2\sigma(F^2)$]	*R1* = 0.0518, *wR2* = 0.1258	
R indices (all data)	*R1* = 0.0990, *wR2* = 0.1511	
Extinction coefficient	0.0043(13)	
Largest diff. peak and hole	0.289 and –0.261 e $Å^{-3}$	

Table A.37: Structure and refinement data.

Atom	x	y	z	U_{eq}
C1	9208(1)	5375(1)	3817(1)	27(1)
C2	9079(2)	4527(1)	4273(1)	32(1)
C3	7892(2)	4164(2)	4268(1)	32(1)
C4	7309(1)	4779(1)	3809(1)	26(1)
C5	10280(1)	6046(1)	3590(1)	27(1)
C6	11390(2)	5470(2)	3871(1)	35(1)
C7	10387(1)	5955(2)	2861(1)	29(1)
C8	10064(2)	4915(2)	2557(1)	35(1)
C9	10214(2)	4769(2)	1908(1)	39(1)
C10	10687(2)	5678(2)	1560(1)	36(1)
C11	11025(2)	6721(2)	1842(1)	37(1)
C12	10878(2)	6843(2)	2495(1)	35(1)
C13	11852(2)	5465(2)	631(1)	42(1)
C14	11792(2)	5038(2)	−37(1)	51(1)
C15	2500	2500	5130(2)	59(1)
C16	2500	2500	4445(2)	37(1)
C17	2500	2500	2223(3)	86(2)
C18	2500	2500	1551(3)	72(2)
C19	7500	7500	1276(3)	162(4)
C20	7500	7500	1959(2)	52(1)
N1	8117(1)	5538(1)	3547(1)	26(1)
N2	2500	2500	3902(2)	51(1)
N3	2500	2500	1008(3)	100(2)
N4	7500	7500	2493(2)	42(1)
O1	10773(1)	5500(1)	897(1)	45(1)
O2	12722(1)	5758(2)	908(1)	67(1)

Table A.38: Atomic coordinates [$\times 10^4$], equivalent isotropic displacement parameters [$Å^2 \times 10^3$] and site occupancy factors. U_{eq} is defined as one third of the trace of the orthogonalized U^{ij} tensor.

5,10,15,20-Tetra-(4-acetoxyphenyl)-5,10,15,20-tetramethyl-calix[4]pyrrole (TBAF complex)

Identification code	**73·TBAF**
Empirical formula	$C_{56}H_{52}N_4O_8$. $NC_{16}H_{36}$. F
Formula weight	1170.47
Temperature	150(2) K
Wavelength	0.71073 Å
Crystal system	Tetragonal
Space group	*P4/ncc*
Unit cell dimensions	a = 17.2489(5) Å
	b = 17.2489(5) Å
	c = 24.0303(8) Å
Volume	7149.6(4) Å^3
Z	4
Density (calculated)	1.087 Mg / m^3
Absorption coefficient	0.072 mm^{-1}
F(000)	2512
Crystal	Colourless needle
Crystal size	0.14 × 0.03 × 0.02 mm^3
θ range for data collection	3.14 – 20.92°
Index ranges	$-17 \le h \le 17$, $-17 \le k \le 17$, $-24 \le l \le 24$
Reflections collected	27239
Independent reflections	1895 [R_{int} = 0.1027]
Completeness to θ = 20.92°	99.1 %
Max. and min. transmission	0.9986 and 0.9899
Refinement method	Full-matrix least-squares on F^2
Data / restraints / parameters	1895 / 56 / 217
Goodness-of-fit on F^2	1.503
Final R indices [$F^2 > 2\sigma(F^2)$]	$R1$ = 0.1126, $wR2$ = 0.3421
R indices (all data)	$R1$ = 0.1244, $wR2$ = 0.3518
Extinction coefficient	0.004(2)
Largest diff. peak and hole	0.667 and –0.351 e Å^{-3}

Table A.39: Structure and refinement data.

Atom	*x*	*y*	*z*	U_{eq}
F1	2500	2500	1144(2)	39(2)
O1	9997(3)	1329(3)	4462(2)	56(2)
N1	11244(3)	2948(3)	6758(2)	44(2)
O2	8751(3)	1048(3)	4591(2)	75(2)
C3	10635(3)	1613(4)	6791(2)	46(2)
C7	10495(3)	1552(4)	6148(3)	46(2)
C8	10051(3)	2112(4)	5879(3)	49(2)
C2	10693(4)	2446(4)	6973(3)	47(2)
C11	10570(4)	845(4)	5291(3)	49(2)
C4	11326(4)	1125(3)	6961(2)	42(2)
C9	9867(4)	2032(4)	5326(3)	53(2)
C12	10754(4)	928(4)	5850(3)	51(2)
C10	10126(4)	1408(4)	5036(3)	51(2)
C1	10241(4)	2872(4)	7322(3)	59(2)
C13	9273(5)	1166(4)	4282(3)	58(2)
C5	11348(4)	515(4)	7318(2)	54(2)
C14	9243(5)	1141(5)	3665(3)	76(2)
C6	9905(4)	1259(4)	7063(3)	61(2)
N2A	2500	2500	3583(4)	63(3)
C17A	1834(7)	2761(9)	3943(6)	72(4)
C18A	1179(7)	3127(8)	3591(5)	141(4)
C19A	520(12)	2910(15)	3929(13)	147(12)
C20A	−158(6)	3491(6)	3907(5)	111(3)
N2B	2500	2500	3583(4)	63(3)
C17B	1836(7)	2772(8)	3210(5)	62(4)
C18B	1179(7)	3127(8)	3591(5)	141(4)
C19B	608(9)	3207(15)	4085(8)	104(7)
C20B	−158(6)	3491(6)	3907(5)	111(3)

Table A.40: Atomic coordinates [$\times 10^4$], equivalent isotropic displacement parameters [$Å^2 \times 10^3$] and site occupancy factors. U_{eq} is defined as one third of the trace of the orthogonalized U^{ij} tensor.

5,11,17,23-Tetra-tert-butyl-25, 27-acetoamidinium--26,28-dihydroxy-calix[4]arene picrate

Identification code	**88·2Picrate**	
Empirical formula	$C_{48}H_{66}N_4O_4(C_6H_2N_3O_7)2.ca.\ 2.25C_2H_5OH$	
Formula weight	1322.9	
Temperature	153 K	
Wavelength	0.71073 Å	
Crystal system	Triclinic	
Space group	$P\bar{1}$	
Unit cell dimensions	a = 11.256(4) Å	α = 86.248(6)°
	b = 12.126(5) Å	β = 89.449(6))°
	c = 24.781(9) Å	γ = 85.085(6)°
Volume	3362(4) Å^3	
Z	2	
Density (calculated)	1.30$_6$ Mg / m^3	
Absorption coefficient	0.098 mm^{-1}	
F(000)	1405	
Crystal	Plate; yellow	
Crystal size	0.20 × 0.12 × 0.10 mm^3	
θ range for data collection	2 – 26°	
Index ranges	$-15 \le h \le 15$, $-16 \le k \le 16$, $0 \le l \le 33$	
Reflections collected	37455	
Independent reflections	16219 [R_{int} = 0.053]	
Absorption correction	Semi–empirical from equivalents	
Max. and min. transmission	0.843 and 0.553	
Refinement method	Full-matrix least-squares on F^2	
Data / restraints / parameters	10356 / - / 888	
Goodness-of-fit on F^2	1.376	
Final R indices [$F^2 > 4\sigma(F^2)$]	*R1* = 0.068, *wR2* = 0.072	
Extinction coefficient	1306(816)	
Largest diff. peak and hole	0.662 and –0.498 e Å^{-3}	

Table A.41: Structure and refinement data

Atom	*x*	*y*	*z*	U_{eq}
O(11)	0.0416(2)	0.7597(2)	0.19929(7)	0.027(1)
C(111)	0.0716(2)	0.6845(2)	0.1582(1)	0.030(2)
C(112)	-0.0385(2)	0.6713(2)	0.1263(1)	0.028(1)
N(111)	-0.0258(2)	0.6278(2)	0.07934(9)	0.030(1)
N(112)	-0.1430(2)	0.7013(2)	0.14627(9)	0.032(1)
C(1)	0.2412(2)	0.8932(2)	0.2042(1)	0.029(1)
C(11)	0.1152(2)	0.7425(2)	0.2452(1)	0.026(1)
C(12)	0.0827(2)	0.6709(2)	0.2879(1)	0.027(1)
C(13)	0.1617(3)	0.6502(2)	0.3311(1)	0.031(2)
C(14)	0.2680(3)	0.7010(2)	0.3333(1)	0.031(2)
C(141)	0.3572(3)	0.6741(3)	0.3796(1)	0.039(2)
C(142)	0.4760(3)	0.6285(4)	0.3565(2)	0.062(3)
C(143)	0.3766(4)	0.7815(4)	0.4074(2)	0.061(3)
C(144)	0.3154(4)	0.5904(4)	0.4223(2)	0.068(3)
C(15)	0.2907(2)	0.7789(2)	0.2914(1)	0.031(2)
C(16)	0.2160(2)	0.8024(2)	0.2469(1)	0.027(1)
C(2)	-0.0367(2)	0.6199(2)	0.2907(1)	0.029(1)
O(21)	-0.2032(2)	0.7928(2)	0.24699(8)	0.032(1)
C(21)	-0.2050(2)	0.7716(2)	0.3026(1)	0.027(1)
C(22)	-0.2844(2)	0.8333(2)	0.3350(1)	0.027(1)
C(23)	-0.2799(2)	0.8108(2)	0.3905(1)	0.030(2)
C(24)	-0.2004(3)	0.7281(2)	0.4154(1)	0.031(2)
C(241)	-0.1960(3)	0.7123(3)	0.4771(1)	0.040(2)
C(242)	-0.3180(4)	0.6879(4)	0.4998(1)	0.068(3)
C(243)	-0.1065(4)	0.6164(4)	0.4968(1)	0.062(3)
C(244)	-0.1552(5)	0.8183(4)	0.4992(2)	0.075(3)
C(25)	-0.1272(2)	0.6662(2)	0.3812(1)	0.030(2)
C(26)	-0.1260(2)	0.6865(2)	0.3253(1)	0.027(1)
C(3)	-0.3700(2)	0.9276(2)	0.3111(1)	0.029(2)
O(31)	-0.2590(2)	1.0106(2)	0.21392(7)	0.029(1)
C(311)	-0.3455(3)	1.0528(3)	0.1744(1)	0.035(2)
C(312)	-0.2984(3)	1.0221(2)	0.1198(1)	0.031(2)
N(311)	-0.1849(2)	0.9964(2)	0.1146(1)	0.035(1)
N(312)	-0.3718(2)	1.0248(2)	0.0789(1)	0.039(2)
C(31)	-0.2524(2)	1.0726(2)	0.2600(1)	0.028(1)
C(32)	-0.1822(2)	1.1614(2)	0.2589(1)	0.029(1)
C(33)	-0.1812(3)	1.2216(2)	0.3051(1)	0.033(2)
C(34)	-0.2439(3)	1.1929(2)	0.3520(1)	0.033(2)
C(341)	-0.2433(3)	1.2593(3)	0.4025(1)	0.042(2)
C(342)	-0.3715(4)	1.3027(3)	0.4153(2)	0.061(3)
C(343)	-0.1929(4)	1.1835(3)	0.4505(1)	0.058(2)

Table A.42: Continued Overleaf

C(344)	-0.1665(4)	1.3576(4)	0.3950(2)	0.071(3)
C(35)	-0.3064(2)	1.0982(2)	0.3526(i)	0.032(2)
C(36)	-0.3115(2)	1.0365(2)	0.3069(l)	b.027(l)
O(41)	-0.0074(2)	0.9787(2)	0.19222(8)	0.034(l)
C(41)	0.0731(2)	1.0459(2)	0.2112(l)	0.028(l)
C(42)	0.1922(2)	1.0092(2)	0.2187(l)	0.027(l)
C(43)	0.2671(2)	1.0824(2)	0.2395(l)	0.032(2)
C(44)	0.2264(3)	1.1896(2)	0.2520(l)	0.034(2)
C(441)	0.3102(3)	1.2694(3)	0.2739(2)	0.046(2)
C(442)*	0.3237(9)	1.3653(8)	0.2330(4)	0.148(9)
C(443)*	0.2587(7)	1.3181(8)	0.3266(4)	0.113(8)
C(444)*	0.4310(6)	1.2201(5)	0.2878(4)	0.090(6)
C2(442')*	0.408(l)	1.283(l)	0.2311(6)	0.073(5)
C(443')*	0.245(l)	1.378(l)	0.2845(5)	0.045(3)
C(444')*	0.361(l)	1.212(l)	0.3267(6)	0.066(4)
C(45)	0.1066(3)	1.2226(2)	0.2425(l)	0.033(2)
C(46)	0.0282(2)	1.1532(2)	0.2220(l)	0.028(l)
C(4)	-0.1021(2)	1.1938(2)	0.2119(l)	0.031(2)
O(101)	-0.1762(2)	0.9574(2)	0.00931(8)	0.046(l)
C(101)	-0.1383(3)	0.8825(3)	-0.0203(l)	0.037(2)
C(102)	-0.0198(3)	0.8240(3)	-0.0159(l)	0.033(2)
N(102)	0.0599(2)	0.8437(2)	0.0278(l)	0.037(2)
O(1021)	0.0221(2)	0.8972(2)	0.06562(9)	0.042(l)
O(1022)	0.1625(2)	0.8003(2)	0.0270(l)	0.055(2)
C(103)	0.0217(3)	0.7440(3)	-0.0496-(l)	0.037(2)
C(104)	-0.0505(3)	0.7140(3)	-0.0900(l)	0.041(2)
N(104)	-0.0068(3)	0.6245(2)	-0.1230(l)	0.052(2)
O(1041)	0.1000(3)	0.5909(2)	-0.1200(l)	0.058(2)
O(1042)	-0.0790(3)	0.5863(2)	-0.1519(l)	0.076(2)
C(105)	-0.1644(3)	0.7648(3)	-0.0978(l)	0.043(2)
C(106)	-0.2059(3)	0.8448(3)	-0.0640(l)	0.040(2)
N(106)	-0.3271(3)	0.8932(3)	-0.0729(l)	0.056(2)
O(1061)	-0.3812(2)	0.9409(3)	-0.0365(l)	0.095(3)
O(1062)	-0.3762(2)	0.8787(3)	-0.11153(1)	0.078(2)
O(201)	-0.2756(2)	0.6139(2)	0.06783(9)	0.050(1)
C(201)	-0.3520(3)	0.6305(2)	0.0318(l)	0.032(2)
C(202)	-0.3442(2)	0.5802(2)	-0.0198(l)	0.029(2)
N(202)	-0.2383(2)	0.5092(2)	-0.0322(1)	0.035(1)
O(2021)	-0.1441(2)	0.5175(2)	-0.00914(9)	0.045(l)
O(2022)	-0.2462(2)	0.4431(2)	-0.0673(l)	0.063(2)
C(203)	-0.4310(3)	0.5938(2)	-0.0585(1)	0.032(2)
C(204)	-0.5342(3)	0.6607(2)	-0.0492(1)	0.032(2)
N(204)	-0.6211(2)	0.6816(2)	-0.0920(1)	0.043(2)
O(2041)	-0.5994(2)	0.6423(3)	-0.13516(l)	0.076(2)

Table A.42: Continued Overleaf

O(2042)	-0.7119(2)	0.7409(2)	-0.0836(1)	0.050(l)
C(205)	-0.5519(3)	0.7118(2)	-0.0009(l)	0.035(2)
C(206)	-0.4646(3)	0.6978(2)	0.0374(l)	0.035(2)
N(206)	-0.4866(3)	0.7550(3)	0.0873(l)	0.052(2)
O(2061)	-0.4041(2)	0.7821(2)	0.1127(l)	0.055(2)
O(2062)	-0.5890(3)	0.7718(4)	0.1021(l)	0.126(3)
C(012)	0.5861(5)	1.5776(4)	0.2138(2)	0.078(3)
C(Oll)	0.6654(4)	1.4905(4)	0.2445(2)	0.069(3)
O(01)	0.7835(3)	1.4795(2)	0.2243(l)	0.072(2)
C(022)	0.0184(4)	0.9478(4)	0.3587(2)	0.068(3)
C(021)	0.1021(5)	1.0139(5)	0.3816(2)	0.095(4)
O(02)	0.0803(5)	1.1283(4)	0.3690(2)	0.053(3)
O(021)	0.2148(7)	1.0148(7)	0.3720(3)	0.108(6)
O(03)	0.4357(9)	1.0328(9)	0.4280(5)	0.064(7)
C(031)	0.4495(9)	0.9897(9)	0.4833(4)	0.084(7)

Table A.42: Atomic coordinates, equivalent isotropic displacement parameters [Å^2] and site occupancy factors. U_{eq} is defined as one third of the trace of the orthogonalized U^{ij} tensor.

5,11,17,23-Tetra-tert-butyl-25,27-acetoamidinium-26,28-dihydroxy-calix[4]arene difluorophosphinate

Identification code	$(\mathbf{88}^{2+})\cdot\mathbf{PF_2O_2}^-$	
Empirical formula	$C_{51}H_{77}F_4N_4O_{11}P_2$	
Formula weight	959.14	
Temperature	150(2) K	
Wavelength	0.71073 Å	
Crystal system	Triclinic	
Space group	P $\bar{1}$	
Unit cell dimensions	a = 12.0665(5) Å	α = 86.4098(18)°
	b = 12.5737(6) Å	β = 79.747(2)°
	c = 20.0201(15) Å	γ = 66.816(4)°
Volume	2747.5(3) Å^3	
Z	2	
Density (calculated)	1.159 Mg / m^3	
Absorption coefficient	0.111 mm^{-1}	
F(000)	1032	
Crystal	Colourless prism	
Crystal size	0.05 × 0.02 × 0.01 mm^3	
θ range for data collection	3.01 – 23.26°	
Index ranges	$-13 \le h \le 13, -13 \le k \le 13, -22 \le l \le 22$	
Reflections collected	31416	
Independent reflections	7824 [R_{int} = 0.2447]	
Completeness to θ = 23.26°	99.2 %	
Max. and min. transmission	0.9989 and 0.9945	
Refinement method	Full-matrix least-squares on F^2	
Data / restraints / parameters	7824 / 390 / 646	
Goodness-of-fit on F^2	0.909	
Final R indices [$F^2 > 2\sigma(F^2)$]	$R1$ = 0.1243, $wR2$ = 0.2996	
R indices (all data)	$R1$ = 0.2668, $wR2$ = 0.3794	
Extinction coefficient	0.015(3)	
Largest diff. peak and hole	0.547 and –0.345 e Å^{-3}	

Table A.43: Structure and refinement data

Atom	*x*	*y*	*z*	U_{eq}
C1	8745(9)	402(8)	8531(5)	44(2)
C2	7947(9)	309(8)	8144(5)	47(3)
C3	8265(9)	−739(9)	7810(5)	54(3)
C4	9336(8)	−1686(8)	7845(5)	42(2)
C5	10104(9)	−1569(9)	8260(5)	52(3)
C6	9825(9)	−530(8)	8607(5)	45(3)
C7	9666(8)	−2787(8)	7454(5)	50(3)
C8	8727(12)	−2755(12)	7049(7)	109(5)
C9	9965(13)	−3806(12)	7950(7)	111(5)
C10	10869(12)	−3007(13)	6946(7)	113(5)
C11	11686(8)	974(8)	8451(5)	37(2)
C12	11747(8)	−162(8)	8527(5)	42(2)
C13	12695(9)	−995(9)	8101(5)	52(3)
C14	13542(8)	−754(8)	7636(5)	41(2)
C15	13394(9)	391(8)	7580(5)	47(3)
C16	12475(8)	1286(8)	7982(5)	44(2)
C17	14528(8)	−1700(8)	7197(5)	51(3)
C18	13963(11)	−2158(11)	6719(6)	86(4)
C19	15266(11)	−2697(10)	7634(6)	83(4)
C20	15464(9)	−1270(9)	6757(5)	66(3)
C21	10320(9)	3450(8)	7351(5)	43(2)
C22	11585(8)	2990(8)	7247(5)	39(2)
C23	12183(9)	2940(8)	6590(5)	51(3)
C24	11594(10)	3299(9)	6036(5)	57(3)
C25	10324(9)	3783(9)	6169(5)	53(3)
C26	9658(8)	3861(8)	6818(5)	42(2)
C27	12314(10)	3177(10)	5320(6)	75(3)
C28	13360(11)	2003(10)	5229(7)	100(5)
C29	12788(15)	4145(13)	5196(9)	140(6)
C30	11511(12)	3271(13)	4780(7)	110(5)
C31	7363(9)	2937(9)	7448(5)	49(3)
C32	7808(9)	3425(8)	6877(5)	46(3)
C33	7845(9)	3007(9)	6260(5)	52(3)
C34	7521(10)	2059(10)	6189(6)	61(3)
C35	7122(9)	1579(9)	6774(6)	56(3)
C36	7069(9)	1964(9)	7408(5)	50(3)
C37A	7575(11)	1610(11)	5487(6)	84(4)
C38A	8786(19)	1540(30)	5072(15)	89(10)
C39A	6620(20)	2690(20)	5151(16)	115(13)
C40A	7210(30)	630(20)	5412(18)	120(13)
C37B	7575(11)	1610(11)	5487(6)	84(4)

Table A.44: Continued Overleaf

C38B	8090(20)	2045(19)	4872(10)	74(8)
C39B	6339(18)	1500(20)	5443(13)	100(10)
C40B	8350(20)	242(14)	5521(12)	91(9)
C41	10756(8)	−442(8)	8990(5)	43(2)
C42	12289(9)	2528(8)	7831(5)	49(3)
C43	8284(9)	4350(9)	6927(5)	54(3)
C44	6787(8)	1318(8)	8039(5)	46(3)
C45	6091(8)	4250(8)	8322(5)	43(2)
C46	6207(9)	4967(8)	8845(5)	43(2)
C47	11141(9)	2044(9)	9477(5)	50(3)
C48	9992(9)	2939(9)	9879(5)	48(3)
O1	8494(6)	1412(5)	8870(4)	62(2)
O2	7259(5)	3352(5)	8099(3)	43(2)
O3	9615(6)	3532(6)	7996(3)	50(2)
O4	10757(6)	1841(5)	8870(3)	45(2)
O5	6900(7)	4800(7)	525(4)	91(3)
O6	8196(7)	5533(7)	942(4)	75(2)
F1	6110(7)	6804(8)	917(5)	134(3)
F2	7563(7)	6230(7)	−123(4)	103(3)
P1	7174(3)	5846(3)	582(2)	65(1)
N1	5212(7)	5576(7)	9246(4)	55(2)
N2	7261(7)	5006(7)	8849(4)	51(2)
N3	10149(8)	3638(7)	10285(4)	61(3)
N4	8926(7)	2947(7)	9828(4)	54(2)
O7	4121(8)	7391(7)	275(5)	84(3)
O9	8695(12)	9317(9)	3782(6)	132(4)
O8	3381(10)	5613(10)	7948(6)	125(4)
C51	9376(11)	9532(10)	3215(6)	72(3)
C50	3732(16)	4801(15)	7386(9)	129(6)
C49	3615(18)	8345(18)	−110(10)	156(7)

Table A.44: Atomic coordinates [$\times 10^4$], equivalent isotropic displacement parameters [$Å^2 \times 10^3$] and site occupancy factors. U_{eq} is defined as one third of the trace of the orthogonalized U^{ij} tensor.

5,11,17,23-Tetra-tert-butyl-25, 27 -3-toluenamidinium-26,28-dihydroxy-calix[4]arene malonate

Identification code	**(89)· Malonate**	
Empirical formula	$C_{60}H_{74}N_4O_4(CH_2(CO_2)_2)_2.4C_2H_5OH.H_2O$	
Formula weight	1219.6	
Temperature	153 K	
Wavelength	0.71073 Å	
Crystal system	Triclinic	
Space group	$P\bar{1}$	
Unit cell dimensions	a = 10.569(3) Å	α = 94.522(5)°
	b = 12.071(3) Å	β = 100.971(5)°
	c = 27.334(7) Å	γ = 95.754(5)°
Volume	3389(2) Å^3	
Z	2	
Density (calculated)	1.19$_5$ Mg / m^3	
Absorption coefficient	0.081 mm^{-1}	
F(000)	1484	
Crystal	Plate; colourless	
Crystal size	0.50 × 0.25 × 0.08 mm^3	
θ range for data collection	2.6 – 22.4°	
Index ranges	$-12 \le h \le 12$, $-14 \le k \le 14$, $0 \le l \le 32$	
Reflections collected	34058	
Independent reflections	11868 [R_{int} = 0.079]	
Absorption correction	None	
Max. and min. transmission	-	
Refinement method	Full-matrix least-squares on F^2	
Data / restraints / parameters	7123 / - / 794	
Goodness-of-fit on F^2	1.562	
Final R indices [$F^2 > 4\sigma(F^2)$]	$R1$ = 0.098, $wR2$ = 0.111	
Extinction coefficient	-	
Largest diff. peak and hole	0.687 and –0.474 e Å^{-3}	

Table A.45: Structure and refinement data

Atom	x	y	z	U_{eq}
O(11)	0.5823(4)	0.2041(3)	0.2343(2)	0.025(2)
C(11)	0.6078(5)	0.2217(4)	0.2861(2)	0.021(3)
C(110)	0.6849(6)	0.2470(5)	0.2113(3)	0.033(4)
C(111)	0.6967(6)	0.1705(5)	0.1672(2)	0.026(4)
C(112)	0.7869(5)	0.1991(5)	0.1389(2)	0.026(4)
C(113)	0.8062(5)	0.1299(4)	0.0998(2)	0.024(4)
C(1131)	0.9048(6)	0.1603(5)	0.0704(2)	0.026(4)
N(1131)	0.9573(5)	0.0836(4)	0.0479(2)	0.030(3)
N(1132)	0.9412(5)	0.2670(4)	0.0668(2)	0.030(3)
C(114)	0.7287(6)	0.0262(5)	0.0867(2)	0.028(4)
C(115)	0.6367(6)	-0.0027(5)	0.1143(3)	0.031(4)
C(116)	0.6193(6)	0.0667(5)	0.1535(3)	0.031(4)
C(12)	0.5605(5)	0.3119(4)	0.3089(2)	0.024(4)
C(13)	0.5866(6)	0.3275(5)	0.3605(2)	0.028(4)
C(14)	0.6521(6)	0.2575(5)	0.3905(2)	0.030(4)
C(141)	0.6832(6)	0.2756(5)	0.4471(3)	0.034(4)
C(142)	0.8289(8)	0.2968(6)	0.4656(3)	0.054(5)
C(143)	0.6247(9)	0.3753(6)	0.4676(3)	0.058(6)
C(144)	0.6291(8)	0.1714(6)	0.4689(3)	0.055(6)
C(15)	0.6930(6)	0.1655(5)	0.3663(2)	0.027(4)
C(16)	0.6705(5)	0.1454(4)	0.3148(2)	0.026(4)
C(1)	0.7097(6)	0.0399(5)	0.2907(2)	0.028(4)
O(21)	0.3130(4)	0.1991(3)	0.2189(2)	0.033(3)
C(21)	0.2641(6)	0.2666(5)	0.2504(2)	0.027(4)
C(22)	0.1363(6)	0.2399(5)	0.2542(2)	0.028(4)
C(23)	0.0813(6)	0.3070(5)	0.2849(3)	0.034(4)
C(24)	0.1517(6)	0.3992(5)	0.3160(3)	0.036(4)
C(241)	0.0926(7)	0.4661(6)	0.3529(3)	0.050(5)
C(242)	0.120(1)	0.5886(6)	0.3502(5)	0.10(1)
C(243)	-0.0479(8)	0.4329(6)	0.3490(4)	0.070(7)
C(244)	0.158(1)	0.4437(8)	0.4066(4)	0.086(8)
C(25)	0.2792(6)	0.4239(5)	0.3113(3)	0.032(4)
C(26)	0.3386(5)	0.3611(5)	0.2803(2)	0.025(4)
C(2)	0.4797(6)	0.3880(5)	0.2788(2)	0.028(4)
O(31)	0.1997(4)	-0.0506(3)	0.1987(2)	0.029(3)
C(31)	0.1660(6)	-0.0469(5)	0.2449(2)	0.025(4)
C(310)	0.1085(6)	-0.1143(5)	0.1572(2)	0.030(4)
C(311)	0.1761(6)	-0.1303(5)	0.1157(2)	0.029(4)
C(312)	0.1814(5)	-0.2355(5)	0.0935(2)	0.024(4)
C(313)	0.2480(5)	-0.2504(4)	0.0555(2)	0.024(4)
C(3131)	0.2553(6)	-0.3646(5)	0.0324(2)	0.028(4)
N(3131)	0.3595(5)	-0.3899(4)	0.0197(2)	0.034(3)

Table A.46: Continued Overleaf

N(3132)	0.1488(5)	-0.4361(4)	0.0250(2)	0.031(3)
C(314)	0.3122(6)	-0.1599(5)	0.0385(2)	0.030(4)
C(315)	0.3049(6)	-0.0533(5)	0.0603(3)	0.035(4)
C(316)	0.2378(6)	-0.0386(5)	0.0982(3)	0.032(4)
C(32)	0.2092(5)	-0.1259(5)	0.2769(2)	0.027(4)
C(33)	0.1923(6)	-0.1144(5)	0.3253(2)	0.030(4)
C(34)	0.1309(6)	-0.0270(5)	0.3440(2)	0.027(4)
C(341)	0.1320(6)	-0.0090(5)	0.3989(2)	0.032(4)
C(342)	0.0445(7)	0.0765(6)	0.4117(3)	0.047(5)
C(343)	0.0849(8)	-0.1189(6)	0.4187(3)	0.056(6)
C(344)	0.2707(7)	0.0280(7)	0.4258(3)	0.052(5)
C(35)	0.0861(6)	0.0456(5)	0.3101(2)	0.029(4)
C(36)	0.1025(5)	0.0381(5)	0.2611(2)	0.025(4)
C(3)	0.0643(6)	0.1308(5)	0.2284(2)	0.030(4)
O(41)	0.4631(4)	-0-0342(3)	0.2367(2)	0.031(3)
C(41)	0.5057(6)	-0.0940(5)	0.2752(2)	0.026(4)
C(42)	0.6306(6)	-0.0616(4)	0.3029(2)	0.025(4)
C(43)	0.6769(6)	-0.1205(5)	0.3420(3)	0.030(4)
C(44)	0.6011(6)	-0.2085(5)	0.3575(2)	0.029(4)
C(441)	0.6558(6)	-0.2682(5)	0.4019(3)	0.032(4)
C(442)	0.7525(7)	-0.3417(6)	0.3900(3)	0.047(5)
C(443)	0.7175(8)	-0.1830(6)	0.4467(3)	0.055(6)
C(444)	0.5475(7)	-0.3400(6)	0.4198(3)	0.048(5)
C(45)	0.4783(6)	-0.2382(5)	0.3290(3)	0.031(4)
C(46)	0.4283(6)	-0.1831(4)	0.2886(2)	0.027(4)
C(4)	0.2902(6)	-0.2135(5)	0.2618(2)	0.028(4)
C(O)	0.8195(6)	-0.2681(5)	0.0744(2)	0.027(4)
C(01)	0.8786(5)	-0.2469(5)	0.0298(2)	0.027(4)
O(011)	0.8922(4)	-0.1476(3)	0.0188(2)	0.034(3)
O(012)	0-9108(4)	-0.3286(3)	0.0055(2)	0.031(3)
C(02)	0.6801(6)	-0.3209(5)	0.0571(3)	0.030(4)
O(021)	0.5950(4)	-0.2621(3)	0.0504(2)	0.043(3)
O(022)	0.6652(4)	-0.4281(3)	0.0525(2)	0.046(3)
O(101)	0.0287(6)	0.5872(5)	0.1727(3)	0.085(5)
C(101)	0.107(l)	0.5062(7)	0.1908(4)	0.076(7)
C(102)	0.186(l)	0.4732(9)	0.1570(4)	0.098(9)
O(201)	0.6080(6)	-0.4575(5)	0.1965(3)	0.076(5)
C(201)	0.524(l)	-0.3750(8)	0.2058(4)	0.075(7)
C(202)	0.490(l)	-0.3116(9)	0.1628(4)	0.087(8)
O(301)	0.8627(8)	-0.3804(6)	0.2311(3)	0.118(7)
C(301)	0.866(l)	-0.2714(9)	0.2576(5)	0.11(1)
C(302)	0.825(l)	-0.1885(9)	0.2229(5)	0.11(1)
O(401)	0.5187(8)	0.4400(6)	0.1049(3)	0.121(7)
C(401)	0.460(2)	0.350(l)	0.0794(4)	0.15(l)

Table A.46: Continued Overleaf

C(402)	0.383(1)	0.2703(8)	0.0992(4)	0.090(8)
0(01)	0.8499(7)	0.4562(4)	0.1035(3)	0.082(5)

Table A.46: Atomic coordinates, equivalent isotropic displacement parameters [Å^2] and site occupancy factors. U_{eq} is defined as one third of the trace of the orthogonalized U^{ij} tensor.

References

(1) Werner, A. *Zeitschr. Anorg. Chem.* **1893**, *3*, 267.

(2) Lehn, J. M. *Angew. Chem. Int. Ed. Engl.* **1988**, *27*, 89.

(3) Pedersen, C. J. *J. Am. Chem. Soc.* **1967**, *89*, 2495.

(4) Pedersen, C. J. *Angew. Chem. Int. Ed. Engl.* **1988**, *27*, 1021.

(5) Cram, D. J. *Angew. Chem. Int. Ed. Engl.* **1988**, *27*, 1009.

(6) Wipff, G.; Kollman, P.; Lehn, J.-M. *J. Mol. Struct.* **1983**, *93*, 153.

(7) Sleiman, H.; Baxter, P. N. W.; Lehn, J.-M.; Rissanen, K. *J. Chem. Soc., Chem. Commun.* **1995**, 715.

(8) Harding, M. M.; Koert, U.; Lehn, J.-M.; Marquis-Rigault, A.; Piguet, C.; Siegel, J. *Helv. Chim. Acta* **1991**, *74*, 594.

(9) Youinou, M.-T.; Rahmouni, N.; Fischer, J.; Osborn, J. A. *Angew. Chem. Int. Ed. Engl.* **1992**, *31*, 733.

(10) Simmons, H. E.; Park, C. H. *J. Am Chem. Soc.* **1968**, *90*, 2428.

(11) Moss, B. *Chemistry & Industry* **1996**, 407.

(12) Higgins, C. *Nature* **1992**, *358*, 536.

(13) Barnard, C. F. J. *Platinum Metals Rev.* **1989**, *33*, 162.

(14) Calnan, B. J.; Tidor, B.; Biancalana, S.; Hudson, D.; Frankel, A. D. *Science* **1991**, *252*, 1167.

(15) Stryer, L. *Biochemistry*; Third ed.; W.H. Freeman, 1988.

(16) Mangani, S.; Ferraroni, M. *Supramolecular Chemstry of anions*; Wiley-VCH: New York, 1997.

(17) Luecke, H.; Quiocho, F. A. *Nature* **1990**, *347*, 402.

(18) Schnebeck, R. D.; Engbersen, E.; Lippert, B. *Angew. Chem. Int. Ed. Engl.* **1999**, *38*, 168.

(19) Kavallieratos, K.; de Gala, S. R.; Austin, D. J.; Crabtree, R. H. *J. Am. Chem. Soc.* **1997**, *119*, 2325.

(20) Choi, K.; Hamilton, A. D. *J. Am. Chem. Soc.* **2001**, *123*, 2456.

(21) Niikura, K.; Bisson, A. P.; Anslyn, E. V. *J. Chem. Soc., Perkin Trans. 2* **1999**, 1111.

(22) Fan, E.; Arman, S. A. V.; Kincaid, S.; Hamilton, A. D. *J. Am. Chem. Soc.* **1993**, *115*, 369.

(23) Xie, H.; Yi, S.; Yang, X.; Wu, S. *New. J. Chem* **1999**, *23*, 1105.

(24) Nam, K. C.; Kang, S. O.; Jeon, H. S. J. *Tetrahedron Letters* **1999**, *40*, 7343.

(25) Ki, Y. J.; Kang, O.; Cho, E. J.; Jeon, S.; Nam, K. C. *Bull. Korean Chem. Soc.* **2000**, *21*, 1152.

(26) Kyne, G. M.; Light, M. E.; Hursthouse, M. B.; de Mendoza, J.; Kilburn, J. D. *J. Chem. Soc., Perkin Trans. 1* **2001**, 1258.

(27) Schmidtchen, F. P. *J. Chem. Soc., Perkin Trans. 2* **1986**, *X*, 135.

(28) Schmidtchen, F. P. *Angew. Chem. Int. Ed. Engl.* **1977**, *16*, 720.

(29) Gale, P. A. *Coord. Chem. Rev.* **2000**, *199*, 181.

(30) Linton, B. R.; Goodman, M. S.; Hamilton, A. D. *Chem. Eur. J.* **2000**, *6*, 2449.

(31) Nishizawa, S.; Kato, Y.; Teramae, N. *J. Am. Chem. Soc.* **1999**, *121*, 9463.

(32) Lawless, L. J.; Blackburn, A. G.; Ayling, A. J.; Perez-Payan, M. N.; Davis, A. P. *J. Chem. Soc., Perkin Trans. 1* **2001**, 1329.

(33) Hosseini, M. W.; Lehn, J. M. *J. Am Chem. Soc.* **1982**, *104*, 3525.

(34) Clifford, T.; Danby, A.; Llinares, J. M.; Mason, S.; Alcock, N. W.; Powell, D.; Aguilar, J. A.; Garcia-España, E.; Bowman-James, K. *Inorg. Chem.* **2001**, *40*, 4710.

(35) Uppadine, L. H.; Drew, M. G. B.; Beer, P. D. *Chem. Commun.* **2001**, 291.

(36) Mahoney, J. M.; Beatty, A. M.; Smith, B. D. *J. Am. Chem. Soc.* **2001**, *123*, 5847.

(37) Coles, S. J.; Gale, P. A.; Hursthouse, M. B. *Cryst. Eng. Comm.* **2001**, 53.

(38) Sessler, J. L.; Gale, P. A. In *The Porphyrin Handbook*; Kadish, K. M., Smith, K. M., Guilard, R., Eds.; Academic Press: San Diego, 2000; Vol. 6, p 257.

(39) Schmuck, C.; Lex, J. *Org. Lett.* **1999**, *1*, 1779.

(40) Schmuck, C. *Chem. Commun.* **1999**, 843.

(41) Schmuck, C.; Heil, M. *Org. Lett.* **2001**, *3*, 1253.

(42) Black, C. B.; Andrioletti, B.; Try, A. C.; Ruiperez, C.; Sessler, J. L. *J. Am. Chem. Soc.* **1999**, *121*, 10438.

(43) Anzenbacher, P.; Try, A. C.; Miyaji, H.; Jursiková, K.; Lynch, V. M.; Marquez, M.; Sessler, J. L. *J. Am Chem. Soc.* **2000**, *122*.

(44) Scherer, M.; Sessler, J. L.; Gebauer, A.; Lynch, V. *Chem. Commun.* **1998**, 85.

(45) Andrievsky, A.; Ahuis, F.; Sessler, J. L.; Vogtle, F.; Gudat, D.; Moini, M. *J. Am. Chem. Soc.* **1998**, *120*, 9712.

(46) Baeyer, A. *Ber. Dtsch. Chem. Ges.* **1886**, *19*, 2184.

(47) Floriani, C. In *The Porphyrin Handbook*; Kadish, K. M., Smith, K. M., Guilard, R., Eds.; Academic Press: San Diego, 2000, Vol. 3, p. 405.

(48) Anzenbacher, P.; Jursikova, K.; Lynch, V. M.; Gale, P. A.; Sessler, J. L. *J. Am. Chem. Soc.* **1999**, *121*, 11020.

(49) Bonomo, L.; Solari, E.; Toraman, G.; Scopelliti, R.; Latronico, M.; Floriani, C. *Chem. Commun.* **1999**, 2413.

(50) Gale, P. A.; Anzenbacher, P.; Sessler, J. L. *Coord. Chem. Rev.* **2001**, *222*, 57.

(51) Sessler, J. L.; Gale, P. A.; Genge, J. W. *Chem. Eur. J.* **1998**, *4*, 1095.

(52) Sessler, J. L.; Anzenbacher, P. J.; Shriver, J. A.; Jurísková, K.; Lynch, V. M.; Marquez, M. *J. Am. Chem. Soc.* **2000**, *122*, 12061.

(53) Cafeo, G.; Kohnke, F. H.; Torre, G. L. L.; White, A. J. P.; Williams, D. J. *Chem. Commun.* **2000**, 1207.

(54) Turner, B.; Shterenberg, A.; M., M. K.; Suwinska, K.; Eichen, Y. *Chem. Commun.* **2001**, 13.

(55) Bucher, C.; Zimmerman, R. S.; Lynch, V.; Sessler, J. L. *J. Am. Chem. Soc.* **2001**, *123*, 9716.

(56) Woodward, R. B. *J. Am. Chem. Soc.* **1983**, *105*, 6429.

(57) Sessler, J. L.; Davis, J. M. *Acc. Chem. Res.* **2001**, *34*, 989.

(58) Sessler, J. L.; Cyr, M.; Furuta, H.; Král, V.; Mody, T.; Morishima, T.; M, M. S.; Weghorn, S. *Pure & Appl. Chem.* **1993**, *65*, 393.

(59) Shionoya, M.; Furuta, H.; Lynch, V.; Harriman, A.; Sessler, J. L. *J. Am. Chem. Soc.* **1992**, *114*, 5714.

(60) Sessler, J. L.; Ford, D. A.; Cyr, M. J.; Furuta, H. *J. Chem. Soc., Chem. Commun.* **1991**, 1733.

(61) Král, V.; Andrievsky, A.; Sessler, J. L. *J. Chem. Soc., Chem. Commun.* **1995**, 2349.

(62) Sessler, J. L.; Andrievsky, A. *Chem. Commun.* **1996**, 1119.

(63) Sessler, J. L.; Seidel, D.; Lynch, V. *J. Am. Chem. Soc.* **1999**, *121*, 11257.

(64) Pflugrath, J. W.; Quicho, F. A. *Nature* **1985**, *314*, 257.

(65) Ohkuma, S.; Sato, T.; Okamoto, M.; Matsuya, H.; Arai, K.; Kataoka, T.; Nagai, K.; Wassermann, H. H. *Biochem. J.* **1998**, *334*, 731.

(66) Gale, P. A.; Camiolo, S.; Chapman, C. P.; Light, M. E.; Hursthouse, M. B. *Tetrahedron Lett.* **2001**, *42*, 5095.

(67) Friedman, M. *J. Org. Chem.* **1965**, *30*, 589.

(68) Gale, P. A.; Camiolo, S.; Tizzard, G. J.; Chapman, C. P.; Light, M. E.; Coles, S. J.; Hursthouse, M. B. *J. Org. Chem.* **2001**, *66*, 7849.

(69) Fisher, H.; Fink, E. *Z. Physiol. Chem.* **1948**, *283*, 152.

(70) Motekaitis, R. J.; Heinert, D. H.; Martell, A. E. *J. Org. Chem.* **1970**, *35*, 2504.

(71) Chang, C. K.; Bag, N. *J. Org. Chem.* **1995**, *60*, 7030.

(72) Hogberg, T.; Strom, P.; Ebner, M.; Ramsby, S. *J. Org. Chem.* **1986**, *52*, 2033.

(73) Basha, A.; Lipton, M.; Weinreb, S. M. *Tet. Lett.* **1977**, *48*, 4171-4174.

(74) Schmuck, C.; Lex, J. *Eur. J. Org. Chem.* **2001**, 1519.

(75) Hynes, M. J. *J. Chem. Soc., Dalton Trans.* **1993**, 311.

(76) Gale, P. A.; Camiolo, S.; Light, M. E.; Hursthouse, M. B. *Tetrahedron Lett.*, **2002**, submitted.

(77) Camiolo, S.; Gale, P. A.; Hursthouse, M. B.; Light, M. E.; Shi, A. J. *Chem. Commun.* **2002**, 758.

(78) Gale, P. A.; Camiolo, S.; Light, M. E.; Hursthouse, M. B. *J. Am. Chem. Soc.*, **2002**, submitted.

(79) Bisson, A. P.; Hunter, C. A.; Morales, J. C.; Young, K. *Chem. Eur. J.* **1998**, *4*, 845.

(80) Pease, A. R.; Jeppesen, J. O.; Stoddart, J. F.; Luo, Y.; Collier, C. P.; Heath, J. R. *Acc. Chem. Res.* **2001**, *34*, 433.

(81) Gale, P. A.; Camiolo, S.; Tizzard, G. J.; Coles, S. J.; Hursthouse, M. B. *Supramol. Chem*, **2002**, submitted.

(82) Shukla, R.; Kida, T.; Smith, B. D. *Org. Lett.* **2000**, *2*, 3099

(83) Hoorn, W. P. v.; Jorgensen, W. L. *J. Org. Chem.* **1999**, *64*, 7439

(84) Gale, P. A.; Sessler, J. L.; Král, V.; Lynch, V. *J. Am. Chem. Soc.* **1996**, *118*, 5140.

(85) Gutsche, C. D. *Calix[4]arenes Revisited*; The Royal Society of Chemistry: Cambridge, 1998.

(86) Arnaud-Neu, F.; Collins, E. M.; Deasy, M.; Ferguson, G.; Harris, S. J.; Kaitner, B.; Lough, A. J.; McKervey, M. A.; Marques, E.; Ruhl, B. L.; Schwing-Weill, M. J.; Seward, E. M. *J. Am Chem. Soc.* **1989**, *111*, 8681.

(87) Camiolo, S.; Gale, P. A. *Chem. Commun.* **2000**, 1129.

(88) Andreetti, G. D.; Ungaro, R.; Pochini, A. *J. Chem. Soc., Chem. Commun.* **1979**, 1005.

(89) Woods, C. J.; Camiolo, S.; Light, M. E.; Coles, S. J.; Hursthouse, M. B.; King, M. A.; Gale, P. A.; Essex, J. W. *J. Am. Chem. Soc.*, **2002**, in press

(90) Gale, P. A.; Sessler, J. L.; Král, V. *Chem. Commun.* **1998**, 1.

(91) Black, D. S.; Kumar, N.; McConnell, D. B. *Tetrahedron* **2001**, *57*, 2203.

(92) Zinke, A.; Kretz, R.; Leggewie, E.; Hossinger, K. *Monatsh.* **1952**, 83.

(93) Baeyer, A. *Chem. Ber.* **1872**, *5*, 25.

(94) Baekeland, L. H. Patent 942,699: U.S.A, 1908.

(95) Cornforth, J. W.; Hart, P. D. A.; Nicholls, G. A.; Rees, R. J. W.; Stock, J. A. *Br. J. Pharmacol.* **1955**, *10*, 73.

(96) Cornforth, J. W.; Morgan, E. D.; Potts, K. T.; Rees, R. J. W. *Tetrahedron* **1973**, *29*, 1659.

(97) Gutsche, C. D.; Iqbal, M.; Stewart, D. *J. Org. Chem.* **1986**, *51*, 742.

(98) Gutsche, C. D.; Dhawan, B.; No, K. H.; Muthukrishnan, R. *J. Am Chem. Soc.* **1981**, *103*, 3782.

(99) Ninagawa, A.; Matsuda, H. *Makromol. Chem. Rapid Commun.* **1982**, *3*, 65.

(100) Nakamoto, Y.; Ishida, S. *Makromol. Chem. Rapid Commun.* **1982**, *3*, 705.

(101) Gutsche, C. D.; Dhawan, D.; Levine, J. A.; No, K. H.; Bauer, L. J. *Tetrahedron* **1983**, *39*, 409

(102) McKervey, M. A.; Seward, E. M.; Ferguson, G.; Ruhl, B.; Harris, S. J. *J. Chem. Soc., Chem. Commun.* **1985**, 388.

(103) Rizzoli, C.; Andreetti, G. D.; Ungaro, R.; Pochini, A. *J. Mol. Struct.* **1982**, *82*, 133.

(104) Bohmer, V.; Goldmann, H.; Kaptein, R.; Zetta, L. *J. Chem. Soc., Chem. Commun.* **1985**, 667.

(105) Gutsche, C. D.; Bauer, L. J. *J. Am Chem. Soc.* **1985**, *107*, 6052.

(106) Shinkai, S.; Osuka, T.; Araki, K.; Matsuda, T. *Bull. Chem. Soc. Jap.* **1989**, *62*, 4055.

(107) Gutsche, C. D.; Nam, K. C. *J. Am. Chem. Soc.* **1988**, *110*, 6153.

(108) Maciel, G. E.; Chuang, I. S. *Macromolecules* **1984**, *17*, 1081.

(109) Beer, P. D.; Gale, P. A.; Hesek, D. *Tetrahedron Lett.* **1995**, *36*, 767.

(110) Beer, P. D.; Gale, P. A.; Chen, Z. *Suprmol. Chem.* **1996**, *7*, 241.

(111) Cameron, B. R.; Loeb, S. J. *Chem. Commun.* **1997**, 573.

(112) Scheerder, J.; Fochi, M.; Engbersen, J. F. J.; Reinhoudt, D. N. *J. Org. Chem.* **1994**, *59*, 7815.

(113) Beer, P. D.; Drew, M. G. B.; Gradwell, K. *J. Chem. Soc., Perkin Trans. 2* **2000**, 511.

(114) Pelizzi, N.; Casnati, A.; Friggeri, A.; Ungaro, R. *J. Chem. Soc. Perkin Trans. 2*, **1998**, 1307.

(115) Gale, P. A. *Tetrahedron Lett.* **1998**, *39*, 3873.

(116) Szemes, F.; Hesek, D.; Chen, Z.; Dent, S. W.; Drew, M. G. B.; Goulden, A. J.; Graydon, A. R.; Grieve, A.; Mortimer, R. J.; Wear, T.; Weightman, J. S.; Beer, P. D. *Inorg. Chem.* **1996**, *35*, 5868.

(117) Garigipati, R. S. *Tetrahedron Lett.* **1990**, *31*, 1969.

(118) Camiolo, S.; Gale, P. A.; Ogden, M. I.; Skelton, B. W.; White, A. H. *J. Chem. Soc. Perkin Trans. 2* **2001**, 1294.

(119) Nagata, H.; In, Y.; Tomoo, K.; Doi, M.; Ishida, T.; Wakahara, A. *Chem. Pharm. Bull.* **1988**, *43*, 1836.

(120) Camiolo, S.; Gale, P. A.; Light, M. E.; Hursthouse, M. B. *Supramol. Chem.* **2001**, *13*, 613.

(121) Reyer, D. L.; Huff, M. F.; Lebioda, L. *Acta Cryst.* **1991**, *C47*, 1167.

(122) Jeffery, J. C.; Jelliss, P. A.; Lebedev, V. N.; Stone, F. G. A. *Organometallics.* **1996**, *15*, 4737.

(123) Gutsche, C. D.; See, K. A. *J. Org. Chem.* **1992**, *57*, 4527.